

Radiative Corrections and Resummation Effects to Higgs Physics in QCD

By
Ajjath A H
PHYS10201604004

The Institute of Mathematical Sciences, Chennai

A thesis submitted to the
Board of Studies in Physical Sciences
In partial fulfilment of requirements
For the Degree of
DOCTOR OF PHILOSOPHY
of
HOMI BHABHA NATIONAL INSTITUTE



August, 2021

Homi Bhabha National Institute

Recommendations of the Viva Voce Board

As members of the Viva Voce Board, we certify that we have read the dissertation prepared by Ms. Ajjath A H entitled "Radiative Corrections and Resummation Effects to Higgs Physics in QCD" and recommend that it maybe accepted as fulfilling the dissertation requirement for the Degree of Doctor of Philosophy.

D. Indumathi

Date: 19.08.2021

Chair - D. Indumathi

V. Ravindran

Date: 19-08-2021

Guide/Convener - V. Ravindran

Shrihari

Date: 19-08-2021

Member 1 - Shrihari Gopalakrishna

Nita Sinha

Date: 19-08-2021

Member 2 - Nita Sinha

S. R. Hassan

Date: 19-08-2021

Member 3 - S.R. Hassan

Asmita Mukherjee

Date: 18-8-2021

External Examiner -

ASMITA MUKHERJEE

Final approval and acceptance of this dissertation is contingent upon the candidate's submission of the final copies of the dissertation to HBNI.

I hereby certify that I have read this dissertation prepared under my direction and recommend that it may be accepted as fulfilling the dissertation requirement.

Date: 19-08-2021

Place: IMSc, Chennai

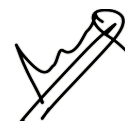
V. Ravindran

Guide - V. Ravindran

STATEMENT BY AUTHOR

This dissertation has been submitted in partial fulfilment of requirements for an advanced degree at Homi Bhabha National Institute (HBNI) and is deposited in the Library to be made available to borrowers under rules of the HBNI.

Brief quotations from this dissertation are allowable without special permission, provided that accurate acknowledgement of source is made. Requests for permission for extended quotation from or reproduction of this manuscript in whole or in part may be granted by the Competent Authority of HBNI when in his or her judgment the proposed use of the material is in the interests of scholarship. In all other instances, however, permission must be obtained from the author.



Ajjath A H

DECLARATION

I, hereby declare that the investigation presented in the thesis has been carried out by me.
The work is original and has not been submitted earlier as a whole or in part for a degree
/ diploma at this or any other Institution / University.


Ajjath A H

List of Publications arising from the thesis¹

Journal

1. “Higgs pair production from bottom quark annihilation to NNLO in QCD”
A. H Ajjath, P. Banerjee, A. Chankraborty, P. K. Dhani, P. Mukherjee, N. Rana and V. Ravindran.
J. High Energ. Phys. (2019), 05, 030.
2. “NNLO QCD \oplus QED corrections to Higgs production in bottom quark annihilation”
A. H Ajjath, P. Banerjee, A. Chakraborty, P. K. Dhani, P. Mukherjee, N. Rana and V. Ravindran.
Phys.Rev.D, (2019), 100 11, 114016

Preprint

1. “On next to soft corrections to Drell-Yan and Higgs Boson productions”
A. H Ajjath, P. Mukherjee and V. Ravindran
[arXiv: 2006.06726 \[hep-ph\]](#) (Communicated to *J. High Energ. Phys.*)
2. “Soft-virtual correction and threshold resummation for n -colorless particles to fourth order in QCD: Part II”
T. Ahmed, **A. H Ajjath**, P. Mukherjee, V. Ravindran, and A. Sankar
[arXiv:2010.02980 \[hep-ph\]](#) (Communicated to *European Physics Journal C*)

¹As it is standard in the High Energy Physics Phenomenology (hep-ph) community the names of the authors on any paper appear in their alphabetical order.

List of other Publications, Not included in the thesis

1. “Resummed prediction for Higgs boson production through $b\bar{b}$ annihilation at N³LL”
A. H Ajjath, A. Chakraborty, G. Das, P. Mukherjee and V. Ravindran.
J. High Energ. Phys., (2019), 11, 006
2. “Polarised Amplitudes and Soft-Virtual Cross Sections for $b\bar{b} \rightarrow ZH$ at NNLO in QCD ”
T. Ahmed, **A. H Ajjath**, L. Chen, P. K. Dhani, P. Mukherjee and V. Ravindran.
J. High Energ. Phys. (2020), 01, 030
3. “Infrared structure of $SU(N) \times U(1)$ gauge theory to three loops”
A. H Ajjath, P. Mukherjee and V. Ravindran.
J. High Energ. Phys. (2020), 08,156
4. “Resummed Drell-Yan cross-section at N³LL”
A. H Ajjath, G. Das, M.C. Kumar, P. Mukherjee, V. Ravindran and K. Samanta.
J. High Energ. Phys. (2020), 10, 153
5. “On next to soft threshold corrections to DIS and SIA processes”
A. H Ajjath, P. Mukherjee, V. Ravindran, A. Sankar, and S. Tiwari
J. High Energ. Phys. (2021), 04, 131
6. “On next to soft corrections for Drell-Yan and Higgs boson rapidity distributions beyond N³LO”
A. H Ajjath, P. Mukherjee, V. Ravindran, A. Sankar, and S. Tiwari
Phys. Rev. D, (2021), 103, L111502
7. “Soft-virtual correction and threshold resummation for n -colorless particles to fourth order in QCD: Part I”
T. Ahmed, **A. H Ajjath**, G. Das, P. Mukherjee, V. Ravindran, and S. Tiwari
[arXiv:2010.02980 \[hep-ph\]](https://arxiv.org/abs/2010.02980) (Communicated to PRD)

Conferences and workshops attended

1. 17 - 21 May 2021 : ***RADCOR - LoopFest 2021***, Florida State University, Virtual Conference.
2. 14 - 18 December 2020: ***DAE-BRNS High Energy Physics Symposium 2020***, National Institute of Science Education and Research (NISER), Odisha, India.
3. 28 - 31 January 2020: ***International Workshop Precision QCD@LHC***, Indian Institute of Technology, Hyderabad, India.
4. 18 - 22 November 2019: ***Madgraph School-2019***, The Institute of Mathematical Sciences, Chennai, India.
5. 01 - 17 April 2019: ***The Myriad Colorful Ways of Understanding Extreme QCD Matter***, International Centre for Theoretical Sciences, Bangalore, India.
6. 25 November - 10 December 2018: ***SERC Main School in Theoretical High Energy Physics-2018***, Indian Institutes of Science Education & Research, Pune.
7. 10 - 14 December 2018 : ***DAE-BRNS High Energy Physics Symposium 2018***, Indian Institute of Technology, Madras, India.
8. 15 July- 03 August 2018 : ***MITP Summer School 2018: Towards the Next Quantum Field Theory of Nature***, Mainz Institute of Theoretical Physics, Germany.
9. 04 - 17 December 2017: ***GIAN School on Infrared Structure of Perturbative Gauge theories***, Indian Institute of Technology, Hyderabad, India.

Presentation and poster

1. 21 May 2021: *Next to soft virtual correction to differential cross section at LHC*, RADCOR - LoopFest 2021, Florida State University, USA, Virtual Conference.
2. 15 December 2020: *Next to soft corrections to Differential rapidity distributions at the hadronic colliders*, DAE-BRNS High Energy Physics Symposium 2020, National Institute of Science Education and Research (NISER), Odisha, India, Virtual Conference.
3. 20 November 2020: *Next to soft corrections to Inclusive cross sections at the colliders*, Forschungsgruppe FOR 2926, Universität Tübingen, Germany, Virtual Seminar.
4. 19 November 2020 : *Next to soft corrections to Inclusive cross sections at the colliders*, CP3 Seminar, Centre for Cosmology, Particle Physics and Phenomenology (CP3), Louvain-la-Neuve, Belgium, Virtual Seminar.
5. 31 January 2020: *Infrared structure of $SU(N) \times U(1)$ gauge theory to three loops* in *International Workshop Precision QCD@LHC*, Indian Institute of Technology, Hyderabad, India.
6. 13 October 2018: *Second order QCD-QED corrections to inclusive Higgs boson production through $b\bar{b}$ annihilation* in *DAE-BRNS High Energy Physics Symposium 2018*, Indian Institute of Technology, Madras, India.



Ajjath A H

*To my parents and siblings
for their unrelenting support...*

ACKNOWLEDGEMENTS

The journey of PhD was not just an academic milestone to me, but a huge step in my life journey with many ups and downs. It wouldn't be possible to wear this crown without the love and support of many amazing people who deserve a mention.

Foremost, it is my supervisor, V. Ravindran, whose incredible mentoring has led me to where I stand right now. Thank you for sharing your ideas and making me understand those and, moreover, for keeping your confidence in me all along my PhD journey. More than a supervisor, you were a good mentor-cum-friend. Thank you for all our academic as well as non-academic discussions, your support in good and bad times and your affection and kindness. Besides your immense knowledge in physics, I thank you for being a wonderful person. Along with Ravindran comes Pooja, my friend-cum-collaborator! It was wonderful to have both of you together in my path, and we had a whole lot of fun in '208'. Our physics and non-physics arguments and discussions in '208' are among the main things I will miss in IMSc. Besides all the fun and physics, Pooja, you were an amazing collaborator one could get. Thank you for pushing me whenever it was required, for your unwavering support, criticism, love and your act of kindness in different situations. We were truly wonderful together! And, I really hope we will do much more in coming years...

Having many people around you who speaks the same language is a privilege only few could afford. Being part of a big QCD-family in India, I am one of those luckiest. I am indebted to Dhani and Pulak for being such outstanding seniors. Besides introducing me to the field of QCD, you people were a pillar of strength in the initial stage of my PhD. Thank you for all your care and love on various occasions. Amlan, you were an excellent addition to our group with all your jokes, fun, and physics. Aparna and Surabhi, you are the two smartest people doing wonders in our group. RADCOR previous night will always be a cherishing memory of our group work, like many others. I am grateful to have seniors like Taushif da and Manoj da: they had answers for each and every of our con-

cerns, be it physics or else. Thank you for being accessible to us at every stage, especially while applying for postdoc. Also, Taushif da, working with you was always great and fun. Goutam da, you have a significant role in my learning of numerical analysis and plotting; thank you for your support and criticisms. I enjoyed discussions with Narayan da, Satyajith da and Maguni da. Kajal, you are an excellent friend-cum-collaborator. Many things to learn from your hard work and dedication.

I would like to express my sincere gratitude to Prakash Mathews and M. C Kumar for various discussions and support. I am grateful to Anurag for organizing many meetings and conferences at IITH, which helped me to meet and interact with various QCD people. I am grateful to Werner Vogelsang for helpful discussion through email and Lorenzo Magnea for his wonderful teachings on QCD infrared structure. I would also like to thank Ekta and Hofie for their help and good moments when I visited Germany.

I would like to express my sincere gratitude to my DC members, Prof. Srihari, Prof. Indumathi, Prof. Nita and Prof. Hassan. Especially I am grateful to Srihari for his questions and concerns in my Doctoral meetings, which had improved my understanding a lot. I also would like to express my sincere gratitude to all my teachers in IMSc, especially Indu Madam. I also would like to express my gratitude to Prof. Murthi sir, who encouraged me all along starting from the IMSc interview.

It is my pleasure to mention Prof. Manoj at IITM, for his support and guidance to get into IMSc. Thank you sir, for all your nice words and encouragement.

It wouldn't be possible to reach where I stand now if it weren't for my excellent teachers. My journey through academia blessed me with many of them whose influence has strengthened me to stick into my passion for research. I take this opportunity to express my sincere gratitude to all of them.

When it comes to physics, the one person I am always indebted is my childhood friend, Sruthil. You are the person who shown me the wonders of physics in my early career.

Discussions with you and our evening readings inspired me to choose this path and stick to it. Thank you for showing me different topics in physics, for our little experiments and moreover for your constant encouragement. All these have done a lot at that stage of my life.

Life in IMSc wouldn't have been the same what it is without my friends. Being away from family and hometown for the first time made it painful in the initial stage; however, it enriched me with a whole lot of experiences and explorations at the personal level. I am thankful to all of you who were part of my life in last five years. I would like to mention some special people who influenced me on various occasions.

Having a 'Malayali' group all along my PhD time was a blessing to me. Sruthy, you were a great companion all along. Thank you for all your unconditional support, love, criticism and a beautiful friendship. Anupam, besides all the helps you have been offering, thank you for being a wonderful person. Renjan, though we were together for a short period, you were a prominent part of my IMSc life. Besides all the fun we had and a lovely friendship, I thank you for all your teachings. Akhil, you are a special friend-cum-brother in IMSc. More than fun, our discussions and endless talks were soothing to me. Thank you for your love and care and also for being supportive on many difficult occasions. Asweel, I enjoyed talking to you and thank you for our special meals during Ramzan. I would also like to thank Prasad, Anju, Goerge and Shruti for being wonderful hosts in several events. I also thank Ratheesh, Jilmy, Arjun and Revathy for many good moments.

My IMSc life would be only physics if it was not for the 'group of unusual people', that I am part of. Besides everything we had together, I am deeply indebted to all of you for including me in the group even I am a 'non-Benagli'. Ujjal, Subhankar, Semanti, Sujoy, Ramit, Gaurav, Soumya: we had numerous experiences and explorations together that only very few lucky researchers could think of. Thank you for all our countless and endless talks, discussions and arguments, our outings, dinners, food orderings, cookings, sports, pictionary, dumb charades, Mafia, watching movies, Birthday and paper celebra-

tions and more than anything our trip and treks. I owe Ujjal and Sujoy the most for initiating most of our trips. Everything started with our first institute trip of 2017 to Chikmaglur. Special mention to Sujoy and Semanti, it was a wonderful experience to co-organize that trip. Later on, Tada trek, Vattakkanal trip, Pichavaram, the great Chandrashila trek, Kudremukh trek, institute trip to Vagamon and finally the lockdown Kolkata and Darjeeling trip; each of these trips was unique in its own way and enlightened me with great experiences. I can't thank enough to each of you for these fantastic experiences, which uplifted me at the personal and professional level. I also take this opportunity to apologize to all of you to make you all talk in English just for me most of the time. I sincerely hope we will keep in touch and make much more trips together.

Sports have been a wonderful part of my IMSc life and helped me physically fit and mentally relaxed. I thank Kd, Renjan, Sujoy, Ujjal, Anupam, Mrigendra, Ramit, Semanti, Piyasa, Pavithra, Chandrani, Surabhi, Mrigendra, Pritam, Selvakumar and many more for the beautiful memories in the Badminton court. I especially thank Anupam, Kd and Renjan for their training in Badminton at various times. I owe IMSc sports committee for including girl's cricket and football tournaments, which open the path to learn them and those beautiful experiences. I owe Ujjal a lot for his training in football. I also thank Sujoy, Subhankar, Tanmoy, Shivam, Semanti, Ramit, Anupam, Sahil, Satyabrata, Ajay, Sabiar, Souvik, Prem and many more for many beautiful memories in football ground. Though I started it very late, it is something I will always cherish. I am also grateful for all the sports activities in IMSc, including cricket, football, badminton, Tennis, Chess and more which kept the environment here refreshing and lively.

It was great to be part of the 2017 fresher's welcome organizations. I especially thank Semanti, Sujoy, Pooja, Shivani, Janani, Mamta, Deepika, Ramit and many more for their co-organizations. Being part of stage performance was always grateful. I thank Semanti, Pooja, Pulak da, Shilpa di, Abhroneel for including me to be part of the outstanding musical performance. I am also grateful to Semanti, Sujoy, Ujjal, Jyotijwal, Subhroneel

da, Ramit, Abhimanyu, Tanmoy, Pavithra, Chandrani, Anupam and Subhasree for the beautiful drama that we could execute. It is also one of the cherishing memories of my PhD life.

Being part of Student mess organization was really wonderful experience. Thank you Ujjal, Ramit, Sujoy and Prateek, I really enjoyed working with you guys and we made it successful!

There were many emotionally downtime during my PhD. I owe Ujjal for being my side all along and extending your unconditional support, love and care. You are one of those exceptionally nice persons I met. Thank you for all your kindness, your time and encouragements, your advice and for all those beautiful experiences. I also thank Pooja, Dhani, Akhil, Sujoy, Subhankar, and Sruthy for your supports in my difficult times.

Khatua and Ujjal, you two made my IMSc life the best. I can't thank you people enough for making my life in IMSc smoother and lively and hopefully we will be in touch. Se-manti, you were an amazing and unique friend throughout my PhD; starting from my roommate to this point, I enjoyed both the warmth and bitterness of our friendship. Sujoy, I thank you for your lovely companionship and support. Ramit, I enjoyed your friendship and intellectual discussions in various topics. I also thank Mrigendra, Tanmoy, Anupam, Chandrani, Arpan, Digjoy and Pavithra for many good moments. Kiddo, you are there in my IMSc memories..

I would like to thank IMSc administration and non teaching staff for their wonderful works and support and keeping the atmosphere here very friendly and active. Special mention to Indra madam for her help and assistance in various administrative related occasions. Also, I would like acknowledge Balaji for his sincerity and appreciable service in canteen related things. I would like to thank Prof. Vani madam also for her help as dean of physics in many academic and administrative works.

I also take this opportunity to thank my friends Kd, Sanjay, Arya, Raji, Aruna, Vishnu,

Rithu, Adnan, Jinu, Sithu, Soni and many more for being part of my life. Sanjay, you are my terrific friend; I can't thank you enough for being my side in my happiness and difficulties. Kd, you are the one who uplifted me from being a silent person to the level I am now. I could never thank you enough. Raji, Vishnu, Rithu, you people are a beautiful part of my life and I enjoy the warmth of your friendship. Adnan, you always motivates me. Arya, I wish if you were there to see me graduate. Your encouragement and caring strengthen me a lot, and you will always be missed.

All those achievements I had in my life would not have been possible without the care and support of my family. I thank my uncle, Ashraf, for supporting me from my childhood; you have a significant role in what I am today. I express my gratitude to all my cousins and relatives for keeping their expectations on me; it has been encouraging all along. Faisalka and Sajikka, I thank you for all your love and caring. Anwar, you don't have any idea how much you encouraged me through your relentless supports, friendship and love; thank you for being an exceptional brother. Anna and Salu, I am grateful to have you in my side as my sisters; you both are my strong pillars of life. Ayan, Pathu, Hamdu, Fajju and Nehu, you people are my little lights of happiness. Last, but indeed not the least, it is my parent's sacrifice, love and prayers which have given me all the strength and courage throughout my life. Your silent support has smoothened my academic career and personal developments. I owe you for keeping your faith in me always, whose importance I cannot ever overlook.

Contents

Summary	1
Synopsis	3
1 Introduction	17
2 Review of perturbative QCD	25
2.1 Basics of QCD	25
2.1.1 QCD Lagrangian	26
2.1.2 Asymptotic freedom and running coupling	29
2.1.3 Parton model and Collinear factorization theorem	32
2.2 Fixed order computations in QCD	36
2.3 Effects of threshold corrections and Resummation	39
2.3.1 Threshold framework	40
2.3.2 Resummation	54
3 Higgs pair production from $b\bar{b}$-annihilation to NNLO in QCD	59

3.1	Prologue	59
3.2	Theoretical Framework	62
3.2.1	The Yukawa interaction	62
3.2.2	Kinematics	63
3.2.3	Classification of Feynman diagrams	64
3.2.4	General structure of amplitude	65
3.3	Calculation of amplitudes	67
3.3.1	Computational details	68
3.3.2	Ultraviolet renormalization	70
3.3.3	Infrared divergences and their factorization	72
3.4	Inclusive Cross Section up to NNLO	74
3.4.1	Cross section for class-A diagrams	75
3.4.2	Cross section for class-B diagrams	77
3.5	Phenomenology	85
3.6	Summary	89
4	NNLO QCD\oplusQED corrections to Higgs production in $b\bar{b}$ annihilation	91
4.1	Prologue	91
4.2	Theoretical framework	93
4.3	Methodology	95
4.4	UV and IR structures in QED and QCD-QED	97

4.4.1	Form factors	99
4.4.2	Soft distributions	105
4.5	Abelianization procedure	110
4.6	Mass factorized partonic cross sections	111
4.7	Numerical Impact	118
4.8	Summary	123
5	Threshold rapidity corrections for n-colorless particles in QCD	125
5.1	Prologue	125
5.2	Soft-virtual rapidity distribution	128
5.2.1	Soft-collinear operator for SV rapidity distribution	131
5.3	Results of SV rapidity distribution	139
5.4	Soft-collinear operator for threshold resummation	149
5.5	Summary	154
6	On next to soft corrections to Drell-Yan and Higgs Boson production	157
6.1	Prologue	157
6.2	Next to SV in z -space	161
6.3	All order predictions for Δ_I	176
6.4	More on the z -space NSV Solution Φ_{nsv}^I	182
6.4.1	On the form of the solution	182
6.4.2	On the Logarithmic Structure	186

6.5	Resummation of next-to-SV in N -space	189
6.6	Physical Evolution Kernel	198
6.7	Summary	201
A	QCD Feynman rules	203
B	Anomalous dimensions	205
C	The relevant coefficients for form factor and Soft-collinear distributions	208
D	Soft-collinear distribution for rapidity distribution	213
E	Resummation coefficients	220
F	Deriving resummation formula for SV and NSV logarithms	226
G	Expansion coefficients $\Gamma_A(x)$ and $\Gamma_B(x)$	229

Summary

The core part of this thesis deals with computing higher order QCD and QED corrections for the processes involving Higgs boson in the final states and the Drell-Yan (DY) process by employing the perturbative theory within the SM.

In the first part, we discuss the fixed order approach to compute higher order corrections concerning two kinds of observables: (1) QCD corrections for the di-Higgs production to second order, and (2) mixed QCD-QED corrections to Higgs production at second order. For both these processes, the dominant gluon contributions are known to unprecedented accuracy, and hence our motive is to capture the corrections arising from the sub-dominant bottom-quark annihilation channel. Computing di-Higgs production provides valuable information on the trilinear self-coupling of Higgs boson and thereby on the shape of Higgs potential. The computation of QCD-QED corrections involves dealing with the interference effects of QCD and QED interactions. Using the exact NNLO result obtained from the fixed order computations, we investigate their ultraviolet and infrared structure. Numerical analysis on both these results at the LHC energy manifests the reduction in unphysical scales, hence confirming the reliability of our results.

In the second half of the thesis, we address in detail the higher order QCD corrections at the threshold approximation. We present a systematic framework for studying the corrections arising from the threshold logarithms – also known as soft-virtual corrections –, in particular, to the differential rapidity distribution for producing arbitrary colorless final states. We also discuss a systematic way of resumming threshold logarithms to all orders

in double Mellin space. Resummation is required due to certain large logarithms at the threshold limit, which may question the reliability of perturbative corrections.

While the singular structure of threshold logarithms dominate, the sub-dominant next-to-threshold corrections are also vital for any precision studies as they give rise to numerically sizeable contributions. This topic is discussed in the last part of the thesis in great detail. These sub-leading logarithms also spoil the reliability of the perturbation series due to its significant contributions at every order. The canonical resolution through resummation for the next to SV terms is unfortunately hard to achieve. Nevertheless, we propose a framework for the same, limiting only to the diagonal partonic channels. We conclude by noting that the NSV logarithms demonstrates a rich perturbative structure that needs to be explored further.

Synopsis

The Standard Model (SM) of elementary particle physics is, perhaps, the pinnacle of human intellectual achievement (to date). It endured all the experimental challenges so far, and its predictions are incredibly consistent with the measurements. Among its notable successes are the observations of W and Z boson in 1983 at CERN, the discovery of top quark in 1995 at Fermi lab, and the recent breakthrough discovery of Higgs boson in 2012 at CERN's Large Hadron Collider (LHC). With its vast predictive successes, the Standard Model is the closest we have for the complete description of the universe at the fundamental level.

However, this is not the complete story: there is ample evidence that SM lacks explanations for yet mysteries in physics. For instance, there is no suitable candidate in SM to explain the dark matter content of the universe, it does not contain mass terms for the neutrinos to describe the neutrino oscillations, there are no explanations for the existence of baryon asymmetry. More fundamentally, it is yet unclear how to incorporate the standard model with the theory of gravity. These mysteries drive us to search for physics beyond the standard model (BSM) hidden in dark processes of the universe. A decade of experiments at LHC via Run-I and Run II phases hints that the effects of new physics might not likely manifest as a direct signal. Instead, they might appear as small systematic deviations from the SM behaviour. Hence, the new physics searches essentially depend on our ability to obtain high-precision theoretical predictions within the Standard Model along with high calibrated measurements at the colliders.

At the experimental end, this undertaking is facilitated by constantly upgrading detectors with large center-of-mass-energy and improved luminosity, thereby pushing down the statistical errors. The upcoming High-Luminosity LHC will further improve the precision, allowing for per cent-level measurements. This scenario calls for immense efforts from the theory side to produce (at least) the same level of precision as of data for a reliable comparison between them both, which is crucial for several essential physics goals of the LHC program.

In improving theoretical precision, higher order quantum chromodynamics (QCD) and electroweak (EW) corrections play an essential role. Over the past few decades, several attempts have been made to incorporate these higher order radiative corrections to observables at colliders. Often observables are expressed in terms of cross-sections, mainly by either differential cross sections in one or more variables or by integrating over the fiducial region of the detector surrounding the particle collision site. A successful methodology to evaluate the cross-section in SM or BSM is based on perturbation theory, under which any observable can be expanded in powers of coupling constants present in the underlying Lagrangian. For instance, for QCD, the corresponding expansion parameter is the strong coupling constant α_s , and their perturbative corrections take the form:

$$\sigma = \sigma^{(0)} + \alpha_s \sigma^{(1)} + \alpha_s^2 \sigma^{(2)} + \dots \quad (1)$$

Here, the first term is leading order (LO) or Born cross-section, second is called next-to-LO (NLO) corrections to Born cross-section and so on so forth. Each new term in the expansion (1.1) put forth new QCD interactions in the form of closed loops or radiations of partons both suppressed by factors of α_s . Despite this suppression, these higher order radiative corrections are crucial for reaching the required precision as that of experiments.

Achieving a full QCD correction to any order is not easy, and with increasing perturbative order, the complexity rises substantially. The non-Abelian nature of the theory and relatively large coupling entails the inclusion of a plethora of sub-processes in the higher

orders, making the task non-trivial. Nevertheless, the tremendous efforts in these directions in the past few decades lead to remarkable achievements. Now we have advanced techniques for the automation of NLO computations, and we are in good shape with next-to-NLO (NNLO). Moreover, we achieved an incredible precision of next-to-next-to-NLO (N³LO) for many important $2 \rightarrow 1$ processes at LHC.

However, with the increase of loops and legs, the complexity proliferates, making the exact computation highly challenging. In this scenario, in the absence of exact fixed order results, one could attempt various methods to capture the dominant contributions to a physical observable by evaluating the quantity in certain limits. In general, the perturbative corrections get contributions from hard, soft and virtual parts corresponding to those arising from energetic, soft and virtual gluons, respectively. For a heavy invariant mass production at the hadron colliders, generically, the dominant contributions originate from the soft regions, and hence these corrections are numerically significant at LHC. Besides, the momenta of all the real emission diagrams in the soft region are assumed to be infinitesimally small, leading to an all order exponentiation of this contribution. Hence, capturing these corrections are crucial for theoretical understanding as well. We call these corrections together with the virtual corrections, in general, soft-virtual (SV) corrections.

This thesis concerns the computations of higher order QCD corrections to inclusive and differential observables for various scattering processes at the colliders. Besides, it also addresses mixed QCD-QED corrections to the inclusive cross-section by considering a specific process. For convenience, the topic is divided into two parts. The first part addresses fixed-order computations, which capture the complete behaviour of a given quantity at a fixed order in coupling constant. Whereas, in the second part, we discuss the soft-virtual approximation for various Sudakov-type processes, by addressing not only the correction but also the question of resummation, which is a necessary ingredient to obtain reliable theoretical predictions at the soft limit. In addition to the leading term in SV corrections, we focus on the structure of sub-leading terms as well. Perturbative corrections

concerning both SV and NSV contributions are called next to SV (NSV) corrections. In subsequent sections, we address the above topics with main focus on the corrections to Higgs production through gluon fusion and/or bottom quark annihilation channel.

Fixed order approach

In this section, we deal with the fixed order calculations till the second order in coupling constant and is comprises of two subsections. In the first, we address complete fixed order corrections to an inclusive reaction associated with Higgs production at LHC. Whereas, in the second part, we discuss a comparative study between QCD, mixed QCD-QED and pure QED at the NNLO.

Di-Higgs production from bottom quark annihilation at NNLO

In all measurements explored so far at LHC, the rates and differential measurements are remarkably consistent with the SM predictions. One of the significant challenges in next LHC phase is constraining Higgs trilinear and quartic self-couplings. The Higgs self-coupling is crucial to understand the Higgs field potential, thereby explaining the electroweak symmetry breaking mechanism. A useful avenue to investigate the trilinear coupling is the production of a pair of Higgs boson at hadron colliders.

Among various partonic channels that contribute to this process, gluon fusion is the dominant one and is well studied both in effective theory as well as in full-QCD. As the precision at the hadron collider improves, it is crucial to incorporate other sub-dominant channels as well into the production mechanism. In this work, we have considered one such channel, namely di-Higgs production in bottom quark annihilation, which is sensitive to the trilinear coupling. For this process, QCD corrections at NLO exist in the literature [1], and hence our aim is to compute the corrections to the inclusive cross-section at

NNLO accuracy.

There are mainly two classes of diagrams that contribute at NNLO, both in virtual and real emission sub-processes. One category is the vertex type diagrams that belongs to class-A. The latter one, we call class-B, are the t- and u-channel diagrams. The loop corrections to class-A are known in the literature till the third order [2]. For class-B diagrams, we produce the virtual corrections at NNLO using in-house routines based on FORM and Mathematica packages. To check the consistency of these corrections, we compared them with the well-known universal structure of two-loop infrared poles as predicted by Catani [3].

Further, using these two-loop results at hand, we have performed the complete NNLO corrections to the inclusive cross-section for the case of class-A diagrams. For class-B diagrams, since the full computation is difficult to attain at present, we compute them at the SV approximation. To obtain the former contributions, we suitably factorized the scattering amplitudes and the phase space and used the available single Higgs production cross-section. The latter one is highly non-trivial, nevertheless, considering the universal nature of soft and collinear components, we obtain the SV contributions till NNLO. Further, we analyze these results numerically at LHC energy in order to estimate their size, which demonstrates that the inclusion of higher-order terms in the perturbative expansion reduces the dependence of unphysical scales in the problem, thereby making the predictions more reliable.

Mixed QCD-QED corrections to $b\bar{b} \rightarrow H$ at NNLO

The efforts to compute the observables related to Higgs production have been going on for a while as those are very sensitive to high scale physics. Since the dominant contribution, which is the gluon fusion channel, is known to unprecedented accuracy, the inclusion of corrections originating from subdominant channels is essential for any consistent study.

One such subdominant channel is the Higgs production from bottom quark annihilation. State-of-the-art for this channel in QCD reached an incredible accuracy of N³LO [4]. These QCD corrections are of the same order as that mixed QCD-EW predictions, despite the smallness of EW coupling in SM. Current or future high-precision experimental measurements and high-luminosity LHC, thus, demands the inclusion of equally precise predictions in mixed QCD-EW theory.

In this context, we explore the possibility of including EW corrections to the aforementioned channel. Since the computation of full EW corrections is more involved, as a first step, we compute all the QED corrections up to second order in the coupling constant α_e , taking into account the non-factorizable or mixed QCD×QED effects through $\alpha_s\alpha_e$ corrections. The computation involves dealing with QED soft and collinear singularities resulting from photons and massless partons along with the corresponding QCD ones.

Understanding the structure of QED infrared (IR) singularities in the presence of QCD ones is a challenging task. We have systematically investigated both QCD and QED IR singularities up to second order in their couplings, taking into account the interference effects. We demonstrate that the IR singularities from QCD, QED and QCD×QED interactions factorize both at the loop corrections as well as at the cross-section level. Besides, by computing the real emission processes in the SV limit, we have studied the structure of the soft distribution function. Using the universal IR structure of the observable, we have determined the mass anomalous dimension of the bottom quark and hence the renormalization constant for the bottom Yukawa. We also discussed the relation between the results from pure QED and pure QCD as well as between QCD × QED through a set of rules known as Abelianization. Using complete NNLO results from QCD, QED and QCD × QED, we performed a systematic study to understand their impact at the LHC energy. We find the corrections from mixed QCD × QED and QED are mild as expected, however these higher order corrections improve the reliability of the predictions.

Resummation at threshold and beyond

While the fixed order calculations are successful for many observables, they are reliable only if the perturbative behaviour of the series is retained. This criteria fails near kinematic threshold due to certain logarithmic enhancements which, hence, has to be resummed to all orders in coupling constant to obtain a reliable approximation. Needless to say, inclusion of such higher order QCD effects not only improves the accuracy of predictions but also reduces the unphysical scale dependence significantly. Moreover, those terms at the kinematic threshold, namely soft-virtual corrections, are often the dominant contributions to the inclusive cross sections, thus computing them in the absence of full NNLO or next to NNLO corrections, is essential in the precision studies.

In this section we focus on the study of SV corrections for inclusive as well as differential observables associated with the Higgs production. This section mainly comprises of two parts. At first, we discuss the SV computations at the threshold addressing differential rapidity distributions. And in the later part, we extend this studies to beyond threshold to obtain so called next-to-SV corrections.

Rapidity resummation for a generic n -colorless final states

Despite its high importance, the differential rapidity distribution and its radiative corrections are computed only for a limited number of scattering processes, unlike the inclusive ones. This section concerns the differential cross-section with respect to the rapidity variable, in particular, we address the question of computing the higher order QCD corrections to this observable for any generic process at a hadron collider with all the final state particles as colorless.

A formalism to incorporate the soft-gluon contribution to the rapidity distribution for the production of a colorless final state in hadron collider is known in the literature [5]. In

this work, we extended that formalism to the case of any number of final state colorless particles. This formalism is based on QCD factorization, which dictates that the soft part of the real emission diagrams factorizes from the hard contribution and renormalization group (RG) invariance.

For the production of an arbitrary number of colorless particles in the hadronic collision, the soft part remains identical to the case of the Sudakov type process since the real emission can only occur from the initial state partons. The main deviation from the Sudakov type formalism arises from the virtual corrections, where the kinematic dependence is much more involved. The rest of the formalism relies essentially on the collinear factorization, the renormalization group invariance, universal IR structure of the scattering amplitudes, and the process independence of the soft-collinear distributions. Besides this, we also use an additional fact that the N^{th} Mellin moment of the differential distribution has a relation with its inclusive counterpart in the large N -limit. The mere use of this fact enables us to get an all order relation between the soft-collinear distribution of inclusive cross-section and that of rapidity. Hence from the given quantity in the inclusive part, we can determine it for rapidity, thereby avoiding the explicit computation of the real emission processes for rapidity distribution.

In this work, we presented a general structure for the SV differential rapidity distribution up to fourth order in the strong coupling constant and the resummed predictions until the third leading logarithms in QCD. These results can be expressed in terms of universal anomalous dimensions along with the process-dependent virtual matrix elements. The former, which comprises of process independent finite segments of soft-collinear distribution and the mass factorized kernels, remains unaltered irrespective of the number of colorless particles in the final states. Furthermore, the soft-collinear distributions for the quark and gluon initiated processes are found to be related to each other through simple quadratic Casimir scaling, known as the maximally non-Abelian property. This is explicitly verified up to $N^3\text{LO}$. In summary, to obtain the fixed order and resummed pre-

diction for the differential rapidity distributions of a generic n -colorless final states, one merely requires the form factor corresponding to the hard process under study provided the soft-collinear distribution for Sudakov type process is known.

NSV corrections and Resummation beyond threshold

In this subsection, we focus on the computation of SV+NSV contributions for certain Sudakov type processes, such as production of a pair of leptons in the Drell-Yan process and Higgs boson in gluon fusion and in bottom quark annihilation. Since the leading term at the SV limit, known as threshold corrections, are well established, in this work, our concern is to study the structure of the next term, which is next-to-SV contributions.

While SV contributions dominate, the next to SV contributions are also numerically sizeable, and hence computing them in the absence of complete result at a given order is essential in precision studies. Lot of progress [6–8] has been made in recent times leading to better understanding of NSV terms. In our work, using IR factorization and renormalization group invariance, we show that both SV and next-to-SV contributions satisfy Sudakov differential equation whose solution provides an all order perturbative result in strong coupling constant. Like SV, next-to-SV contributions also demonstrate IR structure in terms of certain IR anomalous dimensions. However, NSV terms depend, in addition, on certain process dependent functions. In z -space, we show that the next to SV contributions do exponentiate allowing us to predict the corresponding NSV logarithms to all orders. Further, we observe that the NSV part of the solution is invariant under gauge like transformations allowing us to construct class of solutions, all giving identical fixed order predictions for NSV terms of partonic coefficient functions.

The SV and NSV logarithms in the perturbative results, when convoluted with appropriate parton distribution functions to obtain hadronic cross-section, give huge contributions. The presence of these large corrections at every order may invalidate the predictions from

the truncated perturbative series. For the leading SV corrections, resolution to this problem is found by suitably reorganizing the perturbative series, which is widely known as threshold resummation [9, 10]. Whereas, for the subleading terms, a canonical resolution through resummation is unfortunately hard to achieve. In this work, along with understanding the role of NSV terms, we attempt to develop a resummation formalism for inclusive cross-sections, constraining only to the diagonal channels. We derived an integral representation in the z -space for the partonic coefficient function at the exponent level which can be used to study these threshold logarithms in Mellin N -space. Unlike the SV part of the resummed result, the resummation coefficients for NSV terms are found to be controlled not only by process independent anomalous dimensions but also by process dependent coefficients. Indeed, these observations might shed light to many future attempts to understand the nature of NSV logarithms and their phenomenological importance to inclusive observables.

List of Figures

3.1	<i>LO contributions to Higgs boson pair production from gluon fusion channel. . .</i>	61
3.2	<i>Illustration of Class-A diagrams; Born, one and two-loop examples.</i>	65
3.3	<i>Illustration of Class-B diagrams; Born, one and two-loop examples.</i>	65
3.4	<i>Illustration of special set of Class-B diagrams, the singlet contributions.</i>	65
3.5	<i>The total cross section for di-Higgs production in $b\bar{b}$ annihilation at various order in a_s as a function of (μ_R^2/μ_0^2) on left panel with $\mu_F = \mu_0$ and as a function of (μ_F^2/μ_0^2) on right panel with $\mu_R = \mu_0$ with central scale $\mu_0 = 2m_h$ and $\sqrt{s} = 14$ TeV.</i>	86
3.6	<i>The total cross section for di-Higgs production in $b\bar{b}$ annihilation at various order in a_s as a function of the mass scale μ with $(\mu_F = \mu_R = \mu)$ for $\sqrt{s} = 14$ TeV.</i>	87
4.1	<i>Mixed QCD-QED contributions at NNLO. From left the sample diagrams of (1) double virtual, (2) real virtual and (3) double real respectively have shown. Here the wavy line indicates the photon, curly ones the gluon and the dashed line the Higgs boson.</i>	96
4.2	<i>The total cross section at various perturbative orders at energy scales varying from 6 to 22 TeV at LHC. The index ‘ij’ indicates that QCD at ‘i’-th order and QED at ‘j’-th order in perturbative theory are included.</i>	119

4.3	<i>The renormalization scale variation of the total cross section at various perturbative orders in QCD.</i>	121
4.4	<i>The factorization scale variation of the total cross section at various perturbative orders in QCD.</i>	121
4.5	<i>pdf uncertainties.</i>	123

List of Tables

3.1	<i>Inclusive total cross section for the di-Higgs production in dominant gluon fusion chennale and sub-dominant bottom quark annihialtion channel for $\mu_R = \mu_F = m_h/2$.</i>	86
3.2	<i>7-point scale variation for central scale at $m_h = 125\text{GeV}$, $\kappa = 1$</i>	88
3.3	<i>7-point scale variation for central scale at $m_h = 125\text{GeV}$, $\kappa = 2$</i>	89
3.4	<i>%-scale uncertainty at LO, NLO and NNLO</i>	89
4.1	<i>Individual contributions in (pb) to various perturbative orders at $\sqrt{S}=14\text{ TeV}$.</i> .	120
4.2	<i>Individual contributions in (pb) to various perturbative orders at $\sqrt{S}=13\text{ TeV}$.</i> .	120
4.3	<i>7-point scale variation at $\sqrt{S}=13\text{ TeV}$.</i>	122
4.4	<i>Result using different pdfs at $\sqrt{S}=14\text{ TeV}$.</i>	122
4.5	<i>Result using different pdfs at $\sqrt{S}=13\text{ TeV}$.</i>	122
6.1	<i>Towers of Distributions ($\mathcal{D}_i \equiv \mathcal{D}_i(z)$) and NSV logarithms ($L_z^i \equiv \ln^i(1-z)$) that can be predicted for Δ_I using Eq.(6.9). Here $\Psi^{l,(i)}$ and $\Delta_I^{(i)}$ denotes Ψ^l and Δ_I at order a_s^i respectively.</i>	180

6.2	<i>Comparison of $\ln^3(1-z)$ coefficients at the third order against exact results. The left column stands for the exact results and the right column gives the respective contributions when Ψ^I is taken till two loop.</i>	181
6.3	<i>The all order predictions for $1/N$ coefficients of Δ_N^I for a given set of resummation coefficients $\{\bar{g}_{0,i}^I, g_i^I(\omega), \bar{g}_i^I(\omega), h_i^I(\omega)\}$ at a given order. Here $L_N^i = \frac{1}{N} \ln^i(N)$</i>	195
6.4	<i>Values of SV and SV+NSV resummed cross section in 10^{-5} pb/GeV at second logarithmic accuracy in comparison to the fixed order results at different central scales</i>	197
6.5	<i>Comparison of SV and SV+NSV resummed cross section in 10^{-5} pb/GeV for $q\bar{q}$-channel at different central scales.</i>	198

1

Introduction

The richness of diverse phenomena in our universe stems from the physical principles that act at the level of *elementary particles*. Interaction of these particles constitutes the atoms and molecules that define the objects in our everyday world. Search for these particles, deciphering how they interact and what are their properties are centuries-long. The notion of elementary particles has progressed through histories, from ‘*the ancient five*’ to the concept of electrons, protons and neutrons. In the recent past, the protons and neutrons are also found *divisible* in terms of entities called *quarks*. Today, with our current knowledge, we sum up the fundamental constituents of nature as the matter particles – composed of *quarks* and *leptons* – and force carrying particles – known as *bosons*. It is these quarks, leptons and bosons, when cobbled together, account for all the complexity and beauty of our *visible* world at the sub-atomic scale.

The theory that best describes (*so far*) the behaviour of these elementary particles and *almost* all their interactions is called the Standard Model (SM) of particle physics. The development to its current shape took several decades, driven by the collaborative efforts of many brilliant minds around the world. Since its formulation, the SM predictions have been scrutinized and verified through a series of discoveries and experimentation. Among its significant successes are the observations of W and Z boson in 1983 at CERN, the discovery of top quark in 1995 at Fermilab and the recent breakthrough discovery of Higgs boson in 2012 at CERN’s Large Hadron Collider (LHC), which marks the inventory of last, missing particle of SM.

The SM relies on the mathematical framework of Quantum Field theory (QFT), in which particles are described in terms of a dynamical field that pervades space-time. The dynamics of this field are controlled by a Lagrangian constructed from underlying symmetries of the system. These symmetries are primarily classified as global and local or gauge symmetries that enforce the physical properties to be invariant under certain transformations. The global symmetries are associated with properties of the particle and are inherent to the system as a whole. On the other hand, the local gauge symmetry is an internal symmetry related to particle interactions. The modern version of SM relies on the local $SU(3)_C \times SU(2)_L \times U(1)_Y$ gauge symmetry: each of them manifestly gives rise to a fundamental interaction. The $SU(3)_C$ describes the theory of strong interactions – Quantum Chromodynamics (QCD) – with the conserved color charge. Whereas $SU(2)_L$ describes the weak isospin interaction acting only between left-handed fermions, and $U(1)_Y$ is characterized by electromagnetic interactions. The weak and electromagnetic interactions are partly unified in spontaneously broken electroweak (EW) interactions, described by $SU(2)_L \times U(1)_Y$. Each of these interactions is mediated by gauge bosons, which are *gluons* for strong force and *photons*, *W-* and *Z- bosons* for EW interactions.

Three different families of elementary particles characterize the modern SM. The first family consists of matter particles – quarks and leptons of 6 each and comes with half-spin – called *fermions* and are arising from the quantization of fermion fields. The fermions appear in three *generations*, which are identical in every attributes except in their masses. The first generation is responsible for all the stable matter in the universe, while the second and third are less stable heavier particles. The second family of elementary particles are the gauge bosons – quanta of bosonic fields – which are carriers of strong and electroweak interactions. In addition to these gauge bosons, there is a third boson, known as *Higgs boson*, arising from the excitations of *Higgs field*, which represent the third family and the only *known* single scalar particle of SM. The Higgs field is brought into the SM to explain the spontaneous breaking of electroweak symmetry. Unlike the predictions from the gauge symmetries, which enforce the particles to be massless, the

W^- and Z - bosons are found to be massive in reality. This discrepancy is explained through *Brout-Englert-Higgs-Kibble mechanism* [11–15] which implements *spontaneous breaking of electroweak symmetry* to yield mass for these SM particles. This mechanism, however, additionally predicts the existence of the Higgs field – as what we call it today. Although originally conceived to explain the origin of W and Z boson masses, the BEH mechanism later extended to account for the mass of any sub-atomic particles. Particles that interact with the Higgs field acquire masses, and the strength of its coupling with Higgs determines how massive the particle is. Those particles which do not interact with the Higgs field – photons, gluons and possibly neutrinos – remains massless. Built on spontaneously broken electroweak theory with the unbroken strong interaction and incorporating the Higgs mechanism, the SM completely account for the physical realities at the sub-atomic level.

All those achievements obtain for the SM, however, do not stop the need for further exploration. Despite its spectacular success, the SM in its current shape leaves many observed phenomena unexplained. Presently the theory incorporates three out of fundamental forces, while the fourth force and the familiar one in our everyday lives, gravity, as described by the general theory of relativity, is not part of the SM yet. Further, the model fails to explain the existence of neutrino masses and their hierarchy and the origin of matter-antimatter asymmetry in the universe. Also, it does not include a suitable candidate to explain the nature of dark matter and the dark energy content of the universe. These mysteries motivate us to keep searching for physics beyond the standard model (BSM) hidden in the dark recesses of the universe. However, neither any experimental hints exist for the origin of these phenomena *yet*, nor we have any precise energy scale or coupling strength for new physics to explain them. In parallel, many questions remain unanswered about the origin of the Higgs boson: whether it is an elementary particle or a composite state of confined particles, how does its mass generate, or what is the mechanism behind its self-interactions.

To address these questions requires precision measurements of Higgs boson properties and EW interactions above the weak scale, for which the exclusive tools are the high energy colliders. In the last fifty years, we have received an enormous wealth of information from experiments at particle colliders. From CERN's Large Hadron Collider (LHC), which is the largest among all the colliders till today, around fifteen million billion proton-proton collisions are already taken place in a decade. The experiments at LHC via Run-I and Run II phase hint that the new physics effects probably do not appear as clear resonance signals but as tiny systematic deviations from the SM predictions. Hence, the searches for the new physics essentially depend on our ability to obtain high-precision theoretical predictions within the Standard Model combined with the high calibrated measurements at the colliders.

At the experimental end, this undertaking is facilitated by continuously upgrading the detectors with improved collision energy and luminosity. Through LHC histories, the collision energy has improved from 7 to 13 TeV, which possibly will increase to 14 TeV in the next run. The upcoming High-Luminosity LHC will further enhance the precision, allowing for per cent-level estimations, hence providing better chances to track rare phenomena and improve the statistically marginal measurements. This scenario calls for immense efforts from the theory side to produce (at least) the same level of precision as data for a reliable comparison between them both, which is crucial for several essential physics goals of the LHC program.

In improving theoretical precision, higher order QCD and EW corrections play an essential role. Over the past few decades, several attempts have been made to incorporate these higher order radiative corrections into the observables at colliders. Often observables are expressed in terms of *cross sections*, mainly by either differential cross sections in one or more variables or by integrating over the fiducial region of the detector surrounding the particle collision site. A well-employed technique to perform the cross section in SM or BSM is based on perturbation theory; under this prescription, an observable is expanded

in powers of coupling constants present in the underlying Lagrangian. For QCD, the corresponding expansion parameter is the strong coupling constant α_s , whose series plays a dominant role for a large variety of processes at the typical LHC energy scales. For a given process, perturbative QCD (pQCD) corrections take the form:

$$\sigma = \sigma^{(0)} + \alpha_s \sigma^{(1)} + \alpha_s^2 \sigma^{(2)} + \dots \quad (1.1)$$

Here, the first term is leading order (LO) or Born cross section, the second is called next-to-LO (NLO) corrections to Born cross section and so on so forth. Each new term in the expansion (1.1) put forth new QCD interactions in the form of closed loops or radiations of partons both suppressed by factors of α_s . Despite this suppression, these higher order radiative corrections are crucial for achieving the required precision as that of experiments.

Achieving a full QCD correction to any order is not easy, and with increasing perturbative order, the complexity rises substantially. The non-Abelian nature of the theory and relatively large coupling entails the inclusion of a plethora of sub-processes in higher orders, making the task non-trivial. Nevertheless, tremendous efforts in these directions in the past few decades lead to remarkable achievements. Now we have advanced techniques for automating NLO computations, and we are in (almost) good shape with next-to-NLO (NNLO).

However, with the increase in loops and legs, the complexity proliferates, making the exact computation highly challenging. Considering N³LO, the exact computation is available only for the simplest ($2 \rightarrow 1$) processes [4, 16, 17]. In this scenario, in the absence of exact fixed order results, one could attempt different methods to capture the dominant contributions to a physical observable by evaluating the quantity in certain limits. In general, the perturbative corrections get contributions from hard, soft and virtual parts corresponding to those arising from energetic, soft and virtual gluons, respectively. For a heavy invariant mass production at the hadron colliders, such as the Higgs or Z-boson

productions, the dominant contributions originate from the soft regions. Hence, these corrections are numerically significant at LHC. Besides, (almost) zero momenta of real emissions at soft region lead to their all order exponentiation. Hence, capturing these corrections are crucial for theoretical understanding as well. These contributions combined with the pure-virtual corrections, in general, known as soft-virtual (SV) or threshold corrections. The term *threshold* is because these corrections are the ones contributing at the extreme production threshold. It is also known as *soft* due to the soft emissions in this kinematical region. These corrections play a crucial role in the absence of exact predictions at a certain order in the coupling constant.

The core part of this thesis deals with computing higher order QCD and QED corrections for the processes involving Higgs boson in the final states and the Drell-Yan (DY) process by employing the perturbative theory within the SM. The thesis comprises three parts:

1. The fixed order approach – we compute the complete behaviour of inclusive observables at a fixed order in the coupling constant present in the underlying Lagrangian.
2. The threshold approximation – by addressing the QCD correction that appears at the extreme production threshold, we study the general infrared (IR) and ultraviolet (UV) structure of scattering cross sections, considering a differential observable. Following these studies, we are able to develop a framework for resumming the *leading power (LP)* large logarithms at the production threshold.
3. The next-to-threshold or next-to-SV (NSV) approximation – In the last chapter, we extend the study at threshold approximation by including sub-leading corrections that arise from the next to leading large logarithms, also known as *next to LP (NLP) logarithms*. By studying their UV and IR structure, we propose a framework for resumming these NLP logarithms.

Outline

The thesis comprises a selection of published works and preprints that provides a comprehensive picture of higher order computations of physical observables at LHC. A condensed outline of the thesis is as follows.

In chapter 2, we start with a brief overview of the basic principles of QCD and a discussion on methods to compute higher order corrections in perturbative QCD. We also review a framework to compute threshold corrections in great detail, which will play a notable role in our later results.

In chapter 3, we discuss the NNLO computation of di-Higgs productions in the bottom quark annihilation channel. This production channel is a valuable avenue to investigate the trilinear coupling and Higgs potential, which is one of the significant challenges in the next phase of LHC. At NNLO, two classes of diagrams contribute – vertex type diagrams and t - and u - channel ones. For the computations, we use in-house routines based on FORM and Mathematica packages. Since the complete result of t - and u - channels are challenging (at present), we compute them at the SV approximation. Numerical analysis at LHC energy illustrates the reliability of our predictions.

The state-of-the-art QCD corrections have reached such accuracy that requisites the inclusion of precise predictions of mixed QCD-EW theory. This possibility is explored in chapter 4 for the bottom quark induced Higgs boson productions. Since the computation of complete EW corrections is more involved, as a first step, we compute all the QED corrections up to second order in the coupling constant α_e , taking into account the non-factorizable or mixed QCD-QED effects through $\alpha_s\alpha_e$ corrections. The computation involves dealing with QED soft and collinear singularities resulting from photons and massless partons, in addition to the QCD ones. We systematically investigate the structure of QCD and QED IR singularities up to second order in their couplings, taking into account the interference effects. In the process, we obtain the mass anomalous dimension

and renormalization constant of Yukawa coupling as a bonus point. We also discuss a set of rules which connects the QCD, QED and mixed QCD-QED results.

In chapter 5, we discuss the threshold corrections for a differential rapidity observable associated with the Higgs production. In particular, we address the higher order QCD corrections to this observable for generic n -colorless final states. The formalism is based upon the collinear factorization of differential scattering and RG invariance. The soft part remains similar to Sudakov-type processes, while for the virtual corrections, the kinematic dependence is much more involved. In addition to the threshold rapidity corrections, we discuss a framework to resum the threshold logarithms in rapidity variables.

In the last chapter 6, our concern is to extend the threshold framework to include the next-to-threshold or next-to-SV corrections, which attracted considerable attention in recent time. While SV singular structure dominates, the next-to-SV ones are also large and produce numerically sizeable corrections. Hence computing them in the absence of complete result at a given order is essential in precision studies. In this context, we propose a framework with the logic of IR factorization and RG invariance. We show that similar to SV the next-to-SV logarithms also exhibit an all order perturbative structure. This idea enables us to propose a formalism to resum certain next-to-leading power logarithms, which is the first of the kind in literature beyond leading logs.

2 Review of perturbative QCD

To start with, let us review some basics of QCD. It is to be noted that this chapter is by no means intended for a complete review, rather a short introduction to fix the conventions and notations. For more details, the reader is referred to [18–21] and the standard texts.

2.1 Basics of QCD

Quantum Chromodynamics – or QCD – is the theory of quarks, gluons and their interactions. This field theory is a non-Abelian gauge theory based on the SU(3) gauge symmetry. It has a similar structure as QED – electromagnetic interaction – but with a subtle difference that the gauge boson – gluon – carries color charge. Hence in addition to the interaction with quarks, gluons interact among themselves too. Consequent to this fact comes the aspects of asymptotic freedom, which defines the success of QCD to describe the strong interaction. The critical implication of asymptotic freedom is that it explains the point-like behaviour of quark at short distances and offer a mechanism for the strong confining force at large distances. The short distance physics is the realm of perturbative QCD.

In the following, we briefly outline the QCD Lagrangian, followed by the aspects of asymptotic freedom and the running coupling constant. We also discuss parton model and how it modifies when the QCD radiative corrections are applied. In subsequent sections, we briefly address fixed order computation techniques and the threshold framework.

2.1.1 QCD Lagrangian

The perturbative analysis of any process in QFT requires the use of Feynman rules describing the interactions in theory, which can be derived from the underlying Lagrangian density. For an $SU(N_c)$ gauge group encapsulating the interaction of fermions with the non-Abelian gauge bosons, the Lagrangian density is given by:

$$\mathcal{L} = \mathcal{L}_{classical} + \mathcal{L}_{gauge-fixing} + \mathcal{L}_{ghost} \quad (2.1)$$

The classical Lagrangian takes the form:

$$\mathcal{L}_{classical} = -\frac{1}{4}\mathcal{G}_{\mu\nu}^a\mathcal{G}^{a,\mu\nu} + \sum_{f=1}^{n_f}\bar{\psi}_{\alpha,i}^f (i\gamma_{\alpha\beta}^{\mu}\mathcal{D}_{\mu,ij} - m_f\delta_{\alpha\beta}\delta_{ij})\psi_{\beta,j}^f \quad (2.2)$$

These terms represent the interaction of spin-1/2 quarks with mass m_f and massless spin-1 gluons. The gamma matrices satisfy the anti-commutation relation: $\{\gamma^{\mu}, \gamma^{\nu}\} = 2g^{\mu\nu}$. The field strength $\mathcal{G}_{\mu\nu}^a$ is derived from the gluon field G_{μ}^a

$$\mathcal{G}_{\mu\nu}^a = \partial^{\mu}G_{\nu}^a - \partial^{\nu}G_{\mu}^a + \hat{g}_s f^{abc}G_{\mu}^b G_{\nu}^c \quad (2.3)$$

and $\psi_{\alpha,i}^f$ is the fermionic quark field. The third *non-Abelian* term in Eq.(2.3) distinguishes QCD from QED, giving rise to triplet and quartic gluon self-interactions and ultimately to the property of asymptotic freedom. The coupling constant \hat{g}_s determines the strength of interaction between quarks and gluons, and f^{abc} is the structure constants of the $SU(N_c)$ group. The indices in Eq.(2.2) dictates :

$$\begin{aligned} a, b, \dots : & \quad \text{color indices in the adjoint representation} \Rightarrow [1, \dots, N_c^2 - 1], \\ i, j, \dots : & \quad \text{color indices in the fundamental representation} \Rightarrow [1, \dots, N_c], \\ \alpha, \beta, \dots : & \quad \text{Dirac spinor indices} \Rightarrow [1, \dots, d], \\ \mu, \nu, \dots : & \quad \text{Lorentz indices} \Rightarrow [1, \dots, d]. \end{aligned} \quad (2.4)$$

where d is the space-time dimensions. The covariant derivative \mathcal{D}_μ^{ij} acting on the adjoint and fundamental representations takes the form

$$\begin{aligned}\mathcal{D}_{\mu,ab} &= \delta_{ab}\partial_\mu - \hat{g}_s f^{abc} G_\mu^c \\ \mathcal{D}_{\mu,ij} &= \delta_{ij}\partial_\mu - i\hat{g}_s (T^a)_{ij} G_\mu^a\end{aligned}\tag{2.5}$$

respectively. The T^a are the generators of the fundamental representation of $SU(N_c)$, which are related to the structure function through

$$[T^a, T^b] = if^{abc}T^c.\tag{2.6}$$

A representation for T^a is provided by the Gell-Mann matrices, which are traceless and Hermitian and are normalized with

$$\text{tr } T^a T^b = T_F \delta^{ab} \text{ with } T_F = 1/2.\tag{2.7}$$

They also satisfy the completeness relation given by:

$$\sum_a T_{ij}^a T^{akl} = \frac{1}{2} \left(\delta_{il}\delta_{kj} - \frac{1}{N_c} \delta_{ij}\delta_{kl} \right)\tag{2.8}$$

With the above choices, the color matrices obey the following relations, which are often useful in simplifying the color algebra :

$$\begin{aligned}\sum_a (T^a T^a)_{ij} &= C_F \delta_{ij} \\ f^{abc} f^{abd} &= C_A \delta^{cd}\end{aligned}\tag{2.9}$$

where $C_F = \frac{N_c^2-1}{2N_c}$ and $C_A = N_c$ are the quadratic Casimirs of the $SU(N_c)$ group in the fundamental and adjoint representation respectively. For QCD, the $SU(N_c)$ group index $N_c = 3$ and quark flavor $n_f = 6$.

The second term in the Lagrangian in Eq.(2.1) is the gauge fixing term, which is required to perform the perturbation theory consistently. This term originates because, while quantizing, the gluon propagator cannot take an unambiguous form without choosing a gauge. The reason behind this is the presence of gauge degrees of freedom inherent in the classical Lagrangian. The choice of gauge is:

$$\mathcal{L} = -\frac{1}{2\xi} (\partial^\mu G_\mu^a)^2, \quad (2.10)$$

which fixes the gauge in a covariant way with an arbitrary gauge parameter ξ . A typical choice of setting $\xi = 1$ in Eq.(2.10) gives Feynman gauge. In this thesis, we use the Feynman gauge throughout unless we specify otherwise. However, we emphasize that the choice of gauge does not alter the physical results. The immediate consequence of gauge fixing in QCD is that it generates new particles called Faddeev-Popov ghosts – spin-0 particles but having Fermi statistics. The Lagrangian for the ghost field is given by

$$\mathcal{L}_{ghost} = (\partial^\mu \chi^{a*}) \mathcal{D}_{\mu,ab} \chi^b \quad (2.11)$$

where $\mathcal{D}_{\mu,ab}$ is defined in Eq.(2.5). The ghost field χ^a cancel the unphysical degrees of freedom, which would otherwise propagate in covariant gauges. These particles never appear as external physical states but in closed loops interacting with gluons. Now we have the full Lagrangian as given in Eq.(2.1), which can be used to derive all the Feynman rules. See Appendix-A for the complete list of QCD Feynman rules.

There are essentially two first principle approaches to solving the QCD Lagrangian – lattice QCD and perturbative QCD.¹ The complete approach is lattice QCD, where one discretizes the space-time and consider the values of quark and gluon fields at all the edges of the resulting 4-dimensional lattice. The method has been successfully used in a range

¹There are, in addition, effective field theory methods where one can solve the specific limits of QCD with certain inputs taken from lattice or perturbative QCD. Also, there are yet another set of techniques that makes use of *AdS/CFT* correspondence to relate the QCD-like models at the strong coupling to weakly coupled gravitational models

of contexts such as CKM matrix; however, it is implausible to use them for computations of LHC scattering processes with the current knowledge along this direction.

The method that is widely used for collider physics is the perturbative QCD approach, which is based on an order-by-order expansion in the strong coupling constant $\alpha_s = \frac{\hat{g}_s^2}{4\pi} \ll$

1. For a given observable σ , the expansion looks :

$$\sigma = \sigma^0 + \alpha_s \sigma_1 + \alpha_s^2 \sigma_2 + \dots, \quad (2.12)$$

where computing lower-order terms of the series are sufficient, with an understanding that the rest are negligibly small. The coefficients σ_i is computed using Feynman diagrammatic techniques. In this thesis, we deal with the perturbative applications of QCD.

2.1.2 Asymptotic freedom and running coupling

As mentioned earlier, QCD exhibit asymptotic freedom and confinement. Due to the confinement, the quarks and gluons are strongly interacting at low energy, while at high energy, they are asymptotically free and do not interact. Hence, the coupling constant decreases for high energies, enabling the perturbative expansion around the free field theory. The expansion parameter for QCD is the strong coupling constant, α_s , and the series takes the form given in Eq.(2.12). For computations, the standard methodology is to use the Feynman diagrams that contribute to every order in the coupling constant. This comprises loop and phase space integrals at higher orders, which involves divergences beyond the leading order terms. The origin of these divergences can be traced from mainly two categories. The first one is when the loop momenta approach infinity – so-called *ultraviolet* (UV) divergences – and the other category arises when the emissions in the scattering process go soft or collinear to external partons – commonly called *infrared* (IR) divergences. In this section, we focus on UV divergences. Both of these divergences can be regularized using *dimensional regularization* [22], in which the dimensionality of

space-time is analytically continued from 4 to $d = 4 + \epsilon$. Hence divergences will show up poles in ϵ .

The UV divergences can be removed by performing a suitable redefinition of the coupling constants and fields – the process is known as *renormalization*. This redefinition involves absorbing the UV divergences into a few parameters – known as renormalization constant –, and each consists of introducing some scale parameter that is not intrinsic to the theory but tells how we did the renormalization. The new scale is called the renormalization scale. It is to be noted that this scale is an unphysical one, and our physics is independent of them. We denote the unrenormalized or bare physical quantity with a *hat* on the notation and the renormalized ones without the *hat*. Renormalization of a given bare quantity \hat{F} can be represented in general as:

$$\hat{F} = Z_F(\mu_R) F(\mu_R). \quad (2.13)$$

Here the Z_F is the renormalization constant which absorbs all the UV divergences of \hat{F} , and the quantity F is UV finite². For the renormalization procedure, we use minimal subtraction ($\overline{\text{MS}}$) scheme.

Running of QCD coupling

As we have seen, the theory must be renormalized, however, the physics is invariant to the renormalization scale. Running coupling is a consequence of this renormalization group invariance. The fact that the physical quantity $\hat{a}_s \equiv \frac{\hat{g}_s}{4\pi}$ is independent of μ_R leading to the renormalization group (RG) equation :

$$\mu_R^2 \frac{da_s}{d\mu_R^2} = \beta(a_s(\mu_R^2)), \quad \beta(a_s(\mu_R^2)) = - \sum_{n=0}^{\infty} \beta_n a_s^{n+2}(\mu_R^2) \quad (2.14)$$

² The dependence on the μ_R -scale comes only through the presence of g_s

where the available β_i 's [23–30] are

$$\begin{aligned}
\beta_0 &= \frac{11}{3}C_A - \frac{2}{3}n_f, \\
\beta_1 &= \frac{34}{3}C_A^2 - 2n_f C_F - \frac{10}{3}n_f C_A, \\
\beta_2 &= \frac{2857}{54}C_A^3 - \frac{1415}{54}C_A^2 n_f + \frac{79}{54}C_A n_f^2 + \frac{11}{9}C_F n_f^2 - \frac{205}{18}C_F C_A n_f + C_F^2 n_f, \\
\beta_3 &= \left(\frac{17152}{243} + \frac{448}{9}\zeta_3\right)C_A C_F T_F^2 n_f^2 + \left(-\frac{4204}{27} + \frac{352}{9}\zeta_3\right)C_A C_F^2 T_F n_f \\
&\quad + \frac{424}{243}C_A T_F^3 n_f^3 + \left(\frac{7073}{243} - \frac{656}{9}\zeta_3\right)C_A^2 C_F T_F n_f + \left(\frac{7930}{81} + \frac{224}{9}\zeta_3\right)C_A^2 T_F^2 n_f^2 \\
&\quad + \frac{1232}{243}C_F T_F^3 n_f^3 + \left(-\frac{39143}{81} + \frac{136}{3}\zeta_3\right)C_A^3 T_F n_f + \left(\frac{150653}{486} - \frac{44}{9}\zeta_3\right)C_A^4 \\
&\quad + \left(\frac{1352}{27} - \frac{704}{9}\zeta_3\right)C_F^2 T_F^2 n_f^2 + 46 C_F^3 T_F n_f + \left(\frac{512}{9} - \frac{1664}{3}\zeta_3\right)n_f \frac{N_c(N_c^2 + 6)}{48} \\
&\quad + \left(-\frac{704}{9} + \frac{512}{3}\zeta_3\right)n_f^2 \frac{(N_c^4 - 6N_c^2 + 18)}{96N_c^2} + \left(-\frac{80}{9} + \frac{704}{3}\zeta_3\right)\frac{N_c^2(N_c^2 + 36)}{24} \quad (2.15)
\end{aligned}$$

where n_f being the number of light quark flavors and $T_F = 1/2$. Using only β_0 and ignoring the fact that the n_f depends on μ_R we get a simple solution

$$a_s(\mu_R^2) = \frac{a_s(\mu_0^2)}{1 + \beta_0 a_s(\mu_0^2) \ln \frac{\mu_R^2}{\mu_0^2}} = \frac{1}{\beta_0 \ln \frac{\mu_R^2}{\Lambda^2}}, \quad (2.16)$$

where μ_0 is a reference scale. In the second solution, we chose non-perturbative constant Λ as the reference scale. The negative sign in Eq.(2.14) is the origin of asymptotic freedom, which is, in fact, the consequence of the color charge of gluons. As far as the $n_f < 11C_A/2 \equiv 33/2$, the negative sign retains and consequently, the coupling becomes weaker with increasing scales. This essentially leads to a free theory with no interaction between quarks and gluons at high energy or short distances. Conversely, the perturbative coupling grows at low energies or long distance, causing the quarks and gluons to be tightly bound into hadrons. With the large coupling, the perturbative expansion gets unreliable. The scale at which it fails is known in the name of Λ or Λ_{QCD} , which is typically the order of some hundreds MeV, beyond which the realm of non-perturbative physics arises.

Quark masses

Let us conclude this section with a brief discussion on quark masses. The quark masses behave similarly to the gauge coupling itself. Running quark masses can be defined as

$$m(\mu_R^2) = m(\mu_0^2) \exp\left(-\int_{\mu_0}^{\mu_R} \frac{d\lambda}{\lambda} [1 + \gamma_m(a_s(\lambda))]\right) \quad (2.17)$$

Here $\gamma_m(a_s)$ is a perturbative quantity, similar to the $\beta(a_s)$. As μ_R increases, $g(\mu_R)$ decreases and hence $m(\mu_R)$ vanishes. Consequently, the perturbative theory becomes, effectively, a massless theory. From the QCD phenomenology, the light quarks – up, down, strange – can be taken effectively as massless theory, but for the case of heavy quarks – charm, bottom, top – the running mass should be taken into account.

2.1.3 Parton model and Collinear factorization theorem

By itself, asymptotic freedom is a striking result and beautifully explains the behavior of quark-gluon interactions. However, in nature, isolated quarks or gluons do not exist. Not the partons, but protons involves in high energy colliders, but whose interactions cannot be described by perturbative QCD (pQCD) methods. For studying these processes, in general, we adopt *Parton model*, which describe how a hadron interacts via its constituent partons.

The original parton model was proposed by Feynman, which relies on the basic assumption that the hadron interactions are due to the interaction of its constituents. Hence, the structure of the hadron may be described by an instantaneous distribution of partons. This model is proposed in *infinite momentum frame*, where each parton is assumed to carry a fraction of proton momentum, P . That is to say, the i^{th} parton gets the momenta $p_i = x_i P$ following a distribution $\hat{f}_i(x_i)$, where x_i is the fraction defined as $0 \leq x_i \leq 1$. The $\hat{f}_i(x_i)$ is generally called the *parton distribution functions* or in short pdf's. From this, the mo-

momentum sum rules are expected as:

$$\int_0^1 dx \sum_i x \hat{f}_i(x) = 1 \quad (2.18)$$

which is a consequence of the momentum conservation. Also, the proton flavor conservation says:

$$\int_0^1 dx (\hat{f}_u(x) - \hat{f}_{\bar{u}}(x)) = 2, \quad \int_0^1 dx (\hat{f}_d(x) - \hat{f}_{\bar{d}}(x)) = 1 \quad (2.19)$$

Based upon these assumptions, the hadronic cross section, σ , for a high energy process can be expressed in terms of the cross section for partons $\hat{\sigma}$ as:

$$\sigma_{h_1, h_2}(P_1, P_2) = \sum_{a, b} \int_0^1 dx_1 dx_2 \hat{f}_a(x_1) \hat{f}_b(x_2) \hat{\sigma}_{ab}(x_1 P_1, x_2 P_2). \quad (2.20)$$

Here, the partonic cross section is a perturbative quantity, while the pdf's $\hat{f}_i(x)$ are non-perturbative objects.

The above picture is a naive parton model description, which will not survive when QCD corrections are included. Accommodating radiative corrections modify the model to the so-called *improved parton model*, where the pdf's and the partonic cross section acquire a new energy scale dependence. To understand this, let us briefly look into the details of radiative corrections and the divergence structures.

Radiative corrections and factorization

In pQCD, the partonic cross section is expanded in terms of a_s :

$$\hat{\sigma}_{ij} = \sum_l a_s^l \hat{\sigma}_{ij}^{(l)}. \quad (2.21)$$

The coefficients $\hat{\sigma}_{ij}^{(l)}$ are calculated using Feynman diagrammatic approach. In general, these coefficients gets contributions from loop diagrams and real emissions for $l \geq 1$,

which give rise to UV and IR divergences. We have already discussed the origin of UV divergences and how to remove them using UV renormalization.

On the other hand, the IR divergences appear due to soft gluons and massless collinear partons in the loops. They respectively give rise to soft and collinear divergences. In the physical observables, the soft and the collinear divergences coming from virtual diagrams cancel against those resulting from the phase space integrals of the real emission processes. Due to the Kinoshita-Lee-Nauenberg (KLN) theorem [31, 32], the cancellation takes place order by order in perturbation theory. While the soft divergences cancel entirely, the collinear divergences resulting from initial massless states do not cancel at the sub-process level and must be treated separately, which is done using the technique called *mass factorization*. The logic is similar to the renormalization technique: to factor out these initial state collinear divergences in a process independent way and absorb them into the bare parton distribution functions. As in renormalization, this will introduce a new energy scale dependence called factorization scale μ_F . The resulting finite pdf is a measurable quantity. Schematically, we can express the redefined partonic cross section:

$$\hat{\sigma}_{ab}(x_1 P_1, x_2 P_2) = \sum_{c,d} \Gamma_{ac}^T(\mu_F^2) \Delta_{cd}(x_1 P_1, x_2 P_2, \mu_F^2) \Gamma_{db}(\mu_F^2). \quad (2.22)$$

The $\Delta_{ab}(\mu_F^2)$ is a finite quantity, called *partonic coefficient function* and the collinear singularities are encapsulated in $\Gamma(\mu_F^2)$, namely *mass factorization kernels* or Altarelli-Parisi (AP) [33] kernels. Absorbing them into bare pdf's gives the finite pdf:

$$f_i(x, \mu_F^2) = \sum_j \hat{\Gamma}_{ij}(\mu_F^2) f_j(x). \quad (2.23)$$

The resulting finite pdf is a measurable quantity and are universal, which means that it does not depend on the process under study.

Accommodating the radiative corrections and thereby factorization scale dependence in the (naive) parton model modify them to the so-called *improved parton model*. We sum-

marize the details of the improved parton model below.

Improved parton model

For a process:

$$h_1(P_1) + h_2(P_2) \rightarrow F(\{q_i\}) + X \quad (2.24)$$

where two hadrons h_i with momenta P_i , $i = 1, 2$ collide and produces the heavy final state F , the cross section takes the general form in the improved parton model in terms of finite quantities:

$$\sigma_{h_1, h_2}(P_1, P_2) = \sum_{a, b} \int dx_1 dx_2 f_a(x_1, \mu_F^2) f_b(x_2, \mu_F^2) \Delta_{ab}(x_1 P_1, x_2 P_2, \mu_F^2) + \mathcal{O}\left(\frac{\Lambda}{Q}\right). \quad (2.25)$$

The X denotes any final *inclusive* hadrons. In the following we summarize the recipe of improved parton model

- The incoming hadronic beam is equivalent to the incoherent sum of its constituent beams, with its longitudinal momentum distribution defined by the parton distribution functions.
- The short distance partonic cross section is a perturbative quantity:

$$\Delta_{ab}(x_1 P_1, x_2 P_2, \mu_F^2) = \sum_l^\infty a_s^l(\mu_R^2) \Delta_{ab}^{(l)}(x_1 P_1, x_2 P_2, \mu_F^2, \mu_R^2) \quad (2.26)$$

while the long distance pdf's belongs to non-perturbative regime. However, the pdf's are universal, by which we mean that they do not depends on the process of study.

- The evolution of the pdf's with the scale μ_F can be expressed in terms of Dokshitzer-

Gribov-Lipatov-Altarelli-Parisi (DGLAP) equation

$$\mu_F^2 \frac{\partial}{\mu_F^2} f_i(x, \mu_F^2) = \sum_j \int_x^1 \frac{dz}{z} P_{ij}(a_s(\mu_F^2), z) f_j\left(\frac{x}{z}, \mu_F^2\right). \quad (2.27)$$

Here, the P_{ij} are called *splitting functions*.

Together they are called the *collinear factorization theorem*. The factorization scale μ_F is an arbitrary scale whose dependence is compensated between the short and long distances. Note that we have now two unphysical energy scales in the problem – renormalization scale, μ_R , at which a_s is evaluated, and the factorization scale, μ_F , at which the collinear singularities factorize. Both these scales should have the same order, and it has to be chosen of the order of energy scale of the hard process to avoid large logarithms in the perturbative expansion.

Our *goal* is to improve the accuracy of short distance partonic cross sections by computing higher order radiative corrections, which is the topic of concern in this thesis. In the next section, we briefly discuss different approaches for performing the higher order corrections.

2.2 Fixed order computations in QCD

The primary approach to compute the higher order QCD effects is the fixed order expansion. This amounts to expanding the desired observable in powers of the strong coupling constant and then retaining only the first few orders. Being substantially small, each *next* term in the expansion gives minor corrections to the previous one and hence, at least from the naive comparison, the higher order corrections can be disregarded. In that case, the result with the first few orders can be an excellent approximation to the complete result; we call them *fixed order approximation*. Given that the perturbative expansion is well behaved, the fixed order approximation gets closer to the actual value by adding more terms

in the expansion.

Retaining the perturbative expansion of bare partonic cross section to n^{th} -order gives:

$$\hat{\sigma}_{ab}(x_1 P_1, x_2 P_2) = \sum_l^n a_s^l(\mu_R^2) \hat{\sigma}_{ab}^{(l)}(x_1 P_1, x_2 P_2, \mu_R^2) + \mathcal{O}(a_s^{n+1}) \quad (2.28)$$

Since $a_s < 1$, the contributions comes from $\mathcal{O}(a_s^{n+1})$ expected to be small and can be discarded, provided that they are not large enough to surpass the suppression from a_s^{n+1} . The first non-zero term in this expansion is called *leading order* (LO) or *Born approximation*, and the consequent terms refer to *next to LO* (NLO), *next to NLO* (NNLO) corrections and so on. In general, if the expansion is retained to k^{th} order, we call them N^kLO order corrections to the Born.

The leading order term in a perturbative expansion may vary from process to process. For instance, for the case gluon induced Higgs production cross section, the first non zero terms come at a_s^2 order while for the case of Higgs production from bottom quark annihilation, the leading term constitutes to $\mathcal{O}(a_s^0)$ term. Hence the most general perturbative expansion reads:

$$\hat{\sigma}_{ab}(x_1 P_1, x_2 P_2) = a_s^\lambda(\mu_R^2) \sum_{l=0}^n a_s^l(\mu_R^2) \hat{\sigma}_{ab}^{(l)}(x_1 P_1, x_2 P_2, \mu_R^2) + \mathcal{O}(a_s^{n+\lambda+1}) \quad (2.29)$$

where the λ is decided by the LO process. Beyond the LO, the contribution appears from virtual corrections and/or from real radiation corrections. These contributions give rise to loop as well as multi-particle phase space integrals. Looking into more details, consider a partonic sub-process:

$$a(p_1) + b(p_2) \rightarrow F(q) + \sum_{j=1}^m r_j(k_j). \quad (2.30)$$

where the collision of partons a and b produce the final state F along with m partons

through real radiation. The partonic cross section for this process has a general structure:

$$\hat{\sigma}_{ab} = \frac{\mathcal{F}_{ab}}{2\hat{s}} \int dPS_{1+m} |\mathcal{M}_{ab \rightarrow F}|^2. \quad (2.31)$$

Here the $\mathcal{M}_{ab \rightarrow F}$ is constructed from the Feynman diagrams contributing to $a + b \rightarrow F$ order by order in perturbation theory. The \mathcal{F}_{ab} refers to the numerical constant coming from the symmetry factor and/or color and spin averaging. The dPS_{1+m} represents the $(1 + m)$ -particle phase space measure defined by

$$\int dPS_{1+m} = \int d\phi(q) \left(\prod_{j=1}^m d\phi(k_j) \right) (2\pi)^d \delta^{(d)}(p_a + p_b - q - \sum_{j=1}^m k_j) \quad (2.32)$$

At LO, the contribution arises only from the born matrix square, $|\mathcal{M}_{ab \rightarrow F}^{(0)}|^2$, and from one particle phase space. Whereas at NLO, corrections appear from emission of an additional parton ($\hat{\sigma}_{ab}^R$) as well as from one-loop contributions ($\hat{\sigma}_{ab}^V$). This gives rise to :

$$\hat{\sigma}_{ab}^{(1)} = \frac{1}{2\hat{s}} \int dPS_1 \hat{\sigma}_{ab}^V + \int dPS_2 \hat{\sigma}_{ab}^R. \quad (2.33)$$

with

$$\hat{\sigma}_{ab}^V = 2 \operatorname{Re} \left(\mathcal{M}_{ab \rightarrow F}^{(0),\dagger} \mathcal{M}_{ab \rightarrow F}^{(1)} \right), \quad \hat{\sigma}_{ab}^R = |\mathcal{M}_{ab \rightarrow F+1}^{(0)}|^2 \quad (2.34)$$

At NNLO, the contributions are more involved:

$$\hat{\sigma}_{ab}^{(2)} = \frac{1}{2\hat{s}} \int dPS_1 \hat{\sigma}_{ab}^{VV} + \int dPS_2 \hat{\sigma}_{ab}^{RV} + \int dPS_3 \hat{\sigma}_{ab}^{RR}. \quad (2.35)$$

where:

- *double real* (RR) corrections: $\hat{\sigma}_{ab}^{RR} = |\mathcal{M}_{ab \rightarrow F+2}^{(0)}|^2$
- *real virtual* (RV) corrections: $\hat{\sigma}_{ab}^{RV} = 2 \operatorname{Re} \left(\mathcal{M}_{ab \rightarrow F+1}^{(0),\dagger} \mathcal{M}_{ab \rightarrow F+1}^{(1)} \right)$
- *double virtual* (VV) corrections: $\hat{\sigma}_{ab}^{VV} = 2 \operatorname{Re} \left(\mathcal{M}_{ab \rightarrow F}^{(0),\dagger} \mathcal{M}_{ab \rightarrow F}^{(2)} \right) + |\mathcal{M}_{ab \rightarrow F}^{(1)}|^2$

We present the details of these computations in the subsequent chapters. As mentioned earlier, these corrections show up divergences in UV and IR end, which is resolved by using renormalization and mass-factorization techniques and hence obtain a finite partonic coefficient function. In the concluding note, we emphasize that, for the fixed order perturbative theory to be applicable, the contributions at any order should satisfy $\hat{\sigma}_{ab}^{(k)} \ll \hat{\sigma}_{ab}^{(k-1)}$. If the contributions are such that $\hat{\sigma}_{ab}^{(k)} \approx \hat{\sigma}_{ab}^{(k-1)}$, then truncating that perturbative expansion will give rise to unreliable theoretical predictions.

2.3 Effects of threshold corrections and Resummation

The fixed order predictions have limitation in their applicability due to several enhanced logarithms, which are originating from mainly three categories: *UV origin*, *Collinear origin* and *Soft origin*. As discussed in previous sections, the logarithms of UV origin can be absorbed into the running coupling constant and collinear origin into the parton distribution functions. While, for the soft regions, the large logarithms occurs due to soft-gluon emissions. Despite the cancellation of divergences of these soft emissions with those of virtual gluons, the soft gluons effects can still be significant in kinematic configurations where high unbalance between real and virtual contributions persists. In such cases, the fixed order convergence is questionable. An alternative approach to treat these regions is by reorganizing the perturbative expansion by an all-order summation of a class of large logarithms; the technique is known in the name of *resummation*.

In addition to the dominance at the partonic level, for certain observable, the pdfs also get large at soft regions, hence improving their role at the hadronic level. These corrections are, in general, known as *soft corrections*. Supplemented them with the virtual contributions account for the *soft-virtual* or *threshold corrections*. This section briefly reviews a formalism to capture the threshold corrections for the inclusive process and their resummation framework.

2.3.1 Threshold framework

The emission of soft gluons defines the threshold limit, where the final colorless state carries almost all the incoming center of mass energy. Denoting the final state invariant mass as q^2 and $\hat{s} \equiv (p_1 + p_2)^2$ as the center of mass energy of incoming partons, the threshold limit can be defined in terms of the dimensionless partonic scaling variable:

$$z \equiv \frac{q^2}{\hat{s}} \rightarrow 1. \quad (2.36)$$

Recall from the factorization theorem that the finite partonic coefficient function can be related to the bare partonic cross section and mass factorization kernels Γ as:

$$\frac{\Delta_{cd}(z, q^2, \mu_F^2)}{z} = \sum_{a,b} \left(\Gamma_{ca}^T(z, \mu_F^2, \epsilon) \right)^{-1} \otimes \frac{\hat{\sigma}_{ab}(z, q^2, \epsilon)}{z} \otimes \Gamma_{bd}^{-1}(z, \mu_F^2, \epsilon) \quad (2.37)$$

In the threshold limit, this finite partonic coefficient function decomposes into :

$$\Delta_{ij}(z, q^2, \mu_F^2) = \Delta_{ij}^{\text{sv}}(z, q^2, \mu_F^2) + \Delta_{ij}^{\text{hard}}(z, q^2, \mu_F^2) \quad (2.38)$$

where the $\Delta_{ij}^{\text{sv}}(z, q^2, \mu_F^2)$ contain only distributions of the form:

$$\left\{ \delta(1-z), \mathcal{D}_i(z) \equiv \left[\frac{\ln^i(1-z)}{1-z} \right]_+ \right\} \quad (2.39)$$

while the $\Delta_{ij}^{\text{hard}}(z, q^2, \mu_F^2)$ constitutes to all the regular terms in z , which include logarithms of the form $\ln^i(1-z)$ and polynomial of $(1-z)$. Note that logarithms $\ln^i(1-z)$ also give rise to divergences, however they are suppressed to the threshold ones. The corresponding contributions are often called *next-to-soft* or *next-to-threshold* corrections, which will be discussed in detail in subsequent sections.

We focus on SV contributions, which arise only from $\Delta_{q\bar{q}}$ for DY, $\Delta_{b\bar{b}}$ for Higgs boson production in bottom quark annihilation and Δ_{gg} for Higgs boson production in gluon

fusion. For convenience, we denote these coefficient functions collectively by Δ_I with $I = q, b, g$ respectively refers to DY, $b\bar{b} \rightarrow H$ and $gg \rightarrow H$ production processes. In this context, it is sufficient to keep only those components of mass factorization kernels and of $\hat{\sigma}_{ab}$ that upon convolution gives $\delta(1 - z)$ and $\mathcal{D}_i(z)$ terms in (2.37). These contributions only come from diagonal terms/channels. For instance, in the case of DY, the mass factorized result $\Delta_{q\bar{q}}$ either have convolutions involving only diagonal terms/channels, like $\hat{\sigma}_{q\bar{q}} \otimes \Gamma_{qq} \otimes \Gamma_{\bar{q}\bar{q}}$ or those containing one diagonal and a pair of non-diagonal ones/channels, for example $\hat{\sigma}_{qg} \otimes \Gamma_{qq} \otimes \Gamma_{gq}$. The former gives SV terms upon convolutions, while the latter contributes only beyond SV terms. Hence the mass factorized result will be in terms of only diagonal terms/channels, and the sum over different partonic channels can be dropped. The diagonal terms are denoted with index I where $I = q, b, g$ respectively refers $(\sigma_{q\bar{q}}, \Gamma_{qq})$, $(\sigma_{b\bar{b}}, \Gamma_{bb})$, and $(\sigma_{gg}, \Gamma_{gg})$. This gives rise to:

$$\frac{\Delta_I^{\text{sv}}(z, q^2, \mu_F^2)}{z} = \left(\Gamma_I^T(z, \mu_F^2, \epsilon) \right)^{-1} \otimes \frac{\hat{\sigma}_I^{\text{sv}}(z, q^2, \epsilon)}{z} \otimes \Gamma_I^{-1}(z, \mu_F^2, \epsilon) \quad (2.40)$$

The superscript sv indicates that we keep only those terms which gives $\delta(1 - z)$ and \mathcal{D}_j after the aforementioned convolutions.

In constructing threshold enhanced cross section, we start with the decomposition of the cross section in terms of pure virtual contributions \mathcal{F} and soft-collinear distribution function \mathcal{S} in the following way:

$$\hat{\sigma}_I^{\text{sv}}(z, q^2, \epsilon) = \sigma^B(\mu_R^2) \left(Z^I(\mu_R^2) \right)^2 |\mathcal{F}^I(q^2)|^2 \delta(1 - z) \otimes \mathcal{S}_{\text{sv}}^I(z, q^2, \epsilon). \quad (2.41)$$

where σ^B is the born factor. The quantity $\ln \mathcal{S}_{\text{sv}}^I$ is obtained after factoring out the pure virtual contributions from the total inclusive cross section and thus it embeds all the contributions coming from real-virtual and real emission processes only. Consequently, when combined with Eq.(2.40) we get an all-order decomposition formula for the mass-

factorized partonic threshold cross section as,

$$\begin{aligned} \Delta_I^{\text{sv}}(z, q^2, \mu_F^2) &= \sigma^B(\mu_R^2) \left(Z^I(\mu_R^2) \right)^2 |\mathcal{F}^I(q^2)|^2 \delta(1-z) \otimes \ln \mathcal{S}_{\text{sv}}^I(z, q^2, \epsilon) \\ &\otimes \left(\Gamma_I^T(z, \mu_F^2, \epsilon) \right)^{-1} \otimes \Gamma_I^{-1}(z, \mu_F^2, \epsilon). \end{aligned} \quad (2.42)$$

Here, the symbol \otimes denotes the Mellin convolution which is defined for functions $f_i(x_i)$, $i = 1, 2, \dots, n$ as,:

$$(f_1 \otimes f_2 \otimes \dots \otimes f_n)(z) = \prod_{i=1}^n \left(\int dx_i f_i(x_i) \right) \delta(z - x_1 x_2 \dots x_n). \quad (2.43)$$

In consequence to the above decomposition formula, the Δ_I^{sv} can be expressed in terms of certain building blocks: form factor \mathcal{F}^I , soft collinear distribution $\mathcal{S}_{\text{sv}}^I$ and mass factorization Splitting kernels Γ_I . The governing differential equation corresponding to each of these building blocks paves the way to get an all-order structure for Δ_I^{sv} , which we will unravel subsequently. Each of these building blocks has a perturbative expansion in powers of the bare strong coupling constant, which is related to the renormalized one through renormalization constant Z_{a_s} :

$$\hat{a}_s S_\epsilon = \left(\frac{\mu_0^2}{\mu_R^2} \right)^\epsilon Z_{a_s}(\mu_R^2) a_s(\mu_R^2), \quad (2.44)$$

where $S_\epsilon = \exp[(\gamma_E - \ln 4\pi)\epsilon/2]$ with γ_E being the Euler Mascheroni constant. The scale μ_0 is an arbitrary mass scale introduced to make \hat{g}_s dimensionless in d -dimensions. From RG equation, we get

$$\begin{aligned} Z_{a_s}(\mu_R^2) &= 1 + a_s(\mu_R^2) \left[\frac{2}{\epsilon} \beta_0 \right] + a_s^2(\mu_R^2) \left[\frac{4}{\epsilon^2} \beta_0^2 + \frac{1}{\epsilon} \beta_1 \right] + a_s^3(\mu_R^2) \left[\frac{8}{\epsilon^3} \beta_0^3 + \frac{14}{3\epsilon^2} \beta_0 \beta_1 + \frac{2}{3\epsilon} \beta_2 \right] \\ &+ a_s^4(\mu_R^2) \left[\frac{16}{\epsilon^4} \beta_0^4 + \frac{46}{3\epsilon^3} \beta_0^2 \beta_1 + \frac{1}{\epsilon^2} \left(\frac{3}{2} \beta_1^2 + \frac{10}{3} \beta_0 \beta_2 \right) + \frac{1}{2\epsilon} \beta_3 \right]. \end{aligned} \quad (2.45)$$

In the subsequent sections, we discuss the building blocks in detail.

Form factor

The virtual contribution is captured through the form factor, which is defined by the born factorized square matrix element as

$$\mathcal{F}^I = \sum_{k=0}^{\infty} \hat{a}_s^k S_\epsilon^k \left(\frac{Q^2}{\mu^2} \right)^{k \frac{\epsilon}{2}} \mathcal{F}^{I,(k)} \equiv \sum_{k=0}^{\infty} \hat{a}_s^k S_\epsilon^k \left(\frac{Q^2}{\mu^2} \right)^{k \frac{\epsilon}{2}} \frac{\langle \mathcal{M}_I^{(0)} | \mathcal{M}_I^{(k)} \rangle}{\langle \mathcal{M}_I^{(0)} | \mathcal{M}_I^{(0)} \rangle}, \quad (2.46)$$

where $Q^2 = -q^2$ and $\mathcal{M}_I^{(k)}$ is the k -th order unrenormalized matrix element of the underlying partonic process $a(p_1) + \bar{a}(p_2) \rightarrow F(q)$. Form factor for the DY process is the matrix element of vector current $\bar{\psi}_q \gamma_\mu \psi_q$ between on-shell quark states, while for the Higgs boson production in gluon fusion (bottom quark annihilation), it is the matrix element of $G_{\mu\nu}^a G^{\mu\nu a} (\bar{\psi}_b \psi_b)$ between on-shell gluon (bottom quark) states.

In dimensional regularization, the form factor satisfies the following first-order differential equation [34–38]:

$$Q^2 \frac{d}{dQ^2} \ln \mathcal{F}^I(\hat{a}_s, Q^2, \mu^2, \epsilon) = \frac{1}{2} \left[K^I \left(\hat{a}_s, \frac{\mu_R^2}{\mu^2}, \epsilon \right) + G^I \left(\hat{a}_s, \frac{Q^2}{\mu_R^2}, \frac{\mu_R^2}{\mu^2}, \epsilon \right) \right]. \quad (2.47)$$

which follows from the IR factorization, gauge and RG invariances. Here, all the singularities are captured in Q^2 -independent function K^I , whereas G^I collects the remaining terms which are finite as $\epsilon \rightarrow 0$. Further, the RG invariance of \mathcal{F}^I leads to

$$\mu_R^2 \frac{d}{d\mu_R^2} K^I \left(\hat{a}_s, \frac{\mu_R^2}{\mu^2}, \epsilon \right) = -\mu_R^2 \frac{d}{d\mu_R^2} G^I \left(\hat{a}_s, \frac{Q^2}{\mu_R^2}, \frac{\mu_R^2}{\mu^2}, \epsilon \right) = -A^I(a_s(\mu_R^2)) \quad (2.48)$$

where A^I are the standard cusp anomalous dimensions and is a perturbative quantity.

$$A^I = \sum_{k=1}^{\infty} a_s^k(\mu_R^2) A_k^I. \quad (2.49)$$

The solution to the RG Eq.(2.48) is obtained as [39, 40]:

$$K^I\left(\hat{a}_s, \frac{\mu_R^2}{\mu^2}, \epsilon\right) = \sum_{k=1}^{\infty} \hat{a}_s^k S_\epsilon^k \left(\frac{\mu_R^2}{\mu^2}\right)^{k\frac{\epsilon}{2}} K_k^I(\epsilon) \quad (2.50)$$

with

$$\begin{aligned} K_1^I(\epsilon) &= \frac{1}{\epsilon} \left\{ -2A_1^I \right\}, \\ K_2^I(\epsilon) &= \frac{1}{\epsilon^2} \left\{ 2\beta_0 A_1^I \right\} + \frac{1}{\epsilon} \left\{ -A_2^I \right\}, \\ K_3^I(\epsilon) &= \frac{1}{\epsilon^3} \left\{ -\frac{8}{3}\beta_0^2 A_1^I \right\} + \frac{1}{\epsilon^2} \left\{ \frac{2}{3}\beta_1 A_1^I + \frac{8}{3}\beta_0 A_2^I \right\} + \frac{1}{\epsilon} \left\{ -\frac{2}{3}A_3^I \right\}, \\ K_4^I(\epsilon) &= \frac{1}{\epsilon^4} \left\{ 4\beta_0^3 A_1^I \right\} + \frac{1}{\epsilon^3} \left\{ -\frac{8}{3}\beta_0\beta_1 A_1^I - 6\beta_0^2 A_2^I \right\} + \frac{1}{\epsilon^2} \left\{ \frac{1}{3}\beta_2 A_1^I + \beta_1 A_2^I + 3\beta_0 A_3^I \right\} \\ &\quad + \frac{1}{\epsilon} \left\{ -\frac{1}{2}A_4^I \right\} \end{aligned} \quad (2.51)$$

Similarly, RGE of G^I gives the solution:

$$G^I\left(\hat{a}_s, \frac{Q^2}{\mu_R^2}, \frac{\mu_R^2}{\mu^2}, \epsilon\right) = G^I\left(a_s(Q^2), 1, \epsilon\right) + \int_{\frac{Q^2}{\mu_R^2}}^1 \frac{d\lambda^2}{\lambda^2} A^I\left(a_s(\lambda^2 \mu_R^2)\right) \quad (2.52)$$

where the boundary term $G^I\left(a_s(Q^2), 1, \epsilon\right)$ has a perturbative expansion:

$$G^I\left(a_s(Q^2), 1, \epsilon\right) = \sum_{k=1}^{\infty} a_s^k(Q^2) G_k^I(\epsilon). \quad (2.53)$$

Performing the integral in Eq.(2.52) results:

$$\int_{\frac{Q^2}{\mu_R^2}}^1 \frac{d\lambda^2}{\lambda^2} A^I\left(a_s(\lambda^2 \mu_R^2)\right) = \sum_{k=1}^{\infty} \hat{a}_s^k S_\epsilon^k \left(\frac{\mu_R^2}{\mu^2}\right)^{k\frac{\epsilon}{2}} \left[\left(\frac{Q^2}{\mu_R^2}\right)^{k\frac{\epsilon}{2}} - 1 \right] K_k^I(\epsilon). \quad (2.54)$$

Substituting Eq.(2.51),(2.53) and (2.54) in Eq.(2.47) gives the following general structure

for the form factor:

$$\ln \mathcal{F}^I(\hat{a}_s, Q^2, \mu^2, \epsilon) = \sum_{k=1}^{\infty} \hat{a}_s^k S_\epsilon^k \left(\frac{Q^2}{\mu^2} \right)^{k\frac{\epsilon}{2}} \hat{\mathcal{L}}_k^I(\epsilon) \quad (2.55)$$

with

$$\begin{aligned} \hat{\mathcal{L}}_1^I(\epsilon) &= \frac{1}{\epsilon^2} \left\{ -2A_1^I \right\} + \frac{1}{\epsilon} \left\{ G_1^I(\epsilon) \right\}, \\ \hat{\mathcal{L}}_2^I(\epsilon) &= \frac{1}{\epsilon^3} \left\{ \beta_0 A_1^I \right\} + \frac{1}{\epsilon^2} \left\{ -\frac{1}{2} A_2^I - \beta_0 G_1^I(\epsilon) \right\} + \frac{1}{\epsilon} \left\{ \frac{1}{2} G_2^I(\epsilon) \right\}, \\ \hat{\mathcal{L}}_3^I(\epsilon) &= \frac{1}{\epsilon^4} \left\{ -\frac{8}{9} \beta_0^2 A_1^I \right\} + \frac{1}{\epsilon^3} \left\{ \frac{2}{9} \beta_1 A_1^I + \frac{8}{9} \beta_0 A_2^I + \frac{4}{3} \beta_0^2 G_1^I(\epsilon) \right\} \\ &\quad + \frac{1}{\epsilon^2} \left\{ -\frac{2}{9} A_3^I - \frac{1}{3} \beta_1 G_1^I(\epsilon) - \frac{4}{3} \beta_0 G_2^I(\epsilon) \right\} + \frac{1}{\epsilon} \left\{ \frac{1}{3} G_3^I(\epsilon) \right\}, \\ \hat{\mathcal{L}}_4^I(\epsilon) &= \frac{1}{\epsilon^5} \left\{ A_1^I \beta_0^3 \right\} + \frac{1}{\epsilon^4} \left\{ -\frac{3}{2} A_2^I \beta_0^2 - \frac{2}{3} A_1^I \beta_0 \beta_1 - 2\beta_0^3 G_1^I(\epsilon) \right\} \\ &\quad + \frac{1}{\epsilon^3} \left\{ \frac{3}{4} A_3^I \beta_0 + \frac{1}{4} A_2^I \beta_1 + \frac{1}{12} A_1^I \beta_2 + \frac{4}{3} \beta_0 \beta_1 G_1^I(\epsilon) + 3\beta_0^2 G_2^I(\epsilon) \right\} \\ &\quad + \frac{1}{\epsilon^2} \left\{ -\frac{1}{8} A_4^I - \frac{1}{6} \beta_2 G_1^I(\epsilon) - \frac{1}{2} \beta_1 G_2^I(\epsilon) - \frac{3}{2} \beta_0 G_3^I(\epsilon) \right\} \\ &\quad + \frac{1}{\epsilon} \left\{ \frac{1}{4} G_4^I(\epsilon) \right\}. \end{aligned} \quad (2.56)$$

Here, the coefficients G_i^I encapsulated the information about the hard process, while all other factors are universal quantities. It is interesting to note that, at a given order in a_s , coefficients of all the poles but the single one contains only information from the lower orders, and hence can be predicted from the known lower orders. Comparing against the explicit form factor results, it has been observed [41, 42] to satisfy the following decomposition in terms of collinear (B^I), soft (f^I) and UV (γ^I) anomalous dimensions:

$$G_i^I(\epsilon) = 2 \left(B_i^I - \gamma_{i-1}^I \right) + f_i^I + \chi_i^I + \sum_{k=1}^{\infty} \epsilon^k g_i^{I,k}, \quad (2.57)$$

where the constants C_i^I is given by:

$$\begin{aligned}
\chi_1^I &= 0, \\
\chi_2^I &= -2\beta_0 g_1^{I,1}, \\
\chi_3^I &= -2\beta_1 g_1^{I,1} - 2\beta_0 (g_2^{I,1} + 2\beta_0 g_1^{I,2}), \\
\chi_4^I &= -2\beta_2 g_1^{I,1} - 2\beta_1 (g_2^{I,1} + 4\beta_0 g_1^{I,2}) - 2\beta_0 (g_3^{I,1} + 2\beta_0 g_2^{I,2} + 4\beta_0^2 g_1^{I,3}).
\end{aligned} \tag{2.58}$$

The anomalous dimensions are expanded in powers of $a_s(\mu_R^2)$ as

$$Y^I(\mu_R^2) = \sum_{j=1}^{\infty} a_s^j(\mu_R^2) Y_j^I, \tag{2.59}$$

where $Y = A, B, f, \gamma$. As a consequence of recent calculations, the light-like cusp anomalous dimensions are available to four loops [43–47] in QCD. The soft and collinear anomalous dimensions to three loops can be extracted [41, 42] from the quark and gluon collinear anomalous dimensions [48, 49] through the conjecture [41]

$$\gamma^I = 2B^I + f^I. \tag{2.60}$$

The partial results of the soft and collinear anomalous dimensions at four-loop can be obtained from [47, 50–52]. For the reader's convenience, we enlist the values of these anomalous dimensions in Appendix B.

The constants $g_i^{I,k}$ can be extracted from the explicit results of form factors. The computation of quark form factor for DY process and Higgs boson productions are partially available to fourth order in QCD [2, 47, 53–59]. For completeness, we present the results of $g_i^{I,k}$ for quarks in Drell-Yan process, gluon (bottom quark) in Higgs production from gluon fusion (bottom quark annihilation) channel up to third order in Appendix C.

Operator renormalization constant

In certain processes such as Higgs production from gluon fusion, it involves an effective Lagrangian which manifests a non-conserved operator. In such cases, strong coupling renormalization is not sufficient to preserve the UV finiteness of the theory, rather an additional renormalization is required, which is generally called overall operator renormalization. This additional renormalization is performed through the operator renormalization constant Z^I . This is a property inherently associated with the operator and it should not be mix with the UV renormalization constants for the couplings present in the theory. For conserved operator, such as leptonic pair production in DY, this quantity is identically one. The Z^I satisfies the following RG equation:

$$\mu_R^2 \frac{d}{d\mu_R^2} \ln Z^I(\hat{a}_s, \mu_R^2, \mu^2, \epsilon) = \sum_{i=1}^{\infty} a_s^i(\mu_R^2) \gamma_i^I. \quad (2.61)$$

where γ_i^I 's are the UV or mass anomalous dimension. We already come across this quantities in the form factor and are given in Appendix B for $I = q, g, b$. Solving the above RG equation, one obtain the solution for the Z^I as given by:

$$\begin{aligned} Z^I(\hat{a}_s, \mu_R^2, \mu^2, \epsilon) = & 1 + \hat{a}_s \left(\frac{\mu_R^2}{\mu^2} \right)^{\frac{\epsilon}{3}} S_\epsilon \left[\frac{1}{\epsilon} \left(2 \gamma_0^I \right) \right] + \hat{a}_s^2 \left(\frac{\mu_R^2}{\mu^2} \right)^\epsilon S_\epsilon^2 \left[\frac{1}{\epsilon^2} \left(2 (\gamma_0^I)^2 - 2 \beta_0 \gamma_0^I \right) \right. \\ & + \left. \frac{1}{\epsilon} \left(\gamma_1^I \right) \right] + \hat{a}_s^3 \left(\frac{\mu_R^2}{\mu^2} \right)^{3\frac{\epsilon}{2}} S_\epsilon^3 \left[\frac{1}{\epsilon^3} \left(\frac{4}{3} (\gamma_0^I)^3 - 4 \beta_0 (\gamma_0^I)^2 + \frac{8}{3} \beta_0^2 \gamma_0^I \right) \right. \\ & + \left. \frac{1}{\epsilon^2} \left(2 \gamma_0^I \gamma_1^I - \frac{2}{3} \beta_1 \gamma_0^I - \frac{8}{3} \beta_0 \gamma_1^I \right) + \frac{1}{\epsilon} \left(\frac{2}{3} \gamma_2^I \right) \right] \\ & + \hat{a}_s^4 \left(\frac{\mu_R^2}{\mu^2} \right)^{2\epsilon} S_\epsilon^4 \left[\frac{1}{\epsilon^4} \left(\frac{2}{3} (\gamma_0^I)^4 - 4 \beta_0 (\gamma_0^I)^3 + \frac{22}{3} \beta_0^2 (\gamma_0^I)^2 - 4 \beta_0^3 \gamma_0^I \right) \right. \\ & + \left. \frac{1}{\epsilon^3} \left(2 (\gamma_0^I)^2 \gamma_1^I - \frac{4}{3} \beta_1 (\gamma_0^I)^2 - \frac{22}{3} \beta_0 \gamma_0^I \gamma_1^I + \frac{8}{3} \beta_0 \beta_1 \gamma_0^I + 6 \beta_0^2 \gamma_1^I \right) \right. \\ & + \left. \frac{1}{\epsilon^2} \left(\frac{1}{3} (\gamma_1^I)^2 + \frac{4}{3} \gamma_0^I \gamma_2^I - \frac{1}{3} \beta_2 \gamma_0^I - \beta_1 \gamma_1^I - 3 \beta_0 \gamma_2^I \right) + \frac{1}{\epsilon} \left(\frac{1}{2} \gamma_3^I \right) \right] \quad (2.62) \end{aligned}$$

Mass factorization Kernel

The collinear singularities resulting from the massless partons, when their emissions are parallel to any initial states, are removed by absorbing them into bare parton distribution functions. The resulting renormalized pdf's are finite and measurable quantity. This mass factorization procedure is performed at factorization scale μ_F . As discussed before, it introduces mass factorization kernels Γ_I 's which essentially absorbs the initial state collinear singularities. These kernels, in \overline{MS} scheme, satisfies following RG eq:

$$\mu_F^2 \frac{d}{d\mu_F^2} \Gamma_{ij}(z, \mu_F^2, \epsilon) = \frac{1}{2} \sum_k P_{ik}(z, \mu_F^2) \otimes \Gamma_{kj}(z, \mu_F^2, \epsilon) \quad (2.63)$$

where, $P_{ij}(z, \mu_F^2)$ are Altarelli-Parisi splitting functions (matrix valued). Expanding $P_{ij}(z, \mu_F^2)$ and $\Gamma_{ij}(z, \mu_F^2, \epsilon)$ in powers of the strong coupling constant we get

$$P_{ij}(z, \mu_F^2) = \sum_{k=1}^{\infty} a_s^k(\mu_F^2) P_{ij}^{(k-1)}(z). \quad (2.64)$$

As discussed before, since our focus is only SV part of cross section, only diagonal terms of splitting function contributes to our analysis, and hence those give rise to beyond SV are dropped. Hence, by conveniently expressed in terms of index I , we obtain the following structure:

$$P_I^{(k)}(z) = 2 \left(B_{k+1}^I \delta(1-z) + A_{k+1}^I \mathcal{D}_0(z) \right) + P_{reg,I}^{(k)}(z) \quad (2.65)$$

Note here that $P_{reg,I}^{(k)}(z)$ contains terms of the form $\ln(1-z)$ and $\mathcal{O}(1-z)$. We will come across these terms in the subsequent chapters while discussing about the next-to-SV contributions. For the time we focus only on the SV part of splitting functions. After solving RG equation of the kernel in dimensional regularization, we get [39, 40]:

$$\Gamma_I(z, \mu_F^2, \epsilon) = \delta(1-z) + \sum_{k=1}^{\infty} \hat{a}_s^k S_\epsilon^k \left(\frac{\mu_F^2}{\mu^2} \right)^{k \frac{\epsilon}{2}} \hat{\Gamma}_I^{(k)}(z, \epsilon), \quad (2.66)$$

The coefficients $\hat{F}_I^{(k)}$ are expressed in terms of splitting functions:

$$\begin{aligned}
\Gamma_I^{(1)}(z, \epsilon) &= \frac{1}{\epsilon} \left\{ P_I^{(0)}(z) \right\}, \\
\Gamma_I^{(2)}(z, \epsilon) &= \frac{1}{\epsilon^2} \left\{ -\beta_0 P_I^{(0)}(z) + \frac{1}{2} P_I^{(0)}(z) \otimes P_I^{(0)}(z) \right\} + \frac{1}{\epsilon} \left\{ \frac{1}{2} P_I^{(1)}(z) \right\}, \\
\Gamma_I^{(3)}(z, \epsilon) &= \frac{1}{\epsilon^3} \left\{ \frac{4}{3} \beta_0^2 P_I^{(0)} - \beta_0 P_I^{(0)} \otimes P_I^{(0)} + \frac{1}{6} P_I^{(0)} \otimes P_I^{(0)} \otimes P_I^{(0)} \right\} \\
&\quad + \frac{1}{\epsilon^2} \left\{ -\frac{1}{3} \beta_1 P_I^{(0)} + \frac{1}{6} P_I^{(0)} \otimes P_I^{(1)} - \frac{4}{3} \beta_0 P_I^{(1)} + \frac{1}{3} P_I^{(1)} \otimes P_I^{(0)} \right\} \\
&\quad + \frac{1}{\epsilon} \left\{ \frac{1}{3} P_I^{(2)} \right\}, \\
\Gamma_I^{(4)}(z, \epsilon) &= \frac{1}{\epsilon^4} \left\{ -2\beta_0^3 P_I^{(0)} + \frac{11}{6} \beta_0^2 P_I^{(0)} \otimes P_I^{(0)} - \frac{1}{2} \beta_0 P_I^{(0)} \otimes P_I^{(0)} \otimes P_I^{(0)} \right. \\
&\quad \left. + \frac{1}{24} P_I^{(0)} \otimes P_I^{(0)} \otimes P_I^{(0)} \otimes P_I^{(0)} \right\} + \frac{1}{\epsilon^3} \left\{ \frac{4}{3} \beta_0 \beta_1 P_I^{(0)} - \frac{1}{3} \beta_1 P_I^{(0)} \otimes P_I^{(0)} \right. \\
&\quad \left. + \frac{1}{24} P_I^{(0)} \otimes P_I^{(0)} \otimes P_I^{(1)} - \frac{7}{12} \beta_0 P_I^{(0)} \otimes P_I^{(1)} + \frac{1}{12} P_I^{(0)} \otimes P_I^{(1)} \otimes P_I^{(0)} \right. \\
&\quad \left. + 3\beta_0^2 P_I^{(1)} - \frac{5}{4} \beta_0 P_I^{(1)} \otimes P_I^{(0)} + \frac{1}{8} P_I^{(1)} \otimes P_I^{(0)} \otimes P_I^{(0)} \right\} \\
&\quad + \frac{1}{\epsilon^2} \left\{ -\frac{1}{6} \beta_2 P_I^{(0)} + \frac{1}{12} P_I^{(0)} \otimes P_I^{(2)} - \frac{1}{2} \beta_1 P_I^{(1)} + \frac{1}{8} P_I^{(1)} \otimes P_I^{(1)} \right. \\
&\quad \left. - \frac{3}{2} \beta_0 P_I^{(2)} + \frac{1}{4} P_I^{(2)} \otimes P_I^{(0)} \right\} + \frac{1}{\epsilon} \left\{ \frac{1}{4} P_I^{(3)} \right\}. \tag{2.67}
\end{aligned}$$

These quantities are universal and independent of the operator insertion.

Soft Collinear distribution

Since the IR behavior of the pure virtual amplitude is completely universal and independent of the number of external colorless particles, the combined contributions from the real emission diagrams and mass factorization must also exhibit the same universality to get the finite cross section. By employing this universality and imposing the constraint of the finiteness on the cross section, we determine the universal contribution from the latter part to obtain the SV cross section, which we now turn to.

Owing to the decomposition formula given in (2.42) and the universal factorization of the IR singularities, one can write a first order differential equation, similar to the *KG* equation of form factor, for the soft-collinear distribution function as,

$$q^2 \frac{d}{dq^2} \ln \mathcal{S}_{\text{sv}}^I = \frac{1}{2} \left[\overline{K}^I(\hat{a}_s, \frac{\mu_R^2}{\mu^2}, \epsilon, z) + \overline{G}_{\text{sv}}^I(\hat{a}_s, \frac{q^2}{\mu_R^2}, \frac{\mu_R^2}{\mu^2}, \epsilon, z) \right] \quad (2.68)$$

Here the quantity \overline{K}^I embeds all the soft divergences from the real radiation, which cancels with the ones coming from the virtual diagrams. The initial state collinear singularities, which arise from both the virtual and real emission diagrams, are respectively present in \mathcal{F}^I and $\mathcal{S}_{\text{sv}}^I$, and upon incorporating the mass factorization kernels, Γ_I , all of these cease to exist. The final state collinear singularities are guaranteed to cancel upon summing over final states, as dictated by the KLN theorem. Consequently, the SV cross section in (2.42) is free of all the divergences and the finite contributions coming from the soft enhancements associated with the real emission processes are denoted by $\overline{G}_{\text{sv}}^I$ which is a function of (z, ϵ) .

In addition, the RG invariance implies:

$$\mu_R^2 \frac{d}{d\mu_R^2} \overline{K}^I(\hat{a}_s, \frac{\mu_R^2}{\mu^2}, z) = -\mu_R^2 \frac{d}{d\mu_R^2} \overline{G}_{\text{sv}}^I(\hat{a}_s, \frac{q^2}{\mu_R^2}, \frac{\mu_R^2}{\mu^2}, z) = A^I(a_s(\mu_R^2)) \delta(1-z), \quad (2.69)$$

This RG invariance and by demanding the finiteness of SV cross section, supplemented with an understanding on the structure of Feynman integrals provide a unique solution for the IR structure of soft distribution at threshold:

$$\mathcal{S}_{\text{sv}}^I(\hat{a}_s, q^2, \mu^2, z, \epsilon) = C \exp\left(2\Phi_{\text{sv}}^I(\hat{a}_s, q^2, \mu^2, z, \epsilon)\right). \quad (2.70)$$

where the functional form of Φ^I is:

$$\Phi_{\text{sv}}^I = \sum_{i=1}^{\infty} \hat{a}_s^i \left(\frac{q^2(1-z)^2}{\mu^2} \right)^{i\frac{\epsilon}{2}} S_\epsilon^i \left(\frac{i\epsilon}{1-z} \right) \hat{\phi}_i^I(\epsilon). \quad (2.71)$$

The symbol C refers to “ordered exponential” which has the following expansion:

$$Ce^{f(z)} = \delta(1-z) + \frac{1}{1!}f(z) + \frac{1}{2!}(f \otimes f)(z) + \dots \quad (2.72)$$

The symbol \otimes refers to the Mellin convolution and $f(z)$ is a distribution of the kind $\delta(1-z)$ and $\mathcal{D}_i(z)$, where $\mathcal{D}_i(z)$ is defined as,

$$\mathcal{D}_i(z) = \left(\frac{\ln^i(1-z)}{(1-z)} \right)_+ . \quad (2.73)$$

Here the subscript $+$ means that $\mathcal{D}_i(z)$ is a plus distributions. The term $\left(\frac{q^2(1-z)^2}{\mu^2} \right)^{\frac{\epsilon}{2}}$ in the parenthesis of Eq.(2.71) results from two body phase space while $\frac{\hat{\phi}^I(z, \epsilon)}{(1-z)}$ comes from the square of the matrix elements for corresponding amplitudes. In general, the term $q^2(1-z)^2$ inside the parenthesis is the hard scale in the problem and it controls the evolution of Φ^I at every order. The explicit form of the solution in terms of anomalous dimensions and certain universal quantities reads as the following [39, 40]:

$$\begin{aligned} \hat{\phi}_{(1)}^I &= \frac{1}{\epsilon^2} \left(2A_1^I \right) + \frac{1}{\epsilon} \left(\overline{\mathcal{G}}_1^I(\epsilon) \right) \\ \hat{\phi}_{(2)}^I &= \frac{1}{\epsilon^3} \left(-\beta_0 A_1^I \right) + \frac{1}{\epsilon^2} \left(\frac{1}{2} A_2^I - \beta_0 \overline{\mathcal{G}}_1^I(\epsilon) \right) + \frac{1}{2\epsilon} \overline{\mathcal{G}}_2^I(\epsilon) \\ \hat{\phi}_{(3)}^I &= \frac{1}{\epsilon^4} \left(\frac{8}{9} \beta_0^2 A_1^I \right) + \frac{1}{\epsilon^3} \left(-\frac{2}{9} \beta_1 A_1^I - \frac{8}{9} \beta_0 A_2^I - \frac{4}{3} \beta_0^2 \overline{\mathcal{G}}_1^I(\epsilon) \right) \\ &\quad + \frac{1}{\epsilon^2} \left(\frac{2}{9} A_3^I - \frac{1}{3} \beta_1 \overline{\mathcal{G}}_1^I(\epsilon) - \frac{4}{3} \beta_0 \overline{\mathcal{G}}_2^I(\epsilon) \right) + \frac{1}{\epsilon} \left(\frac{1}{3} \overline{\mathcal{G}}_3^I(\epsilon) \right) \\ \hat{\phi}_{(4)}^I &= \frac{1}{\epsilon^5} \left(-\beta_0^3 A_1^I \right) + \frac{1}{\epsilon^4} \left(\frac{2}{3} \beta_0 \beta_1 A_1^I + \frac{3}{2} \beta_0^2 A_2^I - 2\beta_0^3 \overline{\mathcal{G}}_1^I(\epsilon) \right) \\ &\quad - \frac{1}{\epsilon^3} \left(\frac{1}{12} \beta_2 A_1^I - \frac{1}{4} \beta_1 A_2^I - \frac{3}{4} \beta_0 A_3^I + \frac{4}{3} \beta_0 \beta_1 \overline{\mathcal{G}}_1^I(\epsilon) + 3\beta_0^2 \overline{\mathcal{G}}_2^I(\epsilon) \right) \\ &\quad + \frac{1}{\epsilon^2} \left(\frac{1}{8} A_4^I - \frac{1}{6} \beta_2 \overline{\mathcal{G}}_1^I(\epsilon) - \frac{1}{2} \beta_1 \overline{\mathcal{G}}_2^I(\epsilon) - \frac{3}{2} \beta_0 \overline{\mathcal{G}}_3^I(\epsilon) \right) + \frac{1}{\epsilon} \left(\frac{1}{4} \overline{\mathcal{G}}_4^I(\epsilon) \right) \end{aligned} \quad (2.74)$$

where the finite quantity \overline{G}_{sv}^I are related to its renormalized counterparts $\overline{\mathcal{G}}_i^I(\epsilon)$ in the following way:

$$\sum_{i=1}^{\infty} \hat{a}_s^i \left(\frac{q^2(1-z)^2}{\mu^2} \right)^{i\frac{\epsilon}{2}} S_\epsilon^i \overline{G}_{sv,i}^I(\epsilon) = \sum_{i=1}^{\infty} a_s^i (q^2(1-z)^2) \overline{\mathcal{G}}_i^I(\epsilon) \quad (2.75)$$

we find

$$\begin{aligned} \overline{G}_{sv,1}^I(\epsilon) &= \overline{\mathcal{G}}_1^I(\epsilon) \\ \overline{G}_{sv,2}^I(\epsilon) &= \frac{1}{\epsilon} \left(-2\beta_0 \overline{\mathcal{G}}_1^I(\epsilon) \right) + \overline{\mathcal{G}}_2^I(\epsilon) \\ \overline{G}_{sv,3}^I(\epsilon) &= \frac{1}{\epsilon^2} \left(4\beta_0^2 \overline{\mathcal{G}}_1^I(\epsilon) \right) + \frac{1}{\epsilon} \left(-\beta_1 \overline{\mathcal{G}}_1^I(\epsilon) - 4\beta_0 \overline{\mathcal{G}}_2^I(\epsilon) \right) + \overline{\mathcal{G}}_3^I(\epsilon) \\ \overline{G}_{sv,4}^I(\epsilon) &= \frac{1}{\epsilon^3} \left(-8\beta_0^3 \overline{\mathcal{G}}_1^I(\epsilon) \right) + \frac{1}{\epsilon^2} \left(\frac{16}{3} \beta_0 \beta_1 \overline{\mathcal{G}}_1^I(\epsilon) + 12\beta_0^2 \overline{\mathcal{G}}_2^I(\epsilon) \right) \\ &\quad + \frac{1}{\epsilon} \left(-\frac{2}{3} \beta_2 \overline{\mathcal{G}}_1^I(\epsilon) - 2\beta_1 \overline{\mathcal{G}}_2^I(\epsilon) - 6\beta_0 \overline{\mathcal{G}}_3^I(\epsilon) \right) + \overline{\mathcal{G}}_4^I(\epsilon) \end{aligned} \quad (2.76)$$

Through explicit determination of the quantity $\overline{\mathcal{G}}_i^I(\epsilon)$, it was found that it is dependent only on the initial partons and can be further decomposed as:

$$\overline{\mathcal{G}}_i^I(\epsilon) = -f_i^I + \overline{\chi}_i^I + \sum_{k=1}^{\infty} \epsilon^k \overline{\mathcal{G}}_i^{I,k}, \quad \overline{\chi}_i^I = \chi_i^I \Big|_{(g_i^{I,k} \rightarrow \overline{\mathcal{G}}_i^{I,k})}. \quad (2.77)$$

The results of finite coefficients $\overline{\mathcal{G}}_i^{I,k}(\epsilon)$ are given in Appendix C :

One of the most salient features of the Φ_1 is that it satisfies the maximally non-Abelian property:

$$\Phi^g = \frac{C_A}{C_F} \Phi^q, \quad (2.78)$$

This property essentially signifies its universal behavior. Moreover, it is independent

of the external quark flavors, as expected from the infrared behavior of the scattering amplitudes. This is understood as the soft part of the cross section is always independent of any quantum numbers such as spin, color and flavor once the born is factored out; rather, it depends only on the gauge interaction, which is $SU(N_c)$ for the current case. The aforementioned non-Abelian property is explicitly verified to NNLO in refs. [39, 40] and in ref. [60] it is conjectured to be valid even at N^3 LO QCD which is demonstrated through explicit computations in refs. [61, 62]. The flavor dependence of the Φ^I was exploited in ref. [63] to calculate the SV cross section at N^3 LO for the Higgs boson production in bottom quark annihilation. However, whether the validity of this property holds beyond N^3 LO with generalized Casimir scaling [64] needs to be addressed in future.

The SV cross section

Having the IR structure of virtual contributions and real emissions, we get a general structure of SV cross section, with an expansion in powers of coupling constant:

$$\Delta_I^{\text{sv}}(z, q^2, \mu_F^2) = \sum_{i=1}^{\infty} a_s^i(\mu_R^2) \Delta_I^{\text{sv},(i)}(z, q^2, \mu_F^2, \mu_R^2), \quad (2.79)$$

where, $\Delta_I^{\text{sv},(i)}$ defines the finite partonic coefficient function at each order. At the individual level, the building blocks form factor, Splitting kernel and soft-collinear distribution contain singularities. However, together they cancel and give rise to a finite partonic SV cross section, expressed in terms of universal anomalous dimensions and process dependent terms. Substituting explicit results of anomalous dimensions, β -functions and process dependent terms, we obtain the results of Higgs production from gluon fusion and bottom quark annihilation and for the DY process, which is available in [39, 40, 60–63, 65–67].

2.3.2 Resummation

The threshold corrections dominate when the partonic scaling variable approaches its kinematical limit, that is when $z \rightarrow 1$. They manifest in terms of distributions of the form

$$\left\{ \delta(1-z), \mathcal{D}_i(z) \equiv \left[\frac{\ln(1-z)}{1-z} \right]_+ \right\} \quad (2.80)$$

This will be evident by noting:

$$\frac{1}{1-z} \left[(1-z)^2 \right]^{k\frac{\epsilon}{2}} = \frac{1}{k\epsilon} \delta(1-z) + \left(\frac{1}{1-z} \left[(1-z)^2 \right]^{k\frac{\epsilon}{2}} \right)_+ \quad (2.81)$$

When $z \rightarrow 1$, the $\ln(1-z)$ become very large, on the other hand a_s very small so that the product $\equiv a_s \ln(1-z) \sim 1$. In such cases, fixed order truncation will not be justifiable, and one needs to take care of these logarithms to all orders by doing resummation. The Resummation technique provides an alternative perturbative expansion that considers these large logarithms in the expansion and produces reliable results while truncating. In fact, the presence of large logarithms is an artefact of truncating the series. When we expand the series to all orders, it should give a physically acceptable result.

In order to construct a resummation framework, we employ the structure of soft-collinear distribution, which we obtained in last section. Using the relation (2.81), and by factorizing the soft divergences from Eq.(2.71), we obtain an integral representation for the soft collinear distribution :

$$\begin{aligned} \Phi_{sv}^I(\hat{a}_s, q^2, \mu^2, z, \epsilon) &= \left(\frac{1}{1-z} \left\{ \int_{\mu_R^2}^{q^2(1-z)^2} \frac{d\lambda^2}{\lambda^2} A^I(a_s(\lambda^2)) + \bar{G}_{sv}^I(a_s(q^2(1-z)^2), \epsilon) \right\} \right)_+ \\ &+ \delta(1-z) \sum_{i=1}^{\infty} \hat{a}_s^i \left(\frac{q^2}{\mu^2} \right)^{i\frac{\epsilon}{2}} S_\epsilon^i \hat{\phi}_i^I(\epsilon) \\ &+ \left(\frac{1}{1-z} \right)_+ \sum_{i=1}^{\infty} \hat{a}_s^i \left(\frac{\mu_R^2}{\mu^2} \right)^{i\frac{\epsilon}{2}} S_\epsilon^i \bar{K}_i^I(\epsilon) \end{aligned} \quad (2.82)$$

Some remarks are in order. The third line in the above equation exactly cancels with the D_0 term of the mass factorization kernel. The ϕ_i^I in the second line contains both pole and finite terms. The poles cancel with those of form factor and $\delta(1 - z)$ part of mass factorization kernel.

Since the integrand involves many convolutions, it is convenient to solve it Mellin N -space, where all the convolutions turn to normal products. The Mellin transformation of a function $f(z)$ is defined as:

$$M[f](N) = \int_0^1 dz z^{N-1} f(z) \quad (2.83)$$

Also the Mellin transformation of convolutions given in Eq.(2.43) becomes:

$$M[A \otimes B](N) = M[A](N) M[B](N) \quad (2.84)$$

The threshold limit in N -space is defined as:

$$z \rightarrow 1 \text{ transforms to } N \rightarrow \infty \quad (2.85)$$

Similarly, the $\delta(1 - z)$ becomes a constant, and distributions of the form $D_i(z)$ become logarithms of the form $\ln N$.

Adding the form factor and mass factorization kernel with the soft factor given in Eq.(2.82) and performing the coupling constant renormalization and finally solving them in Mellin space we get the resummed formula. In Mellin the finite SV cross section reads as:

$$\begin{aligned} \Delta_N^I &= C_0^I(q^2, \mu_R^2, \mu_F^2) \exp \left[\int_0^1 dz \frac{z^{N-1} - 1}{1 - z} \left\{ \int_{q^2}^{q^2(1-z)^2} \frac{d\lambda^2}{\lambda^2} A^I(a_s(\lambda^2)) + \mathbf{D}^I(a_s(q^2(1-z)^2)) \right\} \right] \\ &= C_0^I(q^2, \mu_R^2, \mu_F^2) \exp \left(\ln g_0^I(a_s(\mu_R^2)) + G_N^I(\omega) \right) \\ &= \bar{g}_0^I(q^2, \mu_R^2, \mu_F^2) \exp \left(G_N^I(\omega) \right) \end{aligned} \quad (2.86)$$

where, $\omega = 2\beta_0 a_s \ln N$ and $\mathbf{D}^I(a_s(q^2(1-z)^2))$ are the well-known threshold exponent in [68] which is related to the SV coefficients though:

$$\begin{aligned} \mathbf{D}^I(a_s(q^2(1-z)^2)) &= \sum_{i=1}^{\infty} a_s^i(q^2(1-z)^2) \mathbf{D}_i^I \\ &= 2 \bar{G}_{\text{sv}}^I(a_s(q^2(1-z)^2), \epsilon) \Big|_{\epsilon=0} \end{aligned} \quad (2.87)$$

The quantity C_0^I is dependent on the hard process under study, which is basically the $\delta(1-z)$ part of form factor and soft factor and is N -independent. The remaining part in the above integral is universal. Mellin transformation in Eq.(2.86) produced an N -dependent ($G_N^I(\omega)$) and N -independent part ($\ln g_0^I$). Adding the N -independent part with the C_0^I produces \bar{g}_0^I .

$$\bar{g}_0^I(q^2, \mu_R^2, \mu_F^2) = C_0^I(q^2, \mu_R^2, \mu_F^2) g_0^I(a_s(\mu_R^2)) \quad (2.88)$$

which can be expanded in terms of $a_s(\mu_R^2)$ as,

$$\bar{g}_0^I(a_s(\mu_R^2)) = \sum_{i=0}^{\infty} a_s^i(\mu_R^2) \bar{g}_{0,i}^I \quad . \quad (2.89)$$

The above integral Eq.(2.86) is first employed in Seminar works by Stermann [69], Catani and Trentedue [68]. The G_N^I collects and resums all large- N logarithms to all orders and can be expressed as a resummed perturbative series as:

$$G_N^I(q^2, \omega) = \ln N g_1^I(q^2, \omega) + g_2^I(q^2, \omega) + a_s g_3^I(q^2, \omega) + a_s^2 g_4^I(q^2, \omega) + \dots \quad (2.90)$$

The coefficients $\bar{g}_{0,i}^I$ and g_i^I are given in Appendix E. Each term in the above perturbative expansion produces all order result. The first term resum every highest logarithm to all orders, the next term resums next to highest logarithms and so on. These terms, together with \bar{g}_0^I in the same accuracy, gives *leading logarithm (LL)*, *next-to-leading logarithms (NLL)* and so on respectively. Adding each term in this perturbative expansion improves

logarithmic accuracy.

We will discuss the resummation framework in great detail in subsequent chapters. In addition to the resummation for threshold logarithms, we propose a framework for resumming the next-to-threshold logarithms in the last chapter.

3 Higgs pair production from $b\bar{b}$ -annihilation to NNLO in QCD

In this chapter, we present the cross section for bottom quark induced di-Higgs productions at NNLO. Among two kind of contributions, we present the exact NNLO corrections for the dominant one. To compute the remaining ones, we adopt the threshold framework that we discussed in last chapter. Numerical analysis establish that the inclusion of higher order terms reduce the uncertainties resulting from the unphysical scales. The materials presented in this chapter are the result of original research done in collaboration with Pooja Mukherjee, V. Ravindran et.al and are based on the published article [70] .

3.1 Prologue

Ever since discovering the Higgs boson [71, 72], understanding this scalar particle's nature has been the critical objective of the LHC and future colliders. The measurements explored so far at the LHC in the Higgs production and decay channels points out towards the particle being the long-sought Higgs boson of SM of elementary particles [73–84]. For instance, the mass of Higgs (125.38 ± 0.14) GeV [85], its zero spin, its couplings to vector bosons and fermions within 5% accuracy [86, 87]. Despite of all these successes of Higgs programme at the LHC, the nature of Higgs potential remains elusive. The relevant parameters to constrain the Higgs potential are the self couplings of Higgs boson such as

trilinear (λ_3^{SM}) and quartic couplings (λ_4^{SM}). As shown, within the SM, the Higgs potential after the electro-weak symmetry breaking (EWSB) takes the form:

$$\mathcal{L} \supset -\frac{m_h^2}{2}\phi^2(x) - \lambda_3^{\text{SM}}v\phi^3(x) - \lambda_4^{\text{SM}}\phi^4(x), \quad \lambda_3^{\text{SM}} = \frac{m_h^2}{2v^2}, \quad \lambda_4^{\text{SM}} = \frac{m_h^2}{8v^2}, \quad (3.1)$$

where $\phi(x)$ denotes the Higgs field and $v \approx 246$ GeV is its vacuum expectation value (vev). In the SM, the Higgs self couplings are related to its mass and the vev of Higgs field, which is linked to the Fermi constant $G_F = 1.166378810^{-5}$ GeV⁻² [88] by $v = (\sqrt{2}G_F)^{-1/2}$. Hence, the SM values for λ_3^{SM} and λ_4^{SM} are found to be ~ 0.13 and ~ 0.03 , respectively. However, these values can be modified by the presence of beyond the SM (BSM) physics scenarios, which, in turn, suggests their independent measurements.

While the quartic Higgs self-coupling (λ_4^{SM}) lies beyond the reach of LHC [89,90], various studies shows that the trilinear self-coupling, (λ_3^{SM}) might be accessible via the Higgs pair production processes [91–98]. Though this measurement is difficult due to the small production cross section and the presence of large QCD backgrounds, the study for the high luminosity LHC indicate that the Higgs boson pair production due to gluon fusion can predict λ_3^{SM} with $O(1)$ accuracy. At present the most stringent constraint on the λ_3 is given by ATLAS and CMS within the range of (-2.3, 10.3) and (-3.3,8.5), respectively, times the SM value [99] with the assumption that no other Higgs boson couplings deviate from their SM value.

A direct way to access the trilinear coupling is the process of producing a pair of Higgs bosons. This can be attained through several partonic channels, viz gluon fusion, vector boson fusion, associated production with a vector boson or a pair of heavy quarks. Among these, the gluon fusion channel has, by far, the largest cross section since it gets the large gluon luminosity at the LHC. On the theoretical side, the state of the art for the gluon fusion channel has reached an impressive accuracy of N³LO in strong coupling constant and also next-to-next-to-leading logarithmic (NNLL) accuracy for the threshold resummation. (See Fig.3.1 for the LO contributions to this channel and for a brief overview

see [100–116]). However, being heavy quark loop-induced (See Fig.3.1), this production channel gets minuscule cross section in the SM. The total Higgs boson pair production

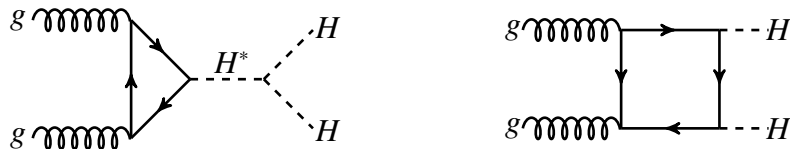


Figure 3.1: *LO contributions to Higgs boson pair production from gluon fusion channel.*

cross section is approximately three orders of magnitude smaller than that of single Higgs production. In addition, the presence of extensive background makes its measurement experimentally challenging. Hence unless contributions from BSM physics enhance the production cross section, measurement of this channel will require a considerable integrated luminosity. On the other hand, in such a scenario, the sub-dominant channels in the SM could possibly become interesting as they would receive substantial contributions from new physics. One such channel is the production of a pair of Higgs bosons in bottom quark annihilation. In certain supersymmetric models, like the Minimal Supersymmetric SM (MSSM) [117], the bottom quark Yukawa coupling is enhanced with respect to the top quark Yukawa coupling, in the large $\tan\beta$ region, where $\tan\beta$ is the ratio of v_{ev} 's of up and down type Higgs fields in the Higgs sector of the MSSM. Hence precise predictions for this channel is of high importance.

While a plethora of work has been performed to reach ultimate precision for the gluon channel, the sub-dominant channels have not received much attention. This chapter mainly concerns the bottom quark annihilation channel where the Higgs boson couples to bottom quarks through the Yukawa coupling. The NLO corrections for this channel was first obtained in [1] and later in [118–120] considering several BSM scenarios. For the latter, the bottom quark annihilation process dominates over the gluon fusion even at the LO level. In addition, their NLO QCD corrections are not only sizeable but also larger than the supersymmetric QCD corrections. To stabilize the cross section with respect to higher order radiative corrections, NNLO corrections to this channel are desirable, which

is the focus of this chapter.

The chapter is organized as follows. In Sec.[3.2], we discuss the Lagrangian, kinematics and the classes of diagrams that are relevant for our computation. The computational details are mentioned in Sec.[3.3] with the structure of UV and IR divergences. We present the relevant analytic results for the inclusive cross sections in Sec.[3.4] and their numerical impact in Sec.[3.5]. Finally, we summarize our findings in Sec.[3.6].

3.2 Theoretical Framework

To begin with, we briefly review the theoretical framework for the production of a pair of Higgs bosons via bottom quark annihilation at hadron colliders. We work in dimensional regularization (DR), in which all the fields and couplings of the Lagrangian and the loop integrals that appear in the Feynman diagrams are analytically continued to $d = 4 + \epsilon$ space-time dimensions. In addition, we perform traces of Dirac γ -matrices in d -dimensions.

3.2.1 The Yukawa interaction

Within SM, the interaction part of the Lagrangian that is responsible for the production is given by,

$$\mathcal{L} = -\lambda_b \phi(x) \bar{\psi}_b(x) \psi_b(x), \quad (3.2)$$

where $\psi_b(x)$ is the bottom quark field. λ_b is the Yukawa coupling which after the EWSB is found to be m_b/v , where m_b is the bottom quark mass and v the vev of the Higgs field. In the SM, the ratio of the top quark Yukawa coupling (λ_t) and the bottom quark Yukawa coupling (λ_b) is found to be approximately 35 *i.e.* $\lambda_t/\lambda_b \approx 35$. In addition, the bottom quark flux in the proton-proton collision is much smaller than the gluon flux. Hence, the

contribution from this channel is sub-dominant as compared to the gluon fusion channel. However, in the MSSM [117], this ratio depends on the value of $\tan\beta$, which can increase the contribution resulting from the bottom quark annihilation channel. At LO,

$$\frac{\lambda_t^{\text{MSSM}}}{\lambda_b^{\text{MSSM}}} = f_\phi(\alpha) \frac{m_t}{m_b} \frac{1}{\tan\beta}, \quad \text{with} \quad f_\phi(\alpha) = \begin{cases} -\cot\alpha & \text{for } \phi = h, \\ \tan\alpha & \text{for } \phi = H, \\ \cot\beta & \text{for } \phi = A, \end{cases} \quad (3.3)$$

where h is the SM like light Higgs boson, H and A are the heavy and the pseudoscalar Higgs bosons, respectively. The parameter α is the angle between weak and mass eigenstates of the neutral Higgs bosons h and H . Since the bottom quark mass is much smaller than the other energy scales that appear at the partonic level, we set the former to zero except in the Yukawa coupling in perturbation theory [121–123]. In particular, the finite mass effects from the bottom quarks are found to be suppressed by the inverse power of the mass of the Higgs boson. The number of active flavors $n_f = 5$ and we work in Feynman gauge.

3.2.2 Kinematics

At the LO, the scattering process responsible for the di-Higgs production in bottom quark annihilation channel is given by

$$b(p_1) + \bar{b}(p_2) \rightarrow H(p_3) + H(p_4), \quad (3.4)$$

where p_1, p_2 are the momenta of incoming bottom, anti-bottom quarks with $p_1^2 = p_2^2 = 0$ and p_3, p_4 are the momenta of the final state Higgs bosons with $p_3^2 = p_4^2 = m_h^2$. The associated Mandelstam variables are,

$$s = (p_1 + p_2)^2, \quad t = (p_1 - p_3)^2, \quad u = (p_2 - p_3)^2, \quad (3.5)$$

which satisfy the relation $s + t + u = 2m_h^2$. For convenience, we use the dimensionless variables x, y and z defined in [124] as follows

$$s = m_h^2 \frac{(1+x)^2}{x}, \quad t = -m_h^2 y, \quad u = -m_h^2 z. \quad (3.6)$$

The variables x, y and z satisfy

$$\frac{(1+x)^2}{x} - y - z = 2. \quad (3.7)$$

The final result will be expressed in term of logarithms and classical polylogarithms, which are functions of these scaling variables.

3.2.3 Classification of Feynman diagrams

Two mechanisms contribute to the production of Higgs pairs through bottom quark annihilation in the standard model. One is the vertex type of digrams, we call them class-A, which contains single Yukawa and trilinear couplings. The latter kind of diagrams is quadratic in Yukawa coupling. At LO, we have three Feynman diagrams, one class-A, and rest class-B diagrams. The same classes of diagrams contribute beyond LO. We elaborate on these classes of diagrams below:

- **Class-A:** It contains diagrams where an off-shell Higgs boson is produced through bottom quark annihilation, which then subsequently decays to double Higgs final states ($H^* \rightarrow HH$). These diagrams are proportional to $\lambda_3^{\text{SM}} \lambda_b$ as can be seen from Fig. 3.2. Note that, the decay part does not get any QCD corrections. Consequently, the QCD corrections to class-A diagrams are identical to those for producing a single Higgs boson in bottom quark annihilation, which is known up to three-loop level in QCD [2]. (Various works on single Higgs production from $b\bar{b}$ -channel can be seen in [2, 63, 125–132])

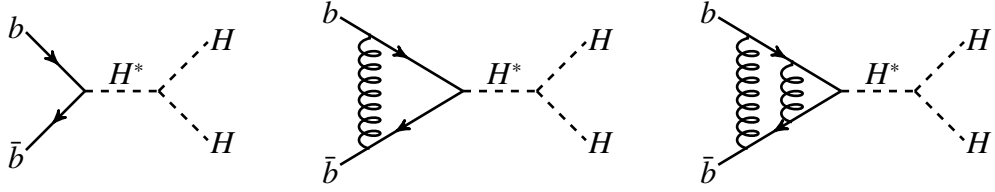


Figure 3.2: Illustration of Class-A diagrams; Born, one and two-loop examples.

- **Class-B:** In this class of diagrams, both the Higgs bosons coupled directly to the bottom quarks. Hence they are proportional to λ_b^2 as shown in Fig. 3.3. For this kind, at two loops level, one encounters a new set of diagrams, the singlet contributions, where the Higgs bosons are produced from a closed bottom quark loop as shown in Fig. 3.4. In the singlet contributions, we have dropped the effects of top quark loops and considered only those coming from bottom quark loops. The top quark contributions are already included in the gluon initiated sub-processes obtained in the heavy top limit in [106] for the Higgs pair production at the LHC.

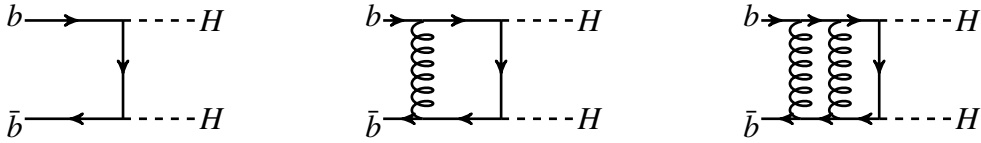


Figure 3.3: Illustration of Class-B diagrams; Born, one and two-loop examples.



Figure 3.4: Illustration of special set of Class-B diagrams, the singlet contributions.

3.2.4 General structure of amplitude

In this section, we describe how the general structure of amplitudes can be obtained using the projector technique for the process given in (3.4). The projectors are defined by analyzing the tensorial structure of the given amplitude, which is valid to all orders in

perturbation theory. Each projector will isolate the coefficients of particular tensor structures. For the given amplitude, since it contains two fermions and two scalars, the general structure takes the form:

$$\begin{aligned}\mathcal{M}_{ij} &= \bar{v}(p_2)(C_1 + C_2 \not{p}_3)u(p_1)\delta_{ij} \\ &\equiv (C_1\mathcal{T}_1 + C_2\mathcal{T}_2)\delta_{ij},\end{aligned}\tag{3.8}$$

where \mathcal{T}_m are the independent tensor with and the $C_m \equiv C_m(x, y, z)$ with $m = 1, 2$ are the corresponding scalar coefficients. Here, the tensor structures \mathcal{T}_m are defined as:

$$\begin{aligned}\mathcal{T}_1 &= \bar{v}(p_2)u(p_1) \\ \mathcal{T}_2 &= \bar{v}(p_2)\not{p}_3u(p_1).\end{aligned}\tag{3.9}$$

The δ_{ij} in Eq.(3.8) is because, in color space, the amplitude is diagonal in the indices (i, j) of the incoming quarks. We use symmetries such as Lorentz covariance, parity and time-reversal invariances to parameterize the amplitude. In addition, we have dropped those terms that vanish when the bottom quarks are massless. The coefficients C_m , $m = 1, 2$, can be determined from the amplitude \mathcal{M}_{ij} by using appropriate projection operators denoted by $\mathcal{P}(C_m)$, *i.e.*,

$$C_m = \frac{1}{N_c} \sum \mathcal{P}(C_m)\mathcal{M}_{ij}\delta_{ij},\tag{3.10}$$

where the sum includes spin, flavors and colors of the external fermions and N_c is the number of colors in $SU(N_c)$ gauge theory. In d -space-time dimensions, the projectors that satisfy $\sum \mathcal{P}(C_m)\mathcal{T}_m = 1$ and $\sum \mathcal{P}(C_m)\mathcal{T}_n = 0 \forall m \neq n$, are found to be

$$\begin{aligned}\mathcal{P}(C_1) &= \frac{1}{2s}\mathcal{T}_1^\dagger, \\ \mathcal{P}(C_2) &= \frac{1}{2[(m_h^2 - t)(m_h^2 - u) - sm_h^2]}\mathcal{T}_2^\dagger.\end{aligned}\tag{3.11}$$

Since the application of projection operators on the amplitude gives only Lorentz scalar functions, the algebraic manipulations with loop integrals become straightforward. The square of the amplitudes that contributes to the total cross section can now be obtained from the coefficients C_1 and C_2 using

$$|\mathcal{M}_{ij}|^2 = N_c \left[|C_1|^2 \mathcal{T}_1 \mathcal{T}_1^\dagger + |C_2|^2 \mathcal{T}_2 \mathcal{T}_2^\dagger + C_1 C_2^\dagger \mathcal{T}_1 \mathcal{T}_2^\dagger + C_1^\dagger C_2 \mathcal{T}_2 \mathcal{T}_1^\dagger \right]. \quad (3.12)$$

Note that these coefficients are, in general, complex due to the Feynman loop integrals. We expand the amplitude \mathcal{M}_{ij} as well as the coefficients C_m in powers of the strong coupling constant defined by $a_s = g_s^2(\mu_R^2)/16\pi^2$, where g_s is the renormalized strong coupling constant and μ_R is the renormalization scale:

$$\mathcal{M}_{ij} = \sum_{l=0}^{\infty} a_s^l \mathcal{M}_{ij}^{(l)}, \quad C_m = \sum_{l=0}^{\infty} a_s^l C_m^{(l)}, \quad (3.13)$$

and consequently

$$\mathcal{M}_{ij}^{(l)} = (C_1^{(l)} \mathcal{T}_1 + C_2^{(l)} \mathcal{T}_2) \delta_{ij}. \quad (3.14)$$

The coefficients $\mathcal{M}_{ij}^{(l)}$ completely describe the amplitudes order by order in perturbation theory. Our next task is to compute these coefficients $C_m^{(l)}$, $m = 1, 2$, up to two loop level, *i.e.*, up to $O(a_s^2)$ in perturbative QCD.

3.3 Calculation of amplitudes

In this section we describe the computational details of the coefficients C_m for the process $b\bar{b} \rightarrow HH$ up to two-loop level in QCD perturbation theory.

3.3.1 Computational details

As can be seen from the form of \mathcal{T}_i in Eq. (3.8), only Class-A diagrams contribute to C_1 and Class-B to C_2 . Since the Class-A diagrams are already computed to three loops in QCD [2], in this section, our focus is to discuss how the scalar function C_2 in Eq. (3.10) is computed order by order in perturbation theory. As we mentioned, we use dimensional regularization, in which the space-time dimensions are taken to be $d = 4 + \epsilon$ and perform traces of Dirac γ -matrices and contraction of Lorentz indices in d -dimensions. For convenience, we work with the bare form of the Lagrangian and evaluate the coefficient C_2 in powers of bare coupling constant \hat{a}_s , where $\hat{a}_s = \hat{g}_s^2/16\pi^2$, \hat{g}_s being the dimensionless strong coupling constant. Beyond LO, one- and two-loop amplitudes containing massless quarks, anti-quarks, and gluons develop UV and IR divergences. These divergences can be regulated using dimensional regularization. We will come to this point in later sections.

To generate Feynman diagrams, we have used QGRAF [133] at every order in the strong coupling constant. Beyond one-loop, a large number of Feynman diagrams contributes to the amplitude. The number of diagrams contributes to tree level, one and two-loop are 2, 10, and 153 respectively, excluding tadpole and self-energy corrections to the external legs. Multiply these amplitudes with the projection operator $\mathcal{P}(C_2)$ defined in Eq. (3.11) will give rise to the scalar function C_2 . Substitution of Feynman rules and computation of various traces involving Dirac and Gell-Mann matrices are done using in-house routines that use publicly available packages such as FORM [134] and Mathematica. At this stage, we end up with a large number of one- and two-loop Feynman integrals. The projection operators guarantee that all the tensor integrals are converted to scalar integrals. We rearrange all the Feynman integrals into a few chosen integral families through shifting of loop momentum. To achieve this, we use the package Reduze2 [135]. At one-loop, the following three integral families can accommodate all the Feynman integrals

$$\{\mathcal{P}_1, \mathcal{P}_{1:i}, \mathcal{P}_{1:i,i+1}, \mathcal{P}_{1:i,i+1,i+2}\}, \quad (3.15)$$

where, i takes one of the values $\{1, 2, 3\}$ whose elements are arranged cyclically. A typical two-loop topology contains at most seven propagators. However, there are nine different Lorentz invariants $(k_i.k_j, k_i.p_j)$ which can appear in the numerator of an integral. Hence, we introduce two auxiliary propagators in each of the two-loop integral families. The following two sets describe the six integral families that we use at two-loops,

$$\begin{aligned} & \{\mathcal{P}_0, \mathcal{P}_1, \mathcal{P}_2, \mathcal{P}_{1:i}, \mathcal{P}_{2:i}, \mathcal{P}_{1:i,i+1}, \mathcal{P}_{2:i,i+1}, \mathcal{P}_{1:i,i+1,i+2}, \mathcal{P}_{2:i,i+1,i+2}\}, \\ & \{\mathcal{P}_0, \mathcal{P}_1, \mathcal{P}_2, \mathcal{P}_{1:i}, \mathcal{P}_{2:i}, \mathcal{P}_{1:i,i+1}, \mathcal{P}_{2:i,i+1}, \mathcal{P}_{0:i+2}, \mathcal{P}_{1:i,i+1,i+2}\}. \end{aligned} \quad (3.16)$$

Here,

$$\begin{aligned} \mathcal{P}_\alpha &= k_\alpha^2, \quad \mathcal{P}_{\alpha:i} = (k_\alpha - p_i)^2, \quad \mathcal{P}_{\alpha:ij} = (k_\alpha - p_i - p_j)^2, \quad \mathcal{P}_{\alpha:ijk} = (k_\alpha - p_i - p_j - p_k)^2, \\ \mathcal{P}_0 &= (k_1 - k_2)^2, \quad \mathcal{P}_{0:i} = (k_1 - k_2 - p_i)^2. \end{aligned}$$

This large number of Feynman integrals belonging to different integral families and can be written in terms of a smaller set of integrals, so-called master integrals (MIs). This can be achieved by using the integration-by-parts (IBP) [136, 137] and the Lorentz Invariance (LI) [138] identities, which are implemented in the Mathematica based package LiteRed [139]. Finally, we obtain 10 and 149 MIs at one- and two-loops, respectively. These MIs are analytically known from the seminal works of Gehrmann and Remiddi [124, 140]. We use them by systematic transformation and hence obtain the two-loop result for the coefficient C_2 which are expressed in terms of Laurent series in ϵ . As mentioned before, these unrenormalized coefficients contain both UV and IR divergences, which appear as poles in ϵ at every order in \hat{a}_s . In previous chapter, we briefly discussed how the renormalization of the strong and the Yukawa couplings render these coefficients UV finite, leaving only IR divergences. In the following section, we demonstrate them in detail by considering the case of $b\bar{b} \rightarrow H$ process.

3.3.2 Ultraviolet renormalization

Beyond LO, the scalar function C_2 computed in powers of the bare coupling constant \hat{a}_s encounters UV and IR divergences. In this section, we describe how to deal with UV divergences. Perturbative expansion of the amplitude for the aforementioned process in terms of the bare strong and Yukawa couplings is given by:

$$\mathcal{M}_{ij} = \left(\frac{\hat{\lambda}_b}{\mu_0^{\epsilon/2}} S_\epsilon \right)^2 \left[\hat{\mathcal{M}}_{ij}^{(0)} + \left(\frac{\hat{a}_s}{\mu_0^\epsilon} S_\epsilon \right) \hat{\mathcal{M}}_{ij}^{(1)} + \left(\frac{\hat{a}_s}{\mu_0^\epsilon} S_\epsilon \right)^2 \hat{\mathcal{M}}_{ij}^{(2)} + \mathcal{O}(\hat{a}_s^3) \right], \quad (3.17)$$

where $\hat{\mathcal{M}}_{ij}^{(l)}$ is the l^{th} loop unrenormalized amplitude. Note that the entire amplitude is proportional to the square of $\hat{\lambda}_b$, the bare Yukawa coupling. Similarly, the coefficient C_2 replicates similar perturbative expansion of the following form,

$$C_2 = \left(\frac{\hat{\lambda}_b}{\mu_0^{\epsilon/2}} S_\epsilon \right)^2 \left[\hat{C}_2^{(0)} + \left(\frac{\hat{a}_s}{\mu_0^\epsilon} S_\epsilon \right) \hat{C}_2^{(1)} + \left(\frac{\hat{a}_s}{\mu_0^\epsilon} S_\epsilon \right)^2 \hat{C}_2^{(2)} + \mathcal{O}(\hat{a}_s^3) \right]. \quad (3.18)$$

To perform the UV renormalization of the amplitudes we use the modified minimal subtraction (\overline{MS}) scheme, where the renormalized strong coupling constant a_s is related to the bare strong coupling constant, \hat{a}_s , through the renormalization constant $Z(\mu_R^2, \epsilon)$ at the renormalization scale μ_R as

$$\frac{\hat{a}_s}{\mu_0^\epsilon} S_\epsilon = \frac{a_s}{\mu_R^\epsilon} Z_{a_s}(\mu_R^2, \epsilon), \quad (3.19)$$

where The scale μ_0 is an arbitrary mass scale introduced to make \hat{g}_s dimensionless in d -dimensions. The coupling renormalization constant $Z(\mu_R^2, \epsilon)$ up to four loop is given by Eq.(2.45). The constants β_0 and β_1 are the coefficients of β function which, for n_f light quark flavors, are given in Eq.(2.15).

Similar to \hat{a}_s , the Yukawa coupling constant $\hat{\lambda}_b$ needs to be renormalized as well, as explained in Sec.[2.3.1]. This has been done as shown below at the renormalization scale

μ_R :

$$\begin{aligned} \frac{\hat{\lambda}_b}{\mu_0^{\epsilon/2}} S_\epsilon &= \frac{\lambda_b}{\mu_R^{\epsilon/2}} Z_\lambda(\mu_R^2, \epsilon) \\ &= \frac{\lambda_b}{\mu_R^{\epsilon/2}} \left[1 + a_s \left(\frac{1}{\epsilon} Z_{\lambda,1}^{(1)} \right) + a_s^2 \left(\frac{1}{\epsilon^2} Z_{\lambda,2}^{(2)} + \frac{1}{\epsilon} Z_{\lambda,1}^{(2)} \right) + \mathcal{O}(a_s^3) \right], \end{aligned} \quad (3.20)$$

where $\lambda_b(\mu_R^2)$ is the renormalized Yukawa coupling and the coefficients $Z_{\lambda,j}^{(i)}$ are given by

$$Z_{\lambda,1}^{(1)} = 6C_F, \quad Z_{\lambda,2}^{(2)} = 18C_F^2 + 6\beta_0 C_F, \quad Z_{\lambda,1}^{(2)} = \frac{3}{2}C_F^2 + \frac{97}{6}C_F C_A - \frac{10}{3}C_F n_f T_F. \quad (3.21)$$

Having the strong as well as Yukawa coupling renormalized, now we can express the coefficient C_2 in terms of the renormalized couplings:

$$C_2 = \left(\frac{\lambda_b}{\mu_R^{\epsilon/2}} \right)^2 \left[C_2^{(0)} + a_s C_2^{(1)} + a_s^2 C_2^{(2)} + \mathcal{O}(a_s^3) \right]. \quad (3.22)$$

where the coefficients $C_2^{(l)}$ are obtained using Eq. (3.19) and (3.20) in Eq. (3.18) and comparing with Eq. (3.22):

$$\begin{aligned} C_2^{(0)} &= \hat{C}_2^{(0)}, \\ C_2^{(1)} &= \frac{12}{\epsilon} C_F \hat{C}_2^{(0)} + \frac{1}{\mu_R^\epsilon} \hat{C}_2^{(1)}, \\ C_2^{(2)} &= \left[\frac{12}{\epsilon^2} (6C_F^2 + \beta_0 C_F) + \frac{1}{\epsilon} \left(3C_F^2 + \frac{97}{3} C_F C_A - \frac{20}{3} C_F n_f T_F \right) \right] \hat{C}_2^{(0)} \\ &\quad + \frac{2}{\mu_R^\epsilon} \left[\frac{\beta_0}{\epsilon} + \frac{6C_F}{\epsilon} \right] \hat{C}_2^{(1)} + \frac{1}{\mu_R^{2\epsilon}} \hat{C}_2^{(2)}. \end{aligned} \quad (3.23)$$

These constants $C_2^{(l)}$, $l = 0, 1, 2$, are now UV finite. However, they are sensitive to IR divergences which will be the topic of our next section.

3.3.3 Infrared divergences and their factorization

Besides UV divergences, the amplitudes beyond LO suffer from infrared divergences, particularly soft and collinear type divergences. The soft ones arise from the soft gluons and the collinear from the massless quarks and gluons in the loops. The details of IR divergences and how we resolve them are given in Sec.[2.1.3].

While all the IR divergences that appear in the amplitudes do not pose any problem for the physical observables, they provide valuable information about the universal structure of the IR divergences in QCD amplitudes. In fact, it can be shown that these divergences systematically factor out from the amplitudes to all orders in perturbation theory [141, 142]. These factored IR divergences demonstrate the universal structure in terms of certain soft and collinear anomalous dimensions. An elegant proposal was put forth by Catani, who predicted IR pole structure of the amplitudes up to two-loop level in non-abelian gauge theory [3]. He demonstrated that the n -particle QCD amplitudes factorize in terms of the universal IR subtraction operator denoted by \mathcal{I} . This \mathcal{I} -operator has a dipole structure [3] containing process independent universal cusp and collinear anomalous dimensions. Thanks to the wealth of results from two-loop calculations of the three-parton $q\bar{q}g$ amplitudes [143] and $2 \rightarrow 2$ scattering amplitudes [144–146], that involve non-trivial color structures [146, 147], the \mathcal{I} -operator is completely known up to two-loop level. In [148], the authors provide further insight on the factorization and resummation properties of QCD amplitudes in the light of Catani’s proposal and demonstrate a connection between divergences governed by soft and collinear anomalous dimensions, see also [149, 150]. Following [3] we express one and two-loop UV renormalized amplitudes in terms of the \mathcal{I} -operator as

$$\begin{aligned}
C_2^{(0)}(\epsilon) &= C_2^{(0),\text{fin}}(\epsilon), \\
C_2^{(1)}(\epsilon) &= 2\mathcal{I}_b^{(1)}(\epsilon)C_2^{(0)}(\epsilon) + C_2^{(1),\text{fin}}(\epsilon), \\
C_2^{(2)}(\epsilon) &= 4\mathcal{I}_b^{(2)}(\epsilon)C_2^{(0)}(\epsilon) + 2\mathcal{I}_b^{(1)}(\epsilon)C_2^{(1)}(\epsilon) + C_2^{(2),\text{fin}}(\epsilon).
\end{aligned} \tag{3.24}$$

The matrix elements of the subtraction operator for the bottom quark, \mathcal{I}_b are given by

$$\begin{aligned}\mathcal{I}_b^{(1)}(\epsilon) &= \frac{e^{-\frac{\epsilon}{2}\gamma_E}}{\Gamma(1+\epsilon/2)} \left(-\frac{4C_F}{\epsilon^2} + \frac{3C_F}{\epsilon} \right) \left(-\frac{s}{\mu_R^2} \right)^{\frac{\epsilon}{2}}, \\ \mathcal{I}_b^{(2)}(\epsilon) &= -\frac{1}{2}\mathcal{I}_b^{(1)}(\epsilon) \left(\mathcal{I}_b^{(1)}(\epsilon) - \frac{2\beta_0}{\epsilon} \right) + \frac{e^{\frac{\epsilon}{2}\gamma_E} \Gamma(1+\epsilon)}{\Gamma(1+\epsilon/2)} \left(-\frac{\beta_0}{\epsilon} + K \right) \mathcal{I}_b^{(1)}(2\epsilon) + 2H_b^{(2)}(\epsilon),\end{aligned}\tag{3.25}$$

with K [3] and $H_b^{(2)}$ [148] are given as follows:

$$\begin{aligned}K &= \left(\frac{67}{18} - \frac{\pi^2}{6} \right) C_A - \frac{10}{9} n_f T_F, \\ H_b^{(2)} &= \left(-\frac{s}{\mu_R^2} \right)^\epsilon \frac{e^{-\frac{\epsilon}{2}\gamma_E}}{\Gamma(1+\epsilon/2)} \frac{1}{\epsilon} \left[C_A C_F \left(-\frac{245}{432} + \frac{23}{16} \zeta_2 - \frac{13}{4} \zeta_3 \right) \right. \\ &\quad \left. + C_F^2 \left(\frac{3}{16} - \frac{3}{2} \zeta_2 + 3\zeta_3 \right) + C_F n_f \left(\frac{25}{216} - \frac{1}{8} \zeta_2 \right) \right].\end{aligned}\tag{3.26}$$

We simplified the expressions $C_2^{(i),\text{fin}}(\epsilon)$ at the level of color factor and also for each color factor, in terms of the *uniform transcendentality*. We find, the resulting expressions are free of IR divergences and hence are finite as $\epsilon \rightarrow 0$. This is following Catani's predictions for the IR poles, which serves as an important check on the correctness of our computation. Although the singlet contributions, which are proportional to the color factor $C_F n_b T_F$, for $n_b = 1$, develops IR divergences at the intermediate stages of the computation, they cancel among themselves to give rise to a finite piece. This is consistent with the IR pole structure predicted by Catani. The finite coefficients, $C_2^{(i),\text{fin}}$, $i = 1, 2$, obtained in Eq. (3.24) contain multiple classical polylogarithms, which are functions of the scaling variables x and y . These polylogarithms can be attributed to different transcendental weights. We present these finite coefficients $C_2^{(i),\text{fin}}, i = 0, 1, 2$ in the attachment with the arXiv submission of [70]

3.4 Inclusive Cross Section up to NNLO

In this section, we describe in detail the computation of inclusive cross section up to NNLO level for producing a pair of Higgs bosons resulting from class-A and class-B diagrams. The hadronic cross section can be expressed in terms of partonic cross sections appropriately convoluted with the corresponding bare parton distribution functions $\hat{f}_{a_i}(x_i)$, $i = 1, 2$ as

$$\sigma^{HH} = \sum_{a_1, a_2} \int dx_1 \hat{f}_{a_1}(x_1) \int dx_2 \hat{f}_{a_2}(x_2) \hat{\sigma}_{a_1 a_2}^{HH}(x_1, x_2, m_h^2), \quad (3.27)$$

where x_i are the momentum fractions of initial state partons and $a_{1,2} = q, \bar{q}, g$. $\hat{\sigma}_{a_1 a_2}^{HH}$ is the UV finite partonic cross section for producing a pair of Higgs bosons along with n_X number of colored particles (partons) through the reactions $a_1(p_1) + a_2(p_2) \rightarrow H(q_1) + H(q_2) + X(k_c)$ and is obtained using

$$\hat{\sigma}_{a_1 a_2}^{HH} = \frac{1}{2s} \prod_{n=1}^2 \int d\phi(q_n) \prod_{c=1}^{n_X} \int d\phi(k_c) \overline{\sum} |\mathcal{M}_{a_1 a_2}|^2 (2\pi)^d \delta^d(p_1 + p_2 - \sum_{n=1}^2 q_n - \sum_{c=1}^{n_X} k_c) \quad (3.28)$$

where p_i, q_i and k_c are the momenta of incoming partons, final state Higgs bosons and partons respectively. In d -dimensions, the phase space measure $d\phi(p)$ of a final state particle with momentum p and mass m is given by

$$d\phi(p) = \frac{d^{d-1} \vec{p}}{(2\pi)^{d-1} 2p^0} \quad (3.29)$$

where $p^0 = \sqrt{m^2 + |\vec{p}|^2}$. $\mathcal{M}_{a_1 a_2}$ is the amplitude for the process $a_1(p_1) + a_2(p_2) \rightarrow H(q_1) + H(q_2) + X(k_c)$ and is calculable order by order in perturbative QCD. The symbol $\overline{\sum}$ indicates that we have to sum over all the quantum numbers of final states, average over initial states and finally include the symmetry factor for final state identical particles. For

convenience, we classify the partonic channels that contribute to $\mathcal{M}_{a_1 a_2}$ into class-A and class-B. We find that these channels do not interfere for the case of inclusive cross section and the invariant mass distribution of Higgs boson pairs. Hence, the hadronic cross section in Eq.(3.27) decompose as:

$$\sigma^{HH} = \sigma_A^{HH} + \sigma_B^{HH} \quad (3.30)$$

We treat them separately and are discussed in the following sections.

3.4.1 Cross section for class-A diagrams

For the class-A diagrams, the amplitude $\mathcal{M}_{a_1 a_2}$ factorizes into a product of two sub amplitudes, where one of them describes the production of a single Higgs boson with virtuality, q^2 and the other encapsulates its decay to a pair of on-shell Higgs bosons. By suitably factorizing the phase space we can describe the entire reaction as a continuous process of producing a single off-shell boson with different virtualities, subsequently decaying to a pair of on-shell Higgs bosons. In other words, we can write $\hat{\sigma}_{a_1 a_2}^{HH}$ for class-A diagrams as

$$\hat{\sigma}_{A, a_1 a_2}^{HH} = \int \frac{dq^2}{2\pi} \hat{\sigma}_{A, a_1 a_2}^{H^*}(x_1, x_2, q^2) |\mathcal{P}_H(q^2)|^2 2q\Gamma_A^{H^* \rightarrow HH}(q^2) \quad (3.31)$$

where the $\mathcal{P}_H(q^2)$ is the Higgs boson propagator, given by

$$\mathcal{P}_H(q^2) = \frac{i}{q^2 - m_h^2 + i\Gamma_h m_h} \quad (3.32)$$

with Γ_h , the decay width of the Higgs boson. The cross section that describes the production of a Higgs boson with virtuality q^2 is given by

$$\hat{\sigma}_{A, a_1 a_2}^{H^*}(x_1, x_2, q^2) = \frac{1}{2s} \prod_{c=1}^{n_X} \int d\phi(k_c) \int d\phi(q) \overline{\sum} |\mathcal{M}_{A, a_1 a_2}^{H^*}|^2 (2\pi)^d \delta^d(p_1 + p_2 - q - \sum_{c=1}^{n_X} k_c). \quad (3.33)$$

Here $\mathcal{M}_{A,a_1a_2}^{H^*}$ is the amplitude for the production of an off-shell Higgs boson with the virtuality q^2 and n_x number of colored particles¹. Similarly, the decay rate $\Gamma_A^{H^* \rightarrow HH}$ is given by

$$\Gamma_A^{H^* \rightarrow HH}(q^2) = \frac{1}{2q} \prod_{n=1}^2 \int d\phi(q_n) \overline{\sum} |\mathcal{M}_A^{H^* \rightarrow HH}|^2 (2\pi)^d \delta^d(q - \sum_{n=1}^2 q_n), \quad (3.34)$$

with $\mathcal{M}_A^{H^* \rightarrow HH}$ describing its decay into a pair of on-shell Higgs bosons. The decay rate $\Gamma_A^{H^* \rightarrow HH}$ is straightforward to compute and in 4-dimensions it is found to be

$$\Gamma_A^{H^* \rightarrow HH}(q^2) = \frac{9\beta(q^2)m_h^4}{32\pi v^2 q}, \quad \beta(q^2) = \sqrt{1 - \frac{4m_h^2}{q^2}}. \quad (3.35)$$

Substituting Eq. (3.31) in Eq. (3.27) and using Eqs. (3.33, 3.34), we obtain σ_A^{HH} in Eq. (3.30):

$$\sigma_A^{HH} = \int \frac{dq^2}{2\pi} D_H(q^2) \sigma_A^{H^*}(q^2) \quad (3.36)$$

with

$$\begin{aligned} \sigma_A^{H^*}(q^2) &= \sum_{a_1, a_2} \int dx_1 \hat{f}_{a_1}(x_1) \int dx_2 \hat{f}_{a_2}(x_2) \hat{\sigma}_{A,a_1a_2}^{H^*}(z, q^2) \\ D_H(q^2) &= 2q \Gamma_A^{H^* \rightarrow HH}(q^2) |\mathcal{P}_H(q^2)|^2 \end{aligned} \quad (3.37)$$

where the partonic scaling variable $z = q^2/s$. Note that $\sigma_A^{H^*}$ is known exactly up to NNLO level [130] and N³LO level [40, 63] in the soft plus virtual approximation for on-shell production of single Higgs boson. Hence, following [130], we can express $\sigma_A^{H^*}(q^2)$ in terms of IR finite coefficients convoluted with renormalized parton distribution functions

¹Note here that, the notation q in the delta function in Eq.(3.33) denotes the momentum of system of colorless states and do *not* confuse with the notation given to represent *quarks*

$f_c(x, \mu_F^2)$ as

$$\sigma_A^{H^*}(q^2) = \sigma_0^{H^*}(q^2, \mu_R^2) \sum_{a_1, a_2} \int dx_1 f_{a_1}(x_1, \mu_F^2) \int dx_2 f_{a_2}(x_2, \mu_F^2) z \Delta_{A, a_1 a_2}(z, q^2, \mu_F^2, \mu_R^2) \quad (3.38)$$

where $\sigma_0^{H^*}(q^2, \mu_R^2) = \pi m_b^2(\mu_R^2)/(6q^2 v^2)$. The partonic coefficient function $\Delta_{A, a_1 a_2}$ can be expanded in powers of strong coupling constant as

$$\Delta_{A, a_1 a_2}(z, q^2, \mu_F^2, \mu_R^2) = \sum_{i=0}^{\infty} a_s^i(\mu_R^2) \Delta_{A, a_1 a_2}^{(i)}(z, q^2, \mu_F^2, \mu_R^2). \quad (3.39)$$

Substituting Eq. (3.38) in Eq. (3.36) and making suitable change of variables, we obtain

$$\sigma_A^{HH} = \sum_{a_1 a_2} \int_{\tau}^1 \frac{dx}{2\pi} \Phi_{a_1 a_2}(x, \mu_F^2) \int_{\frac{\tau}{x}}^1 dz \left[\sigma_0^{H^*}(q^2, \mu_R^2) D_H(q^2) \Delta_{A, a_1 a_2}(z, q^2, \mu_F^2, \mu_R^2) \right]_{q^2 = xzS} \quad (3.40)$$

where $\tau = 4m_b^2/S$, $S = s/x_1 x_2$, the hadronic center of mass energy of incoming hadrons and the partonic flux $\Phi_{a_1 a_2}(x, \mu_F^2)$ is given by

$$\Phi_{a_1 a_2}(x, \mu_F^2) = \int_x^1 \frac{dy}{y} f_{a_1}(y, \mu_F^2) f_{a_2}\left(\frac{x}{y}, \mu_F^2\right). \quad (3.41)$$

In the next section, we use Eq. (3.40) to obtain the numerical impact of class-A diagrams to the inclusive production cross section.

3.4.2 Cross section for class-B diagrams

We now describe how the contributions from class-B diagrams in Eq. (3.30) can be obtained. Since class-B diagrams comprise t - and u - channels, the corresponding amplitudes do not factorize like class-A diagrams. This makes the computation technically more challenging beyond NLO level. However, one can obtain certain dominant contri-

butions of class-B processes resulting from soft gluon emission as they are process independent. Using the contributions from soft gluons, as described in Sec.[2.3.1], and those from the two-loop virtual processes computed in the previous sections, we can readily calculate the soft plus virtual contribution up to NNLO level, a first step towards obtaining the total NNLO contribution from class-B.

For the class-B, the leading order contribution results from the Born process $b+\bar{b} \rightarrow H+H$ contain t and u channels. At NLO, one loop virtual corrections to Born and real emission processes $b + \bar{b} \rightarrow H + H + g$ and $b(\bar{b}) + g \rightarrow H + H + b(\bar{b})$ contribute. The UV divergences that are present in the virtual processes to Born processes are removed using \overline{MS} renormalization scheme. The soft and final state collinear divergences in both virtual as well as real emission processes cancel among each other while the initial state collinear divergences are factored out and absorbed into bare bottom quark densities in the \overline{MS} scheme through the mass factorization. For the sub-process $b(\bar{b}) + g \rightarrow H + H + b(\bar{b})$, we encounter only collinear divergences, and they are removed by mass factorization. We achieve this by using the semi-analytical method, namely the two cut off phase space slicing [151], which is summarised in the section below.

NLO corrections to class B: Phase space slicing approach

In this section, we summarise the computation of NLO corrections of class-B diagrams using the *phase space slicing* approach. The same approach has been used for the first computation of NLO correction to the production of a pair of Higgs bosons in bottom quark annihilation process [1]. In this method, for the real process $b+\bar{b} \rightarrow H+H+g$, two slicing parameters δ_s and δ_c are introduced to separate three-body phase space into *soft*, *hard collinear* and *hard non-collinear regions*. Whereas, for the real process $g + b(\bar{b}) \rightarrow H + H + b(\bar{b})$, we need to introduce only δ_c as these are free from soft divergences. The slicing parameter δ_s divides the real emission phase space into soft and hard regions. Soft region is the part of phase space where the energy of gluon in the center-of-mass frame of

incoming partons is required to be less than $\delta_s \sqrt{s}/2$, and the rest is called hard region. The latter contains collinear configurations where the two massless partons become collinear to each other, leading to collinear singularities. Similarly, the δ_c is used to divide the hard region into *hard-collinear* and *hard non-collinear* regions denoted respectively by \mathcal{HC} and $\overline{\mathcal{HC}}$. Keeping these slicing parameters δ_s and δ_c infinitesimally small, the virtual loop integrals and the soft and collinear sensitive phase space integrals are computed within the method of dimensional regularization. The corresponding singularities show up as poles in dimensional regularization parameter ϵ .

We describe below the essential steps that are followed in dealing with IR singularities in phase space slicing method. We start with UV finite hadronic cross section at NLO level, denoted by $d\sigma^{HH+1}$. It gets contribution from real emission partonic sub-process $a_1 + a_2 \rightarrow HH + a_3$ where the final state consists of a pair of Higgs bosons HH and a_3 , a single partonic state. We divide the phase space of a_3 into three regions using two slicing parameters as

$$d\sigma^{HH+1}(\delta_s, \delta_c, \epsilon) = d\sigma^{HH,S}(\delta_s, \epsilon) + d\sigma^{HH,\mathcal{HC}}(\delta_s, \delta_c, \epsilon) + d\sigma^{HH,\overline{\mathcal{HC}}}(\delta_s, \delta_c). \quad (3.42)$$

The soft ($d\sigma^{HH,S}(\delta_s, \epsilon)$) and hard-collinear ($d\sigma^{HH,\mathcal{HC}}(\delta_s, \delta_c, \epsilon)$) contributions can be computed analytically when the slicing parameters are infinitesimally small within the dimensional regularization. Soft and collinear singularities appear as poles in ϵ and are cancelled against those resulting from the virtual diagrams as well as from the counterterms that are used to perform mass factorization. In other words, the following sum, denoted by $d\sigma_{\text{NLO}}^{HH}$ is finite as $\epsilon \rightarrow 0$:

$$d\sigma_{\text{NLO}}^{HH}(\mu_F^2) = d\sigma^{HH,\mathcal{V}}(\epsilon) + d\sigma^{HH+1}(\delta_s, \delta_c, \epsilon) + d\sigma^{HH,\text{CT}}(\delta_s, \delta_c, \epsilon, \mu_F^2) \quad (3.43)$$

where $d\sigma^{HH,\mathcal{V}}(\epsilon)$ is the contribution from virtual corrections to Born level processes. The counter term $d\sigma^{HH,\text{CT}}(\delta_s, \delta_c, \epsilon, \mu_F^2)$ that removes the initial state collinear singularities is

defined at the factorization scale μ_F . While the sum given by

$$d\sigma^{S+\mathcal{V}+\mathcal{H}C+\text{CT}}(\delta_s, \delta_c, \mu_F^2) = d\sigma^{HH,S}(\delta_s, \epsilon) + d\sigma^{HH,\mathcal{V}}(\epsilon) \\ + d\sigma^{HH,\mathcal{H}C}(\delta_s, \delta_c, \epsilon) + d\sigma^{HH,\text{CT}}(\delta_s, \delta_c, \epsilon, \mu_F^2). \quad (3.44)$$

is free from soft and collinear poles in ϵ , it depends on the slicing parameters. However, when the above sum is added to the hard non-collinear contributions ($d\sigma^{HH,\overline{\mathcal{H}C}}$), that is,

$$d\sigma_{\text{NLO}}^{HH}(\mu_F^2) = \lim_{\delta_s, \delta_c \rightarrow 0} \left(d\sigma^{S+\mathcal{V}+\mathcal{H}C+\text{CT}}(\delta_s, \delta_c) + d\sigma^{HH,\overline{\mathcal{H}C}}(\delta_s, \delta_c) \right) \quad (3.45)$$

the resulting contribution, Eq. (3.45), is guaranteed to be independent of the slicing parameters in the limit when they are taken to be infinitesimally small. For the sub-process, $g + b(\bar{b}) \rightarrow H + H + b(\bar{b})$, we encounter only collinear divergences and hence we require a single slicing parameter δ_c to obtain infrared safe observable.

For completeness, we present the individual contributions that are required in phase space slicing method to obtain inclusive cross section up to NLO level from class B diagrams. The virtual contribution for the sub-process initiated by b and \bar{b} is found to be

$$d\sigma^{HH,\mathcal{V}} = a_s(\mu_F^2) \left(\frac{s}{\mu_F^2} \right)^{\frac{\epsilon}{2}} \frac{\Gamma(1 + \frac{\epsilon}{2})}{\Gamma(1 + \epsilon)} dx_1 dx_2 \left[C_F \left(-\frac{16}{\epsilon^2} + \frac{12}{\epsilon} \right) \right. \\ \times d\sigma_{bb}^{HH,(0)}(x_1, x_2, \epsilon) (f_b(x_1) f_{\bar{b}}(x_2) + (x_1 \leftrightarrow x_2)) \\ \left. + d\sigma_{bb,\text{fin}}^{HH,\mathcal{V}}(x_1, x_2, \epsilon) (f_b(x_1) f_{\bar{b}}(x_2) + (x_1 \leftrightarrow x_2)) \right] \quad (3.46)$$

after setting renormalization scale $\mu_R = \mu_F$. The finite part of the virtual corrections, $d\sigma_{bb,\text{fin}}^{HH,\mathcal{V}}$ can be obtained in terms of C_2 given in Eq. (3.14). The soft contribution is given by

$$d\sigma^{HH,S} \simeq a_s(\mu_F^2) \left(\frac{s}{\mu_F^2} \right)^{\frac{\epsilon}{2}} \frac{\Gamma(1 + \frac{\epsilon}{2})}{\Gamma(1 + \epsilon)} C_F \left(\frac{16}{\epsilon^2} + \frac{16 \ln \delta_s}{\epsilon} + 8 \ln^2 \delta_s \right)$$

$$\times \left(d\sigma_{b\bar{b}}^{HH,(0)}(x_1, x_2, \epsilon) f_b(x_1) f_{\bar{b}}(x_2) + (x_1 \leftrightarrow x_2) \right) dx_1 dx_2. \quad (3.47)$$

The sum of hard-collinear and counter term contributions from both $b\bar{b}$ annihilation and $gb(\bar{b})$ scattering processes, is found to be:

$$\begin{aligned} d\sigma^{\mathcal{HC}+\text{CT}} &= a_s(\mu_F^2) \left(\frac{s}{\mu_F^2} \right)^{\frac{\epsilon}{2}} \frac{\Gamma(1 + \frac{\epsilon}{2})}{\Gamma(1 + \epsilon)} dx_1 dx_2 \\ &\times \left[d\sigma_{b\bar{b}}^{HH,(0)}(x_1, x_2, \epsilon) \left\{ \frac{1}{2} f_b(x_1, \mu_F^2) \tilde{f}_{\bar{b}}(x_2, \mu_F^2) + \frac{1}{2} \tilde{f}_{\bar{b}}(x_1, \mu_F) f_b(x_2, \mu_F^2) \right. \right. \\ &\left. \left. + 2 \left(-\frac{1}{\epsilon} + \frac{1}{2} \ln \frac{s}{\mu_F^2} \right) A_{b \rightarrow b+g} f_{\bar{b}}(x_1, \mu_F) f_b(x_2, \mu_F) + (x_1 \leftrightarrow x_2) \right\} \right]. \quad (3.48) \end{aligned}$$

Using the diagonal splitting function $P_{bb}(z)$, we find

$$A_{b \rightarrow b+g} \equiv \int_{1-\delta_s}^1 \frac{dz}{z} P_{bb}(z) = 4C_F \left(2 \ln \delta_s + \frac{3}{2} \right), \quad (3.49)$$

and from the non-diagonal ones, we obtain

$$\tilde{f}_{\bar{b}}(x, \mu_F^2) = \int_x^{1-\delta_s} \frac{dz}{z} f_b\left(\frac{x}{z}, \mu_F^2\right) \tilde{P}_{bb}(z) + \int_x^1 \frac{dz}{z} f_g\left(\frac{x}{z}, \mu_F^2\right) \tilde{P}_{bg}(z), \quad (3.50)$$

with

$$\tilde{P}_{ij}(z) = P_{ij}(z) \ln \left(\delta_c \frac{1-z}{z} \frac{s}{\mu_F^2} \right) + 2P'_{ij}(z), \quad (3.51)$$

where $P'_{ij}(z)$ [151] are ϵ dependent part of splitting functions, that is

$$P_{ij}(z, \epsilon) = P_{ij}(z) + \epsilon P'_{ij}(z). \quad (3.52)$$

Adding all the order a_s pieces together: the virtual cross section $d\sigma^{HH,\mathcal{V}}$ in Eq. (3.46), the soft piece $d\sigma^{HH,S}$ in Eq. (3.47) and the mass factorized hard-collinear contribution $d\sigma^{HH,\mathcal{HC}+\text{CT}}$ as given in Eq. (3.48), we find that the poles in ϵ cancel in the sum given in Eq. (3.45) giving IR finite NLO contribution from class-B diagrams.

NNLO corrections to class B: Soft-Virtual approach

Going beyond NLO for the class-B diagrams requires a dedicated computation taking into account pure virtual contributions presented in last section, the double real and single real-virtual contributions. The inclusion of the later contributions is beyond the scope of the present work. However, we can compute the SV contribution resulting from class-B diagrams. To achieve this, we follow the general formalism presented in Sec.[2.3.1], which is applicable to both classes of diagrams.

We begin with the UV finite partonic cross section for producing a pair of Higgs bosons and n_X partons, namely for the process $b(p_1) + \bar{b}(p_2) \rightarrow H(q_1) + H(q_2) + X(k_c)$,

$$\hat{\sigma}_{b\bar{b}} = \frac{1}{2s} \prod_{n=1}^2 \int d\phi(q_n) \prod_{c=1}^{n_X} \int d\phi(k_c) \overline{\sum} |\mathcal{M}_{b\bar{b}}|^2 (2\pi)^d \delta^d\left(p_1 + p_2 - \sum_{n=1}^2 q_n - \sum_{c=1}^{n_X} k_c\right) \quad (3.53)$$

where c counts the number of partons in the final state. The dominant soft gluon contributions to partonic reactions are proportional to terms such as $\delta(1-z)$ and $+$ distributions of kind $\mathcal{D}_j(z) \equiv \left[\frac{\ln(1-z)}{1-z}\right]_+$. Such contributions result only from bottom quark annihilation sub-processes. They themselves do not constitute infrared safe observables until we include pure virtual contributions and mass factorization counter-terms. The resulting one is called SV contribution.

In the soft limit, the square of the real emission partonic matrix elements factorises into hard and soft parts and similarly the phase space splits into their respective parts. The soft part when combined with the pure virtual corrections and the mass factorization counter terms, will give infrared safe SV part of the cross section:

$$\begin{aligned} \hat{\sigma}_{b\bar{b}}^{\text{sv}} &= \int \frac{dq^2}{q^2} \frac{1}{2s} \prod_{n=1}^2 \int d\phi(q_n) \overline{\sum} |\mathcal{M}_{b\bar{b}}^{(0)}|^2 (2\pi)^d \delta^d\left(p_1 + p_2 - \sum_n q_n\right) \\ &\quad \times \int d\phi(q) \prod_{c=1}^{n_X} \int d\phi(k_c) \overline{\sum} |\mathcal{M}^{\text{sv}}|^2 (2\pi)^d \delta^d\left(p_1 + p_2 - q - \sum_c k_c\right) \end{aligned} \quad (3.54)$$

where $\mathcal{M}_{b\bar{b}}^{(0)}$ is the Born amplitude for producing a pair of Higgs bosons in bottom quark annihilation and \mathcal{M}^{sv} is the SV part of amplitude $\mathcal{M}_{b\bar{b}}$. The second line of the above equation can be computed order by order in perturbation theory for any colorless state with momentum q in a process independent way as the amplitude for the production of a pair of Higgs bosons factorises out at every order. Beyond LO, the virtual corrections to Born amplitudes and multiple soft gluon emissions arising from tree level as well as from loop corrected amplitudes contribute to the SV. While the singularities from soft gluons cancel between real and virtual amplitudes, the initial state collinear singularities can be removed only after adding appropriate mass factorization counter terms computed in the soft limit at the factorization scale μ_F . The resulting hadronic cross section will be free of soft and collinear singularities:

$$\begin{aligned} \sigma^{\text{HH,sv}} &= \int \frac{dq^2}{q^2} \sum_{b,\bar{b}} \int dx_1 f_b(x_1, \mu_F^2) \int dx_2 f_{\bar{b}}(x_2, \mu_F^2) \frac{1}{2s} \prod_{n=1}^2 \int d\phi(q_n) \\ &\times (2\pi)^d \delta^d\left(p_1 + p_2 - \sum_{n=1}^2 q_n\right) \overline{\sum}_{i=A,B} \sum_{i=A,B} \Delta_{i,b}^{\text{sv}}(\{p_j \cdot q_k\}, z, q^2, \mu_F^2, \mu_R^2) \end{aligned} \quad (3.55)$$

where $z = q^2/s$, i runs over both the classes of diagrams. Following the threshold framework in Sec.[2.3.1], the finite coefficients $\Delta_{i,b}^{\text{sv}}$ can be computed order by order in perturbation theory using one and two-loop virtual amplitudes, soft distribution function and diagonal mass factorization kernels. We expand $\Delta_{i,b}^{\text{sv}}$ in powers of strong coupling constant as,

$$\Delta_{i,b}^{\text{sv}} = \sum_{j=0}^{\infty} a_s^j(q^2) \Delta_{i,b}^{\text{sv},(j)}(q^2) \quad (3.56)$$

where we have set $\mu_R^2 = \mu_F^2 = q^2$. The coefficients, $\Delta_{i,b}^{\text{sv},(j)}$ for $j = 0, 1, 2$ can be expressed in terms of the cusp A_j^q , the soft f_j^q and the collinear B_j^q anomalous dimensions that are present in the virtual amplitudes and in the soft distribution function [40]:

$$\Delta_{i,b}^{\text{sv},(0)} = \delta(1-z) |\mathcal{M}_{i,0}^{(0)}|^2,$$

$$\begin{aligned}
\Delta_{i,b}^{\text{sv},(1)} &= \delta(1-z) \left\{ |\mathcal{M}_{i,0}^{(0)}|^2 \left(2\overline{\mathcal{G}}_1^{q,1} \right) + \mathcal{M}_{i,0}^{(1)} \mathcal{M}_{i,0}^{\star(0)} + \mathcal{M}_{i,0}^{(0)} \mathcal{M}_{i,0}^{\star(1)} \right\} + \mathcal{D}_0(z) |\mathcal{M}_{i,0}^{(0)}|^2 \left(-2f_1^q \right) \\
&\quad + \mathcal{D}_1(z) |\mathcal{M}_{i,0}^{(0)}|^2 \left(4A_1^q \right), \\
\Delta_{i,b}^{\text{sv},(2)} &= \delta(1-z) \left\{ |\mathcal{M}_{i,0}^{(1)}|^2 + |\mathcal{M}_{i,0}^{(0)}|^2 \left(\overline{\mathcal{G}}_2^{q,1} + 2(\overline{\mathcal{G}}_1^{q,1})^2 + 2\beta_0 \overline{\mathcal{G}}_1^{q,2} - 8\zeta_3 A_1^q f_1^q \right) \right. \\
&\quad - 2\zeta_2 (f_1^q)^2 - \frac{4}{5} \zeta_2^2 (A_1^q)^2 + \mathcal{M}_{i,0}^{(2)} \mathcal{M}_{i,0}^{\star(0)} + \mathcal{M}_{i,2}^{(1)} \mathcal{M}_{i,-2}^{\star(1)} \\
&\quad + \mathcal{M}_{i,2}^{(1)} \mathcal{M}_{i,0}^{\star(0)} (4A_1^q) + \mathcal{M}_{i,1}^{(1)} \mathcal{M}_{i,-1}^{\star(1)} + \mathcal{M}_{i,1}^{(1)} \mathcal{M}_{i,0}^{\star(0)} \left(-2f_1^q - 4B_1^q \right) + \mathcal{M}_{i,-1}^{(1)} \mathcal{M}_{i,1}^{\star(1)} \\
&\quad + \mathcal{M}_{i,-2}^{(1)} \mathcal{M}_{i,2}^{\star(1)} + \mathcal{M}_{i,0}^{(1)} \mathcal{M}_{i,0}^{\star(0)} \left(2\overline{\mathcal{G}}_1^{q,1} \right) + \mathcal{M}_{i,0}^{(0)} \mathcal{M}_{i,0}^{\star(2)} + \mathcal{M}_{i,0}^{(0)} \mathcal{M}_{i,2}^{\star(1)} \left(4A_1^q \right) \\
&\quad + \mathcal{M}_{i,0}^{(0)} \mathcal{M}_{i,1}^{\star(1)} \left(-2f_1^q - 4B_1^q \right) + \mathcal{M}_{i,0}^{(0)} \mathcal{M}_{i,0}^{\star(1)} \left(2\overline{\mathcal{G}}_1^{q,1} \right) \left. \right\} + \mathcal{D}_0(z) \left\{ |\mathcal{M}_{i,0}^{(0)}|^2 \left(-2f_2^q - 4f_1^q \overline{\mathcal{G}}_1^{q,1} \right) \right. \\
&\quad - 4\beta_0 \overline{\mathcal{G}}_1^{q,1} + 16\zeta_3 (A_1^q)^2 + 8\zeta_2 A_1^q f_1^q + \mathcal{M}_{i,0}^{(1)} \mathcal{M}_{i,0}^{\star(0)} \left(-2f_1^q \right) + \mathcal{M}_{i,0}^{(0)} \mathcal{M}_{i,0}^{\star(1)} \left(-2f_1^q \right) \left. \right\} \\
&\quad + \mathcal{D}_1(z) \left\{ |\mathcal{M}_{i,0}^{(0)}|^2 \left(4(f_1^q)^2 + 4A_2^q + 8A_1^q \overline{\mathcal{G}}_1^{q,1} + 4\beta_0 f_1^q - 16\zeta_2 (A_1^q)^2 \right) \right. \\
&\quad + \mathcal{M}_{i,0}^{(1)} \mathcal{M}_{i,0}^{\star(0)} \left(4A_1^q \right) + \mathcal{M}_{i,0}^{(0)} \mathcal{M}_{i,0}^{\star(1)} \left(4A_1^q \right) \left. \right\} \\
&\quad + \mathcal{D}_2(z) |\mathcal{M}_{i,0}^{(0)}|^2 \left\{ -12A_1^q f_1^q - 4\beta_0 A_1^q \right\} + \mathcal{D}_3(z) |\mathcal{M}_{i,0}^{(0)}|^2 \left\{ 8(A_1^q)^2 \right\}, \tag{3.57}
\end{aligned}$$

where $\zeta_2 = 1.64493407 \dots$, $\zeta_3 = 1.20205690 \dots$ and $\mathcal{M}_{i,k}^{(j)}$ are obtained from Eq. (3.14) by defining $\mathcal{M}_{mn} = \mathcal{M} \delta_{mn}$ and expanding in powers of ϵ as

$$\mathcal{M}_i^{(j)}(\epsilon) = \sum_{k=-2j}^{\infty} \epsilon^k \mathcal{M}_{i,k}^{(j)}. \tag{3.58}$$

The cusp, collinear and soft anomalous dimensions are given in Appendix B. The universal constants $\overline{\mathcal{G}}_k^{q,(j)}$ for the quark-initiated process are given by:

$$\begin{aligned}
\overline{\mathcal{G}}_1^{q,1} &= C_F (-3\zeta_2), \\
\overline{\mathcal{G}}_1^{q,2} &= C_F \left(\frac{7}{3} \zeta_3 \right), \\
\overline{\mathcal{G}}_2^{q,1} &= C_F n_f \left(-\frac{328}{81} + \frac{70}{9} \zeta_2 + \frac{32}{3} \zeta_3 \right) + C_A C_F \left(\frac{2428}{81} - \frac{469}{9} \zeta_2 + 4\zeta_2^2 - \frac{176}{3} \zeta_3 \right). \tag{3.59}
\end{aligned}$$

Finally, defining $\bar{\Delta}_b^{\text{sv}}(z, q^2, \mu_F^2, \mu_R^2)$ by

$$\begin{aligned} \bar{\Delta}_{b\bar{b}}^{\text{sv}}(z, q^2, \mu_F^2, \mu_R^2) &= \frac{1}{2s} \prod_{n=1}^2 \int d\phi(q_n) (2\pi)^d \delta^d\left(p_1 + p_2 - \sum_{n=1}^2 q_n\right) \\ &\times \sum \overline{|\mathcal{M}_{b\bar{b}}^{(0)}|^2} \sum_{i=1}^2 \Delta_{i,b}^{\text{sv}}(\{p_j \cdot q_k\}, z, q^2, \mu_F^2, \mu_R^2), \end{aligned} \quad (3.60)$$

we obtain $\sigma^{\text{HH,sv}}$:

$$\sigma^{\text{HH,sv}} = \int_{\tau}^1 dx \Phi_{a_1 a_2}(x, \mu_F^2) \int_{\frac{\tau}{x}}^1 dz \bar{\Delta}_{a_1 a_2}^{\text{sv}}(z, q^2, \mu_F^2, \mu_R^2) \Big|_{q^2=xzS}. \quad (3.61)$$

We have used the above formula to study the numerical impact of SV part of the partonic cross section resulting from class-B diagrams up to NNLO level on the inclusive production of a pair of Higgs bosons.

3.5 Phenomenology

In this section, we present in detail the numerical impact of our analytical results obtained in the previous sections. We mainly focus on the inclusive cross section for producing a pair of Higgs bosons at the LHC with the center-of-mass energy $\sqrt{S} = 14$ TeV. We use MMHT2014(68cl) PDF set [152] and the corresponding α_s through the LHAPDF-6 [153] interface at every order in perturbation theory. We use the running bottom quark mass renormalized in \overline{MS} [130] scheme with the boundary condition $\bar{m}_b(m_b) = 4.7$ GeV. Both $\alpha_s(\mu_R^2)$ and $m_b(\mu_R^2)$ at various orders in perturbation theory are evolved using appropriate QCD β -function coefficients and quark mass anomalous dimensions. Similarly, the PDFs are evolved to factorization scale μ_F using the splitting functions computed to desired accuracy in the perturbation theory. We choose the Higgs boson mass $m_h = 125$ GeV and its total decay width $\Gamma_h = 0.001$ GeV. In our analysis, we have included all the partonic channels upto NNLO level for the class-A diagrams while for the class-B, we could do this only up to NLO level, however, at NNLO level we have included SV contributions.

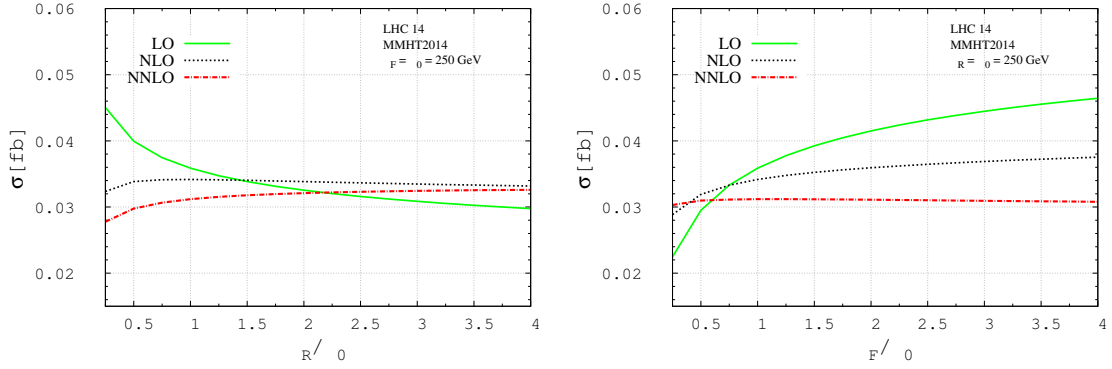


Figure 3.5: The total cross section for di-Higgs production in $b\bar{b}$ annihilation at various order in a_s as a function of (μ_R^2/μ_0^2) on left panel with $\mu_F = \mu_0$ and as a function of (μ_F^2/μ_0^2) on right panel with $\mu_R = \mu_0$ with central scale $\mu_0 = 2m_h$ and $\sqrt{s} = 14$ TeV.

We find that this approximation does not change our conclusion as the dominant contribution results from class-A. To illustrate this point we state some of our observations from our numerical results. We find that the *LO contributions from class-A diagrams are three orders of magnitude larger than those from class-B diagrams*. We also find that NLO contributions change the LO cross section by -1.096% and at the NNLO level the change is about -8.095% . The numerical result manifests the fact that the SV contribution presented in this work not only gets the dominant contribution from class-A but also the stability of our NNLO result for di-Higgs production from the $b\bar{b}$ annihilation channel. We find that the *contribution from bottom quark annihilation processes is three orders of magnitude smaller than from the gluon fusion processes [110]* (See Table 3.1). However, former ones need to be included for the precision studies at the LHC.

Channel	LO[fb]	NLO[fb]	NNLO[fb]
$b\bar{b} \rightarrow H$	0.02821	0.03169	0.02970
$gg \rightarrow H$	17.06	31.89	37.55

Table 3.1: Inclusive total cross section for the di-Higgs production in dominant gluon fusion channel and sub-dominant bottom quark annihilation channel for $\mu_R = \mu_F = m_h/2$.

Having studied the size of the corrections both at NLO and NNLO level, it is important to

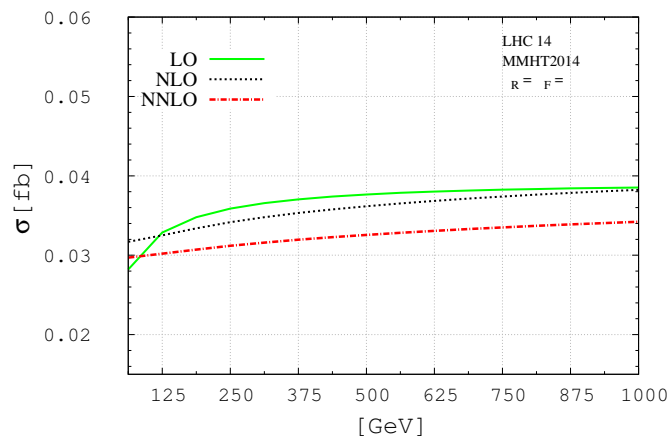


Figure 3.6: The total cross section for di-Higgs production in $b\bar{b}$ annihilation at various order in a_s as a function of the mass scale μ with $(\mu_F = \mu_R = \mu)$ for $\sqrt{s} = 14$ TeV.

quantify the uncertainties resulting from the mass scales introduced in our calculations. Recall that the renormalization of the UV and the initial state collinear divergences enforces the introduction of mass scales namely μ_R and μ_F respectively. The μ_R dependency shows up in the coupling constant $a_s(\mu_R^2)$, the mass $m_b(\mu_R^2)$ and in the mass factorized partonic cross sections at various orders in perturbations theory. The coupling constants are evolved using the appropriate QCD β -function coefficients and quark mass anomalous dimensions. The μ_F scale dependency comes from the PDFs that are evolved using splitting functions computed in the perturbation series. But the cross section, like every other physical observables, is expected to be independent of these arbitrary mass scales. This crude fact manifests the scale independency if we sum the perturbative predictions to all orders in perturbation theory. Since we have truncated the series, there is a residual scale dependency. In the following we aim to study this by varying both μ_R and μ_F scales.

In Fig. 3.5, we show the variation of our fixed order predictions with respect to μ_R (on the left panel) and μ_F (on the right panel) for a particular choice of central scale $\mu_0 = 250$ GeV. We can see that except for the small μ_R and μ_F region, which is in the region below $\mu_R = m_h$, there is an overall reduction of the scale dependency with increasing order of perturbation theory. We observe that both NLO and NNLO results attain a much faster

stability against the variation of the scales than the LO cross section. At the leading order, there are no μ_R or μ_F scale dependent logarithms that can compensate those coming from the Yukawa coupling and parton distribution functions, and hence LO has large scale dependency. However, the inclusion of higher order terms that contain logarithms of

$(\frac{\mu_R}{\kappa m_h}, \frac{\mu_F}{\kappa m_h})$	LO[fb] $\times 10^{-1}$	NLO[fb] $\times 10^{-1}$	NNLO[fb] $\times 10^{-1}$
(2,2)	0.3587	0.3416	0.3119
(2,1)	0.2951	0.3191	0.3098
(1,2)	0.3994	0.3384	0.2976
(1,1)	0.3286	0.3250	0.3020
(1,1/2)	0.2502	0.3032	0.3031
(1/2,1)	0.3704	0.3246	0.2879
(1/2,1/2)	0.2821	0.3169	0.2970

Table 3.2: 7-point scale variation for central scale at $m_h = 125\text{GeV}$, $\kappa = 1$

these scales provide partial cancellation at every order in perturbation theory. Hence the inclusion of NLO and NNLO pieces reduces the dependency on the scales considerably. In Fig. 3.6, we have set $\mu_R = \mu_F$ and varied the cross section with respect to a single scale μ . It can be observed that LO attains stability much faster compared to the case when μ_R is not equal to μ_F . This can be comprehended from Fig. 3.5, where the LO contribution behaves exactly in an opposite way with respect to the variation of both the mass scales. So the stability in the leading order seen in Fig. 3.6 attributes to the fact that there is a significant cancellation happening between the μ_R and μ_F scale variations of the cross section. We also show the 7-point scale variation for the central scale at $m_h = 125\text{ GeV}$ in Table 3.2. This variation spans the entire region from $\mu_R, \mu_F = m_h/2$ to $\mu_R, \mu_F = 2m_h$ and hence captures the uncertainty in this region. The 7-point scale variation for a different value of central scale is also shown in Table 6.4. Table 6.5 contains the %-uncertainty from the scale variation at two different central scales. It can be seen that the leading order cross section has a huge scale uncertainty which implies the unreliability of the result. But the scale dependency starts to reduce when we include the higher order corrections.

$(\frac{\mu_R}{\kappa m_h}, \frac{\mu_F}{\kappa m_h})$	LO[fb] $\times 10^{-1}$	NLO[fb] $\times 10^{-1}$	NNLO[fb] $\times 10^{-1}$
(2,2)	0.3765	0.3617	0.3256
(2,1)	0.3254	0.3384	0.3210
(1,2)	0.4150	0.3594	0.3110
(1,1)	0.3587	0.3416	0.3119
(1,1/2)	0.2951	0.3191	0.3098
(1/2,1)	0.3994	0.3384	0.2976
(1/2,1/2)	0.3286	0.3250	0.3020

Table 3.3: 7-point scale variation for central scale at $m_h = 125\text{GeV}$, $\kappa = 2$

Central Scale(GeV)	LO[fb] $\times 10^{-1}$	NLO[fb] $\times 10^{-1}$	NNLO[fb] $\times 10^{-1}$
125	0.3286 ^{+21.546%} _{-23.859%}	0.3250 ^{+5.108%} _{-6.708%}	0.3020 ^{+3.278%} _{-4.669%}
250	0.3587 ^{+15.696%} _{-17.731%}	0.3416 ^{+5.210%} _{-6.587%}	0.3119 ^{+4.392%} _{-4.585%}

Table 3.4: %-scale uncertainty at LO, NLO and NNLO

3.6 Summary

To summarize, we have systematically computed the inclusive cross section for the production of a pair of Higgs bosons in the bottom quark annihilation up to NNLO level in perturbative QCD. We find that the diagrams contributing at NNLO can be classified to two classes, with no interference terms between them. For obtaining the corrections coming from class-A, we use the result of single Higgs production from bottom annihilation channel. For class-B, the evaluation of full NNLO inclusive corrections are hard to achieve. However, we obtained the correction at the soft limit using the threshold framework explained in chapter 3. We have analyzed these results numerically at the LHC energy, which demonstrates that the inclusion of higher order terms reduces the renormalization and factorization scale uncertainties, and hence making the predictions more reliable.

4 NNLO QCD \oplus QED corrections to Higgs production in $b\bar{b}$ annihilation

In this chapter, we investigate the NNLO corrections resulting from the interference of QCD and QED interactions for the bottom quark induced Higgs productions. We also discuss their general structure using the threshold framework presented in chapter 3. In the process, we obtain the QED mass anomalous dimensions upto second order. The materials presented in this chapter are the result of original research done in collaboration with Pooja Mukherjee, V. Ravindran et.al and are based on the published article [154].

4.1 Prologue

The efforts to compute the observables related to top quarks and Higgs bosons have been going on for a while as these observables are sensitive to high scale physics. Since the dominant contributions to these processes are known to unprecedented accuracy, the inclusion of sub-dominant contributions and radiative corrections is essential for any consistent study. This chapter explores the possibility of including EW corrections to Higgs boson production in bottom quark annihilation, which is sub-dominant. While this is a sub-dominant process at the LHC, in certain BSM contexts, the rates are significantly appreciable, leading to interesting phenomenological studies.

Unlike the dominant channel, which is gluon-induced Higgs boson production, the bot-

tom quark annihilation channel has not received much attention in the context of EW corrections, presumably because it is already sub-dominant at the LHC. The complete EW corrections are much involved. Hence in this chapter, as a first step towards this, we attempt to include the QED corrections to the inclusive production for the aforementioned channel. Though these corrections are sub-dominating for the collider physics, however, from the naive power counting the QED coupling constant $\alpha \sim \alpha_s^2$, where α_s is the QCD one. Hence we expect that, the corrections obtained from this work could be comparable to the fixed [4] and resummed [155] results solely from third order in perturbative QCD.

Recently in [156], a suitable algorithm, called *Abelianization*, has been developed by studying the group theory structure of QCD and QED amplitudes that contribute to the partonic sub-processes of DY production. The algorithm contains a set of transformations on the color factors/Casimirs of $SU(N_c)$ that transforms QCD results for the partonic sub-processes to the corresponding QED results. This way both pure QED and the mixed QCD-QED contributions to inclusive production cross section for the Z boson in DY process have been obtained in [156] at NNLO level. Following this approach, we can in principle proceed to obtain pure QED and mixed QCD-QED contributions to the bottom quark annihilation process from the QCD results. However, in order to scrutinize the very approach of Abelianization, we explicitly compute the pure QED and mixed QCD-QED corrections to inclusive production of the Higgs boson in bottom quark annihilation up to NNLO level in $U(1)$ and $SU(N_c) \times U(1)$. In addition, we reproduce the same for the production of Z boson in DY process.

The computation beyond the leading order involves evaluation of virtual and real emission processes. As discussed before, these contributions are sensitive to UV, soft and collinear divergences. We compute them in dimensional regularization, hence divergences appear as poles in dimensional parameter $\epsilon = d-4$, where d being the space-time dimension. The UV divergences are removed in $\overline{\text{MS}}$ scheme. While the soft divergences cancel between virtual and real emission processes in the inclusive cross section, the collinear divergences

are removed by mass factorization. Both the UV and mass factorization counter terms are determined using factorization property of the inclusive cross section and obtain collinear finite contributions to the Higgs boson production in bottom quark annihilation and Z boson production in DY. In the process, we also obtain the universal IR anomalous dimensions and consequently the renormalization constant for the Yukawa coupling up to two-loop level in both QED and mixed QCD-QED ones.

We begin the chapter with a discussion on the theoretical framework in Sec.[4.2]. In Sec.[4.3], we briefly describe the methodology to compute higher order QCD and QED corrections to various partonic and photonic channels contributing to the inclusive cross section. We also investigate the UV and IR structure of the form factors and cross sections using K+G equation and obtain the mass factorized cross sections, which is done in Sec.[4.4]. Further the Abelianization procedure is discussed in Sec.[4.5]. Finally, the phenomenological impact of our theoretical predictions are presented in Sec.[4.7] and summarize in Sec.[4.8].

4.2 Theoretical framework

The Lagrangian corresponds to the gauge group $SU(N_c) \times U(1)$, where $SU(N_c)$ is the gauge group for strong interaction and $U(1)$ for electromagnetic interaction, is given by:

$$\mathcal{L} = \bar{\psi}^i \left(i\gamma_\mu D_{ij}^\mu - m\delta_{ij} \right) \psi^j - \frac{1}{4} \mathcal{G}_{\mu\nu}^a \mathcal{G}^{a\mu\nu} - \frac{1}{4} \mathcal{F}_{\mu\nu} \mathcal{F}^{\mu\nu} - \frac{1}{2\xi} \left(\partial^\mu G_\mu^a \right)^2. \quad (4.1)$$

Here ψ^m represents the fermionic field in the fundamental representation of the $SU(N_c)$ group with $m = 1, \dots, N_c$ and ξ is the gauge fixing parameter. The covariant derivative $D_{ij}^\mu = \partial^\mu \delta_{ij} - ig_s (T^c)_{ij} G_c^\mu - ieA^\mu \delta_{ij}$. The gluonic and photonic field strength tensors takes the form in terms of gluon gauge field G_μ^a and photon gauge fields A_μ respectively as:

$$\mathcal{G}_{\mu\nu}^a = \partial_\mu G_\nu^a - \partial_\nu G_\mu^a + ig_s f^{abc} G_\mu^b G_\nu^c,$$

$$\mathcal{F}_{\mu\nu} = \partial_\mu A_\nu - \partial_\nu A_\mu,$$

Here both G_μ^a , ($a = 1, \dots, N_c^2 - 1$) and A_μ belong to the adjoint representation. We use the standard perturbation theory for our computations in which various quantities are expressed in powers of $a_s = g_s^2/16\pi^2$ and $a_e = e^2/16\pi^2$. Here g_s and e are strong and electromagnetic coupling constants respectively. We treat the quarks and leptons massless as we are interested in quantities in the high energy limit. The computations beyond LO involves virtual and real emission processes which are often sensitive to divergences coming from UV and IR end. The IR divergences arises: (1) from massless gluons of $SU(N_c)$ and massless photons of $U(1)$, and (2) (almost) massless collinear quarks and leptons. We perform these higher order computations in dimensional regularisation where the divergences appears in terms of $\epsilon = d - 4$, with d being the space-time dimension. Also we use \overline{MS} -scheme to renormalize the fields and the couplings in the theory. The number of active flavors is taken to be $n_f = 5$ and we work in the Feynman gauge.

For the Higgs boson production from bottom quark annihilation, the Lagrangian includes additional interaction term described by the Yukawa interaction λ_b , which is given in Eq.(3.2). The Yukawa coupling which, after the EW symmetry breaking, is found to be m_b/v , where v is the vacuum expectation value (vev) of the Higgs field $\phi(x)$. The $\psi_b(x)$ and m_b denote the bottom quark field and mass, respectively.

As discussed in the previous chapter, in the SM, the Higgs boson production through bottom quark annihilation is sub-dominant compared to gluon fusion through top quark loop. One finds that the bottom Yukawa coupling is 35 times smaller than top quark Yukawa coupling and in addition, the bottom quark flux in the proton-proton collision is much smaller than the gluon flux. However, in certain BSM scenarios such as the MSSM [117], the ratio of the $vevs$ of Higgs doublets can increase the contributions resulting from the bottom quark annihilation channel (See (3.2.1) for more details).

The inclusive cross section for the production of a colorless state, such as Higgs produc-

tion from gluon fusion or bottom quark annihilation, in the hadronic collisions is given by

$$\sigma(S, q^2) = \sigma_B(\mu_R^2) \sum_{cd} \int dx_1 dx_2 f_c(x_1, \mu_F^2) f_d(x_2, \mu_F^2) \Delta_{cd}(s, q^2, \mu_F^2, \mu_R^2), \quad (4.2)$$

where σ_B is the Born cross section and $f_a(x_i, \mu_F^2)$ are pdf's for $a = q, \bar{q}, g$ and photon distribution function (phdf) if $a = \gamma$. The scaling variables x_i is their momentum fractions. The partonic sub-process contributions Δ_{cd} are normalized by the Born cross section. The scales μ_R and μ_F are renormalization and factorization scales. S and $s = x_1 x_2 S$ are hadronic and partonic center of mass energy, respectively. q^2 is the invariant mass of the final colorless state. Δ_{cd} can be expanded in powers of the QCD coupling constant $a_s = g_s^2(\mu_R^2)/16\pi^2$ and QED coupling constant $a_e = e^2(\mu_R^2)/16\pi^2$, g_s and e being the strong and electromagnetic coupling constants, respectively. That is, after suppressing μ_R and μ_F dependence,

$$\Delta_{cd}(z, q^2, \mu_F^2, \mu_R^2) = \sum_{i,j=0}^{\infty} a_s^i(\mu_R^2) a_e^j(\mu_R^2) \Delta_{cd}^{(i,j)}(z, q^2, \mu_F^2, \mu_R^2), \quad (4.3)$$

with $\Delta_{cd}^{(0,0)} = \delta(1 - z)$ and $z = q^2/s$. Unlike the $\Delta_{cd}^{(i)}$ given in Eq.(3.39), where the index i dictates the perturbative order of QCD corrections, here we have two indices (i, j) to represent the same for both QCD and QED respectively. In the following, we describe the methodology to compute $\Delta_{cd}^{(i,j)}$ up to second order in the couplings.

4.3 Methodology

In this section, we briefly describe how higher order perturbative corrections $\Delta_{cd}^{(i,j)}$ in Eq. (4.3) are computed. Beyond LO, the partonic channels consists of one and two loop virtual sub processes, real-virtual and single and double-real emissions (See Sec.[2.2]). Some sample diagrams are presented in Fig. 4.1. Sub-processes involving virtual di-

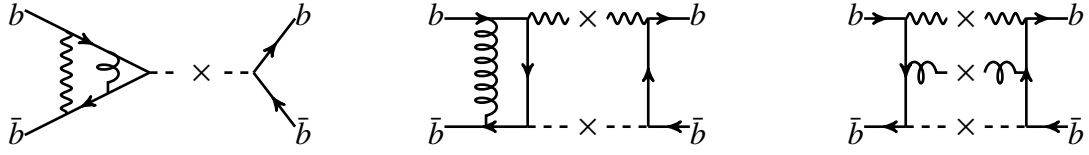


Figure 4.1: *Mixed QCD-QED contributions at NNLO. From left the sample diagrams of (1) double virtual, (2) real virtual and (3) double real respectively have shown. Here the wavy line indicates the photon, curly ones the gluon and the dashed line the Higgs boson.*

agrams are sensitive to UV singularities. Due to the presence of massless gluons and photons, we encounter soft singularities in both virtual and real emission sub-processes. In addition, we encounter collinear singularities as well, since the quarks are treated massless. We use dimensional regularization to regulate all these singularities.

To generate Feynman diagrams we have used the program QGRAF [133]. An in-house FORM [134] code is used to perform all the symbolic manipulations, e.g. performing Dirac, $SU(N_c)$ color and Lorentz algebra. We encounter a large number of loop integrals at this stage coming from the virtual diagrams. In order to reduce them to a minimum set of master integrals, we use IBP identities through a Mathematica based package, namely LiteRed [139]. For the virtual processes, at two loop level, the form factors in QCD, QED and mixed QCD \times QED require four MIs. For those processes that involve pure real emissions with or without virtual diagrams, we use the method of reverse unitarity that allows one to use IBP identities to reduce the resulting phase-space integrals to a set of few MIs. These MIs are matching with those given in [157]. For the RV type of processes at NNLO level we need 9 MIs for QCD and 8 MIs for both QED and mixed QCD-QED. Whereas, for the pure real emissions at NNLO, 24 MIs are required for QCD, QED and mixed QCD-QED processes. Substituting these MIs, we obtain contributions to each sub-process with their singularities expressed in terms of ϵ . We discuss the structure of these singularities in the following section.

4.4 UV and IR structures in QED and QCD-QED

Having computed all the partonic channels that contribute to the hadronic cross sections in QED and QCD-QED, now we can investigate the underlying UV and IR structure of U(1) gauge theory and the mixed gauge groups with massless fermions, which is the focus of this section. For the SU(N_c) group, similar studies can be found in [3, 49, 148, 158–161]. In order to explore the IR structure, we study the production of a Z -boson namely the Drell-Yan process, in addition to Higgs productions, in hadron colliders to the same accuracy in QCD, QED and QCD-QED.

To start with, we focus on the UV divergences coming from the virtual sub processes. In order to avoid those divergences, we renormalize the coupling constants a_c using suitable renormalization constants Z_{a_c} , where $c = s, e$ corresponds to QCD and QED coupling constants respectively. The Z_{a_c} relate the bare couplings \hat{a}_c to the renormalized ones $a_c(\mu_R^2)$ at the renormalization scale μ_R in the following way,

$$\frac{\hat{a}_c}{(\mu_0^2)^{\frac{\epsilon}{2}}} S_\epsilon = \frac{a_c(\mu_R^2)}{(\mu_R^2)^{\frac{\epsilon}{2}}} Z_{a_c}(a_s(\mu_R^2), a_e(\mu_R^2), \epsilon), \quad (4.4)$$

where $a_c = \{a_s, a_e\}$. Recall: $\hat{a}_s = \hat{g}_s^2/16\pi^2$ and $\hat{a}_e = \hat{e}^2/16\pi^2$ and $S_\epsilon \equiv \exp[(\gamma_E - \ln 4\pi) \frac{\epsilon}{2}]$. μ_0 is an arbitrary mass scale introduced to make \hat{a}_s and \hat{a}_e dimensionless in d -dimensions. Since the bare coupling constants \hat{a}_c is independent of the renormalisation scale μ_R , the couplings $a_c(\mu_R^2)$ satisfy the renormalisation group equations given by:

$$\mu_R^2 \frac{d}{d\mu_R^2} \ln Z_{a_c} = \frac{\epsilon}{2} + \beta_{a_c}(a_s(\mu_R^2), a_e(\mu_R^2)). \quad (4.5)$$

When both the interactions are simultaneously present in the perturbation theory, the beta functions β_{a_c} will involve both the couplings a_s and a_e , as given by:

$$\beta_{a_s} = - \sum_{i,j=0}^{\infty} \beta_{ij} a_s^{i+2} a_e^j, \quad \beta_{a_e} = - \sum_{i,j=0}^{\infty} \beta'_{ij} a_e^{j+2} a_s^i. \quad (4.6)$$

As can be seen from above expressions, the mixing of both these couplings in the beta functions start to appear from the third order onward, where $(i + j) \geq 3$ in Eq.(4.6). (More details can be found in [162]).

Substituting Eq.(4.6) in Eq.(4.5) and solving for the renormalization constants Z_{a_c} up to two-loops, we obtain

$$\begin{aligned} Z_{a_s} &= 1 + a_s \left(\frac{2\beta_{00}}{\epsilon} \right) + a_s a_e \left(\frac{\beta_{01}}{\epsilon} \right) + a_s^2 \left(\frac{4\beta_{00}^2}{\epsilon^2} + \frac{\beta_{10}}{\epsilon} \right) \\ Z_{a_e} &= 1 + a_e \left(\frac{2\beta'_{00}}{\epsilon} \right) + a_e a_s \left(\frac{\beta'_{10}}{\epsilon} \right) + a_e^2 \left(\frac{4\beta'_{00}{}^2}{\epsilon^2} + \frac{\beta'_{01}}{\epsilon} \right) \end{aligned} \quad (4.7)$$

In the present case, only one loop β i.e. β_{00} and β'_{00} appear. They, along with the other β 's [162, 163], are given by¹.

$$\begin{aligned} \beta_{00} &= \frac{11}{3} C_A - \frac{4}{3} n_f T_F, & \beta'_{00} &= -\frac{4}{3} \left(N_c \sum_q e_q^2 + \sum_l e_l^2 \right), \\ \beta_{01} &= -2 \left(\sum_q e_q^2 + \sum_l e_l^2 \right), & \beta'_{01} &= -4 \left(N_c \sum_q e_q^4 + \sum_l e_l^4 \right), \\ \beta_{10} &= \left(\frac{34}{3} C_A^2 - \frac{20}{3} C_A n_f T_F - 4 C_F n_f T_F \right), & \beta'_{10} &= -4 C_F \left(N_c \sum_q e_q^2 + \sum_l e_l^2 \right). \end{aligned} \quad (4.8)$$

Recall that $C_A = N_c$ and $C_F = (N_c^2 - 1)/2N_c$. $n_f(n_l)$ are the number of active quark (lepton) flavors and e_q, e_l refers to electric charge for quark q and lepton l respectively.

In addition to the QCD and QED coupling renormalization, we perform the renormalization for the Yukawa coupling through overall operator renormalization constant $Z_\lambda^b(a_s, a_e)$, which satisfies the RG equation:

$$\mu_R^2 \frac{d}{d\mu_R^2} \ln Z_\lambda^b = \frac{\epsilon}{4} + \gamma_b^{(i,j)}(a_s(\mu_R^2), a_e(\mu_R^2)) \quad (4.9)$$

¹Note that β_{j0} are pure QCD beta's as given in Eq.(2.14). We define them again, since we need to take care of both QCD and QED indices simultaneously.

whose solution in terms of the anomalous dimensions $\gamma_b^{(i,j)}$ up to two loops is found to be

$$\begin{aligned}
Z_{\lambda_b}(a_s, a_e, \epsilon) = & 1 + a_s \left\{ \frac{1}{\epsilon} (2\gamma_b^{(1,0)}) \right\} + a_s^2 \left\{ \frac{1}{\epsilon^2} (2(\gamma_b^{(1,0)})^2 + 2\beta_{00}\gamma_b^{(1,0)}) + \frac{1}{\epsilon} \gamma_b^{(2,0)} \right\} \\
& + a_e \left\{ \frac{1}{\epsilon} (2\gamma_b^{(0,1)}) \right\} + a_e^2 \left\{ \frac{1}{\epsilon^2} (2(\gamma_b^{(0,1)})^2 + 2\beta'_{00}\gamma_b^{(0,1)}) + \frac{1}{\epsilon} \gamma_b^{(0,2)} \right\} \\
& + a_s a_e \left\{ \frac{1}{\epsilon^2} (4\gamma_b^{(1,0)}\gamma_b^{(0,1)}) + \frac{1}{\epsilon} (\gamma_b^{(1,1)}) \right\}. \tag{4.10}
\end{aligned}$$

Note that while the UV singularities factorize through Z_{λ_b} , singularities from QCD and QED mix from two loop onward. For QCD, $\gamma_b^{(i,0)}$ is known to four loops [164]. Using universal IR structure of the amplitudes and cross sections in QED, we determine $\gamma_b^{(i,j)}$ up to two loops in QED i.e. for $(i, j) = (0, 1), (0, 2)$ and in QCD-QED i.e. for $(i, j) = (1, 1)$.

As discussed in Sec.[2.3.1], the IR structure of partonic cross section in the soft-virtual limit is constructed using the form factors, soft distributions and mass factorization kernels. We have already seen the structure of these quantities in the QCD perturbation theory in previous chapters. Now in this section, we study their structure for the case of mixed QCD-QED and pure QED.

4.4.1 Form factors

We begin with the discussion on the form factors (FF). The bare form factor is denoted by $\hat{\mathcal{F}}_I(\hat{a}_s, \hat{a}_e, Q^2, \mu^2)$, where $I = q, b$ denotes the DY process and the Higgs boson production in bottom quark annihilation respectively. As mentioned, our computations are performed in the perturbative framework where both QCD as well as QED interactions are taken into account simultaneously. Hence all the quantities, including form factor, depend on both QCD and QED coupling constants. In addition, we find that the UV renormalized form factors demonstrate the factorization of IR singularities. Using gauge and renormalization group invariance, we propose Sudakov integro-differential equation for these FFs,

analogous to the QCD one. In dimensional regularization, they take the following form:

$$Q^2 \frac{d}{dQ^2} \ln \hat{\mathcal{F}}_I = \frac{1}{2} \left[K_I(\{\hat{a}_c\}, \frac{\mu_R^2}{\mu^2}, \epsilon) + G_I(\{\hat{a}_c\}, \frac{Q^2}{\mu_R^2}, \frac{\mu_R^2}{\mu^2}, \epsilon) \right], \quad (4.11)$$

where $\{a_c\} = \{a_s, a_e\}$ and $Q^2 = -q^2$ is the invariant mass of the final state particle:

$$q^2 = \begin{cases} m_{l+l-}^2 & \text{for Drell-Yan,} \\ m_h^2 & \text{for Higgs production,} \end{cases} \quad (4.12)$$

where m_{l+l-} is the invariant mass of the lepton pairs. Explicit computation of the form factors shows that IR singularities, resulting from QCD and QED interactions not only factorize but also mix beyond one loop level. In other words, if we factorize IR singularities from the FFs, the resulting IR singular function can not be written as a product of pure QCD and pure QED functions. More specifically, there will be terms proportional to $a_s^i a_e^j$, where $i, j > 0$, which will not allow factorization of QCD and QED ones. Hence, K_I will have IR poles in ϵ from pure QED and pure QCD in every order in perturbation theory and in addition, from QCD-QED for the orders starting from $\mathcal{O}(a_s a_e)$. On the other hand, overall factorization of IR singularities implies that all the IR singularities contributes to the constants K_I , while the G_I s will have IR finite contributions when $\epsilon \rightarrow 0$. Since, the IR singularities of FFs have dipole structure, K_I will be independent of q^2 while G_I s are contains logarithms in q^2 . Since the $\hat{\mathcal{F}}_I$ are renormalization group (RG) invariant, so does the sum $K_I + G_I$. Thus, the RG invariance of $\hat{\mathcal{F}}_I$ implies

$$\mu_R^2 \frac{d}{d\mu_R^2} K_I(\{\hat{a}_c\}, \frac{\mu_R^2}{\mu^2}, \epsilon) = -\mu_R^2 \frac{d}{d\mu_R^2} G_I(\{\hat{a}_c\}, \frac{Q^2}{\mu_R^2}, \frac{\mu_R^2}{\mu^2}, \epsilon) = -A_I(\{a_c(\mu_R^2)\}), \quad (4.13)$$

where A_I are the cusp anomalous dimensions. The solutions to the above RG equations for K_I can be obtained by expanding the cusp anomalous dimensions (A_I) in powers of

renormalized coupling constants $a_s(\mu_R^2)$ and $a_e(\mu_R^2)$ as

$$A_I(\{a_c(\mu_R^2)\}) = \sum_{i,j} a_s^i(\mu_R^2) a_e^j(\mu_R^2) A_I^{(i,j)}, \quad A_I^{(0,0)} = 0, \quad (4.14)$$

and K_I as

$$K_I(\mu_R^2, \epsilon) = \sum_{i,j} \hat{a}_s^i \hat{a}_e^j \left(\frac{\mu_R^2}{\mu^2}\right)^{(i+j)\frac{\epsilon}{2}} S_\epsilon^{(i+j)} K_I^{(i,j)}(\epsilon), \quad K_I^{(0,0)} = 0, \quad (4.15)$$

where $A^{(i,0)}$ and $A^{(0,i)}$ result from pure QCD and pure QED interactions and $A^{(i,j)}$ with $i, j > 0$ from QCD-QED. The perturbative solutions to the RG equation for K_I in Eq.(4.13) are found using RG equations for the couplings a_s and a_e :

$$\begin{aligned} K_I^{(1,0)} &= \frac{1}{\epsilon} \left(-2A_I^{(1,0)} \right), & K_I^{(2,0)} &= \frac{1}{\epsilon^2} \left(2\beta_{00} A_I^{(1,0)} \right) + \frac{1}{\epsilon} \left(-A_I^{(2,0)} \right), \\ K_I^{(0,1)} &= \frac{1}{\epsilon} \left(-2A_I^{(0,1)} \right), & K_I^{(0,2)} &= \frac{1}{\epsilon^2} \left(2\beta'_{00} A_I^{(0,1)} \right) + \frac{1}{\epsilon} \left(-A_I^{(0,2)} \right). \\ K_I^{(1,1)} &= \frac{1}{\epsilon} \left(-A_I^{(1,1)} \right). \end{aligned} \quad (4.16)$$

Unlike K_I , G_I do not contain any IR singularities but depend only on Q^2 and hence we expand them as

$$G_I\left(\{\hat{a}_c\}, \frac{Q^2}{\mu_R^2}, \frac{\mu_R^2}{\mu^2}, \epsilon\right) = G_I(\{a_c(Q^2)\}, 1, \epsilon) + \int_{\frac{Q^2}{\mu_R^2}}^1 \frac{d\lambda^2}{\lambda^2} A_I(\{a_c(\lambda^2 \mu_R^2)\}) \quad (4.17)$$

where the first term is the boundary condition on each G_I at $\mu_R^2 = Q^2$. Expanding A_I in powers of a_s and a_e and using RG equations for QCD and QED couplings, we obtain

$$\int_{\frac{Q^2}{\mu_R^2}}^1 \frac{d\lambda^2}{\lambda^2} A_I(\{a_c(\lambda^2 \mu_R^2)\}) = \sum_{i,j} \hat{a}_s^i \hat{a}_e^j \left(\frac{\mu_R^2}{\mu^2}\right)^{(i+j)\frac{\epsilon}{2}} \times S_\epsilon^{(i+j)} \left[\left(\frac{Q^2}{\mu^2}\right)^{(i+j)\frac{\epsilon}{2}} - 1 \right] K^{(i,j)}(\epsilon). \quad (4.18)$$

Expanding the finite function $G_I(a_s(Q^2), a_e(Q^2), 1, \epsilon)$ as,

$$G_I(\{a_c(Q^2)\}, 1, \epsilon) = \sum_{i,j} a_s^i(Q^2) a_e^j(Q^2) G_I^{(i,j)}(\epsilon), \quad (4.19)$$

substituting the solutions of K_I and G_I in Eq.(4.11) and performing the integration over Q^2 we get

$$\ln \hat{\mathcal{F}}_I = \sum_{i,j} \hat{a}_s^i \hat{a}_e^j \left(\frac{Q^2}{\mu^2} \right)^{(i+j)\frac{\epsilon}{2}} S_\epsilon^{(i+j)} \hat{\mathcal{L}}_{F_I}^{(i,j)}(\epsilon), \quad (4.20)$$

where,

$$\begin{aligned} \hat{\mathcal{L}}_{F_I}^{(1,0)} &= \frac{1}{\epsilon^2} \left(-2A_I^{(1,0)} \right) + \frac{1}{\epsilon} \left(G_I^{(1,0)}(\epsilon) \right). \\ \hat{\mathcal{L}}_{F_I}^{(0,1)} &= \frac{1}{\epsilon^2} \left(-2A_I^{(0,1)} \right) + \frac{1}{\epsilon} \left(G_I^{(0,1)}(\epsilon) \right). \\ \hat{\mathcal{L}}_{F_I}^{(2,0)} &= \frac{1}{\epsilon^3} \left(\beta_{00} A_I^{(1,0)} \right) + \frac{1}{\epsilon^2} \left(-\frac{1}{2} A_I^{(2,0)} - \beta_{00} G_I^{(1,0)}(\epsilon) \right) + \frac{1}{2\epsilon} \left(G_I^{(2,0)}(\epsilon) \right). \\ \hat{\mathcal{L}}_{F_I}^{(0,2)} &= \frac{1}{\epsilon^3} \left(\beta'_{00} A_I^{(0,1)} \right) + \frac{1}{\epsilon^2} \left(-\frac{1}{2} A_I^{(0,2)} - \beta'_{00} G_I^{(0,1)}(\epsilon) \right) + \frac{1}{2\epsilon} \left(G_I^{(0,2)}(\epsilon) \right). \\ \hat{\mathcal{L}}_{F_I}^{(1,1)} &= \frac{1}{\epsilon^2} \left(-\frac{1}{2} A_I^{(1,1)} \right) + \frac{1}{2\epsilon} \left(G_I^{(1,1)}(\epsilon) \right). \end{aligned} \quad (4.21)$$

The derivations are followed the same way as the case of QCD, which in detail are given in Sec.[2.3.1]. Similar to the QCD [41, 42], the finite coefficients $G_I^{(i,j)}(\epsilon)$ are observed to satisfy the following decomposition in terms of collinear ($B_I^{(i,j)}$), soft ($f_I^{(i,j)}$) and UV ($\gamma_I^{(i,j)}$) anomalous dimensions as

$$G_I^{(i,j)}(\epsilon) = 2(B_I^{(i,j)} - \gamma_I^{(i,j)}) + f_I^{(i,j)} + \chi_I^{(i,j)} + \sum_{k=1} \epsilon^k g_{I,i,j}^k \quad (4.22)$$

with

$$\begin{aligned} \chi_I^{(1,0)} &= 0, \quad \chi_I^{(0,1)} = 0, \quad \chi_I^{(1,1)} = 0, \\ \chi_I^{(2,0)} &= -2\beta_{00} g_{I,10}^1, \quad \chi_I^{(0,2)} = -2\beta'_{00} g_{I,01}^1. \end{aligned} \quad (4.23)$$

Now we have the general structure of form factor up to second order in coupling constants for QCD, QED and QCD-QED as given in Eq. (4.20) . Also we explicitly computed the virtual corrections for Drell-Yan process and bottom quark induced Higgs production,

which are performed using the methodology described in the previous section. By comparing the explicit computations with the general structure of form factor, we can obtain many useful information which is our next focus.

The analytic expression for the unrenormalized form factor ($\hat{\mathcal{F}}_I$) in powers of (\hat{a}_s) and (\hat{a}_e) takes the following form:

$$\begin{aligned}\hat{\mathcal{F}}_I &= 1 + \hat{a}_s \left(\frac{Q^2}{\mu^2}\right)^{\frac{\epsilon}{2}} \mathcal{S}_\epsilon [C_F \mathcal{F}_1^I] + \hat{a}_s^2 \left(\frac{Q^2}{\mu^2}\right)^\epsilon \mathcal{S}_\epsilon^2 [C_F^2 \mathcal{F}_{2,0}^I + C_A C_F \mathcal{F}_{2,1}^I + C_{F n_f} T_F \mathcal{F}_{2,2}^I] \\ &\quad + \hat{a}_e \left(\frac{Q^2}{\mu^2}\right)^{\frac{\epsilon}{2}} \mathcal{S}_\epsilon [e_I^2 \mathcal{F}_1^I] + \hat{a}_e^2 \left(\frac{Q^2}{\mu^2}\right)^\epsilon \mathcal{S}_\epsilon^2 [e_I^4 \mathcal{F}_{2,0}^I + e_I^2 (N \sum_q e_q^2 + \sum_l e_l^2) \mathcal{F}_{2,2}^I] \\ &\quad + \hat{a}_s \hat{a}_e \left(\frac{Q^2}{\mu^2}\right)^\epsilon \mathcal{S}_\epsilon^2 [2C_F e_I^2 \mathcal{F}_{2,0}^I].\end{aligned}\tag{4.24}$$

$I = q, b$ denotes the Drell-Yan pair production and the Higgs boson production in bottom quark annihilation, respectively. The coefficients $\mathcal{F}_1^q, \mathcal{F}_{2,0}^q, \mathcal{F}_{2,1}^q$ and $\mathcal{F}_{2,2}^q$ are

$$\begin{aligned}\mathcal{F}_1^q &= -\frac{8}{\epsilon^2} + \frac{6}{\epsilon} - 8 + \zeta_2 + \epsilon \left(8 - \frac{3}{4}\zeta_2 - \frac{7}{3}\zeta_3\right) + \epsilon^2 \left(-8 + \zeta_2 + \frac{47}{80}\zeta_2^2 + \frac{7}{4}\zeta_3\right) + \epsilon^3 \left(8 - \zeta_2\right. \\ &\quad \left.- \frac{141}{320}\zeta_2^2 - \frac{7}{3}\zeta_3 + \frac{7}{24}\zeta_2\zeta_3 - \frac{31}{20}\zeta_5\right) + \epsilon^4 \left(-8 + \zeta_2 + \frac{47}{80}\zeta_2^2 + \frac{949}{4480}\zeta_2^3 + \frac{7}{3}\zeta_3\right. \\ &\quad \left.- \frac{7}{32}\zeta_2\zeta_3 - \frac{49}{144}\zeta_3^2 + \frac{93}{80}\zeta_5\right), \\ \mathcal{F}_{2,0}^q &= \frac{32}{\epsilon^4} - \frac{48}{\epsilon^3} + \frac{1}{\epsilon^2} \left(82 - 8\zeta_2\right) + \frac{1}{\epsilon} \left(-\frac{221}{2} + \frac{128}{3}\zeta_3\right) + \frac{1151}{8} + \frac{17}{2}\zeta_2 - 13\zeta_2^2 - 58\zeta_3 \\ &\quad + \epsilon \left(-\frac{5741}{32} - \frac{213}{8}\zeta_2 + \frac{171}{10}\zeta_2^2 + \frac{839}{6}\zeta_3 - \frac{56}{3}\zeta_2\zeta_3 + \frac{92}{5}\zeta_5\right) + \epsilon^2 \left(\frac{27911}{128}\right. \\ &\quad \left.+ \frac{1839}{32}\zeta_2 - \frac{3401}{80}\zeta_2^2 + \frac{223}{20}\zeta_3 - \frac{6989}{24}\zeta_3 + \frac{27}{2}\zeta_2\zeta_3 + \frac{652}{9}\zeta_3^2 - \frac{231}{10}\zeta_5\right), \\ \mathcal{F}_{2,1}^q &= \frac{44}{3\epsilon^3} - \frac{1}{\epsilon^2} \left(\frac{332}{9} - 4\zeta_2\right) + \frac{1}{\epsilon} \left(\frac{4129}{54} + \frac{11}{3}\zeta_2 - 26\zeta_3\right) - \frac{89173}{648} - \frac{119}{9}\zeta_2 + \frac{44}{5}\zeta_2^2 \\ &\quad + \frac{467}{9}\zeta_3 + \epsilon \left(\frac{1775893}{7776} + \frac{6505}{216}\zeta_2 - \frac{1891}{120}\zeta_2^2 - \frac{3293}{27}\zeta_3 + \frac{89}{6}\zeta_2\zeta_3 - \frac{51}{2}\zeta_5\right) \\ &\quad + \epsilon^2 \left(-\frac{33912061}{93312} - \frac{146197}{2592}\zeta_2 + \frac{2639}{72}\zeta_2^2 - \frac{809}{280}\zeta_3^2 + \frac{159949}{648}\zeta_3 - \frac{397}{36}\zeta_2\zeta_3\right. \\ &\quad \left.- \frac{569}{12}\zeta_3^2 + \frac{3491}{60}\zeta_5\right),\end{aligned}$$

$$\begin{aligned}
\mathcal{F}_{2,2}^q = & -\frac{16}{3\epsilon^3} + \frac{112}{9\epsilon^2} + \frac{1}{\epsilon} \left(-\frac{706}{27} - \frac{4}{3}\zeta_2 \right) + \frac{7541}{162} + \frac{28}{9}\zeta_2 - \frac{52}{9}\zeta_3 + \epsilon \left(-\frac{150125}{1944} \right. \\
& - \frac{353}{54}\zeta_2 + \frac{41}{30}\zeta_2^2 + \frac{364}{27}\zeta_3 \left. \right) + \epsilon^2 \left(\frac{2877653}{23328} + \frac{7541}{648}\zeta_2 - \frac{287}{90}\zeta_2^2 - \frac{4589}{162}\zeta_3 \right. \\
& \left. - \frac{13}{9}\zeta_2\zeta_3 - \frac{121}{15}\zeta_5 \right). \tag{4.25}
\end{aligned}$$

Similarly, the coefficients $\mathcal{F}_1^b, \mathcal{F}_{2,0}^b, \mathcal{F}_{2,1}^b$ and $\mathcal{F}_{2,2}^b$ are

$$\begin{aligned}
\mathcal{F}_1^b = & -\frac{8}{\epsilon^2} - 2 + \zeta_2 + \epsilon \left(2 - \frac{7}{3}\zeta_3 \right) + \epsilon^2 \left(-2 + \frac{1}{4}\zeta_2 + \frac{47}{80}\zeta_2^2 \right) + \epsilon^3 \left(2 - \frac{1}{4}\zeta_2 - \frac{7}{12}\zeta_3 \right. \\
& \left. + \frac{7}{24}\zeta_2\zeta_3 - \frac{31}{20}\zeta_5 \right) + \epsilon^4 \left(-2 + \frac{1}{4}\zeta_2 + \frac{47}{320}\zeta_2^2 + \frac{949}{4480}\zeta_2^3 + \frac{7}{12}\zeta_3 - \frac{49}{144}\zeta_3^2 \right), \\
\mathcal{F}_{2,0}^b = & \frac{32}{\epsilon^4} + \frac{1}{\epsilon^2} (16 - 8\zeta_2) + \frac{1}{\epsilon} \left(-16 - 12\zeta_2 + \frac{128}{3}\zeta_3 \right) + 22 + 12\zeta_2 - 13\zeta_2^2 - 30\zeta_3 \\
& + \epsilon \left(-32 - 18\zeta_2 + \frac{48}{5}\zeta_2^2 + \frac{202}{3}\zeta_3 - \frac{56}{3}\zeta_2\zeta_3 + \frac{92}{5}\zeta_5 \right) + \epsilon^2 \left(48 + \frac{53}{2}\zeta_2 - \frac{213}{10}\zeta_2^2 \right. \\
& \left. + \frac{223}{20}\zeta_2^3 - \frac{436}{3}\zeta_3 + \frac{1}{2}\zeta_2\zeta_3 + \frac{652}{9}\zeta_3^2 - \frac{63}{2}\zeta_5 \right), \\
\mathcal{F}_{2,1}^b = & \frac{44}{3\epsilon^3} + \frac{1}{\epsilon^2} \left(-\frac{134}{9} + 4\zeta_2 \right) + \frac{1}{\epsilon} \left(\frac{440}{27} + \frac{11}{3}\zeta_2 - 26\zeta_3 \right) - \frac{1655}{81} - \frac{103}{18}\zeta_2 + \frac{44}{5}\zeta_2^2 \\
& + \frac{305}{9}\zeta_3 + \epsilon \left(\frac{6353}{243} + \frac{245}{27}\zeta_2 - \frac{1171}{120}\zeta_2^2 - \frac{2923}{54}\zeta_3 + \frac{89}{6}\zeta_2\zeta_3 - \frac{51}{2}\zeta_5 \right) \\
& + \epsilon^2 \left(-\frac{49885}{1458} - \frac{4733}{324}\zeta_2 + \frac{11819}{720}\zeta_2^2 - \frac{809}{280}\zeta_2^3 + \frac{7667}{81}\zeta_3 - \frac{127}{36}\zeta_2\zeta_3 \right. \\
& \left. - \frac{569}{12}\zeta_3^3 + \frac{2411}{60}\zeta_5 \right), \\
\mathcal{F}_{2,2}^b = & -\frac{16}{3\epsilon^3} + \frac{40}{9\epsilon^2} + \frac{1}{\epsilon} \left(-\frac{184}{27} - \frac{4}{3}\zeta_2 \right) + \frac{832}{81} + \frac{10}{9}\zeta_2 - \frac{52}{9}\zeta_3 + \epsilon \left(-\frac{3748}{243} - \frac{46}{27}\zeta_2 \right. \\
& \left. + \frac{41}{30}\zeta_2^2 + \frac{130}{27}\zeta_3 \right) + \epsilon^2 \left(\frac{16870}{729} + \frac{208}{81}\zeta_2 - \frac{41}{36}\zeta_2^2 - \frac{598}{81}\zeta_3 - \frac{13}{9}\zeta_2\zeta_3 - \frac{121}{15}\zeta_5 \right). \tag{4.26}
\end{aligned}$$

Compring these explicit form factor results with the general expression in Eq.(4.20), we obtain the structure of the cusp anomalous dimensions ($A_I^{(i,j)}$) for the case of QED and mixed QCD-QED. For QCD they are known to 4-loop and presented in Appendix B. We

find $A_I^{(i,j)}$ up to two loops as:

$$\begin{aligned}
A_I^{(1,0)} &= 4C_F, & A_I^{(2,0)} &= 8C_A C_F \left(\frac{67}{18} - \zeta_2 \right) + 8C_F n_f T_F \left(-\frac{10}{9} \right), \\
A_I^{(0,1)} &= 4e_I^2, & A_I^{(0,2)} &= 8e_I^2 \left(N \sum_{k=1}^{n_f} e_k^2 + \sum_{l=1}^{n_l} e_l^2 \right) \left(-\frac{10}{9} \right), \\
A_I^{(1,1)} &= 0.
\end{aligned} \tag{4.27}$$

Unlike $A_I^{(i,j)}$, the other anomalous dimensions $B_I^{(i,j)}$, $f_I^{(i,j)}$ and $\gamma_I^{(i,j)}$ can not be disentangled either from $\hat{\mathcal{F}}_q$ or $\hat{\mathcal{F}}_b$ alone. In order to disentangle $B_I^{(i,j)}$ and $f_I^{(i,j)}$, we study the partonic cross sections resulting from soft gluon and soft photon emissions, namely soft distributions, in the next section.

4.4.2 Soft distributions

Before going to the extraction of soft or collinear anomalous dimension, let us briefly describe how we obtain the soft contributions arises from the real emission sub-processes. This has been discussed in detail for the case of QCD in Sec.[2.3.1]. The soft distributions, Φ_J , are governed by the cusp and soft anomalous dimensions, where $J = q, b, g$ refers to DY process, Higgs production from bottom quark annihilation and gluon fusion respectively. For the case of QCD, one finds that the quark and gluon soft distributions are related through $\Phi_b = \Phi_q = (C_F/C_A) \Phi_g$, which is found to be true up to three loop level [39, 40, 60]. This relation is expected to hold since the Φ_q and Φ_g are defined by the expectation value of certain gauge invariant bi-local quark and gluon operators computed between on-shell quark and gluons fields. The Wilson lines made up of gauge fields make these bi-local operators gauge invariant. (See [68, 69, 165–169] for more details).

We can use the partonic sub-processes of either DY process or the Higgs boson production in bottom quark annihilation namely $\hat{\sigma}_{q\bar{q}}$ or $\hat{\sigma}_{b\bar{b}}$ normalized by the square of the bare form factor $\hat{\mathcal{F}}_q$ or $\hat{\mathcal{F}}_b$ to obtain Φ_I . In general Φ_I , which is function of the scaling variable

$z = q^2/s$, is defined as,

$$C \exp(2\Phi_I(z)) = \frac{\hat{\sigma}_{\bar{II}}(z)}{Z_I^2 |\hat{\mathcal{F}}_I|^2} \quad I = q, b \quad (4.28)$$

with $Z_q = 1$ and $Z_b = Z_{\lambda_b}$ being the overall renormalization constant. Recall that the Drell-Yan process does not require additional operator renormalization and hence $Z_q = 1$ and the corresponding UV anomalous dimensions $\gamma_q = 0$. Whereas, the Yukawa coupling require additional renormalization which is dictated by nonzero γ_b 's. The symbol C refers to ‘‘ordered exponential’’ as given in Eq.(2.72).

We can compute the UV finite $\hat{\sigma}_{\bar{II}}$ at every order in renormalized perturbation theory. Since, we have not determined Z_{λ_b} , we can only compute the unrenormalized partonic cross section $\tilde{\sigma}_{\bar{II}} = \hat{\sigma}_{\bar{II}}/Z_I^2$. From the explicit results for $\tilde{\sigma}_{\bar{II}}$ and the form factors $\hat{\mathcal{F}}_I$, using Eq.(4.28) we obtain Φ_I up to second order in a_s , a_e and $a_s a_e$. We find $\Phi_q = \Phi_b$ up to second order in the couplings demonstrating the universality.

In [39, 40], it was shown that the soft distribution function Φ_I satisfies Sudakov integro-differential equation analogous to the form factor $\hat{\mathcal{F}}_I$ (See Eq.(4.11)) due to similar IR structures that both of them have, order by order in perturbation theory. That is, Φ_I satisfies

$$q^2 \frac{d}{dq^2} \Phi_I = \frac{1}{2} \left[\bar{K}_I(\{\hat{a}_c\}, \frac{\mu_R^2}{\mu^2}, \epsilon, z) + \bar{G}_{sv,I}(\{\hat{a}_c\}, \frac{q^2}{\mu_R^2}, \frac{\mu_R^2}{\mu^2}, \epsilon, z) \right], \quad (4.29)$$

where, the IR singularities are contained in \bar{K} and the finite part in \bar{G} . The RG invariance of Φ_I implies

$$\mu_R^2 \frac{d}{d\mu_R^2} \bar{K}_I = -\mu_R^2 \frac{d}{d\mu_R^2} \bar{G}_{sv,I} = A_I(\{a_c(\mu_R^2)\}) \delta(1-z). \quad (4.30)$$

Note that, the same anomalous dimensions govern the evolution of both \bar{K}_I and \bar{G}_I . This ensures that the soft distribution function contains right soft singularities to cancel those

from the form factor leaving bare partonic cross section to contain only initial state collinear singularities. The later will be removed by mass factorization by appropriate DGLAP kernels. Expanding $\overline{K}_I(\{a_c\})$ and $\overline{G}_{sv,I}(\{a_c(q^2)\}, 1, \epsilon, z)$ in powers of $\{a_c\}$ as has been done for $K_I(\{a_c\})$ and $G_I(\{a_c\})$ (see Eq.(4.15) and (4.19)), with the replacements of $K_I^{(i,j)}$ by $\overline{K}_I^{(i,j)}$ and

$$\overline{G}_{sv,I}(\{a_c(q^2)\}, 1, \epsilon, z) = \sum_{i,j} a_s^i(q^2) a_e^j(q^2) \overline{G}_{sv,I}^{(i,j)}(\epsilon, z), \quad (4.31)$$

the solution to Eq.(4.29) is found to be

$$\Phi_I(\{\hat{a}_c\}, q^2, \mu^2, \epsilon, z) = \sum_{i,j} \hat{a}_s^i \hat{a}_e^j \left(\frac{q^2(1-z)^2}{\mu^2} \right)^{(i+j)\frac{\epsilon}{2}} S_\epsilon^{(i+j)} \left(\frac{(i+j)\epsilon}{1-z} \right) \hat{\phi}_I^{(i,j)}(\epsilon) \quad (4.32)$$

where,

$$\hat{\phi}_I^{(i,j)}(\epsilon) = \frac{1}{(i+j)\epsilon} \left[\overline{K}_I^{(i,j)}(\epsilon) + \overline{G}_{sv,I}^{(i,j)}(\epsilon) \right]. \quad (4.33)$$

The coefficients $\overline{G}_{sv,I}^{(i,j)}(\epsilon)$ are related to the finite function $\overline{G}_{sv,I}(\{a_c(q^2)\}, 1, \epsilon, z)$ defined in Eq.(4.31) through the distributions $\delta(1-z)$ and $\mathcal{D}_j(z)$. Thus expanding $\overline{G}^{(i,j)}(\epsilon)$ in terms of the $a_s(q^2(1-z)^2)$ and $a_e(q^2(1-z)^2)$ we write,

$$\sum_{i,j} \hat{a}_s^i \hat{a}_e^j \left(\frac{q_z^2}{\mu^2} \right)^{(i+j)\frac{\epsilon}{2}} S_\epsilon^{(i+j)} \overline{G}_{sv,I}^{(i,j)}(\epsilon) = \sum_{i,j} a_s^i(q_z^2) a_e^j(q_z^2) \overline{\mathcal{G}}_I^{(i,j)}(\epsilon) \quad (4.34)$$

where $q_z^2 = q^2(1-z)^2$. The IR finite $\overline{\mathcal{G}}_I^{(i,j)}(\epsilon)$ are observed [39, 40] to satisfy the following relation:

$$\overline{\mathcal{G}}_I^{(i,j)}(\epsilon) = -f_I^{(i,j)} + \overline{\chi}_I^{(i,j)} + \sum_{k=1} \epsilon^k \overline{\mathcal{G}}_{I,ij}^{(k)}, \quad (4.35)$$

where, for up to two loops

$$\begin{aligned}\bar{\chi}_I^{(1,0)} &= 0, & \bar{\chi}_I^{(0,1)} &= 0, & \bar{\chi}_I^{(1,1)} &= 0, \\ \bar{\chi}_I^{(2,0)} &= -2\beta_{00} \bar{\mathcal{G}}_{I,10}^{(1)}, & \bar{\chi}_I^{(1,0)} &= -2\beta'_{00} \bar{\mathcal{G}}_{I,01}^{(1)}.\end{aligned}\quad (4.36)$$

The constants $\bar{\mathcal{G}}_{I,i,j}^{(k)}$ up to two loops are found to be:

$$\begin{aligned}\bar{\mathcal{G}}_{I,10}^{(1)} &= C_F(-3\zeta_2), & \bar{\mathcal{G}}_{I,10}^{(2)} &= C_F\left(\frac{7}{3}\zeta_3\right), & \bar{\mathcal{G}}_{I,10}^{(3)} &= C_F\left(-\frac{3}{16}\zeta_2^2\right), \\ \bar{\mathcal{G}}_{I,01}^{(1)} &= e_b^2(-3\zeta_2), & \bar{\mathcal{G}}_{I,01}^{(2)} &= e_b^2\left(\frac{7}{3}\zeta_3\right), & \bar{\mathcal{G}}_{I,01}^{(3)} &= e_b^2\left(-\frac{3}{16}\zeta_2^2\right), \\ \bar{\mathcal{G}}_{I,11}^{(1)} &= 0, \\ \bar{\mathcal{G}}_{I,20}^{(1)} &= C_F n_f T_F \left(-\frac{656}{81} + \frac{140}{9}\zeta_2 + \frac{64}{3}\zeta_3\right) + C_A C_F \left(\frac{2428}{81} - \frac{469}{9}\zeta_2 + 4\zeta_2^2 - \frac{176}{3}\zeta_3\right), \\ \bar{\mathcal{G}}_{I,02}^{(1)} &= e_b^2 \left(N \sum_q e_q^2 + \sum_l e_l^2\right) \left(-\frac{656}{81} + \frac{140}{9}\zeta_2 + \frac{64}{3}\zeta_3\right).\end{aligned}\quad (4.37)$$

Comparing the soft distribution functions Φ_I , $I = q, b$, obtained from the explicit computation up to second order in coupling constants against the formal solution given in Eq.(4.32), we can obtain $A_I^{(i,j)}$ and $f_I^{(i,j)}$ for $(i, j) = (1, 0), (0, 1), (1, 1), (2, 0), (0, 2)$. We obtain:

$$\begin{aligned}f_I^{(1,0)} &= f_I^{(0,1)} = f_I^{(1,1)} = 0 \\ f_I^{(2,0)} &= C_A C_F \left(-\frac{22}{3}\zeta_2 - 28\zeta_3 + \frac{808}{27}\right) + C_F n_f T_F \left(\frac{8}{3}\zeta_2 - \frac{224}{27}\right), \\ f_I^{(0,2)} &= e_I^2 \left(N \sum_q e_q^2 + \sum_l e_l^2\right) \left(\frac{8}{3}\zeta_2 - \frac{224}{27}\right).\end{aligned}\quad (4.38)$$

Now that we have $f_I^{(i,j)}$, it is straightforward to obtain $B_q^{(i,j)}$ in Eq. (4.22) from the explicit results on $G_q^{(i,j)}$ as $\gamma_q^{(i,j)} = 0$ for DY. This way we obtain,

$$\begin{aligned}B_q^{(1,0)} &= 3C_F, & B_q^{(0,1)} &= 3e_q^2, & B_q^{(1,1)} &= C_F e_q^2 (3 - 24\zeta_2 + 48\zeta_3), \\ B_q^{(2,0)} &= \frac{1}{2} \left\{ C_F^2 (3 - 24\zeta_2 + 48\zeta_3) + C_A C_F \left(\frac{17}{3} + \frac{88}{3}\zeta_2 - 24\zeta_3\right) + C_F n_f T_F \left(-\frac{4}{3} - \frac{32}{3}\zeta_2\right) \right\},\end{aligned}$$

$$B_q^{(0,2)} = \frac{1}{2} \left\{ e_q^4 (3 - 24\zeta_2 + 48\zeta_3) + e_q^2 \left(N \sum_{q'} e_{q'}^2 + \sum_l e_l^2 \right) \left(-\frac{4}{3} - \frac{32}{3} \zeta_2 \right) \right\}. \quad (4.39)$$

Considering $B_b^{(i,j)} = B_q^{(i,j)}$, we determine the UV anomalous dimension $(\gamma_b^{(i,j)})$ from $G_b^{(i,j)}$ of Eq.(4.22) which is known to second order. They are found to be:

$$\begin{aligned} \gamma_b^{(1,0)} &= 3C_F, & \gamma_b^{(0,1)} &= 3e_b^2, & \gamma_b^{(1,1)} &= 3C_F e_b^2, \\ \gamma_b^{(2,0)} &= \frac{3}{2} C_F^2 + \frac{97}{6} C_A C_F - \frac{10}{3} C_F n_f T_F, \\ \gamma_b^{(0,2)} &= \frac{3}{2} e_b^4 - \frac{10}{3} e_b^2 \left(N \sum_{k \in Q} e_k^2 + \sum_l e_l^2 \right). \end{aligned} \quad (4.40)$$

Alternatively, taking $B_b^{(i,j)} = B_q^{(i,j)}$ and $f_b^{(i,j)} = f_q^{(i,j)}$, we can determine $\gamma_b^{(i,j)}$ by comparing the difference $G_b^{(i,j)} - G_q^{(i,j)}$ obtained using DY and Higgs boson form factors $\hat{\mathcal{F}}_q$ and $\hat{\mathcal{F}}_b$ at $\epsilon = 0$ against the formal decomposition of $G_I^{(i,j)}$ given in Eq.(4.22). Substituting the above UV anomalous dimensions in Eq.(4.10), we obtain Z_{λ_b} to second order in the couplings.

Using the renormalization constants Z_{a_s} , Z_{a_e} and Z_{λ_b} for the coupling constants a_s , a_e and the Yukawa coupling, we obtain UV finite partonic cross sections. The soft and collinear singularities arising from gluons/photons/fermions in the virtual sub-processes cancel against those from the real sub-processes when all the degenerate states are summed up. The remaining initial state collinear singularities are removed by mass factorization. Collinear factorization allows us to determine the mass factorization kernels Γ_{qq} and Γ_{qg} up to two-loop level for U(1) and SU(N_c) × U(1) cases. Since Γ_{qq} and Γ_{qg} are governed by the splitting functions P_{qq} and P_{qg} , we extract them to second order in couplings. In [170], these splitting functions up to NNLO level, both in QED and QCD×QED, were obtained using the Abelianization procedure. The splitting functions that we have obtained by demanding finiteness of the mass factorised cross section, agree with those in [170]. The resulting expression for the finite partonic cross section is presented in later sections. Before going to that, let us briefly discuss the abelianization procedure which is the focus of next section.

4.5 Abelianization procedure

In [156], QCD-QED corrections to the DY process were obtained by studying the $SU(N_c)$ color factors in Feynman diagrams that contribute to QCD corrections. This led to an algorithm namely Abelianization procedure which provides a set of rules that transform QCD results into pure QED and mixed QCD×QED results. Unlike in [156], without resorting to Abelianization rules, we have performed explicit calculation to obtain the contributions resulting from all the partonic and photonic channels taking into account both UV and mass factorization counter terms. Using these results at NNLO in QCD, QCD-QED and in QED, we find a set of rules that can relate QCD and QED results. Note that if there is a gluon in the initial state, averaging over its color factor gives a factor $(1/(N_c^2 - 1))$. This is absent for the processes where photon is present instead of gluon in the initial state. Also, for pure QCD or QED, the gluons or photons are degenerate and hence one needs to account for a factor of 2. Taking this in account, we obtain a set of relations among QCD and QED results, which are found to be consistent with the procedure used in [156]. These relations are listed in the following tables for various scattering channels:

Rule 1 : *quark-quark initiated cases*

QCD	QCD-QED	QED
C_F^2	$2C_F e_b^2$	e_b^4
$C_F C_A$	0	0
$C_F n_f T_F$	0	$e_b^2 (N_c \sum_q e_q^2 + \sum_l e_l^2)$
$C_F T_F$	0	$N_c e_b^2 e_q^{2*}$

* $e_q^2 = e_b^2$ when both initial quarks are bottom quarks.

Rule 2 : *quark-gluon initiated cases*: After multiplying $2C_A C_F$ for the initial state gluon

QCD	QCD-QED	QED
$C_A C_F^2$	$C_A C_F e_b^2$	$C_A e_b^4$
$C_A^2 C_F$	0	0

Rule 3 : *gluon-gluon initiated cases* After multiplying $2C_A C_F$ for each initial state gluon

QCD	QCD-QED	QED
$C_A^2 C_F^2$	$C_A^2 C_F e_b^2$	$C_A^2 e_b^4$
$C_A^3 C_F$	0	0

4.6 Mass factorized partonic cross sections

In this section, we present the finite partonic cross sections $\Delta_{cd}^{(i,j)}$ that we obtained after mass factorization. Expanding these cross section in powers of strong and electromagnetic coupling constants:

$$\Delta_{cd}(z, q^2, \mu_F^2, \mu_R^2) = \sum_{i,j=0}^{\infty} a_s^i(\mu_R^2) a_e^j(\mu_R^2) \Delta_{cd}^{(i,j)}(z, q^2, \mu_F^2, \mu_R^2), \quad (4.41)$$

In QCD, $\Delta_{cd}^{i,0}$ for bottom quark annihilation is known [130, 171], but we present here for completeness. In the following, $\Delta_{cd}^{i,0}$, $i = 1, 2$ is in $SU(N_c)$ gauge theory, while $\Delta_{cd}^{0,j}$, $j = 1, 2$ is in $U(1)$ gauge theory.

$$\begin{aligned} \Delta_{b\bar{b}}^{(0,0)} &= \delta(1-z), \\ \Delta_{b\bar{b}}^{(1,0)} &= \mathbf{C}_F \left[\delta(1-z) \left\{ -4 + 8\zeta_2 \right\} + 16\mathcal{D}_1(z) + \left\{ 4(1-z) - 8(1+z) \ln(1-z) \right. \right. \\ &\quad \left. \left. - \frac{4(1+z^2)}{(1-z)} \ln(z) \right\} \right], \\ \Delta_{bg}^{(1,0)} &= -\frac{1}{2}(-1+z)(-3+7z) + 2(1-2z+2z^2) \ln(1-z) + (-1+2z-2z^2) \ln(z), \\ \Delta_{b\bar{b}}^{(2,0)} &= \mathbf{C}_F^2 \left[\delta(1-z) \left\{ 16 + \frac{8}{5}\zeta_2^2 - 60\zeta_3 \right\} + 256\mathcal{D}_0(z)\zeta_3 + \mathcal{D}_1(z) \left\{ -64 - 128\zeta_2 \right\} \right. \\ &\quad \left. + 128\mathcal{D}_3(z) + \left\{ -4(-26+11z+13z^2) + \frac{8}{1-z}(-7-10z+11z^2) \ln(1-z) \ln(z) \right. \right. \\ &\quad \left. \left. - \frac{4}{1-z}(23+39z^2) \ln^2(1-z) \ln(z) + \frac{2}{1-z}(7+30z-34z^2+12z^3) \ln^2(z) \right. \right. \\ &\quad \left. \left. + \frac{16}{1-z}(2+5z^2) \ln(1-z) \ln^2(z) - \frac{2}{3(1-z)}(1+15z^2+4z^3) \ln^3(z) \right. \right. \end{aligned}$$

$$\begin{aligned}
& + \frac{8}{1-z}(-16 + 13z - 6z^2 + 6z^3)\text{Li}_2(1-z) + \frac{8}{1-z}(7 - 9z^2)\ln(1-z)\text{Li}_2(1-z) \\
& - \frac{16}{1-z}(3 + z^2 + 2z^3)\ln(z)\text{Li}_2(1-z) + \frac{48}{1-z}(-1 + 2z^2)\text{Li}_3(1-z) \\
& - \frac{8}{1-z}(9 + 9z^2 + 8z^3)\text{S}_{1,2}(1-z) + 8(11 - 10z)\zeta_2 - \frac{16}{1-z}(-2 - 7z^2 + z^3)\ln(z)\zeta_2 \\
& - 128(1+z)\zeta_3 + 12(-4 + 9z)\ln(1-z) + 64(1+z)\zeta_2\ln(1-z) \\
& - 32(1-z)\ln^2(1-z) - 64(1+z)\ln^3(1-z) + \frac{4}{1-z}(16 - z + z^2)\ln(z) \\
& - 48z^2\zeta_2\ln(1+z) + 16(-1 + 2z)\ln(z)\ln(1+z) + 40z^2\ln^2(z)\ln(1+z) \\
& - 48z^2\ln(z)\ln^2(1+z) + 16(-1 + 2z)\text{Li}_2(-z) + 48z^2\ln(z)\text{Li}_2(-z) \\
& - 96z^2\ln(1+z)\text{Li}_2(-z) - 16z^2\text{Li}_3(-z) - 96z^2\text{S}_{1,2}(-z) \Bigg\} \\
& + \mathbf{C}_A \mathbf{C}_F \left[\delta(1-z) \left\{ \frac{166}{9} + \frac{232}{9}\zeta_2 - \frac{12}{5}\zeta_2^2 - 8\zeta_3 \right\} + \mathcal{D}_0(z) \left\{ -\frac{1616}{27} + \frac{176\zeta_2}{3} + 56\zeta_3 \right\} \right. \\
& + \mathcal{D}_1(z) \left\{ \frac{1072}{9} - 32\zeta_2 \right\} - \frac{176}{3}\mathcal{D}_2(z) + \left\{ \frac{2}{27}(-595 + 944z + 351z^2) \right. \\
& - \frac{4}{3(1-z)}(61 - 31z + 40z^2)\ln(z) + \frac{32}{3(1-z)}(7 + 4z^2)\ln(1-z)\ln(z) \\
& - \frac{1}{3(1-z)}(61 + 48z - 13z^2 + 36z^3)\ln^2(z) + \frac{8}{(1-z)}(1 + z^2)\ln(1-z)\ln^2(z) \\
& - \frac{2}{3(1-z)}(3 + 7z^2 - 2z^3)\ln^3(z) - \frac{4}{3(1-z)}(-29 + 27z - 27z^2 + 18z^3)\text{Li}_2(1-z) \\
& + \frac{8}{(1-z)}(1 + z^2)\ln(1-z)\text{Li}_2(1-z) + \frac{8}{(1-z)}(3 + 2z^3)\ln(z)\text{Li}_2(1-z) \\
& - \frac{28}{(1-z)}(1 + z^2)\text{Li}_3(1-z) + \frac{8}{(1-z)}(1+z)(5 - 5z + 4z^2)\text{S}_{1,2}(1-z) \\
& - \frac{4}{3}(22 + 25z)\zeta_2 - 28(1+z)\zeta_3 - \frac{4}{9}(-40 + 299z)\ln(1-z) + 16(1+z)\zeta_2\ln(1-z) \\
& + \frac{88}{3}(1+z)\ln^2(1-z) + \frac{8}{(1-z)}(1+z)(1-z+z^2)\zeta_2\ln(z) + 24z^2\zeta_2\ln(1+z) \\
& - 8(-1 + 2z)\ln(z)\ln(1+z) - 20z^2\ln^2(z)\ln(1+z) + 24z^2\ln(z)\ln^2(1+z) \\
& - 8(-1 + 2z)\text{Li}_2(-z) - 24z^2\ln(z)\text{Li}_2(-z) + 48z^2\ln(1+z)\text{Li}_2(-z) + 8z^2\text{Li}_3(-z) \\
& \left. + 48z^2\text{S}_{1,2}(-z) \right] \\
& + \mathbf{C}_F \mathbf{n}_F \mathbf{T}_F \left[\delta(1-z) \left\{ \frac{16}{9} - \frac{80}{9}\zeta_2 + 16\zeta_3 \right\} + \mathcal{D}_0(z) \left\{ \frac{448}{27} - \frac{64}{3}\zeta_2 \right\} - \frac{320}{9}\mathcal{D}_1(z) \right. \\
& \left. + \frac{64}{3}\mathcal{D}_2(z) + \left\{ \frac{8}{3(1-z)}(7 - 4z + 7z^2)\ln(z) - \frac{8}{27}(1 + 55z) \right\} \right]
\end{aligned}$$

$$\begin{aligned}
& -\frac{64}{3(1-z)}(1+z^2)\ln(1-z)\ln(z) + \frac{4}{3(1-z)}(5+7z^2)\ln^2(z) + \frac{32}{3}(1+z)\zeta_2 \\
& + \frac{64}{9}(1+4z)\ln(1-z) - \frac{32}{3}(1+z)\ln^2(1-z) - \frac{16}{3(1-z)}\text{Li}_2(1-z) \Bigg\} \Bigg] \\
& + \mathbf{C}_F \mathbf{T}_F \left[\frac{2}{27z}(-1+z)(208-635z+487z^2) - \frac{16}{9z}(-1+z)(4-53z+22z^2)\ln(1-z) \right. \\
& - \frac{16}{3z}(-1+z)(4+7z+4z^2)\ln^2(1-z) + 16(-1+4z+4z^2)\ln(1-z)\ln(z) \\
& + \frac{8}{3z}(16-3z+21z^2+8z^3)\text{Li}_2(1-z) + 64(1+z)\ln(1-z)\text{Li}_2(1-z) \\
& - \frac{16}{3z}(4+3z-3z^2-3z^3)\zeta_2 + \frac{4}{9}(87-252z+38z^2)\ln(z) - 32(1+z)\zeta_2\ln(z) \\
& + 32(1+z)\ln^2(1-z)\ln(z) - 2(1+5z+12z^2)\ln^2(z) + \frac{20}{3}(1+z)\ln^3(z) \\
& - 32(1+z)\ln(1-z)\ln^2(z) - \frac{32}{3}z^2\ln(z)\ln(1+z) - 16(1+z)\ln(z)\text{Li}_2(1-z) \\
& \left. - \frac{32}{3}z^2\text{Li}_2(-z) - 64(1+z)\text{Li}_3(1-z) + 32(1+z)\mathbf{S}_{1,2}(1-z) \right\} \Bigg], \\
\Delta_{bb}^{(2,0)} = & \mathbf{C}_F^2 \left[2(-1+z)(57-13z) + \frac{16}{1+z}(1+z^2)\ln(1-z)\ln^2(z) \right. \\
& - \frac{4}{3(1+z)}(3+7z^2+2z^3)\ln^3(z) + \frac{4}{1+z}(9+19z^2)\ln^2(z)\ln(1+z) \\
& - \frac{8}{1+z}(-1+5z^2)\ln(z)\ln^2(1+z) - 8(-7-5z+3z^2)\text{Li}_2(1-z) \\
& - \frac{16}{1+z}(-3-2z^2+z^3)\ln(z)\text{Li}_2(1-z) - \frac{64}{1+z}(1+z^2)\ln(1-z)\text{Li}_2(-z) \\
& + \frac{8(5+11z^2)}{1+z}\ln(z)\text{Li}_2(-z) - \frac{16}{1+z}(-1+5z^2)\ln(1+z)\text{Li}_2(-z) \\
& + \frac{8}{1+z}(-7-z-8z^2+2z^3)\text{Li}_3(1-z) - \frac{8}{1+z}(1+3z^2)\text{Li}_3(-z) \\
& + \frac{64}{1+z}(1+z^2)\text{Li}_3\left(\frac{1-z}{1+z}\right) - \frac{64}{1+z}(1+z^2)\text{Li}_3\left(-\frac{1-z}{1+z}\right) \\
& - \frac{8}{1+z}(-9+z-4z^2+2z^3)\mathbf{S}_{1,2}(1-z) - \frac{16}{1+z}(-1+5z^2)\mathbf{S}_{1,2}(-z) \\
& + 32(1+z)\ln(1-z)\ln(z) - \frac{64}{1+z}(1+z^2)\ln(1-z)\ln(z)\ln(1+z) + 8\zeta_2 \\
& - \frac{32}{1+z}(1+z^2)\ln(1-z)\zeta_2 - \frac{8}{1+z}(-1+5z^2)\ln(1+z)\zeta_2 - \frac{8}{1+z}(1+z^2)\zeta_3 \\
& + 64(1-z)\ln(1-z) + 4(-8+5z)\ln(z) + \frac{16}{1+z}(1+2z^2)\zeta_2\ln(z) \\
& \left. - 4(1+2z+3z^2)\ln^2(z) + 16\ln(z)\ln(1+z) + 16\text{Li}_2(-z) \right]
\end{aligned}$$

$$\begin{aligned}
& + \mathbf{C}_A \mathbf{C}_F \left[57 - 70z + 13z^2 - \frac{8}{1+z}(1+z^2) \ln(1-z) \ln^2(z) \right. \\
& + \frac{2}{3(1+z)}(3+7z^2+2z^3) \ln^3(z) + \frac{32}{1+z}(1+z^2) \ln(1-z) \ln(z) \ln(1+z) \\
& - \frac{2}{1+z}(9+19z^2) \ln^2(z) \ln(1+z) + \frac{4}{1+z}(-1+5z^2) \ln(z) \ln^2(1+z) \\
& + 4(-7-5z+3z^2) \text{Li}_2(1-z) - \frac{8}{1+z}(3+2z^2-z^3) \ln(z) \text{Li}_2(1-z) \\
& + \frac{32}{1+z}(1+z^2) \ln(1-z) \text{Li}_2(-z) - \frac{4}{1+z}(5+11z^2) \ln(z) \text{Li}_2(-z) \\
& + \frac{8}{1+z}(-1+5z^2) \ln(1+z) \text{Li}_2(-z) + \frac{4}{1+z}(7+z+8z^2-2z^3) \text{Li}_3(1-z) \\
& + \frac{4}{1+z}(1+3z^2) \text{Li}_3(-z) - \frac{32}{1+z}(1+z^2) \text{Li}_3\left(\frac{1-z}{1+z}\right) + \frac{32}{1+z}(1+z^2) \text{Li}_3\left(\frac{-1+z}{1+z}\right) \\
& + \frac{4}{1+z}(-9+z-4z^2+2z^3) \text{S}_{1,2}(1-z) + \frac{8}{1+z}(-1+5z^2) \text{S}_{1,2}(-z) - 4\zeta_2 \\
& + \frac{16}{1+z}(1+z^2) \ln(1-z) \zeta_2 + \frac{4}{1+z}(-1+5z^2) \ln(1+z) \zeta_2 + \frac{4}{1+z}(1+z^2) \zeta_3 \\
& + 32(-1+z) \ln(1-z) - 2(-8+5z) \ln(z) - \frac{8}{1+z}(1+2z^2) \zeta_2 \ln(z) - 8 \text{Li}_2(-z) \\
& \left. - 16(1+z) \ln(1-z) \ln(z) + 2(1+2z+3z^2) \ln^2(z) - 8 \ln(z) \ln(1+z) \right] \\
& + \mathbf{C}_F \mathbf{T}_F \left[\frac{2}{27z}(-1+z)(208-707z+703z^2) - \frac{16}{9z}(z-1)(4-53z+22z^2) \ln(1-z) \right. \\
& - \frac{16}{3z}(-1+z)(4+7z+4z^2) \ln^2(1-z) + 16(-1+4z+4z^2) \ln(1-z) \ln(z) \\
& - \frac{2}{3}(3+15z+40z^2) \ln^2(z) + \frac{8}{3z}(16-3z+21z^2+8z^3) \text{Li}_2(1-z) \\
& + 64(1+z) \ln(1-z) \text{Li}_2(1-z) + \frac{16}{3z}(-1+z)(4+7z+4z^2) \zeta_2 \\
& + \frac{4}{9}(93-264z+20z^2) \ln(z) - 32(1+z) \zeta_2 \ln(z) + 32(1+z) \ln^2(1-z) \ln(z) \\
& - 32(1+z) \ln(1-z) \ln^2(z) + \frac{20}{3}(1+z) \ln^3(z) - 16(1+z) \ln(z) \text{Li}_2(1-z) \\
& \left. - 64(1+z) \text{Li}_3(1-z) + 32(1+z) \text{S}_{1,2}(1-z) \right], \\
\mathcal{A}_{ub}^{(2,0)} = & \mathbf{C}_F \mathbf{T}_F \left[\frac{1}{27z}(-1+z)(208-707z+703z^2) - \frac{8}{9z}(-1+z)(4-53z+22z^2) \ln(1-z) \right. \\
& - \frac{8}{3z}(-1+z)(4+7z+4z^2) \ln^2(1-z) + 8(-1+4z+4z^2) \ln(1-z) \ln(z) \\
& - \frac{1}{3}(3+15z+40z^2) \ln^2(z) + \frac{4}{3z}(16-3z+21z^2+8z^3) \text{Li}_2(1-z) \\
& \left. + 32(1+z) \ln(1-z) \text{Li}_2(1-z) + \frac{8}{3z}(-1+z)(4+7z+4z^2) \zeta_2 \right]
\end{aligned}$$

$$\begin{aligned}
& + \frac{2}{9}(93 - 264z + 20z^2) \ln(z) - 16(1+z)\zeta_2 \ln(z) + 16(1+z) \ln^2(1-z) \ln(z) \\
& - 16(1+z) \ln(1-z) \ln^2(z) + \frac{10}{3}(1+z) \ln^3(z) - 8(1+z) \ln(z) \text{Li}_2(1-z) \\
& - 32(1+z) \text{Li}_3(1-z) + 16(1+z) \text{S}_{1,2}(1-z) \Big], \\
\Delta_{ui}^{(2,0)} = & \mathbf{C}_F \mathbf{T}_F \left[-\frac{16}{3}(-1+z)(-1+3z) - \frac{16}{3}z^2 \zeta_2 + \frac{8}{3}(1+z)(-1+3z) \ln(z) + \frac{8}{3}z^2 \ln^2(z) \right. \\
& \left. - \frac{32}{3}z^2 \ln(z) \ln(1+z) - \frac{32}{3}z^2 \text{Li}_2(-z) \right], \\
\Delta_{bg}^{(2,0)} = & \mathbf{C}_F \left[\frac{1}{4}(-129 + 658z - 549z^2) + (64 - 197z + 136z^2) \ln(1-z) \right. \\
& - 3(11 - 32z + 23z^2) \ln^2(1-z) + \frac{35}{3}(1 - 2z + 2z^2) \ln^3(1-z) \\
& + 4(7 - 32z + 27z^2) \ln(1-z) \ln(z) - 3(7 - 14z + 22z^2) \ln^2(1-z) \ln(z) \\
& + \frac{1}{4}(-19 + 140z - 76z^2) \ln^2(z) + 4(3 - 6z + 10z^2) \ln(1-z) \ln^2(z) \\
& + \frac{1}{6}(-9 + 18z - 52z^2) \ln^3(z) - 4(1+z)(1+3z) \ln(z) \ln(1+z) \\
& - (13 + 16z - 28z^2) \text{Li}_2(1-z) - 2(1 - 2z + 26z^2) \ln(1-z) \text{Li}_2(1-z) \\
& - 4(1+z)(1+3z) \text{Li}_2(-z) + 6(-1 + 2z + 6z^2) \text{Li}_3(1-z) \\
& - 2(7 - 14z + 34z^2) \text{S}_{1,2}(1-z) + 2(5 - 16z + 6z^2) \zeta_2 - 8(1 - 2z + 2z^2) \ln(1-z) \zeta_2 \\
& + 2(19 - 38z + 50z^2) \zeta_3 - \frac{1}{2}(35 - 301z + 214z^2) \ln(z) + 8(1 - 2z + 6z^2) \zeta_2 \ln(z) \\
& \left. - 2(-1 + 2z) \ln(z) \text{Li}_2(1-z) - 16z^2 \ln(z) \text{Li}_2(-z) + 32z^2 \text{Li}_3(-z) \right] \\
& + \mathbf{C}_A \left[\frac{1}{54z}(-208 + 1185z - 2598z^2 + 1513z^3) \right. \\
& + \frac{1}{9z}(16 - 228z + 57z^2 + 182z^3) \ln(1-z) + \frac{1}{3z}(1-z)(16+z+145z^2) \ln^2(1-z) \\
& + \frac{13}{3}(1 - 2z + 2z^2) \ln^3(1-z) + 2(1 - 28z + 62z^2) \ln(1-z) \ln(z) \\
& + 2(1 + 22z - 6z^2) \ln^2(1-z) \ln(z) + \frac{1}{6}(-3 + 108z - 292z^2) \ln^2(z) \\
& + 2(-3 - 14z + 2z^2) \ln(1-z) \ln^2(z) + 2(1+z)(3+5z) \ln(z) \ln(1+z) \\
& - 8(1 + 2z + 2z^2) \ln(1-z) \ln(z) \ln(1+z) + 6(1 + 2z + 2z^2) \ln^2(z) \ln(1+z) \\
& \left. + \frac{2}{3z}(16 - 12z + 48z^2 + 53z^3) \text{Li}_2(1-z) + 2(13 + 22z + 10z^2) \ln(1-z) \text{Li}_2(1-z) \right]
\end{aligned}$$

$$\begin{aligned}
& - 8(-1+z)^2 \ln(z) \text{Li}_2(1-z) + 2(1+z)(3+5z) \text{Li}_2(-z) \\
& - 8(1+2z+2z^2) \ln(1-z) \text{Li}_2(-z) + 8(1+2z+2z^2) \ln(z) \text{Li}_2(-z) \\
& - 4(7+18z+6z^2) \text{Li}_3(1-z) - 4(1+2z+2z^2) \text{Li}_3(-z) \\
& - 8(1+2z+2z^2) \text{Li}_3\left(-\frac{1-z}{1+z}\right) + 8(1+2z+2z^2) \text{Li}_3\left(\frac{1-z}{1+z}\right) \\
& + \frac{8}{3z}(-2+3z-15z^2+20z^3) \zeta_2 - 16(1-z+2z^2) \ln(1-z) \zeta_2 - 2(1+4z+2z^2) \zeta_3 \\
& + \frac{1}{9}(102-66z-565z^2) \ln(z) + 8z(-5+2z) \zeta_2 \ln(z) + \frac{1}{3}(5+14z) \ln^3(z) \\
& + 16(1+3z+z^2) \text{S}_{1,2}(1-z) \Big],
\end{aligned}$$

$$\begin{aligned}
\Delta_{gg}^{(2,0)} = & 2(-1+z)(10+59z) - (2(-1+z)(23+75z) \ln(1-z)) \\
& + 16(-1+z)(1+3z) \ln^2(1-z) - 4(-5-16z+4z^2) \ln(1-z) \ln(z) \\
& - 8(1+2z)^2 \ln^2(1-z) \ln(z) + 4(1+2z)^2 \ln(1-z) \ln^2(z) \\
& - \frac{2}{3}(1+4z+8z^2) \ln^3(z) + 6(1+2z+2z^2) \ln^2(z) \ln(1+z) \\
& - 4(1+2z+2z^2) \ln(z) \ln^2(1+z) + 4(-1+4z+14z^2) \text{Li}_2(1-z) \\
& - 16(1+2z)^2 \ln(1-z) \text{Li}_2(1-z) - 4(1+2z)^2 \ln(z) \text{Li}_2(1-z) \\
& + 4(3+6z+2z^2) \ln(z) \text{Li}_2(-z) - 8(1+2z+2z^2) \ln(1+z) \text{Li}_2(-z) \\
& + 16(1+2z)^2 \text{Li}_3(1-z) + 4(-3-6z+2z^2) \text{Li}_3(-z) - 4(3+18z+14z^2) \text{S}_{1,2}(1-z) \\
& - 4(-4-9z+12z^2) \zeta_2 + 8(-1-2z+z^2) \zeta_3 + (-15-48z+121z^2) \ln(z) \\
& + 8(1+4z+5z^2) \zeta_2 \ln(z) - 2(2+15z+4z^2) \ln^2(z) - 4(1+2z+2z^2) \zeta_2 \ln(1+z) \\
& + 8z \ln(z) \ln(1+z) + 8z \text{Li}_2(-z) - 8(1+2z+2z^2) \text{S}_{1,2}(-z) \\
& + \frac{\mathbf{C}_A^2}{(\mathbf{N}^2 - \mathbf{1})} \left[\frac{1}{3}(-1+z)(1+249z) + \frac{2}{3}z(3+25z) \ln^2(z) \right. \\
& + \frac{8}{3}z(-3+2z) \ln(z) \ln(1+z) - 6(1+2z+2z^2) \ln^2(z) \ln(1+z) \\
& + 4(1+2z+2z^2) \ln(z) \ln^2(1+z) + \frac{8}{3}z(-3+2z) \text{Li}_2(-z) \\
& - 12(1+2z+2z^2) \ln(z) \text{Li}_2(-z) + 8(1+2z+2z^2) \ln(1+z) \text{Li}_2(-z) \\
& + 12(1+2z+2z^2) \text{Li}_3(-z) - 4(1-2z+2z^2) \text{S}_{1,2}(1-z) + \frac{4}{3}z(-3+2z) \zeta_2 \\
& \left. + 8(1+2z+2z^2) \zeta_3 - \frac{2}{3}(-2+40z+87z^2) \ln(z) + 4(1+2z+2z^2) \zeta_2 \ln(1+z) \right]
\end{aligned}$$

$$+ 8(1 + 2z + 2z^2)S_{1,2}(-z) \Big]. \quad (4.42)$$

The corresponding results from the QED and QCD×QED are found to be

$$\Delta_{b\bar{b}}^{(1,1)} = \Delta_{b\bar{b}}^{(2,0)} \Big|_{C_F^2 \rightarrow 2C_F e_b^2, C_A C_F \rightarrow 0, C_F n_f T_F \rightarrow 0, C_F T_F \rightarrow 0} \quad (4.43)$$

$$\Delta_{bb}^{(1,1)} = \Delta_{bb}^{(2,0)} \Big|_{C_F^2 \rightarrow 2C_F e_b^2, C_A C_F \rightarrow 0, C_F n_f T_F \rightarrow 0, C_F T_F \rightarrow 0} \quad (4.44)$$

$$\Delta_{ub}^{(1,1)} = 0 \quad (4.45)$$

$$\Delta_{u\bar{u}}^{(1,1)} = 0 \quad (4.46)$$

$$\Delta_{bg}^{(1,1)} = \frac{1}{2C_A C_F} \left[\left(2C_A C_F \Delta_{bg}^{(2,0)} \right) \Big|_{C_A C_F^2 \rightarrow C_A C_F e_b^2, C_A^2 C_F \rightarrow 0} \right] = \Delta_{bg}^{(2,0)} \Big|_{C_F \rightarrow e_b^2, C_A \rightarrow 0} \quad (4.47)$$

$$\Delta_{b\gamma}^{(1,1)} = \left(2C_A C_F \Delta_{bg}^{(2,0)} \right) \Big|_{C_A C_F^2 \rightarrow C_A C_F e_b^2, C_A^2 C_F \rightarrow 0} \quad (4.48)$$

$$\Delta_{g\gamma}^{(1,1)} = \frac{1}{2C_A C_F} \left[\left(4C_A^2 C_F^2 \Delta_{gg}^{(2,0)} \right) \Big|_{C_A^2 C_F^2 \rightarrow C_A^2 C_F e_b^2, C_A^3 C_F \rightarrow 0} \right] = \left(2C_A C_F \Delta_{gg}^{(2,0)} \right) \Big|_{C_A C_F \rightarrow C_A e_b^2, C_A^2 \rightarrow 0} \quad (4.49)$$

Partonic cross sections contributing to pure NLO and NNLO QED corrections:

$$\Delta_{b\bar{b}}^{(0,1)} = \Delta_{b\bar{b}}^{(1,0)} \Big|_{C_F \rightarrow e_b^2} \quad (4.50)$$

$$\Delta_{b\gamma}^{(0,1)} = \left(2C_A C_F \Delta_{bg}^{(1,0)} \right) \Big|_{C_A C_F \rightarrow C_A e_b^2} \quad (4.51)$$

$$\Delta_{b\bar{b}}^{(0,2)} = \Delta_{b\bar{b}}^{(2,0)} \Big|_{C_F^2 \rightarrow e_b^4, C_A C_F \rightarrow 0, C_F n_f T_F \rightarrow e_b^2 (N \sum_q e_q^2 + \sum_l e_l^2), C_F T_F \rightarrow N e_b^4} \quad (4.52)$$

$$\Delta_{bb}^{(0,2)} = \Delta_{bb}^{(2,0)} \Big|_{C_F^2 \rightarrow e_b^4, C_A C_F \rightarrow 0, C_F n_f T_F \rightarrow e_b^2 (N \sum_q e_q^2 + \sum_l e_l^2), C_F T_F \rightarrow N e_b^4} \quad (4.53)$$

$$\Delta_{ub}^{(0,2)} = \Delta_{ub}^{(2,0)} \Big|_{C_F T_F \rightarrow N e_b^2 e_u^2} \quad (4.54)$$

$$\Delta_{u\bar{u}}^{(0,2)} = \Delta_{u\bar{u}}^{(2,0)} \Big|_{C_F T_F \rightarrow N e_b^2 e_u^2} \quad (4.55)$$

$$\Delta_{b\gamma}^{(0,2)} = \left(2C_A C_F \Delta_{bg}^{(2,0)} \right) \Big|_{C_A C_F^2 \rightarrow C_A e_b^4, C_A^2 C_F \rightarrow 0} \quad (4.56)$$

$$\Delta_{\gamma\gamma}^{(0,2)} = \left(4C_A^2 C_F^2 \Delta_{gg}^{(2,0)} \right) \Big|_{C_A^2 C_F^2 \rightarrow C_A^2 e_b^4, C_A^3 C_F \rightarrow 0} \quad (4.57)$$

The constants $\zeta_i = \sum_{k=1}^{\infty} \frac{1}{k^i}$, $k \in \mathbb{N}$ denote the Riemann's ζ -functions. In our results, we

have ζ_2 and ζ_3 which take the values:

$$\begin{aligned}\zeta_2 &= 1.64493406684822643647\dots \\ \zeta_3 &= 1.20205690315959428540\dots\end{aligned}\tag{4.58}$$

Also, the Spence functions [172, 173] $\text{Li}_2(x)$ and $\text{Li}_3(x)$ are defined by

$$\begin{aligned}\text{Li}_2(x) &= \sum_{k=1}^{\infty} \frac{x^k}{k^2} = - \int_0^x \frac{\ln(1-t)}{t} dt, \\ \text{Li}_3(x) &= \sum_{k=1}^{\infty} \frac{x^k}{k^3} = \int_0^x \frac{\text{Li}_2(t)}{t} dt,\end{aligned}\tag{4.59}$$

and the Nielsen function $\text{S}_{1,2}(x)$ as

$$\text{S}_{1,2}(x) = \frac{1}{2} \int_0^1 \frac{dt}{t} \ln^2(1-tx).\tag{4.60}$$

In the next section, we study the numerical impact of the these partonic cross sections at the LHC energies.

4.7 Numerical Impact

In this section, we study the numerical impact of pure QED and mixed QCD-QED corrections over the dominant QCD corrections up to NNLO level to the production of the Higgs boson in bottom quark annihilation at the LHC. We focus mainly for the center of mass energy of $\sqrt{S} = 13$ TeV. Since we include QED effects, we need phdf inside the proton in addition to the standard pdfs. For this purpose, we use NNPDF 3.1 LUXqed set [174], MRST [175], CT14 [176] and PDF4LHC17. The pdfs, phdfs and the strong coupling constant a_s can be obtained using the LHAPDF-6 [153] interface. We have used the following input parameters for the masses and the couplings:

$$\begin{aligned}
m_W &= 80.4260 \text{ GeV} & m_b(m_b) &= 4.70 \text{ GeV} \\
m_Z &= 91.1876 \text{ GeV} & \alpha_s(m_h) &= 0.113 \\
m_h &= 125.09 \text{ GeV} & \alpha_e &= 1/128.0
\end{aligned}$$

Both $a_s(\mu_R)$ and $m_b(\mu_R)$ are evolved using appropriate QCD β -function coefficients and quark mass anomalous dimensions respectively. However, we have considered fixed $\alpha_e = 4\pi a_e$ throughout the computation.

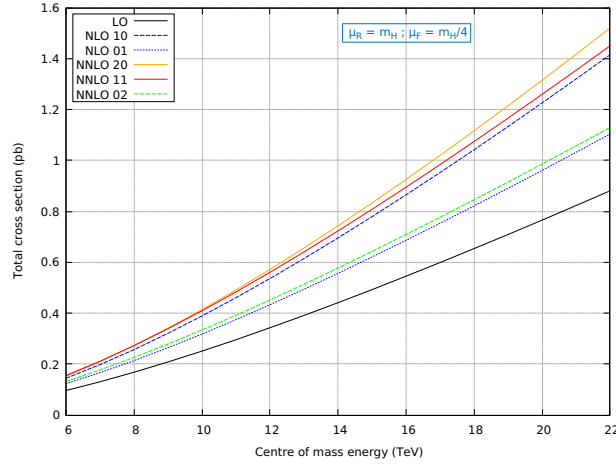


Figure 4.2: *The total cross section at various perturbative orders at energy scales varying from 6 to 22 TeV at LHC. The index ‘ij’ indicates that QCD at ‘i’-th order and QED at ‘j’-th order in perturbative theory are included.*

The Higgs boson production cross section from bottom quark annihilation at the present energy of LHC is not substantial. For example, at 13 TeV, the third order QCD corrections contribute almost 1% to the NNLO, while the mixed QCD-QED corrections contribute around 0.1% on top off the NNLO contributions. However, for the high luminosity LHC, measuring them at higher center of mass energy would give larger contributions and it will improve the precision. Hence, we have first studied how the cross section varies with the center of mass energy of LHC. In Fig. 4.2, we plot the inclusive production cross sections at various orders in perturbative QCD and QED for the range of CM energies between $\sqrt{S} = 6$ to 22 TeV. In the inset, the index ‘ij’ indicates that QCD at ‘i’-th order and QED at ‘j’-th order in perturbative theory are included. In Fig. 4.2, we have used NNPDF31_lo_as_0118, NNPDF31_nlo_as_0118_luxqed and

NNPDF31_nnlo_as_0118_luxqed for LO, NLO and NNLO, respectively. The scales (μ_R) and (μ_F) are kept fixed at m_h and $m_h/4$, respectively. We note that in Fig. 4.2, the pure QED contributions are large. This is due to the fact that we consider leading order QCD running of Yukawa coupling which gives larger Born contribution compared to pure QCD. However, if we consider same running of Yukawa coupling, the NLO QCD effects are 50 - 500 times larger than NLO QED effects, depending on the scale choice.

	$\Delta^{(0,0)}$	$\Delta^{(1,0)}$	$\Delta^{(0,1)}$	$\Delta^{(2,0)}$	$\Delta^{(1,1)}$	$\Delta^{(0,2)}$	Total
Δ_{00}	1.0181						1.0181
Δ_{10}	1.1362	-0.1810					0.9552
Δ_{01}	1.2219		0.0030				1.2249
Δ_{20}	1.1433	-0.1683		-0.1935			0.7816
Δ_{11}	1.1542	-0.1699	0.0029		-0.0005		0.9867
Δ_{02}	1.2422		0.0031			$-3 \cdot 10^{-5}$	1.2453

Table 4.1: Individual contributions in (pb) to various perturbative orders at $\sqrt{S}=14$ TeV.

	$\Delta^{0,0}$	$\Delta^{1,0}$	$\Delta^{0,1}$	$\Delta^{2,0}$	$\Delta^{1,1}$	$\Delta^{0,2}$	Total
Δ_{00}	0.3911						0.3911
Δ_{10}	0.4588	0.1557					0.6145
Δ_{01}	0.4935		0.0003				0.4938
Δ_{20}	0.4726	0.1614		0.0220			0.6561
Δ_{11}	0.4771	0.1630	0.0003		$1.5 \cdot 10^{-4}$		0.6406
Δ_{02}	0.5135		0.0003			$6 \cdot 10^{-6}$	0.5139

Table 4.2: Individual contributions in (pb) to various perturbative orders at $\sqrt{S}=13$ TeV.

In order to understand this in more detail, we study the impact of different contributions to the cross sections resulting from QCD, QED and mixed QCD-QED at various orders in perturbation theory. The results are tabulated in Table 4.1 for $\sqrt{S} = 14$ TeV and for the scale choice $\mu_R = \mu_F = m_h$. The $\Delta^{(i,j)}$ indicates sole i -th order QCD and j -th order QED corrections to the total contribution. Whereas the Δ_{ij} indicates the total contribution. For instance, Δ_{11} means $\Delta^{(0,0)} + \Delta^{(1,0)} + \Delta^{(0,1)} + \Delta^{(1,1)}$, or in other figures which is denoted by either LO, NLO or NNLO *e.g.* Δ_{11} means NNLO₁₁. In Table 4.2, a similar study has been performed for $\sqrt{S} = 13$ TeV and the scales $\mu_R = m_h$, $\mu_F = m_h/4$.

As we discussed, the fixed order predictions depend on the renormalization and factorization scales. The uncertainty resulting from the choice of the scales quantify the missing higher order contributions. We have studied their dependency by varying them independently around a central scale. Fig. 4.3 shows the dependence of the cross section on the renormalization scale for the fixed choice of the factorization scale $\mu_F = m_H/4$. It clearly demonstrates the importance of higher order corrections as the μ_R variation is much more stable at NNLO₂₀ compared to the lower orders.

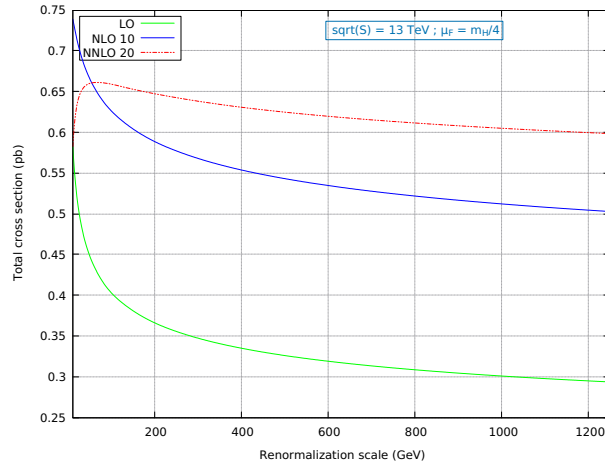


Figure 4.3: *The renormalization scale variation of the total cross section at various perturbative orders in QCD.*

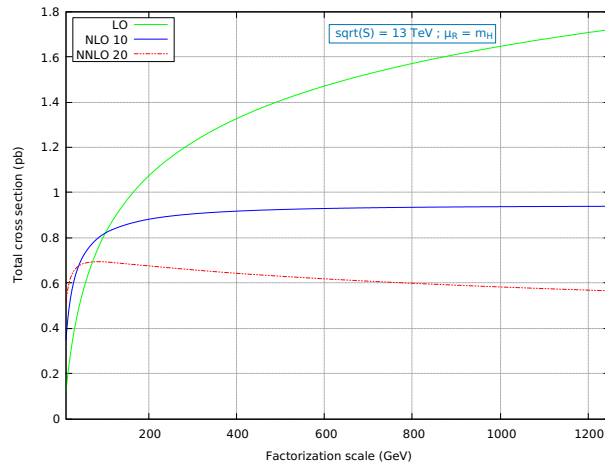


Figure 4.4: *The factorization scale variation of the total cross section at various perturbative orders in QCD.*

In Fig. 4.4, we present the dependence on the factorization scale keeping the renormalization scale fixed at m_h . Similar to the μ_R variation, μ_F variation improves after adding higher order corrections. To illustrate their dependence when both the scales are changed simultaneously, we present the cross section by performing 7-point scale variation and the results are listed in Table 4.3. We used NNPDF31_nnlo_as_0118_luxqed for this study.

$\left(\frac{\mu_R}{m_h}, \frac{\mu_F}{m_h}\right)$	$\left(2, \frac{1}{2}\right)$	$\left(2, \frac{1}{4}\right)$	$\left(1, \frac{1}{2}\right)$	$\left(1, \frac{1}{4}\right)$	$\left(1, \frac{1}{8}\right)$	$\left(\frac{1}{2}, \frac{1}{4}\right)$	$\left(\frac{1}{2}, \frac{1}{8}\right)$
NNLO ₂₀ (pb)	0.707	0.643	0.690	0.656	0.562	0.661	0.606
NNLO ₁₁ (pb)	0.759	0.602	0.780	0.641	0.445	0.682	0.498
NNLO ₀₂ (pb)	0.728	0.465	0.804	0.514	0.250	0.574	0.279

Table 4.3: 7-point scale variation at $\sqrt{S}=13$ TeV.

The perturbative predictions also depend on the choice of pdfs and phdfs. There are several groups which fit them and are widely used in the literature for the phenomenological studies. In order to estimate the uncertainty resulting from the choice of pdfs and phdfs we present the NNLO results from various pdf sets in Table 4.4 for $\sqrt{S}=14$ TeV and $\mu_R = \mu_F = m_h$. In Table 4.5, we repeat the study for $\sqrt{S}=13$ TeV and $\mu_R = m_h$ and $\mu_F = m_h/4$.

	MRST	NNPDF	CT14	PDF4LHC
NNLO ₂₀ (pb)	0.7805	0.7816	0.7574	0.8546
NNLO ₁₁ (pb)	0.9691	0.9867	0.9644	1.0625
NNLO ₀₂ (pb)	1.2020	1.2453	1.2288	1.3123

Table 4.4: Result using different pdfs at $\sqrt{S}=14$ TeV.

	MRST	NNPDF	CT14	PDF4LHC
NNLO ₂₀ (pb)	0.6610	0.6561	0.6398	0.7178
NNLO ₁₁ (pb)	0.6451	0.6406	0.6259	0.6996
NNLO ₀₂ (pb)	0.5252	0.5139	0.5030	0.5605

Table 4.5: Result using different pdfs at $\sqrt{S}=13$ TeV.

We have also studied the uncertainties resulting from the choice of pdf set [153]. Using NNPDF31, in Fig 4.5, we plot the variation of the cross section with respect to different choices of pdf and phdf replica. The central value and pdf uncertainties are given by the average and standard deviation over the replica sample, and are denoted in Fig 4.5 by the thick line and shaded region, respectively.

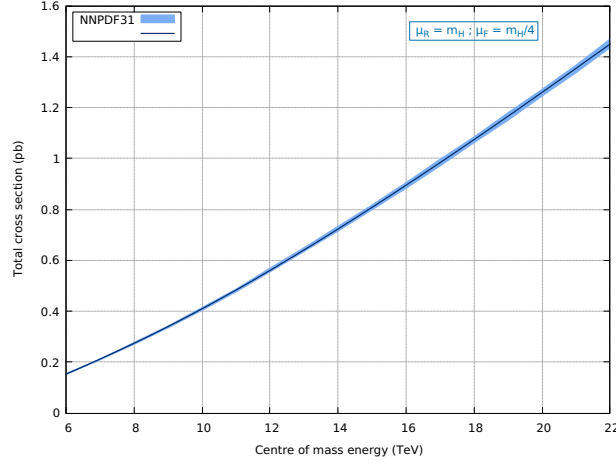


Figure 4.5: *pdf uncertainties.*

4.8 Summary

In this chapter we explored the possibility of including mixed QCD-QED as well as pure QED corrections to Higgs boson production in bottom quark annihilation channel. The computation involves dealing with QED soft and collinear singularities resulting from photons and the massless partons along with the corresponding QCD ones. We have systematically investigated the structure of these singularities up to second order in the QCD and QED couplings, taking into account the interference effects. We observe that, while the IR singularities factorize as a whole, the IR singularities from QCD do not factorize from that of QED leading to mixed/non-factorizable QCD-QED IR singularities. In addition, by computing the real emission processes in the limit when the photons/gluons become soft, we have studied the structure of soft distribution function. Using the universal

IR structure of the observable, we have determined the mass anomalous dimension of the bottom quark and hence the renormalization constant for the bottom Yukawa. We also discussed the relation between the results from pure QED, pure QCD and mixed QCD-QED through a set of rules which is found to be consistent with the so-called Abelianization procedure given in [156] for the case DY. Having obtained the complete NNLO results from QED and QCD-QED, we have systematically included them in the NNLO QCD study to understand their impact at the LHC energy. We find that the corrections are mild as expected, however, these higher order corrections from QED and mixed QCD-QED improve the reliability of the predictions.

5 Threshold rapidity corrections for n -colorless particles in QCD

In this chapter, we extend the threshold framework to obtain threshold rapidity distribution for a generic n -number of colorless productions. We present a universal soft collinear operator, which when applied to the virtual corrections of any colorless production process will give rise to SV or threshold corrections. Besides, we also provide a universal operator to perform the threshold resummation to N^3LL logarithmic accuracy. The materials presented in this chapter are the result of original research done in collaboration with Pooja Mukherjee, V. Ravindran et.al and are based on the article [177]

5.1 Prologue

Among different observables, the differential cross-section allows a wider range of comparisons with the experimental data. Over the past few decades several attempts have been made to incorporate the higher order QCD and EW radiative corrections to this observable. The topic of this chapter is concerning the differential cross-section with respect to rapidity, in particular, we address the question of computing the higher order QCD corrections to this observable for *any generic process* at hadron colliders with all the final state particles as *colorless*.

Despite its high importance, unlike the inclusive cross-section, the differential rapidity

distribution and its radiative corrections are computed only for a limited number of scattering processes. The rapidity distributions in Drell-Yan and of the scalar Higgs boson were computed to NNLO QCD in [178, 179] and [180], respectively. In case of the scalar Higgs boson produced through gluon fusion, the N³LO QCD correction was incorporated in [181]. Shortly before, it was approximated in [182] in the formalism of q_T -subtraction. For the Higgs boson production through bottom quark annihilation, it was computed to NNLO in [183].

Needless to say, achieving a full QCD correction to any order is not easy and with increasing perturbative order, the complexity level increase substantially which often prevents us from achieving it. In this context, SV approximation play an essential role, to obtain large contributions. In previous chapters, we discussed the threshold framework in the context of inclusive corrections. In this chapter we focus on the structure of differential scattering cross sections. These topic is studied in the past in [5, 184], where the authors present a formalism to incorporate the soft-gluon contribution to the rapidity distribution for the production of *a single colorless* final state. In the present work, we extend this formalism to the case of *any number of final state colorless particles* in hadronic collisions.

The formalism is based on QCD factorization, which dictates that the soft part of the real emission diagrams factorizes from the hard contribution, and renormalization group (RG) invariance. The factorized soft part is conjectured to fulfil a Sudakov type KG differential equation with respect to the final state invariant mass square. As a consequence, it is found to get exponentiated which not only provides us with the fixed order result under soft limit but also enables us to perform a resummation in the soft limit. For the production of arbitrary number of colorless particles in hadronic collision, the soft part essentially remains identical to the case of Sudakov type ($2 \rightarrow 1$)-process since the real emission can only takes place from the initial state partons. Using this idea, we extend the formalism [5] to the case of $2 \rightarrow n$ scattering, where n denotes the number of final state colorless particles. For this purpose, we combine the virtual matrix element that captures

the process dependence, the universal soft part and the mass-factorization kernels in an elegant way. In addition, we also show how naturally it leads to the threshold resummation for the same observable.

In the literature, several results for the rapidity resummation employing different methods are available. In [185], following the conjecture given in [186], the resummation of rapidity of W^\pm gauge boson and in [187] of Drell-Yan are computed in Mellin-Fourier (M-F) space. A detailed theoretical underpinnings and phenomenological implications of threshold resummation of rapidity are examined in [188] emphasizing the role of prescriptions that take care of diverging series at a given logarithmic accuracy. Our method belongs to a category, so called direct QCD approach [68], which is based on [5, 184, 189], where we resums the soft gluons in two dimensional Mellin space (M-M). In [190], the merits of different approaches are discussed in details.

One of the salient features of our formalism is that the soft part that enters into the rapidity distribution is shown to be connected to the respective part of inclusive cross-section through a very simple relation involving gamma function of the dimensional regulator. This relation was used to extract the required soft part from the respective quantity of the SV cross-section [60, 191]. The main *goal* of this chapter is to present the formal methodology of computing threshold rapidity corrections for any generic process of $2 \rightarrow n$ kind at hadron collider.

The chapter is organized as follows: in Sec.[5.2], we introduce the notion of soft-virtual correction in the context of differential rapidity distribution and then describe our formalism in details in Sec.[5.2.1]. The universality of soft part leads us to define a quantity called the differential soft-collinear operator that essentially captures the process independent part, is also introduced in Sec. 5.2.1. In Sec.[5.4], we extend our formalism to incorporate the threshold resummation of the rapidity distribution.

5.2 Soft-virtual rapidity distribution

We begin by introducing the regime of soft gluon contribution to differential rapidity distribution for the production of n -number of colorless particles in hadron collisions within the framework of perturbative QCD. Our prescription that we will develop subsequently to capture this contribution is within the scope of QCD improved parton model where the collinear divergences factorize to all orders in strong coupling constant $\alpha_s = g_s^2/4\pi$. We consider a generic hadronic collision between two hadrons $H_{1,(2)}$ having momentum $P_{1,(2)}$ that produces a final state consisting of n -number of colorless particles, denoted as $F_i(q_i)$

$$H_1(P_1) + H_2(P_2) \rightarrow \sum_{i=1}^n F_i(q_i) + X. \quad (5.1)$$

Through the quantity X , we represent an inclusive hadronic state. q_i stands for the momentum of corresponding colorless particle F_i . We denote the invariant mass square of the final state by q^2 which is related to the momenta $\{q_i\}$ through $q^2 = (\sum_i q_i)^2$. Without loss of generality, the rapidity of the final state invariant mass system is defined as

$$y \equiv \frac{1}{2} \ln \left(\frac{P_2 \cdot q}{P_1 \cdot q} \right). \quad (5.2)$$

The differential rapidity distribution at the hadronic level can be written as

$$\begin{aligned} \frac{d^2}{dy dq^2} \sigma(\tau, q^2, y) &= \sigma_B(\tau, q^2) W(\tau, q^2, y) \quad \text{with} \\ W &= \sum_{a,b=q,\bar{q},g} \int_0^1 dx_1 \int_0^1 dx_2 f_a(x_1, \mu_F^2) f_b(x_2, \mu_F^2) \int_0^1 dz \delta(\tau - zx_1 x_2) \\ &\quad \times \int [dPS_m] |\overline{\mathcal{M}}_{ab}|^2 \delta\left(y - \frac{1}{2} \ln \left(\frac{P_2 \cdot q}{P_1 \cdot q} \right)\right). \end{aligned} \quad (5.3)$$

Here, σ_B is the LO contribution normalized by the delta function. The dimensionless variables, $\tau \equiv \frac{q^2}{S}$ and $z \equiv \frac{q^2}{\hat{s}}$, where S and \hat{s} are respectively the hadronic and partonic center-of-mass energies. We denote the fraction of the initial state hadronic momentum

carried by the partons (a, b) that take part in the scattering at the partonic level as $x_{1(2)}$, and these are constrained through the relation $\tau = z x_1 x_2$ as reflected by the presence of the respective δ -function in the definition of W . The $f_{a(b)}$ are the pdf's renormalized at the factorization scale μ_F and the coupling constant is renormalized at the scale μ_R . The mass-factorized scattering matrix element is denoted through $\overline{\mathcal{M}}_{ab}$ containing an overline to signify the sum and average over all the quantum numbers for the final and initial state particles, respectively. The corresponding m -particle phase space is $[dPS_m]$. Note that the numerical value of the integer m depends on the number of radiated partons which is solely controlled by the perturbative order we are interested in.

We confine ourselves to the regime where the leading order processes can only be initiated through color neutral quark or gluon channels,

$$q(p_1) + \bar{q}(p_2) \rightarrow \sum_{i=1}^n F_i(q_i) \quad \text{and} \quad g(p_1) + g(p_2) \rightarrow \sum_{i=1}^n F_i(q_i) \quad (5.4)$$

with the corresponding momenta $p_{1(2)}$. Moreover, we are interested in computing the differential rapidity distribution only in the soft limit which constrained all the partonic radiation to be only soft. In order to define the soft limit for the rapidity distribution, we choose to work with a set of symmetric scaling variables $x_{1(2)}^0$ instead of y and τ which are related through

$$y \equiv \frac{1}{2} \ln \left(\frac{x_1^0}{x_2^0} \right) \quad \text{and} \quad \tau \equiv x_1^0 x_2^0. \quad (5.5)$$

Note that unlike the inclusive cross-section, the choice of variables which one needs to take in order to define the soft limit is not unique and as it turns out, our choice of these new set of variables is crucial for our prescription. In terms of these variables, the partonic contributions arising from the subprocesses are found to depend on the ratios

$$z_i \equiv \frac{x_i^0}{x_i}, \quad (5.6)$$

which play the role of scaling variables at the partonic level. After evaluating the δ -function integration over z , the $W(\tau, q^2, y)$ in (5.3) can be rewritten as

$$W(x_1^0, x_2^0, q^2) = \sum_{a,b} \int_{x_1^0}^1 \frac{dz_1}{z_1} \int_{x_2^0}^1 \frac{dz_2}{z_2} f_a\left(\frac{x_1^0}{z_1}, \mu_F^2\right) f_b\left(\frac{x_2^0}{z_2}, \mu_F^2\right) \Delta_{d,ab}(z_1, z_2, q^2, \{p_j \cdot q_k\}, \mu_F^2) \quad (5.7)$$

with the coefficient function defined as:

$$\Delta_{d,ab}(z_1, z_2, q^2, \{p_j \cdot q_k\}, \mu_F^2) = \int [dPS_m] |\overline{\mathcal{M}}_{ab}|^2 \delta\left(y - \frac{1}{2} \ln\left(\frac{P_2 \cdot q}{P_1 \cdot q}\right)\right). \quad (5.8)$$

Being a scattering process containing n -number of final state colorless particles, the partonic coefficient function does, in fact, depend on the Mandelstam variables constructed out of all the independent external momenta which is concisely denoted through $\{p_j \cdot q_k\}$. In order to find the definition of soft limit in terms of the new partonic scaling variables, we take the double Mellin moment of W with respect to the variables $N_{1(2)}$ which turns out to be

$$\begin{aligned} W(N_1, N_2) &\equiv \int dx_1^0 (x_1^0)^{N_1-1} \int dx_2^0 (x_2^0)^{N_2-1} W(x_1^0, x_2^0) \\ &= \sum_{ab} f_a(N_1) f_b(N_2) \Delta_{d,ab}(N_1, N_2). \end{aligned} \quad (5.9)$$

All the quantities with functional dependence of $N_{1(2)}$ are in Mellin space where the soft limit is defined by the simultaneous limit of $N_{1(2)} \rightarrow \infty$. In terms of partonic scaling variables this condition gets translated to $z_{1(2)} \rightarrow 1$. Note that we normalize the coefficient function $\Delta_{d,ab}$ in such a way that at the leading order W satisfies

$$W(x_1^0, x_2^0, q^2, \mu_R^2) = W_B \equiv \delta(1 - x_1^0) \delta(1 - x_2^0). \quad (5.10)$$

In the following section, we will present the prescription to calculate the infrared safe SV differential rapidity distribution to N⁴LO in QCD for any $2 \rightarrow n$ scattering process which

can be computed order by order in perturbation theory in terms of $a_s(\mu_R^2) \equiv \alpha_s(\mu_R^2)/4\pi$:

$$\mathcal{A}_{d,ab}^{\text{SV}}(z_1, z_2, q^2, \{p_j \cdot q_k\}, \mu_F^2) = \alpha_s^\lambda(\mu_R^2) \sum_{k=0}^{\infty} a_s^k(\mu_R^2) \mathcal{A}_{d,ab}^{(k),\text{SV}}(z_1, z_2, q^2, \{p_j \cdot q_k\}, \mu_F^2, \mu_R^2). \quad (5.11)$$

λ is the order of strong coupling constant at the leading order partonic process.

5.2.1 Soft-collinear operator for SV rapidity distribution

In this section, we setup a framework to compute the soft-virtual corrections to the rapidity distribution to all orders in strong coupling constant. The infrared safe SV rapidity distribution can be obtained by combining the UV renormalized virtual matrix elements with the soft gluon contribution and performing appropriate mass factorization to get rid of initial state collinear singularities. It is well-known that the combined soft and collinear divergences, conveniently denoted as IR, in virtual matrix elements factorize from the corresponding UV renormalized part to all orders in perturbation theory. In dimensional regularization we can write

$$\mathcal{M}_{ab,\text{fin}}(\{p_j\}, \{q_k\}, \mu_R^2) = \lim_{\epsilon \rightarrow 0} Z_{ab,\text{IR}}^{-1}(q^2, \mu_R^2, \epsilon) \mathcal{M}_{ab}(\{p_j\}, \{q_k\}, \epsilon) \quad (5.12)$$

with the space-time dimensions $d = 4 + \epsilon$. Without loss of generality, we choose the renormalization scale to be equal to the scale of aforementioned factorization which, of course, in general can be different. Upon multiplying the renormalization constant $Z_{ab,\text{IR}}$, the IR divergent part of the UV renormalized matrix element \mathcal{M}_{ab} gets compensated and we end up with the finite part of the matrix element $\mathcal{M}_{ab,\text{fin}}$. The renormalization constant is a universal quantity as it is independent of the details of the process, it only depends on the nature of external color particles. It is fully independent of the number and nature of external colorless particles.

Expanding the $Z_{I,\text{IR}}(q^2, \mu_R^2, \epsilon)$ in powers of $a_s(\mu_R^2)$ ¹:

$$Z_{I,\text{IR}}(q^2, \mu_R^2, \epsilon) = 1 + \sum_{k=1}^{\infty} a_s^k(\mu_R^2) Z_{I,\text{IR}}^{(k)}(q^2, \epsilon) \quad (5.13)$$

with the coefficients $Z_{I,\text{IR}}^{(k)}$ up to four loops by setting $\mu_R^2 = q^2$:

$$\begin{aligned} Z_{I,\text{IR}}^{(1)} &= \frac{1}{\epsilon^2} \left\{ -2A_1^I \right\} + \frac{1}{\epsilon} \left\{ f_1^I + 2B_1^I - \pi A_1^I i \right\}, \\ Z_{I,\text{IR}}^{(2)} &= \frac{1}{\epsilon^4} \left\{ 2(A_1^I)^2 \right\} + \frac{1}{\epsilon^3} \left\{ -2A_1^I f_1^I - 4A_1^I B_1^I - 3\beta_0 A_1^I + 2\pi(A_1^I)^2 i \right\} + \frac{1}{\epsilon^2} \left\{ \frac{1}{2}(f_1^I)^2 + 2B_1^I f_1^I \right. \\ &\quad \left. + 2(B_1^I)^2 - \frac{1}{2}A_2^I + \beta_0 f_1^I + 2\beta_0 B_1^I - 3\zeta_2(A_1^I)^2 - \pi A_1^I f_1^I i - 2\pi A_1^I B_1^I i - \pi\beta_0 A_1^I i \right\} + \frac{1}{\epsilon} \left\{ \right. \\ &\quad \left. \frac{1}{2}f_2^I + B_2^I - \frac{1}{2}\pi A_2^I i \right\}, \\ Z_{I,\text{IR}}^{(3)} &= \frac{1}{\epsilon^6} \left\{ -\frac{4}{3}(A_1^I)^3 \right\} + \frac{1}{\epsilon^5} \left\{ 2(A_1^I)^2 f_1^I + 4(A_1^I)^2 B_1^I + 6\beta_0(A_1^I)^2 - 2\pi(A_1^I)^3 i \right\} + \frac{1}{\epsilon^4} \left\{ -A_1^I (f_1^I)^2 \right. \\ &\quad \left. - 4A_1^I B_1^I f_1^I - 4A_1^I (B_1^I)^2 + A_1^I A_2^I - 5\beta_0 A_1^I f_1^I - 10\beta_0 A_1^I B_1^I - \frac{44}{9}\beta_0^2 A_1^I + 6\zeta_2(A_1^I)^3 \right. \\ &\quad \left. + 2\pi(A_1^I)^2 f_1^I i + 4\pi(A_1^I)^2 B_1^I i + 5\pi\beta_0(A_1^I)^2 i \right\} + \frac{1}{\epsilon^3} \left\{ \frac{1}{6}(f_1^I)^3 + B_1^I (f_1^I)^2 + 2(B_1^I)^2 f_1^I \right. \\ &\quad \left. + \frac{4}{3}(B_1^I)^3 - \frac{1}{2}A_2^I f_1^I - A_2^I B_1^I - A_1^I f_2^I - 2A_1^I B_2^I - \frac{16}{9}\beta_1 A_1^I + \beta_0 (f_1^I)^2 + 4\beta_0 B_1^I f_1^I \right. \\ &\quad \left. + 4\beta_0 (B_1^I)^2 - \frac{10}{9}\beta_0 A_2^I + \frac{4}{3}\beta_0^2 f_1^I + \frac{8}{3}\beta_0^2 B_1^I - 3\zeta_2(A_1^I)^2 f_1^I - 6\zeta_2(A_1^I)^2 B_1^I - 6\zeta_2\beta_0(A_1^I)^2 \right. \\ &\quad \left. - \frac{1}{2}\pi A_1^I (f_1^I)^2 i - 2\pi A_1^I B_1^I f_1^I i - 2\pi A_1^I (B_1^I)^2 i + \frac{3}{2}\pi A_1^I A_2^I i - 2\pi\beta_0 A_1^I f_1^I i - 4\pi\beta_0 A_1^I B_1^I i \right. \\ &\quad \left. - \frac{4}{3}\pi\beta_0^2 A_1^I i + \pi\zeta_2(A_1^I)^3 i \right\} + \frac{1}{\epsilon^2} \left\{ \frac{1}{2}f_1^I f_2^I + B_2^I f_1^I + B_1^I f_2^I + 2B_1^I B_2^I - \frac{2}{9}A_3^I + \frac{2}{3}\beta_1 f_1^I \right. \\ &\quad \left. + \frac{4}{3}\beta_1 B_1^I + \frac{2}{3}\beta_0 f_2^I + \frac{4}{3}\beta_0 B_2^I - 3\zeta_2 A_1^I A_2^I - \frac{1}{2}\pi A_2^I f_1^I i - \pi A_2^I B_1^I i - \frac{1}{2}\pi A_1^I f_2^I i - \pi A_1^I B_2^I i \right. \\ &\quad \left. - \frac{2}{3}\pi\beta_1 A_1^I i - \frac{2}{3}\pi\beta_0 A_2^I i \right\} + \frac{1}{\epsilon} \left\{ \frac{1}{3}f_3^I + \frac{2}{3}B_3^I - \frac{1}{3}\pi A_3^I i \right\}, \\ Z_{I,\text{IR}}^{(4)} &= \frac{1}{\epsilon^8} \left\{ \frac{2}{3}(A_1^I)^4 \right\} + \frac{1}{\epsilon^7} \left\{ -\frac{4}{3}(A_1^I)^3 f_1^I - \frac{8}{3}(A_1^I)^3 B_1^I - 6\beta_0(A_1^I)^3 + \frac{4}{3}\pi(A_1^I)^4 i \right\} \\ &\quad + \frac{1}{\epsilon^6} \left\{ (A_1^I)^2 (f_1^I)^2 + 4(A_1^I)^2 B_1^I f_1^I + 4(A_1^I)^2 (B_1^I)^2 - (A_1^I)^2 A_2^I + 8\beta_0(A_1^I)^2 f_1^I \right. \\ &\quad \left. + 16\beta_0(A_1^I)^2 B_1^I + \frac{257}{18}\beta_0^2(A_1^I)^2 - 6\zeta_2(A_1^I)^4 - 2\pi(A_1^I)^3 f_1^I i - 4\pi(A_1^I)^3 B_1^I i \right. \\ &\quad \left. - 8\pi\beta_0(A_1^I)^3 i \right\} + \frac{1}{\epsilon^5} \left\{ -\frac{1}{3}A_1^I (f_1^I)^3 - 2A_1^I B_1^I (f_1^I)^2 - 4A_1^I (B_1^I)^2 f_1^I - \frac{8}{3}A_1^I (B_1^I)^3 \right. \end{aligned}$$

¹See [41, 158, 192, 193] for an elaborated discussion on the universality of subleading infrared poles in form factors.

$$\begin{aligned}
& + A_1^l A_2^l f_1^l + 2A_1^l A_2^l B_1^l + (A_1^l)^2 f_2^l + 2(A_1^l)^2 B_2^l + \frac{32}{9}\beta_1(A_1^l)^2 - \frac{7}{2}\beta_0 A_1^l (f_1^l)^2 \\
& - 14\beta_0 A_1^l B_1^l f_1^l - 14\beta_0 A_1^l (B_1^l)^2 + \frac{67}{18}\beta_0 A_1^l A_2^l - \frac{95}{9}\beta_0^2 A_1^l f_1^l - \frac{190}{9}\beta_0^2 A_1^l B_1^l - \frac{25}{3}\beta_0^3 A_1^l \\
& + 6\zeta_2(A_1^l)^3 f_1^l + 12\zeta_2(A_1^l)^3 B_1^l + 21\zeta_2\beta_0(A_1^l)^3 + \pi(A_1^l)^2 (f_1^l)^2 i + 4\pi(A_1^l)^2 B_1^l f_1^l i \\
& + 4\pi(A_1^l)^2 (B_1^l)^2 i - 2\pi(A_1^l)^2 A_2^l i + 7\pi\beta_0(A_1^l)^2 f_1^l i + 14\pi\beta_0(A_1^l)^2 B_1^l i + \frac{95}{9}\pi\beta_0^2(A_1^l)^2 i \\
& - 2\pi\zeta_2(A_1^l)^4 i \Big\} + \frac{1}{\epsilon^4} \left\{ \frac{1}{24}(f_1^l)^4 + \frac{1}{3}B_1^l (f_1^l)^3 + (B_1^l)^2 (f_1^l)^2 + \frac{4}{3}(B_1^l)^3 f_1^l + \frac{2}{3}(B_1^l)^4 \right. \\
& - \frac{1}{4}A_2^l (f_1^l)^2 - A_2^l B_1^l f_1^l - A_2^l (B_1^l)^2 + \frac{1}{8}(A_2^l)^2 - A_1^l f_1^l f_2^l - 2A_1^l B_2^l f_1^l - 2A_1^l B_1^l f_2^l \\
& - 4A_1^l B_1^l B_2^l + \frac{4}{9}A_1^l A_3^l - \frac{28}{9}\beta_1 A_1^l f_1^l - \frac{56}{9}\beta_1 A_1^l B_1^l + \frac{1}{2}\beta_0 (f_1^l)^3 + 3\beta_0 B_1^l (f_1^l)^2 \\
& + 6\beta_0 (B_1^l)^2 f_1^l + 4\beta_0 (B_1^l)^3 - \frac{29}{18}\beta_0 A_2^l f_1^l - \frac{29}{9}\beta_0 A_2^l B_1^l - \frac{17}{6}\beta_0 A_1^l f_2^l - \frac{17}{3}\beta_0 A_1^l B_2^l \\
& - \frac{20}{3}\beta_0 \beta_1 A_1^l + \frac{11}{6}\beta_0^2 (f_1^l)^2 + \frac{22}{3}\beta_0^2 B_1^l f_1^l + \frac{22}{3}\beta_0^2 (B_1^l)^2 - \frac{13}{6}\beta_0^2 A_2^l + 2\beta_0^3 f_1^l + 4\beta_0^3 B_1^l \\
& - \frac{3}{2}\zeta_2(A_1^l)^2 (f_1^l)^2 - 6\zeta_2(A_1^l)^2 B_1^l f_1^l - 6\zeta_2(A_1^l)^2 (B_1^l)^2 + \frac{15}{2}\zeta_2(A_1^l)^2 A_2^l - 9\zeta_2\beta_0(A_1^l)^2 f_1^l \\
& - 18\zeta_2\beta_0(A_1^l)^2 B_1^l - 11\zeta_2\beta_0^2(A_1^l)^2 + \frac{3}{2}\zeta_2(A_1^l)^4 - \frac{1}{6}\pi A_1^l (f_1^l)^3 i - \pi A_1^l B_1^l (f_1^l)^2 i \\
& - 2\pi A_1^l (B_1^l)^2 f_1^l i - \frac{4}{3}\pi A_1^l (B_1^l)^3 i + \frac{3}{2}\pi A_1^l A_2^l f_1^l i + 3\pi A_1^l A_2^l B_1^l i + \pi(A_1^l)^2 f_2^l i \\
& + 2\pi(A_1^l)^2 B_2^l i + \frac{28}{9}\pi\beta_1(A_1^l)^2 i - \frac{3}{2}\pi\beta_0 A_1^l (f_1^l)^2 i - 6\pi\beta_0 A_1^l B_1^l f_1^l i - 6\pi\beta_0 A_1^l (B_1^l)^2 i \\
& + \frac{40}{9}\pi\beta_0 A_1^l A_2^l i - \frac{11}{3}\pi\beta_0^2 A_1^l f_1^l i - \frac{22}{3}\pi\beta_0^2 A_1^l B_1^l i - 2\pi\beta_0^3 A_1^l i + \pi\zeta_2(A_1^l)^3 f_1^l i \\
& + 2\pi\zeta_2(A_1^l)^3 B_1^l i + 3\pi\zeta_2\beta_0(A_1^l)^3 i \Big\} + \frac{1}{\epsilon^3} \left\{ \frac{1}{4}(f_1^l)^2 f_2^l + \frac{1}{2}B_2^l (f_1^l)^2 + B_1^l f_1^l f_2^l + 2B_1^l B_2^l f_1^l \right. \\
& + (B_1^l)^2 f_2^l + 2(B_1^l)^2 B_2^l - \frac{2}{9}A_3^l f_1^l - \frac{4}{9}A_3^l B_1^l - \frac{1}{4}A_2^l f_2^l - \frac{1}{2}A_2^l B_2^l - \frac{2}{3}A_1^l f_3^l - \frac{4}{3}A_1^l B_3^l \\
& - \frac{5}{4}\beta_2 A_1^l + \frac{2}{3}\beta_1 (f_1^l)^2 + \frac{8}{3}\beta_1 B_1^l f_1^l + \frac{8}{3}\beta_1 (B_1^l)^2 - \frac{3}{4}\beta_1 A_2^l + \frac{7}{6}\beta_0 f_1^l f_2^l + \frac{7}{3}\beta_0 B_2^l f_1^l \\
& + \frac{7}{3}\beta_0 B_1^l f_2^l + \frac{14}{3}\beta_0 B_1^l B_2^l - \frac{7}{12}\beta_0 A_3^l + 2\beta_0 \beta_1 f_1^l + 4\beta_0 \beta_1 B_1^l + \beta_0^2 f_2^l + 2\beta_0^2 B_2^l \\
& - 3\zeta_2 A_1^l A_2^l f_1^l - 6\zeta_2 A_1^l A_2^l B_1^l - \frac{3}{2}\zeta_2(A_1^l)^2 f_2^l - 3\zeta_2(A_1^l)^2 B_2^l - 4\zeta_2\beta_1(A_1^l)^2 - 7\zeta_2\beta_0 A_1^l A_2^l \\
& - \frac{1}{4}\pi A_2^l (f_1^l)^2 i - \pi A_2^l B_1^l f_1^l i - \pi A_2^l (B_1^l)^2 i + \frac{1}{4}\pi(A_2^l)^2 i - \frac{1}{2}\pi A_1^l f_1^l f_2^l i - \pi A_1^l B_2^l f_1^l i \\
& - \pi A_1^l B_1^l f_2^l i - 2\pi A_1^l B_1^l B_2^l i + \frac{8}{9}\pi A_1^l A_3^l i - \frac{4}{3}\pi\beta_1 A_1^l f_1^l i - \frac{8}{3}\pi\beta_1 A_1^l B_1^l i - \frac{7}{6}\pi\beta_0 A_2^l f_1^l i \\
& - \frac{7}{3}\pi\beta_0 A_2^l B_1^l i - \frac{7}{6}\pi\beta_0 A_1^l f_2^l i - \frac{7}{3}\pi\beta_0 A_1^l B_2^l i - 2\pi\beta_0 \beta_1 A_1^l i - \pi\beta_0^2 A_2^l i + \frac{3}{2}\pi\zeta_2(A_1^l)^2 A_2^l i \Big\} \\
& + \frac{1}{\epsilon^2} \left\{ \frac{1}{8}(f_2^l)^2 + \frac{1}{3}f_1^l f_3^l + \frac{2}{3}B_3^l f_1^l + \frac{1}{2}B_2^l f_2^l + \frac{1}{2}(B_2^l)^2 + \frac{2}{3}B_1^l f_3^l + \frac{4}{3}B_1^l B_3^l - \frac{1}{8}A_4^l \right.
\end{aligned}$$

$$\begin{aligned}
& + \frac{1}{2}\beta_2 f_1^l + \beta_2 B_1^l + \frac{1}{2}\beta_1 f_2^l + \beta_1 B_2^l + \frac{1}{2}\beta_0 f_3^l + \beta_0 B_3^l - \frac{3}{4}\zeta_2(A_2^l)^2 - 2\zeta_2 A_1^l A_3^l \\
& - \frac{1}{3}\pi A_3^l f_1^l i - \frac{2}{3}\pi A_3^l B_1^l i - \frac{1}{4}\pi A_2^l f_2^l i - \frac{1}{2}\pi A_2^l B_2^l i - \frac{1}{3}\pi A_1^l f_3^l i - \frac{2}{3}\pi A_1^l B_3^l i - \frac{1}{2}\pi \beta_2 A_1^l i \\
& - \frac{1}{2}\pi \beta_1 A_2^l i - \frac{1}{2}\pi \beta_0 A_3^l i \} + \frac{1}{\epsilon} \left\{ \frac{1}{4}f_4^l + \frac{1}{2}B_4^l - \frac{1}{4}\pi A_4^l i \right\}. \tag{5.14}
\end{aligned}$$

The anomalous dimensions that appear in the aforementioned results are expanded as:

$$X^l(\mu_R^2) = \sum_{j=1}^{\infty} a_s^j(\mu_R^2) X_j^l, \tag{5.15}$$

where $X = A, B, f$. For processes involving only conserved operator, such as Drell-Yan, the coupling constant renormalization is sufficient to get rid of all the UV divergences. However, for other processes, such as the Higgs boson production in heavy quark effective theory, additional operator renormalization is required. This is a property inherent to the operator itself.

In order to get the infrared safe and finite differential rapidity distribution, we need to combine the UV renormalized virtual matrix element to the real emission contributions in the soft limit and perform mass factorization which ensures the removal of collinear singularities arising from the initial state colored particles. Therefore, the universal nature of IR divergences in virtual matrix element implies that the combined contribution from the real emission diagrams and mass-factorization kernels must exhibit the same universality. By employing the criteria of universal IR structure and imposing the finiteness property of the rapidity distribution, we develop the prescription to compute the rapidity distribution under SV approximation for any generic $2 \rightarrow n$ scattering process and present the result in terms of universal quantities to N⁴LO QCD. Once the pure virtual matrix element for any process of the kind under consideration becomes available, our expression can immediately be employed to calculate the SV rapidity distribution at that order in QCD.

We propose that the coefficient function for the rapidity distribution in Eq.(5.11) can be written as a Mellin convolution of the pure virtual contribution \mathcal{F} , soft-collinear distribu-

tion Φ_d and mass-factorization kernel Γ , which read as

$$\begin{aligned} \mathcal{A}_{d,I}^{\text{sv}}(z_1, z_2, q^2, \{p_j \cdot q_k\}, \mu_F^2) &= |\mathcal{M}_I^{(0)}|^2 |\mathcal{F}^I(\{p_j \cdot q_k\}, q^2, \epsilon)|^2 \delta(1 - z_1) \delta(1 - z_2) \\ &\otimes C \exp \left[2\Phi_{d,\text{sv}}^I(z_1, z_2, q^2, \epsilon) - C \ln \Gamma_I(z_1, \mu_F^2, \epsilon) \delta(1 - z_2) \right. \\ &\quad \left. - C \ln \Gamma_I(z_2, \mu_F^2, \epsilon) \delta(1 - z_1) \right]. \end{aligned} \quad (5.16)$$

Since we are confining our discussion to only those scattering processes with initial state quark-antiquark pair of same flavours or a pair of gluon, we conveniently use the index I , where $I = q, b, g$ respectively refers to Drell-Yan process, Higgs production via bottom quark annihilation and from gluon fusion channel. The pure virtual contribution is captured through the form factor $\mathcal{F}_{a\bar{a}}$ that is defined as

$$\mathcal{F}^I = 1 + \sum_{k=1}^{\infty} a_s^k \mathcal{F}^{I,(k)} \equiv 1 + \sum_{k=1}^{\infty} a_s^k \frac{\langle \mathcal{M}_I^{(0)} | \mathcal{M}_I^{(k)} \rangle}{\langle \mathcal{M}_I^{(0)} | \mathcal{M}_I^{(0)} \rangle}, \quad (5.17)$$

where $\mathcal{M}_I^{(k)}$ represents the k -th order UV renormalized matrix element of the underlying partonic level process $a(p_1) + \bar{a}(p_2) \rightarrow \sum_{i=1}^n F_i(q_i)$. The symbol ‘‘C’’ stands for the convolution whose actions on a distribution $g(z_1, z_2)$ is defined as

$$C e^{g(z_1, z_2)} = \delta(1 - z_1) \delta(1 - z_2) + \frac{1}{1!} g(z_1, z_2) + \frac{1}{2!} (g \otimes g)(z_1, z_2) + \dots, \quad (5.18)$$

where \otimes denotes Mellin convolution. In the context of SV corrections, we encounter only $\delta(1 - z_i)$ and $\mathcal{D}_j(z_i)$, where

$$\mathcal{D}_j(z_i) \equiv \left[\frac{\ln^j(1 - z_i)}{(1 - z_i)} \right]_+. \quad (5.19)$$

The contribution from the real emission diagrams is contained in soft-collinear distribution $\Phi_{d,\text{sv}}^I$. The soft divergences arising from the real emission and virtual diagrams, which are respectively encapsulated in $\Phi_{d,\text{sv}}$ and \mathcal{F} , get cancelled. The final state collinear singularity is guaranteed to go away, as dictated by KLN theorem, once the sum over all

the final states is performed. The mass factorization kernel takes care of the initial state collinear singularities. As a result, the coefficient function $\mathcal{A}_{d,I}^{\text{sv}}$ in (5.16) becomes finite. By demanding the finiteness of this quantity we can put a constraint on the soft-collinear distribution which turns out to be a Sudakov type RG equation. This has profound implications which not only reveals a significant amount of insights about the IR world but also it enables us to perform threshold resummation as we will see in the next section. To be more precise, the solution of the RG equation results an all order exponentiation of the soft-collinear distribution. So, the whole job of computing the SV correction depends on our ability to determine and explore the unknown distribution $\Phi_{d,\text{sv}}^I$ to which we now turn to.

As we have discussed, the soft-collinear distribution essentially captures the contribution arising from real emission diagrams which only can occur from colored partons. Naturally, $\Phi_{d,\text{sv}}^I$ for Sudakov form factor i.e. $2 \rightarrow 1$ and $2 \rightarrow n$ scattering should essentially be identical. The presence of more Mandelstam variables in the latter process just makes it more involved in its kinematic dependence when it is expressed in terms of $\{p_j \cdot q_k\}$. However, in terms of the total invariant mass square of the final state colorless particles i.e. q^2 , it has to be exactly same as that of Sudakov process. In [5], it was conjectured to satisfy a integro-differential RG equation to all orders in QCD coupling constant. The underlying reason behind this all order conjecture is inspired by the akin integro-differential Sudakov equation [35–37] fulfilled by the form factor whose solution is present explicitly to five loops order in massless QCD in [39, 40, 42, 194]. By integrating the differential rapidity distribution, we get the inclusive cross-section. Upon taking the Mellin moment with respect to the same Mellin variable N of this relation we get

$$\int_0^1 dx_1^0 \int_0^1 dx_2^0 (x_1^0 x_2^0)^{N-1} \frac{d\sigma}{dy} = \int_0^1 d\tau \tau^{N-1} \sigma. \quad (5.20)$$

By taking the limit $N \rightarrow \infty$ on both sides of this relation, we can relate the soft-collinear distributions in rapidity and that of inclusive cross-section. This is remarkable in a sense

that given the soft-collinear distribution for inclusive cross-section, we can automatically calculate it for the rapidity. Since this is the only quantity that is unknown in comparison to the ingredients for the computation of SV cross-section, we can immediately calculate the SV rapidity distribution. The $\Phi_{d,sv}^I$ for the Sudakov form factor is determined to NNLO in [5] and in [195] at N³LO in QCD. In the work presented in this chapter, for the first time, we present the general analytical form of $\Phi_{d,sv}^I$ in terms of universal quantities at N⁴LO for any generic $2 \rightarrow n$ scattering. One of the most notable features of this quantity is it satisfies the maximally non-Abelian property:

$$\Phi_{d,sv}^I = \frac{C_A}{C_F} \Phi_{d,sv}^g, \quad (5.21)$$

where the C_A and C_F are the quadratic Casimirs in Adjoint and fundamental representations of $SU(N_c)$, respectively. This essentially signifies the universality of the real emission in the soft limit. Needless to say, it is also quark flavour blind. This relation was explicitly verified to NNLO in [5] and at N³LO in [195]. We expect the Casimir scaling to hold true to all orders in perturbation theory since it originates entirely from the soft-collinear part of the differential cross-section, and therefore it would indeed be interesting to see whether truly it holds beyond N³LO with generalised Casimir scaling [64].

We decompose all the quantities into its singular (sing) and finite (fin) parts as

$$\begin{aligned} \Phi_{d,sv}^I &= \Phi_{d,sing}^I + \Phi_{d,fin}^I, \\ \ln \Gamma_I &= \ln \Gamma_{I,sing} + \ln \Gamma_{I,fin}, \end{aligned} \quad (5.22)$$

Then, Eq.(5.16) can be recast into

$$\begin{aligned} \Delta_{d,I}^{sv} &= |\mathcal{M}_I^{(0)}|^2 |\mathcal{F}_{fin}^I(\{p_j \cdot q_k\}, q^2, \mu_R^2)|^2 \delta(1-z_1) \delta(1-z_2) \\ &\otimes C \exp \left[2\Phi_{d,fin}^I(z_1, z_2, q^2, \mu_R^2) - C \ln \Gamma_{I,fin}(z_1, \mu_F^2, \mu_R^2) \delta(1-z_2) \right. \\ &\quad \left. - C \ln \Gamma_{I,fin}(z_2, \mu_F^2, \mu_R^2) \delta(1-z_1) \right] \otimes \mathbf{I}_{d,I}^{sv}, \end{aligned} \quad (5.23)$$

where

$$\mathbf{I}_{d,I}^{\text{sv}} = |Z_{I,\text{IR}}(q^2, \mu_R^2, \epsilon)|^2 \delta(1-z) \otimes C \exp \left[2\Phi_{d,\text{sing}}^I(z_1, z_2, q^2, \mu_R^2, \epsilon) - C \ln \Gamma_{I,\text{sing}}(z_1, \mu_R^2, \epsilon) \delta(1-z_2) - C \ln \Gamma_{I,\text{sing}}(z_2, \mu_R^2, \epsilon) \delta(1-z_1) \right]. \quad (5.24)$$

Through the decomposition of the quantities into singular and finite parts in Eq.(5.22), we put together all the singular components of the rapidity distribution into $\mathbf{I}_{d,I}^{\text{sv}}$ which must be unit distribution $\delta(1-z_1)\delta(1-z_2)$ in order to get a finite $\Delta_{d,I}^{\text{sv}}$. In Eq. (5.23), the form factor and the leading order matrix element are the only process dependent quantity. The remaining part which comprises of the finite segments of the soft-collinear distribution and mass factorization kernel is a process independent universal quantity which we call as *differential soft-collinear operator*

$$\mathbf{S}_d^I(z_1, z_2, q^2, \mu_R^2, \mu_F^2) \equiv C \exp \left[2\Phi_{d,\text{fin}}^I(z_1, z_2, q^2, \mu_R^2) - C \ln \Gamma_{I,\text{fin}}(z_1, \mu_R^2, \mu_F^2) \delta(1-z_2) - C \ln \Gamma_{I,\text{fin}}(z_2, \mu_R^2, \mu_F^2) \delta(1-z_1) \right]. \quad (5.25)$$

The expression of \mathbf{S}_d^I being process independent can be used for any generic $2 \rightarrow n$ scattering process. Hence Eq. (5.23) reads as

$$\Delta_{d,I}^{\text{sv}} = |\mathcal{M}_I^{(0)}|^2 |\mathcal{F}_{I,\text{fin}}|^2 \delta(1-z_1) \delta(1-z_2) \otimes \mathbf{S}_d^I \quad (5.26)$$

We can calculate the SV coefficient function for the rapidity distribution order by order in perturbation theory by expanding it in powers of a_s according to Eq.(5.11). The results of \mathbf{S}_d^I for any generic process up to N⁴LO QCD is given in Appendix D for $\mu_R^2 = \mu_F^2 = q^2$. Also, the universal light-like cusp-, soft- and collinear anomalous dimensions are given in Appendix B. The anomalous dimensions are expanded in powers of $a_s(\mu_R^2)$ as

$$X^I(\mu_R^2) = \sum_{j=1}^{\infty} a_s^j(\mu_R^2) X_j^I, \quad (5.27)$$

where $X = A, B, f$. Thanks to recent calculations, the light-like cusp anomalous dimensions are available to four loops [43–47] in QCD. The soft and collinear anomalous dimensions can be extracted [41, 42] from the quark and gluon collinear anomalous dimensions [48, 49] through the conjecture [41]

$$\gamma^I = 2B^I + f^I \quad (5.28)$$

to three loops. At four loop, only partial results are available in [47, 50–52].

5.3 Results of SV rapidity distribution

In this section, we present the explicit results of $\Delta_{d,I}^{\text{sv}}$ defined in (5.26) for the Drell-Yan ($I = q$), and the Higgs boson productions through gluon fusion ($I = g$) as well as bottom quark annihilation ($I = b$) at fourth order in coupling constant. Expanding them in powers of $a_s(\mu_R^2)$ through

$$\begin{aligned} \Delta_{d,I}^{\text{sv}}(\{p_j \cdot q_k\}, z_1, z_2, q^2, \mu_F^2) &= \delta(1 - z_1)\delta(1 - z_2)|\mathcal{M}_{I,\text{fin}}^{(0)}|^2 \\ &+ \sum_{i=1}^{\infty} a_s^i(\mu_R^2)\Delta_{d,I}^{\text{sv},(i)}(\{p_j \cdot q_k\}, z_1, z_2, q^2, \mu_F^2, \mu_R^2). \end{aligned} \quad (5.29)$$

Setting $\mu_F^2 = \mu_R^2 = q^2$, in the following, we provide only the new results, and the old results for Drell-Yan and Higgs boson productions can be found in [5, 132, 195]. The results with explicit dependence on μ_R and μ_F are provided up to N⁴LO in the ancillary files supplied with the arXiv submission of [177].

$$\begin{aligned} \Delta_{d,g}^{\text{sv},(4)} &= \delta(1 - z_1)\delta(1 - z_2) \left[n_f \frac{d_F^{abcd} d_A^{abcd}}{N_A} \left\{ \chi_5^g - \frac{2560}{3} \zeta_2 \zeta_5 - \frac{512}{3} \zeta_2 \zeta_3 + 512 \zeta_2^2 \right\} \right. \\ &+ n_f^2 \frac{d_F^{abcd} d_F^{abcd}}{N_A} \left\{ -\frac{9008}{9} - 960 \zeta_5 + 1520 \zeta_3 + 512 \zeta_3^2 + \frac{384}{5} \zeta_2^2 \right\} + \frac{d_A^{abcd} d_A^{abcd}}{N_A} \left\{ \chi_7^g \right. \\ &\left. + \frac{7040}{3} \zeta_2 \zeta_5 + \frac{256}{3} \zeta_2 \zeta_3 - 768 \zeta_2 \zeta_3^2 - 256 \zeta_2^2 - \frac{15872}{35} \zeta_2^4 \right\} + n_f \left\{ -\frac{1}{3} \tilde{\mathcal{G}}_3^{g,(2)} \right\} \end{aligned}$$

$$\begin{aligned}
& + C_F n_f^3 \left\{ -\frac{233953}{972} + \frac{640}{27} \zeta_5 + \frac{4060}{27} \zeta_3 + \frac{376}{3} \zeta_2 - \frac{640}{9} \zeta_2 \zeta_3 + \frac{112}{45} \zeta_2^2 \right\} \\
& + C_F^2 n_f^2 \left\{ \frac{11401}{54} + \frac{3920}{3} \zeta_5 - \frac{5044}{3} \zeta_3 + \frac{896}{3} \zeta_3^2 - \frac{50}{9} \zeta_2 + \frac{32}{3} \zeta_2 \zeta_3 - \frac{212}{15} \zeta_2^2 \right. \\
& + \left. \frac{13696}{945} \zeta_2^3 \right\} + C_F n_f \left\{ \chi_4^g \right\} + C_A \left\{ \frac{11}{6} \tilde{\mathcal{G}}_3^{g,(2)} \right\} + C_A n_f^3 \left\{ -\frac{943703}{5832} - \frac{566}{27} \zeta_5 \right. \\
& - \left. \frac{57182}{729} \zeta_3 + \frac{1156}{9} \zeta_2 + \frac{3332}{81} \zeta_2 \zeta_3 + \frac{10141}{405} \zeta_2^2 \right\} + C_A C_F n_f^2 \left\{ \frac{49991435}{11664} - \frac{23572}{27} \zeta_5 \right. \\
& - \left. \frac{357994}{243} \zeta_3 - \frac{3214}{9} \zeta_3^2 - \frac{6509}{18} \zeta_2 - \frac{1640}{9} \zeta_2 \zeta_3 - \frac{101459}{540} \zeta_2^2 - \frac{2756}{189} \zeta_2^3 \right\} \\
& + C_A C_F^2 n_f \left\{ \frac{153625}{162} + \chi_3^g - \frac{17656}{3} \zeta_7 + \frac{29728}{9} \zeta_5 + \frac{222683}{54} \zeta_3 - \frac{3824}{3} \zeta_3^2 \right. \\
& + \left. \frac{2227}{9} \zeta_2 - 1280 \zeta_2 \zeta_5 + 1104 \zeta_2 \zeta_3 + \frac{4032}{5} \zeta_2^2 - \frac{2464}{3} \zeta_2^2 \zeta_3 - \frac{415952}{945} \zeta_2^3 \right\} \\
& + C_A^2 n_f^2 \left\{ \frac{3373102453}{839808} - \frac{5957}{27} \zeta_5 + \frac{1583227}{1944} \zeta_3 + \frac{4504}{27} \zeta_3^2 - \frac{43937939}{34992} \zeta_2 \right. \\
& + \left. \frac{10277}{54} \zeta_2 \zeta_3 - \frac{2169709}{3240} \zeta_2^2 - \frac{1567}{135} \zeta_2^3 \right\} + C_A^2 C_F n_f \left\{ -\frac{495711665}{69984} + \chi_2^g \right. \\
& + \left. \frac{28744}{9} \zeta_7 + \frac{1077758}{405} \zeta_5 + \frac{186703}{729} \zeta_3 - \frac{178784}{81} \zeta_3^2 - \frac{5080535}{1944} \zeta_2 + \frac{1120}{9} \zeta_2 \zeta_5 \right. \\
& + \left. \frac{194875}{81} \zeta_2 \zeta_3 + \frac{443861}{1080} \zeta_2^2 + \frac{76904}{45} \zeta_2^2 \zeta_3 + \frac{24368}{105} \zeta_2^3 \right\} + C_A^3 n_f \left\{ \frac{8163906247}{472392} \right. \\
& + \left. \chi_1^g - \frac{383989}{63} \zeta_7 + \frac{7783846}{1215} \zeta_5 - \frac{142069663}{26244} \zeta_3 + \frac{2132341}{729} \zeta_3^2 + \frac{6135005}{8748} \zeta_2 \right. \\
& + \left. \frac{77156}{135} \zeta_2 \zeta_5 - \frac{568195}{243} \zeta_2 \zeta_3 + \frac{101328101}{29160} \zeta_2^2 - \frac{134854}{81} \zeta_2^2 \zeta_3 + \frac{178103}{315} \zeta_2^3 \right\} \\
& + C_A^4 \left\{ \frac{24881127343}{1889568} + \chi_6^g + \frac{1024}{45} \zeta_{5,3} + \frac{2029709}{42} \zeta_7 - \frac{9370337}{486} \zeta_5 \right. \\
& - \left. \frac{293538695}{13122} \zeta_3 - \frac{304447}{45} \zeta_3 \zeta_5 + \frac{6412558}{729} \zeta_3^2 + \frac{339046381}{52488} \zeta_2 + \frac{433642}{135} \zeta_2 \zeta_5 \right. \\
& - \left. \frac{4939438}{729} \zeta_2 \zeta_3 - \frac{35402}{27} \zeta_2 \zeta_3^2 - \frac{107201743}{14580} \zeta_2^2 + \frac{1731257}{405} \zeta_2^2 \zeta_3 + \frac{5324869}{3780} \zeta_2^3 \right. \\
& - \left. \frac{33921919}{15750} \zeta_2^4 \right\} + \frac{1}{4} \tilde{\mathcal{G}}_4^{g,(1)} + \delta(1-z_1) \bar{\mathcal{D}}_0 \left[n_f \frac{d_F^{abcd} d_A^{abcd}}{N_A} \left\{ 384 + 2b_{4,d_F^{abcd} d_A^{abcd}}^g \right. \right. \\
& + \left. \left. \frac{21760}{9} \zeta_5 + \frac{5312}{9} \zeta_3 - \frac{1216}{3} \zeta_3^2 - \frac{4544}{3} \zeta_2 - 128 \zeta_2 \zeta_3 + \frac{320}{3} \zeta_2^2 - \frac{9472}{315} \zeta_2^3 \right\} \right. \\
& + \left. \frac{d_A^{abcd} d_A^{abcd}}{N_A} \left\{ -f_{4,d_F^{abcd} d_A^{abcd}}^g \right\} + C_A n_f^3 \left\{ \frac{5216}{2187} + \frac{80}{81} \zeta_3 - \frac{800}{81} \zeta_2 + \frac{16}{9} \zeta_2^2 \right\} + C_A C_F n_f^2 \left\{ \right. \right. \\
& - \left. \left. \frac{155083}{486} + 16 \zeta_5 + \frac{1912}{9} \zeta_3 + \frac{1400}{9} \zeta_2 - \frac{320}{3} \zeta_2 \zeta_3 + \frac{32}{3} \zeta_2^2 \right\} + C_A C_F^2 n_f \left\{ -\frac{27949}{108} \right. \right. \\
& + \left. \left. 2b_{4,n_f C_F^3}^g - \frac{3872}{3} \zeta_5 + \frac{1120}{9} \zeta_3 - 368 \zeta_3^2 - 320 \zeta_2 + \frac{512}{3} \zeta_2 \zeta_3 + \frac{668}{5} \zeta_2^2 \right. \right. \\
& + \left. \left. \frac{117344}{315} \zeta_2^3 \right\} + C_A^2 n_f^2 \left\{ -\frac{1543153}{5832} + \frac{1936}{9} \zeta_5 + \frac{1240}{9} \zeta_3 + \frac{258130}{729} \zeta_2 - \frac{3536}{27} \zeta_2 \zeta_3 \right\}
\end{aligned}$$

$$\begin{aligned}
& - \frac{1504}{45} \zeta_2^2 \Big\} + C_A^2 C_F n_f \Big\{ \frac{2798681}{972} + 2b_{4,n_f C_F^2 C_A}^q + \frac{10952}{9} \zeta_5 - \frac{70426}{27} \zeta_3 + \frac{7816}{3} \zeta_3^2 \\
& - \frac{4925}{9} \zeta_2 - \frac{368}{9} \zeta_2 \zeta_3 - \frac{24400}{27} \zeta_2^2 - \frac{1328}{7} \zeta_2^3 \Big\} + C_A^3 n_f \Big\{ \frac{17665315}{5832} - b_{4,n_f C_F^2 C_A}^q \\
& - \frac{1}{2} b_{4,n_f C_F^3}^q - \frac{1}{24} b_{4,d_F^{abcd} d_F^{abcd}}^q - \frac{83128}{27} \zeta_5 - \frac{177566}{27} \zeta_3 + \frac{604}{9} \zeta_3^2 - \frac{1991747}{729} \zeta_2 \\
& + \frac{8848}{3} \zeta_2 \zeta_3 + \frac{195944}{405} \zeta_2^2 - \frac{2696}{945} \zeta_2^3 \Big\} + C_A^4 \Big\{ - \frac{40498399}{4374} + \frac{1}{24} f_{4,d_F^{abcd} d_A^{abcd}}^q \\
& + 9380 \zeta_7 + \frac{83240}{9} \zeta_5 + \frac{2047084}{81} \zeta_3 - \frac{36652}{3} \zeta_3^2 + \frac{4083193}{729} \zeta_2 - 7264 \zeta_2 \zeta_5 \\
& - \frac{312316}{27} \zeta_2 \zeta_3 + \frac{76708}{405} \zeta_2^2 + \frac{7568}{15} \zeta_2^2 \zeta_3 - \frac{25036}{315} \zeta_2^3 \Big\} + \\
& \delta(1 - z_1) \overline{\mathcal{D}}_1 \Big[n_f \frac{d_F^{abcd} d_A^{abcd}}{N_A} \Big\{ - \frac{1280}{3} \zeta_5 - \frac{256}{3} \zeta_3 + 256 \zeta_2 \Big\} + \frac{d_A^{abcd} d_A^{abcd}}{N_A} \Big\{ \frac{3520}{3} \zeta_5 \\
& + \frac{128}{3} \zeta_3 - 384 \zeta_3^2 - 128 \zeta_2 - \frac{7936}{35} \zeta_2^3 \Big\} + C_A n_f^3 \Big\{ - \frac{4000}{729} + \frac{320}{27} \zeta_2 \Big\} + C_A C_F n_f^2 \Big\{ \\
& \frac{57890}{81} - \frac{4576}{9} \zeta_3 - \frac{976}{9} \zeta_2 - \frac{128}{45} \zeta_2^2 \Big\} + C_A C_F^2 n_f \Big\{ \frac{3004}{9} - 1600 \zeta_5 + \frac{2960}{3} \zeta_3 \Big\} \\
& + C_A^2 n_f^2 \Big\{ \frac{544699}{729} - \frac{464}{9} \zeta_3 - \frac{33344}{81} \zeta_2 - \frac{832}{45} \zeta_2^2 \Big\} + C_A^2 C_F n_f \Big\{ - \frac{410057}{81} + 800 \zeta_5 \\
& + \frac{28480}{9} \zeta_3 + \frac{2920}{9} \zeta_2 + 256 \zeta_2 \zeta_3 + \frac{704}{45} \zeta_2^2 \Big\} + C_A^3 n_f \Big\{ - \frac{6305477}{729} + 2000 \zeta_5 \\
& + \frac{136664}{27} \zeta_3 + \frac{232048}{81} \zeta_2 - 3040 \zeta_2 \zeta_3 + \frac{36128}{135} \zeta_2^2 \Big\} + C_A^4 \Big\{ \frac{14936741}{729} - 6600 \zeta_5 \\
& - \frac{798056}{27} \zeta_3 + \frac{34816}{3} \zeta_3^2 - \frac{413360}{81} \zeta_2 + 15312 \zeta_2 \zeta_3 - \frac{131072}{135} \zeta_2^2 + \frac{1696}{105} \zeta_2^3 \Big\} + \\
& \mathcal{D}_0 \overline{\mathcal{D}}_0 \Big[n_f \frac{d_F^{abcd} d_A^{abcd}}{N_A} \Big\{ - \frac{640}{3} \zeta_5 - \frac{128}{3} \zeta_3 + 128 \zeta_2 \Big\} + \frac{d_A^{abcd} d_A^{abcd}}{N_A} \Big\{ \frac{1760}{3} \zeta_5 + \frac{64}{3} \zeta_3 \\
& - 192 \zeta_3^2 - 64 \zeta_2 - \frac{3968}{35} \zeta_2^3 \Big\} + C_A n_f^3 \Big\{ - \frac{2000}{729} + \frac{160}{27} \zeta_2 \Big\} + C_A C_F n_f^2 \Big\{ \frac{28945}{81} \\
& - \frac{2288}{9} \zeta_3 - \frac{488}{9} \zeta_2 - \frac{64}{45} \zeta_2^2 \Big\} + C_A C_F^2 n_f \Big\{ \frac{1502}{9} - 800 \zeta_5 + \frac{1480}{3} \zeta_3 \Big\} + C_A^2 n_f^2 \Big\{ \\
& \frac{544699}{1458} - \frac{232}{9} \zeta_3 - \frac{16672}{81} \zeta_2 - \frac{416}{45} \zeta_2^2 \Big\} + C_A^2 C_F n_f \Big\{ - \frac{410057}{162} + 400 \zeta_5 \\
& + \frac{14240}{9} \zeta_3 + \frac{1460}{9} \zeta_2 + 128 \zeta_2 \zeta_3 + \frac{352}{45} \zeta_2^2 \Big\} + C_A^3 n_f \Big\{ - \frac{6305477}{1458} + 1000 \zeta_5 \\
& + \frac{68332}{27} \zeta_3 + \frac{116024}{81} \zeta_2 - 1520 \zeta_2 \zeta_3 + \frac{18064}{135} \zeta_2^2 \Big\} + C_A^4 \Big\{ \frac{14936741}{1458} - 3300 \zeta_5 \\
& - \frac{399028}{27} \zeta_3 + \frac{17408}{3} \zeta_3^2 - \frac{206680}{81} \zeta_2 + 7656 \zeta_2 \zeta_3 - \frac{65536}{135} \zeta_2^2 + \frac{848}{105} \zeta_2^3 \\
& \Big\} + \Big\{ z_1 \leftrightarrow z_2 \Big\}. \tag{5.30}
\end{aligned}$$

$$\begin{aligned}
\Delta_{d,q}^{\text{sv},(4)} = & \delta(1-z_1)\delta(1-z_2) \left[n_f \frac{d_F^{abcd} d_F^{abcd}}{N_F} \left\{ \frac{3190}{3} - 1240\zeta_7 + \frac{95098}{27}\zeta_5 - \frac{13414}{27}\zeta_3 + \frac{680}{9}\zeta_3^2 \right. \right. \\
& - \frac{21566}{9}\zeta_2 - \frac{1568}{3}\zeta_2\zeta_5 - 140\zeta_2\zeta_3 + \frac{30592}{45}\zeta_2^2 - \frac{3952}{15}\zeta_2^2\zeta_3 + \frac{41620}{189}\zeta_2^3 \left. \right\} \\
& + \frac{d_F^{abcd} d_A^{abcd}}{N_F} \left\{ \chi_{10}^q + \frac{7040}{3}\zeta_2\zeta_5 + \frac{256}{3}\zeta_2\zeta_3 - 768\zeta_2\zeta_3^2 - 256\zeta_2^2 - \frac{15872}{35}\zeta_2^4 \right\} \\
& + n_f \left\{ -\frac{1}{3}\tilde{\mathcal{G}}_3^{q,(2)} \right\} + C_{Fn_f n_{fv}} N_4 \left\{ -\frac{392}{9} + \frac{440}{9}\zeta_5 - 28\zeta_3 + \frac{176}{3}\zeta_3^2 - \frac{556}{9}\zeta_2 \right. \\
& - \frac{56}{3}\zeta_2\zeta_3 + \frac{76}{9}\zeta_2^2 + \frac{1408}{135}\zeta_2^3 \left. \right\} + C_{Fn_f^3} \left\{ \frac{65633}{1944} - \frac{238}{27}\zeta_5 - \frac{3416}{729}\zeta_3 - \frac{39398}{729}\zeta_2 \right. \\
& + \frac{404}{81}\zeta_2\zeta_3 - \frac{3511}{405}\zeta_2^2 \left. \right\} + C_{Fn_f n_{fv}}^2 N_4 \left\{ \frac{3334}{3} + \frac{1}{8}\chi_5^q - \frac{8542}{3}\zeta_7 + \frac{38468}{27}\zeta_5 + \frac{4840}{27}\zeta_3 \right. \\
& - \frac{4592}{9}\zeta_3^2 + \frac{10706}{9}\zeta_2 - 464\zeta_2\zeta_5 + \frac{902}{3}\zeta_2\zeta_3 - \frac{4024}{45}\zeta_2^2 - \frac{784}{3}\zeta_2^2\zeta_3 + \frac{11254}{135}\zeta_2^3 \left. \right\} \\
& + C_{Fn_f^2}^2 \left\{ -\frac{1194071}{5832} + \frac{1876}{27}\zeta_5 - \frac{425615}{729}\zeta_3 + \frac{286}{27}\zeta_3^2 + \frac{108874}{729}\zeta_2 + \frac{10120}{27}\zeta_2\zeta_3 \right. \\
& + \frac{5401}{60}\zeta_2^2 + \frac{18868}{945}\zeta_2^3 \left. \right\} + C_{Fn_f^3}^3 \left\{ -\frac{7723623865}{419904} + \chi_3^q - \frac{473078}{63}\zeta_7 + \frac{1268018}{81}\zeta_5 \right. \\
& + \frac{10401064}{243}\zeta_3 - \frac{674818}{81}\zeta_3^2 - \frac{12237605}{648}\zeta_2 - \frac{8464}{9}\zeta_2\zeta_5 + \frac{364040}{81}\zeta_2\zeta_3 \\
& + \frac{1994819}{1215}\zeta_2^2 - \frac{327928}{135}\zeta_2^2\zeta_3 - \frac{2803408}{2835}\zeta_2^3 \left. \right\} + C_F^4 \left\{ -\frac{6246665}{128} + \chi_9^q + \frac{5152}{3}\zeta_{5,3} \right. \\
& + \frac{164740}{7}\zeta_7 + \frac{1550732}{15}\zeta_5 - \frac{144091}{2}\zeta_3 - \frac{658688}{45}\zeta_3\zeta_5 + \frac{292424}{27}\zeta_3^2 \\
& - \frac{1762043}{48}\zeta_2 + \frac{2576}{5}\zeta_2\zeta_5 + \frac{203056}{9}\zeta_2\zeta_3 + \frac{59264}{27}\zeta_2\zeta_3^2 - \frac{90321}{10}\zeta_2^2 + \frac{19856}{15}\zeta_2^2\zeta_3 \\
& + \frac{3412928}{315}\zeta_2^3 - \frac{507968}{1575}\zeta_2^4 \left. \right\} + C_A \left\{ \frac{11}{6}\tilde{\mathcal{G}}_3^{q,(2)} \right\} + C_A C_{Fn_f n_{fv}} N_4 \left\{ -\frac{1870}{3} + \frac{1}{8}\chi_4^q \right. \\
& - \frac{8272}{9}\zeta_5 - \frac{1034}{9}\zeta_3 + \frac{3784}{3}\zeta_3^2 - \frac{2860}{3}\zeta_2 - 330\zeta_2\zeta_3 + \frac{2156}{15}\zeta_2^2 + \frac{107008}{315}\zeta_2^3 \left. \right\} \\
& + C_A C_{Fn_f^2} \left\{ -\frac{667210703}{839808} + \frac{8152}{27}\zeta_5 + \frac{2099687}{2916}\zeta_3 + \frac{68}{9}\zeta_3^2 + \frac{42932371}{34992}\zeta_2 \right. \\
& - \frac{13396}{27}\zeta_2\zeta_3 + \frac{15877}{108}\zeta_2^2 - \frac{3517}{315}\zeta_2^3 \left. \right\} + C_A C_{Fn_f^3} \left\{ \frac{161137649299}{1889568} + \chi_2^q - 1722\zeta_7 \right. \\
& - \frac{8225273}{486}\zeta_5 - \frac{5024904581}{52488}\zeta_3 + \frac{11407462}{729}\zeta_3^2 + \frac{1790660321}{34992}\zeta_2 + \frac{187004}{135}\zeta_2\zeta_5 \\
& - \frac{898147}{81}\zeta_2\zeta_3 - \frac{125343967}{29160}\zeta_2^2 + \frac{146510}{81}\zeta_2^2\zeta_3 + \frac{20536}{27}\zeta_2^3 \left. \right\} \\
& + C_A C_F^3 \left\{ \frac{154126124135}{839808} + \chi_8^q - \frac{23024}{15}\zeta_{5,3} + \frac{23357}{21}\zeta_7 - \frac{272959751}{1620}\zeta_5 \right. \\
& - \frac{1562360669}{11664}\zeta_3 + \frac{43564}{5}\zeta_3\zeta_5 + \frac{6415507}{162}\zeta_3^2 + \frac{1143090157}{7776}\zeta_2 + \frac{265036}{45}\zeta_2\zeta_5 \left. \right\}
\end{aligned}$$

$$\begin{aligned}
& -\frac{6518455}{81}\zeta_2\zeta_3 - \frac{28928}{9}\zeta_2\zeta_3^2 - \frac{52425877}{9720}\zeta_2^2 + \frac{393476}{27}\zeta_2^2\zeta_3 - \frac{24147386}{2835}\zeta_2^3 \\
& - \frac{2236966}{875}\zeta_2^4 \Big\} + C_A^2 C_F n_f \Big\{ -\frac{7253202277}{104976} + \chi_1^q - \frac{211}{9}\zeta_7 + \frac{394286}{45}\zeta_5 \\
& + \frac{141306569}{2916}\zeta_3 - \frac{62306}{9}\zeta_3^2 - \frac{175686721}{4374}\zeta_2 - \frac{2672}{3}\zeta_2\zeta_5 + \frac{204071}{27}\zeta_2\zeta_3 \\
& + \frac{361903}{216}\zeta_2^2 - \frac{9104}{45}\zeta_2^2\zeta_3 - \frac{4261}{105}\zeta_2^3 \Big\} + C_A^2 C_F^2 \Big\{ -\frac{139605518111}{472392} + \chi_7^q \\
& - \frac{7184}{45}\zeta_{5,3} + \frac{112505}{9}\zeta_7 + \frac{491406151}{4860}\zeta_5 + \frac{31284635423}{104976}\zeta_3 - \frac{7567}{9}\zeta_3\zeta_5 \\
& - \frac{45139415}{729}\zeta_3^2 - \frac{39174091799}{209952}\zeta_2 - \frac{1163402}{135}\zeta_2\zeta_5 + \frac{60145883}{729}\zeta_2\zeta_3 - \frac{7018}{27}\zeta_2\zeta_3^2 \\
& + \frac{628489141}{29160}\zeta_2^2 - \frac{1136015}{81}\zeta_2^2\zeta_3 + \frac{135362}{45}\zeta_2^3 + \frac{17432749}{15750}\zeta_2^4 \Big\} + C_A^3 C_F \Big\{ \\
& \frac{29551452589}{209952} + \chi_6^q + \frac{2321}{18}\zeta_7 - \frac{736349}{30}\zeta_5 - \frac{175768027}{1458}\zeta_3 + \frac{41129}{2}\zeta_3^2 \\
& + \frac{1547277107}{17496}\zeta_2 + \frac{19976}{3}\zeta_2\zeta_5 - \frac{920596}{27}\zeta_2\zeta_3 - 32\zeta_2\zeta_3^2 - \frac{1404395}{162}\zeta_2^2 \\
& + \frac{113432}{45}\zeta_2^2\zeta_3 + \frac{79827}{140}\zeta_2^3 - \frac{40064}{105}\zeta_2^4 \Big\} + \frac{1}{4}\tilde{\mathcal{G}}_4^{q,(1)} \Big] + \delta(1-z_1)\bar{\mathcal{D}}_0 \Big[n_f \frac{d^{abcd} d^{abcd}}{N_F} \Big\{ \\
& 384 + 2b_{4,d_F}^q \frac{d^{abcd} d^{abcd}}{d_F} + \frac{21760}{9}\zeta_5 + \frac{5312}{9}\zeta_3 - \frac{1216}{3}\zeta_3^2 - \frac{4544}{3}\zeta_2 - 128\zeta_2\zeta_3 + \frac{320}{3}\zeta_2^2 \\
& - \frac{9472}{315}\zeta_2^3 \Big\} + \frac{d^{abcd} d^{abcd}}{N_F} \Big\{ -f_{4,d_F}^q \frac{d^{abcd} d^{abcd}}{d_A} \Big\} + C_F n_f^3 \Big\{ \frac{5216}{2187} + \frac{80}{81}\zeta_3 - \frac{800}{81}\zeta_2 + \frac{16}{9}\zeta_2^2 \Big\} \\
& + C_F^2 n_f^2 \Big\{ -\frac{142769}{1458} + \frac{1168}{9}\zeta_5 + \frac{8552}{27}\zeta_3 - \frac{71900}{729}\zeta_2 - \frac{6272}{27}\zeta_2\zeta_3 + \frac{1504}{27}\zeta_2^2 \Big\} \\
& + C_F^3 n_f \Big\{ -\frac{80221}{108} + 2b_{4,n_f C_F}^q - \frac{7712}{3}\zeta_5 + \frac{14800}{9}\zeta_3 + 1168\zeta_3^2 - \frac{8210}{27}\zeta_2 \\
& + \frac{4576}{9}\zeta_2\zeta_3 + \frac{8108}{45}\zeta_2^2 + \frac{117344}{315}\zeta_2^3 \Big\} + C_F^4 \Big\{ 7680\zeta_7 - 6144\zeta_5 + 4088\zeta_3 - 1920\zeta_3^2 \\
& - 4608\zeta_2\zeta_5 + 3904\zeta_2\zeta_3 - \frac{6656}{5}\zeta_2^2\zeta_3 \Big\} + C_A C_F n_f^2 \Big\{ -\frac{898033}{5832} + \frac{304}{3}\zeta_5 + \frac{2456}{81}\zeta_3 \\
& + \frac{75718}{243}\zeta_2 + \frac{80}{9}\zeta_2\zeta_3 - \frac{3104}{45}\zeta_2^2 \Big\} + C_A C_F^2 n_f \Big\{ -\frac{955285}{2916} + 2b_{4,n_f C_F^2 C_A}^q - \frac{104}{3}\zeta_5 \\
& - \frac{25124}{27}\zeta_3 + \frac{4072}{3}\zeta_3^2 + \frac{1781395}{729}\zeta_2 + \frac{12880}{9}\zeta_2\zeta_3 - \frac{675088}{405}\zeta_2^2 - \frac{12976}{105}\zeta_2^3 \Big\} \\
& + C_A C_F^3 \Big\{ -\frac{103222}{27} + 8576\zeta_5 - \frac{57095}{9}\zeta_3 - 5008\zeta_3^2 + \frac{18479}{9}\zeta_2 - 2304\zeta_2\zeta_5 \\
& - \frac{14936}{9}\zeta_2\zeta_3 + \frac{8968}{45}\zeta_2^2 + \frac{4672}{5}\zeta_2^2\zeta_3 - \frac{704}{5}\zeta_2^3 \Big\} + C_A^2 C_F n_f \Big\{ \frac{10761379}{5832} - \frac{1}{2}b_{4,n_f C_F^3}^q \\
& - b_{4,n_f C_F^2 C_A}^q - \frac{1}{24}b_{4,d_F}^q \frac{d^{abcd} d^{abcd}}{d_F} - \frac{14776}{27}\zeta_5 - \frac{210778}{81}\zeta_3 - \frac{4868}{9}\zeta_3^2 - \frac{654449}{243}\zeta_2 \\
& + \frac{6640}{9}\zeta_2\zeta_3 + \frac{138808}{135}\zeta_2^2 - \frac{65192}{945}\zeta_2^3 \Big\} + C_A^2 C_F^2 \Big\{ \frac{7543094}{729} + \frac{58624}{9}\zeta_5
\end{aligned}$$

$$\begin{aligned}
& -\frac{134305}{27}\zeta_3 - 2032\zeta_3^2 - \frac{7337465}{729}\zeta_2 - 768\zeta_2\zeta_5 - \frac{72640}{27}\zeta_2\zeta_3 + \frac{193424}{81}\zeta_2^2 \\
& + \frac{1840}{3}\zeta_2^2\zeta_3 - \frac{1232}{15}\zeta_2^3 \Big\} + C_A^3 C_F \Big\{ -\frac{28325071}{4374} + \frac{1}{24}f_4^{abcd} d_F^{abcd} + 1700\zeta_7 \\
& - \frac{24920}{9}\zeta_5 + 9600\zeta_3 - \frac{2332}{3}\zeta_3^2 + \frac{1642195}{243}\zeta_2 + 416\zeta_2\zeta_5 - \frac{30772}{9}\zeta_2\zeta_3 \\
& - \frac{78188}{45}\zeta_2^2 + 288\zeta_2^2\zeta_3 + \frac{45188}{315}\zeta_2^3 \Big\} \\
& + \delta(1 - z_1) \overline{\mathcal{D}}_1 \Big[n_f \frac{d_F^{abcd} d_A^{abcd}}{N_F} \Big\{ -\frac{1280}{3}\zeta_5 - \frac{256}{3}\zeta_3 + 256\zeta_2 \Big\} + \frac{d_F^{abcd} d_A^{abcd}}{N_F} \Big\{ \frac{3520}{3}\zeta_5 \\
& + \frac{128}{3}\zeta_3 - 384\zeta_3^2 - 128\zeta_2 - \frac{7936}{35}\zeta_2^3 \Big\} + C_F n_f^3 \Big\{ -\frac{4000}{729} + \frac{320}{27}\zeta_2 \Big\} \\
& + C_F^2 n_f N_4 \Big\{ 32 - \frac{640}{3}\zeta_5 + \frac{112}{3}\zeta_3 + 80\zeta_2 - \frac{16}{5}\zeta_2^2 \Big\} + C_F^2 n_f^2 \Big\{ -\frac{72590}{729} - \frac{30688}{81}\zeta_3 \\
& + \frac{11408}{81}\zeta_2 + \frac{5632}{135}\zeta_2^2 \Big\} + C_F^3 n_f \Big\{ -\frac{4310}{9} + \frac{10816}{9}\zeta_5 + \frac{29456}{27}\zeta_3 - \frac{5576}{27}\zeta_2 \\
& - \frac{22400}{9}\zeta_2\zeta_3 + \frac{27968}{135}\zeta_2^2 \Big\} + C_F^4 \Big\{ -\frac{11198}{3} + 5312\zeta_5 - 1840\zeta_3 + \frac{18304}{3}\zeta_3^2 \\
& - \frac{6652}{3}\zeta_2 + 1280\zeta_2\zeta_3 + \frac{592}{5}\zeta_2^2 + \frac{97408}{315}\zeta_2^3 \Big\} + C_A C_F n_f^2 \Big\{ \frac{58045}{243} - \frac{208}{9}\zeta_3 \\
& - \frac{7616}{27}\zeta_2 + \frac{64}{5}\zeta_2^2 \Big\} + C_A C_F^2 n_f \Big\{ \frac{2300107}{729} + 128\zeta_5 + \frac{234368}{81}\zeta_3 - \frac{18100}{9}\zeta_2 \\
& - \frac{1408}{3}\zeta_2\zeta_3 - \frac{51536}{135}\zeta_2^2 \Big\} + C_A C_F^3 \Big\{ 12062 - \frac{110752}{9}\zeta_5 - \frac{214592}{27}\zeta_3 + \frac{15808}{3}\zeta_3^2 \\
& + \frac{21554}{27}\zeta_2 + \frac{111008}{9}\zeta_2\zeta_3 - \frac{211376}{135}\zeta_2^2 - \frac{71168}{315}\zeta_2^3 \Big\} + C_A^2 C_F n_f \Big\{ -\frac{571387}{243} \\
& - \frac{1360}{9}\zeta_5 + \frac{3128}{3}\zeta_3 + \frac{58000}{27}\zeta_2 + 32\zeta_2\zeta_3 - \frac{3872}{15}\zeta_2^2 \Big\} + C_A^2 C_F^2 \Big\{ -\frac{11106458}{729} \\
& - 816\zeta_5 + \frac{6164}{81}\zeta_3 + \frac{752}{3}\zeta_3^2 + \frac{594406}{81}\zeta_2 + 1648\zeta_2\zeta_3 + \frac{58972}{135}\zeta_2^2 + \frac{38944}{315}\zeta_2^3 \Big\} \\
& + C_A^3 C_F \Big\{ \frac{4520317}{729} + \frac{15400}{9}\zeta_5 - \frac{51032}{9}\zeta_3 - 16\zeta_3^2 - \frac{140200}{27}\zeta_2 + 528\zeta_2\zeta_3 \\
& + \frac{3520}{3}\zeta_2^2 - \frac{20032}{105}\zeta_2^3 \Big\} + \mathcal{D}_0 \overline{\mathcal{D}}_0 \Big[n_f \frac{d_F^{abcd} d_A^{abcd}}{N_F} \Big\{ -\frac{640}{3}\zeta_5 - \frac{128}{3}\zeta_3 + 128\zeta_2 \Big\} \\
& + \frac{d_F^{abcd} d_A^{abcd}}{N_F} \Big\{ \frac{1760}{3}\zeta_5 + \frac{64}{3}\zeta_3 - 192\zeta_3^2 - 64\zeta_2 - \frac{3968}{35}\zeta_2^3 \Big\} + C_F n_f^3 \Big\{ -\frac{2000}{729} \\
& + \frac{160}{27}\zeta_2 \Big\} + C_F^2 n_f N_4 \Big\{ 16 - \frac{320}{3}\zeta_5 + \frac{56}{3}\zeta_3 + 40\zeta_2 - \frac{8}{5}\zeta_2^2 \Big\} + C_F^2 n_f^2 \Big\{ -\frac{36295}{729} \\
& - \frac{15344}{81}\zeta_3 + \frac{5704}{81}\zeta_2 + \frac{2816}{135}\zeta_2^2 \Big\} + C_F^3 n_f \Big\{ -\frac{2155}{9} + \frac{5408}{9}\zeta_5 + \frac{14728}{27}\zeta_3 \\
& - \frac{2788}{27}\zeta_2 - \frac{11200}{9}\zeta_2\zeta_3 + \frac{13984}{135}\zeta_2^2 \Big\} + C_F^4 \Big\{ -\frac{5599}{3} + 2656\zeta_5 - 920\zeta_3 + \frac{9152}{3}\zeta_3^2 \\
& - \frac{3326}{3}\zeta_2 + 640\zeta_2\zeta_3 + \frac{296}{5}\zeta_2^2 + \frac{48704}{315}\zeta_2^3 \Big\} + C_A C_F n_f^2 \Big\{ \frac{58045}{486} - \frac{104}{9}\zeta_3 - \frac{3808}{27}\zeta_2
\end{aligned}$$

$$\begin{aligned}
& + \frac{32}{5} \zeta_2^2 \Big\} + C_A C_F^2 n_f \Big\{ \frac{2300107}{1458} + 64 \zeta_5 + \frac{117184}{81} \zeta_3 - \frac{9050}{9} \zeta_2 - \frac{704}{3} \zeta_2 \zeta_3 \\
& - \frac{25768}{135} \zeta_2^2 \Big\} + C_A C_F^3 \Big\{ 6031 - \frac{55376}{9} \zeta_5 - \frac{107296}{27} \zeta_3 + \frac{7904}{3} \zeta_3^2 + \frac{10777}{27} \zeta_2 \\
& + \frac{55504}{9} \zeta_2 \zeta_3 - \frac{105688}{135} \zeta_2^2 - \frac{35584}{315} \zeta_2^3 \Big\} + C_A^2 C_F n_f \Big\{ - \frac{571387}{486} - \frac{680}{9} \zeta_5 \\
& + \frac{1564}{3} \zeta_3 + \frac{29000}{27} \zeta_2 + 16 \zeta_2 \zeta_3 - \frac{1936}{15} \zeta_2^2 \Big\} + C_A^2 C_F^2 \Big\{ - \frac{5553229}{729} - 408 \zeta_5 \\
& + \frac{3082}{81} \zeta_3 + \frac{376}{3} \zeta_3^2 + \frac{297203}{81} \zeta_2 + 824 \zeta_2 \zeta_3 + \frac{29486}{135} \zeta_2^2 + \frac{19472}{315} \zeta_2^3 \Big\} \\
& + C_A^3 C_F \Big\{ \frac{4520317}{1458} + \frac{7700}{9} \zeta_5 - \frac{25516}{9} \zeta_3 - 8 \zeta_3^2 - \frac{70100}{27} \zeta_2 + 264 \zeta_2 \zeta_3 + \frac{1760}{3} \zeta_2^2 \\
& - \frac{10016}{105} \zeta_2^3 \Big\} \Big] + \{z_1 \leftrightarrow z_2\}. \tag{5.31}
\end{aligned}$$

$$\begin{aligned}
\Delta_{d,b}^{\text{sv},(4)} = & \delta(1-z_1)\delta(1-z_2) \Big[n_f \frac{d_F^{abcd} d_F^{abcd}}{N_F} \Big\{ - \frac{2560}{3} \zeta_2 \zeta_5 - \frac{512}{3} \zeta_2 \zeta_3 + 512 \zeta_2^2 \Big\} \\
& + \frac{d_F^{abcd} d_A^{abcd}}{N_F} \Big\{ \frac{7040}{3} \zeta_2 \zeta_5 + \frac{256}{3} \zeta_2 \zeta_3 - 768 \zeta_2 \zeta_3^2 - 256 \zeta_2^2 - \frac{15872}{35} \zeta_2^4 \Big\} \\
& + n_f \Big\{ - \frac{1}{3} \tilde{\mathcal{G}}_3^{b,(2)} \Big\} + C_F n_f^3 \Big\{ - \frac{580}{729} - \frac{238}{27} \zeta_5 - \frac{3686}{729} \zeta_3 - \frac{3758}{729} \zeta_2 + \frac{404}{81} \zeta_2 \zeta_3 \\
& - \frac{335}{81} \zeta_2^2 \Big\} + C_F^2 n_f^2 \Big\{ - \frac{1341097}{11664} - \frac{3488}{27} \zeta_5 - \frac{245390}{729} \zeta_3 + \frac{286}{27} \zeta_3^2 + \frac{241525}{729} \zeta_2 \\
& + \frac{12856}{27} \zeta_2 \zeta_3 - \frac{3065}{36} \zeta_2^2 + \frac{18868}{945} \zeta_2^3 \Big\} + C_F^3 n_f \Big\{ \frac{42292165}{52488} - \frac{473078}{63} \zeta_7 \\
& + \frac{5271502}{405} \zeta_5 + \frac{3163859}{486} \zeta_3 - \frac{271510}{81} \zeta_3^2 - \frac{352162}{81} \zeta_2 - \frac{8464}{9} \zeta_2 \zeta_5 + \frac{317420}{81} \zeta_2 \zeta_3 \\
& - \frac{778774}{1215} \zeta_2^2 - \frac{327928}{135} \zeta_2 \zeta_3 + \frac{179864}{405} \zeta_2^3 \Big\} + C_F^4 \Big\{ \frac{31207}{2} + \frac{5152}{3} \zeta_{5,3} + 17448 \zeta_7 \\
& + \frac{579184}{15} \zeta_5 - \frac{236447}{3} \zeta_3 - \frac{658688}{45} \zeta_3 \zeta_5 + \frac{363374}{27} \zeta_3^2 - \frac{56399}{6} \zeta_2 + \frac{33008}{5} \zeta_2 \zeta_5 \\
& + \frac{57568}{9} \zeta_2 \zeta_3 + \frac{59264}{27} \zeta_2 \zeta_3^2 - \frac{50856}{5} \zeta_2^2 + \frac{14248}{5} \zeta_2^2 \zeta_3 + \frac{256712}{45} \zeta_2^3 - \frac{507968}{1575} \zeta_2^4 \Big\} \\
& + C_A \Big\{ \frac{11}{6} \tilde{\mathcal{G}}_3^{b,(2)} \Big\} + C_A C_F n_f^2 \Big\{ \frac{198202909}{839808} + \frac{7396}{27} \zeta_5 + \frac{1477931}{2916} \zeta_3 + \frac{68}{9} \zeta_3^2 \\
& + \frac{3988867}{34992} \zeta_2 - \frac{12460}{27} \zeta_2 \zeta_3 + \frac{34049}{540} \zeta_2^2 - \frac{3517}{315} \zeta_2^3 \Big\} + C_A C_F^2 n_f \Big\{ \frac{893866105}{472392} \\
& - 1722 \zeta_7 - \frac{19235759}{1215} \zeta_5 - \frac{767605141}{26244} \zeta_3 + \frac{8355031}{729} \zeta_3^2 + \frac{71947313}{8748} \zeta_2 \\
& + \frac{187004}{135} \zeta_2 \zeta_5 - \frac{861269}{81} \zeta_2 \zeta_3 + \frac{254215}{5832} \zeta_2^2 + \frac{146510}{81} \zeta_2^2 \zeta_3 + \frac{874568}{945} \zeta_2^3 \Big\}
\end{aligned}$$

$$\begin{aligned}
& + C_A C_F^3 \left\{ -\frac{61739114}{6561} - \frac{23024}{15} \zeta_{5,3} + \frac{432101}{21} \zeta_7 - \frac{36539051}{405} \zeta_5 + \frac{44371336}{729} \zeta_3 \right. \\
& + \frac{43564}{5} \zeta_3 \zeta_5 + \frac{699449}{81} \zeta_3^2 + \frac{7935479}{243} \zeta_2 - \frac{48124}{9} \zeta_2 \zeta_5 - \frac{3288814}{81} \zeta_2 \zeta_3 \\
& \left. - \frac{28928}{9} \zeta_2^2 \zeta_3 + \frac{16395079}{1215} \zeta_2^2 + \frac{1575124}{135} \zeta_2^2 \zeta_3 - \frac{20261636}{2835} \zeta_2^3 - \frac{2236966}{875} \zeta_2^4 \right\} \\
& + C_A^2 C_F n_f \left\{ \frac{11380577}{6561} - \frac{211}{9} \zeta_7 + \frac{345056}{45} \zeta_5 + \frac{47301911}{2916} \zeta_3 - \frac{55286}{9} \zeta_3^2 \right. \\
& \left. - \frac{17328527}{2187} \zeta_2 - \frac{2672}{3} \zeta_2 \zeta_5 + \frac{186359}{27} \zeta_2 \zeta_3 + \frac{268843}{216} \zeta_2^2 - \frac{9104}{45} \zeta_2^2 \zeta_3 - \frac{1237}{15} \zeta_2^3 \right\} \\
& + C_A^2 C_F^2 \left\{ \frac{4432795339}{472392} - \frac{7184}{45} \zeta_{5,3} + \frac{95771}{9} \zeta_7 + \frac{14489696}{243} \zeta_5 + \frac{261351839}{6561} \zeta_3 \right. \\
& - \frac{7567}{9} \zeta_3 \zeta_5 - \frac{49177675}{1458} \zeta_3^2 - \frac{462645803}{13122} \zeta_2 - \frac{653282}{135} \zeta_2 \zeta_5 + \frac{40089554}{729} \zeta_2 \zeta_3 \\
& \left. - \frac{7018}{27} \zeta_2^2 \zeta_3 - \frac{17427029}{7290} \zeta_2^2 - \frac{1030139}{81} \zeta_2^2 \zeta_3 + \frac{117904}{315} \zeta_2^3 + \frac{17432749}{15750} \zeta_2^4 \right\} \\
& + C_A^3 C_F \left\{ -\frac{634801943}{52488} + \frac{2321}{18} \zeta_7 - \frac{570359}{30} \zeta_5 - \frac{92733521}{2916} \zeta_3 + \frac{32549}{2} \zeta_3^2 \right. \\
& + \frac{164602591}{8748} \zeta_2 + \frac{19976}{3} \zeta_2 \zeta_5 - \frac{725170}{27} \zeta_2 \zeta_3 - 32 \zeta_2^2 \zeta_3 - \frac{8169839}{1620} \zeta_2^2 \\
& \left. + \frac{113432}{45} \zeta_2^2 \zeta_3 + \frac{112079}{140} \zeta_2^3 - \frac{40064}{105} \zeta_2^4 \right\} + \frac{1}{4} \tilde{\mathcal{G}}_4^{b,(1)} + n_f \left\{ \frac{1}{4} \chi_1^b \right\} + n_f^0 \left\{ \frac{1}{4} \chi_2^b \right\} \\
& + \delta(1 - z_1) \bar{\mathcal{D}}_0 \left[n_f \frac{d_F^{abcd} d_F^{abcd}}{N_F} \left\{ 384 + 2b^q_{4,d_F^{abcd} d_F^{abcd}} + \frac{21760}{9} \zeta_5 + \frac{5312}{9} \zeta_3 \right. \right. \\
& \left. \left. - \frac{1216}{3} \zeta_3^2 - \frac{4544}{3} \zeta_2 - 128 \zeta_2 \zeta_3 + \frac{320}{3} \zeta_2^2 - \frac{9472}{315} \zeta_2^3 \right\} + \frac{d_F^{abcd} d_A^{abcd}}{N_F} \left\{ -f_{4,d_F^{abcd} d_A^{abcd}}^q \right\} \right. \\
& \left. + C_F n_f^3 \left\{ \frac{5216}{2187} + \frac{80}{81} \zeta_3 - \frac{800}{81} \zeta_2 + \frac{16}{9} \zeta_2^2 \right\} + C_F^2 n_f^2 \left\{ -\frac{309953}{1458} + \frac{1168}{9} \zeta_5 + \frac{8168}{27} \zeta_3 \right. \right. \\
& \left. \left. + \frac{43552}{729} \zeta_2 - \frac{6272}{27} \zeta_2 \zeta_3 + \frac{928}{27} \zeta_2^2 \right\} + C_F^3 n_f \left\{ -\frac{48157}{108} + 2b^q_{4,n_f C_F^3} - \frac{7712}{3} \zeta_5 \right. \right. \\
& \left. \left. - \frac{2368}{9} \zeta_3 + 1168 \zeta_3^2 - \frac{292}{27} \zeta_2 + \frac{6880}{9} \zeta_2 \zeta_3 + \frac{2012}{45} \zeta_2^2 + \frac{117344}{315} \zeta_2^3 \right\} + C_F^4 \left\{ 7680 \zeta_7 \right. \right. \\
& \left. \left. - 1536 \zeta_5 + 512 \zeta_3 - 1920 \zeta_3^2 - 4608 \zeta_2 \zeta_5 + 1536 \zeta_2 \zeta_3 - \frac{6656}{5} \zeta_2^2 \zeta_3 \right\} + C_A C_F n_f^2 \left\{ \right. \\
& \left. - \frac{898033}{5832} + \frac{304}{3} \zeta_5 + \frac{2456}{81} \zeta_3 + \frac{75718}{243} \zeta_2 + \frac{80}{9} \zeta_2 \zeta_3 - \frac{3104}{45} \zeta_2^2 \right\} + C_A C_F^2 n_f \left\{ \right. \\
& \left. \frac{5590667}{2916} + 2b^q_{4,n_f C_F^2 C_A} - \frac{104}{3} \zeta_5 - \frac{63782}{27} \zeta_3 + \frac{4072}{3} \zeta_3^2 + \frac{146491}{729} \zeta_2 + \frac{15760}{9} \zeta_2 \zeta_3 \right. \\
& \left. - \frac{516976}{405} \zeta_2^2 - \frac{12976}{105} \zeta_2^3 \right\} + C_A C_F^3 \left\{ -\frac{12928}{27} + 8576 \zeta_5 + 928 \zeta_3 - 6160 \zeta_3^2 \right. \\
& \left. - \frac{6592}{27} \zeta_2 - 2304 \zeta_2 \zeta_5 - \frac{34736}{9} \zeta_2 \zeta_3 + \frac{23488}{45} \zeta_2^2 + \frac{4672}{5} \zeta_2^2 \zeta_3 - \frac{704}{5} \zeta_2^3 \right\} \\
& \left. + C_A^2 C_F n_f \left\{ \frac{10761379}{5832} - \frac{1}{2} b^q_{4,n_f C_F} - b^q_{4,n_f C_F C_A} - \frac{1}{24} b^q_{4,d_F^{abcd} d_F^{abcd}} - \frac{14776}{27} \zeta_5 \right. \right.
\end{aligned}$$

$$\begin{aligned}
& -\frac{210778}{81}\zeta_3 - \frac{4868}{9}\zeta_3^2 - \frac{654449}{243}\zeta_2 + \frac{6640}{9}\zeta_2\zeta_3 + \frac{138808}{135}\zeta_2^2 - \frac{65192}{945}\zeta_2^3 \Big\} \\
& + C_A^2 C_F^2 \left\{ \frac{785732}{729} + \frac{37888}{9}\zeta_5 + \frac{176600}{27}\zeta_3 - 3040\zeta_3^2 - \frac{1902716}{729}\zeta_2 - 768\zeta_2\zeta_5 \right. \\
& - \frac{136144}{27}\zeta_2\zeta_3 + \frac{529936}{405}\zeta_2^2 + \frac{1840}{3}\zeta_2^2\zeta_3 - \frac{1232}{15}\zeta_2^3 \Big\} + C_A^3 C_F \left\{ -\frac{28325071}{4374} \right. \\
& + \frac{1}{24} f_4^{q, d_F^{abcd} d_A^{abcd}} + 1700\zeta_7 - \frac{24920}{9}\zeta_5 + 9600\zeta_3 - \frac{2332}{3}\zeta_3^2 + \frac{1642195}{243}\zeta_2 \\
& \left. + 416\zeta_2\zeta_5 - \frac{30772}{9}\zeta_2\zeta_3 - \frac{78188}{45}\zeta_2^2 + 288\zeta_2^2\zeta_3 + \frac{45188}{315}\zeta_2^3 \Big\} \right] \\
& + \delta(1 - z_1) \overline{\mathcal{D}}_1 \left[n_f \frac{d_F^{abcd} d_A^{abcd}}{N_F} \left\{ -\frac{1280}{3}\zeta_5 - \frac{256}{3}\zeta_3 + 256\zeta_2 \right\} + \frac{d_F^{abcd} d_A^{abcd}}{N_F} \left\{ \frac{3520}{3}\zeta_5 \right. \right. \\
& + \frac{128}{3}\zeta_3 - 384\zeta_3^2 - 128\zeta_2 - \frac{7936}{35}\zeta_2^3 \Big\} + C_F n_f^3 \left\{ -\frac{4000}{729} + \frac{320}{27}\zeta_2 \right\} \\
& + C_F^2 n_f^2 \left\{ \frac{123010}{729} - \frac{30112}{81}\zeta_3 - \frac{4720}{81}\zeta_2 + \frac{5632}{135}\zeta_2^2 \right\} + C_F^3 n_f \left\{ 108 + \frac{10816}{9}\zeta_5 \right. \\
& + \frac{60560}{27}\zeta_3 - \frac{14624}{27}\zeta_2 - \frac{22400}{9}\zeta_2\zeta_3 + \frac{58208}{135}\zeta_2^2 \Big\} + C_F^4 \left\{ \frac{4312}{3} + 3392\zeta_5 \right. \\
& - 4752\zeta_3 + \frac{18304}{3}\zeta_3^2 - \frac{2968}{3}\zeta_2 + 704\zeta_2\zeta_3 - \frac{1056}{5}\zeta_2^2 + \frac{97408}{315}\zeta_2^3 \Big\} + C_A C_F n_f^2 \left\{ \right. \\
& \frac{58045}{243} - \frac{208}{9}\zeta_3 - \frac{7616}{27}\zeta_2 + \frac{64}{5}\zeta_2^2 \Big\} + C_A C_F^2 n_f \left\{ -\frac{1243577}{729} + 128\zeta_5 + \frac{281600}{81}\zeta_3 \right. \\
& + \frac{2416}{3}\zeta_2 - \frac{1408}{3}\zeta_2\zeta_3 - \frac{64064}{135}\zeta_2^2 \Big\} + C_A C_F^3 \left\{ -\frac{7496}{9} - \frac{102112}{9}\zeta_5 - \frac{180032}{27}\zeta_3 \right. \\
& + \frac{15808}{3}\zeta_3^2 + \frac{102728}{27}\zeta_2 + \frac{112736}{9}\zeta_2\zeta_3 - \frac{340112}{135}\zeta_2^2 - \frac{71168}{315}\zeta_2^3 \Big\} \\
& + C_A^2 C_F n_f \left\{ -\frac{571387}{243} - \frac{1360}{9}\zeta_5 + \frac{3128}{3}\zeta_3 + \frac{58000}{27}\zeta_2 + 32\zeta_2\zeta_3 - \frac{3872}{15}\zeta_2^2 \right\} \\
& + C_A^2 C_F^2 \left\{ \frac{2420680}{729} - 336\zeta_5 - \frac{638128}{81}\zeta_3 + \frac{752}{3}\zeta_3^2 - \frac{178496}{81}\zeta_2 + 1696\zeta_2\zeta_3 \right. \\
& + \frac{151312}{135}\zeta_2^2 + \frac{38944}{315}\zeta_2^3 \Big\} + C_A^3 C_F \left\{ \frac{4520317}{729} + \frac{15400}{9}\zeta_5 - \frac{51032}{9}\zeta_3 - 16\zeta_3^2 \right. \\
& - \frac{140200}{27}\zeta_2 + 528\zeta_2\zeta_3 + \frac{3520}{3}\zeta_2^2 - \frac{20032}{105}\zeta_2^3 \Big\} + \mathcal{D}_0 \overline{\mathcal{D}}_0 \left[n_f \frac{d_F^{abcd} d_A^{abcd}}{N_F} \left\{ -\frac{640}{3}\zeta_5 \right. \right. \\
& - \frac{128}{3}\zeta_3 + 128\zeta_2 \Big\} + \frac{d_F^{abcd} d_A^{abcd}}{N_F} \left\{ \frac{1760}{3}\zeta_5 + \frac{64}{3}\zeta_3 - 192\zeta_3^2 - 64\zeta_2 - \frac{3968}{35}\zeta_2^3 \right\} \\
& + C_F n_f^3 \left\{ -\frac{2000}{729} + \frac{160}{27}\zeta_2 \right\} + C_F^2 n_f^2 \left\{ \frac{61505}{729} - \frac{15056}{81}\zeta_3 - \frac{2360}{81}\zeta_2 + \frac{2816}{135}\zeta_2^2 \right\} \\
& + C_F^3 n_f \left\{ 54 + \frac{5408}{9}\zeta_5 + \frac{30280}{27}\zeta_3 - \frac{7312}{27}\zeta_2 - \frac{11200}{9}\zeta_2\zeta_3 + \frac{29104}{135}\zeta_2^2 \right\} \\
& + C_F^4 \left\{ \frac{2156}{3} + 1696\zeta_5 - 2376\zeta_3 + \frac{9152}{3}\zeta_3^2 - \frac{1484}{3}\zeta_2 + 352\zeta_2\zeta_3 - \frac{528}{5}\zeta_2^2 \right. \\
& \left. + \frac{48704}{315}\zeta_2^3 \right\} + C_A C_F n_f^2 \left\{ \frac{58045}{486} - \frac{104}{9}\zeta_3 - \frac{3808}{27}\zeta_2 + \frac{32}{5}\zeta_2^2 \right\}
\end{aligned}$$

$$\begin{aligned}
& + C_A C_F^2 n_f \left\{ -\frac{1243577}{1458} + 64\zeta_5 + \frac{140800}{81}\zeta_3 + \frac{1208}{3}\zeta_2 - \frac{704}{3}\zeta_2\zeta_3 - \frac{32032}{135}\zeta_2^2 \right\} \\
& + C_A C_F^3 \left\{ -\frac{3748}{9} - \frac{51056}{9}\zeta_5 - \frac{90016}{27}\zeta_3 + \frac{7904}{3}\zeta_3^2 + \frac{51364}{27}\zeta_2 + \frac{56368}{9}\zeta_2\zeta_3 \right. \\
& - \left. \frac{170056}{135}\zeta_2^2 - \frac{35584}{315}\zeta_2^3 \right\} + C_A^2 C_F n_f \left\{ -\frac{571387}{486} - \frac{680}{9}\zeta_5 + \frac{1564}{3}\zeta_3 + \frac{29000}{27}\zeta_2 \right. \\
& + \left. 16\zeta_2\zeta_3 - \frac{1936}{15}\zeta_2^2 \right\} + C_A^2 C_F^2 \left\{ \frac{1210340}{729} - 168\zeta_5 - \frac{319064}{81}\zeta_3 + \frac{376}{3}\zeta_3^2 \right. \\
& - \left. \frac{89248}{81}\zeta_2 + 848\zeta_2\zeta_3 + \frac{75656}{135}\zeta_2^2 + \frac{19472}{315}\zeta_2^3 \right\} + C_A^3 C_F \left\{ \frac{4520317}{1458} + \frac{7700}{9}\zeta_5 \right. \\
& - \left. \frac{25516}{9}\zeta_3 - 8\zeta_3^2 - \frac{70100}{27}\zeta_2 + 264\zeta_2\zeta_3 + \frac{1760}{3}\zeta_2^2 - \frac{10016}{105}\zeta_2^3 \right\} + \left\{ z_1 \leftrightarrow z_2 \right\}.
\end{aligned} \tag{5.32}$$

The symbols χ_j^q and χ_j^g denote the unknown coefficients of the color factors in four loop form factors of the Drell-Yan and of the Higgs boson production through gluon fusion, respectively. For the case of Higgs boson production in bottom quark annihilation, only the n_f^3 and n_f^2 contributions to the four loop form factor are available in the literature [56]. As a result, the unknown coefficients corresponding to $O(n_f)$ and $O(n_f^0)$ color factors are denoted by χ_1^b and χ_2^b , respectively. Also the symbols $f_{4,d_F^{abcd}d_A^{abcd}}^q$ and $b_{4,j}^q$, where $j = \{d_F^{abcd}d_A^{abcd}, n_f C_F^3, n_f C_F^2 C_A, d_F^{abcd}d_A^{abcd}, C_F^2 C_A^2, C_F^3 C_A, C_F^4\}$ are the unknown coefficients of the color factors in four loop soft and collinear anomalous dimensions. In the aforementioned equations, n_{fv} is proportional to the charge weighted sum of the quark flavours and $N_4 = (n_c^2 - 4)/n_c$ [58]. Following [46], we have

$$\frac{d_A^{abcd}d_A^{abcd}}{N_A} = \frac{N_c^2(N_c^2 + 36)}{24}, \quad \frac{d_F^{abcd}d_A^{abcd}}{N_A} = \frac{N_c(N_c^2 + 6)}{48}, \quad \frac{d_F^{abcd}d_F^{abcd}}{N_A} = \frac{N_c^4 - 6N_c^2 + 18}{96N_c^2}, \tag{5.33}$$

$$C_A = N_c, \quad C_F = \frac{N_c^2 - 1}{2N_c}, \quad N_A = N_c^2 - 1, \quad N_F = N_c. \tag{5.34}$$

5.4 Soft-collinear operator for threshold resummation

In this section, we develop the resummation formalism for the differential distribution with respect to the rapidity variable y , for the production of n -colorless particles. Earlier we have seen that differential soft-collinear operator, \mathbf{S}_d^l in Eq.(5.25), embeds universality of all the soft enhancements associated with the soft gluon emissions. Besides being the process independent operator, interestingly it also exhibits an exponential behaviour. Recall that the threshold resummation [196] relies on the fact that the soft contribution exponentiates to all orders in perturbation theory, owing to the Sudakov differential equation and the renormalization group invariance. Following the same argument we proceed towards the resummation formalism for differential cross-section as well.

The relevance of resummation of differential cross-section arises from the fact that, in the limit $z_{1(2)} \rightarrow 1$, the logarithms of type $\left(a_s^n \ln^{m_1}(1 - z_1) \ln^{m_2}(1 - z_2)\right)/((1 - z_1)(1 - z_2))$ for $m_1 + m_2 \leq 2(n - 1)$, give rise to large contributions which could potentially spoil the reliability of the perturbative series. Hence a systematic way of exponentiating these large logarithms and resumming them to all orders in perturbation theory becomes indispensable. In [68] it was shown, in the context of differential distribution with respect to the Feynman variable x_F , that the potential logarithms which give dominant contributions in certain kinematic regions can be resummed to all orders in perturbation theory in Mellin-Mellin (M-M) space approach. This approach was also extended to rapidity distributions in the earlier works (See [189, 197] for details). Note that this approach is different from the Mellin-Fourier (M-F) approach [186] proposed by Laenen & Sterman. In M-F formalism partonic cross-section is expressed in terms of scaling variable z and rapidity variable y and then the threshold limit is taken only for $z \rightarrow 1$ which resums delta $(\delta(1 - z))$ and distributions $(D_i(z))$, but for rapidity variable y only delta $(\delta(y))$ piece is resummed. In [197], a detailed numerical comparison has been made in between M-M and M-F approach and found that both the approaches converges to a few percent correc-

tion to the fixed order prediction at NNLL level. In the following we further extend the M-M approach and derive the resummation formalism for the production of n -colorless particles in a partonic collision.

Within the framework of M-M approach, both the partonic scaling variables $z_{1(2)}$ are simultaneously taken to the threshold limit 1 and the corresponding delta, $\delta(1 - z_i)$, and plus distributions, $D_i(z_i) \equiv \left[\frac{\ln^l(1-z_i)}{1-z_i} \right]_+$, are resummed to all orders in perturbation theory. Due to the involvement of convolutions in the $z_{1(2)}$ space, the resummation is performed in two dimensional Mellin space where the differential cross-section is expressed in terms of simple normal products. In the following we derive the generic formalism in terms of the Mellin variables N_1 and N_2 corresponding to the z_1 and z_2 variables, respectively. Hence the threshold limit $z_{1(2)} \rightarrow 1$ translate to $N_{1(2)} \rightarrow \infty$ in Mellin space and the large logarithms proportional to $\ln N_{1(2)}$ are resummed to all orders in perturbation theory.

To derive the all order behaviour of the SV differential cross-section, $\mathcal{A}_{d,I}^{\text{SV}}(z_1, z_2)$, in the two dimensional Mellin space with $\bar{N}_i = N_i e^{\gamma_E}$, we begin with the Mellin moment of the same, which takes the following form:

$$\tilde{\mathcal{A}}_{d,I}^{\text{SV}}(\bar{N}_1, \bar{N}_2) = \left[\prod_{i=1,2} \int_0^1 dz_i z_i^{N_i-1} \right] \mathcal{A}_{d,I}^{\text{SV}}(\{p_j \cdot q_k\}, z_1, z_2). \quad (5.35)$$

γ_E is the Euler-Mascheroni constant. In the previous section in (5.16), $\mathcal{A}_{d,I}^{\text{SV}}$ is decomposed into constituents corresponding to the virtual as well as the soft-collinear real emission contributions. Now in this section, we further decompose those contributions into a process dependent and a process independent quantities. We denote the process dependent coefficient $C_{d,0}^I$ in the context of $2 \rightarrow n$ scattering process as,

$$C_{d,0}^I(\{p_j \cdot q_k\}, q^2, \mu_F^2) = |\mathcal{M}_I^{(0)}|^2 |\mathcal{F}_{I,\text{fin}}(\{p_j \cdot q_k\}, q^2, \mu_R^2)|^2 S_{d,\delta}^{I,\text{res}}(q^2, \mu_R^2, \mu_F^2). \quad (5.36)$$

Here $C_{d,0}^I$ accounts for all the finite contributions coming from the virtual corrections and the coefficients proportional to $\delta(1 - z_1)\delta(1 - z_2)$ of the real emission contributions.

Besides, it also contains the finite part of the mass factorized kernel $\Gamma_{I,\text{fin}}$ in terms of $\ln(\mu_F^2/\mu_R^2)$ which results from the coupling constant renormalization. The quantity $S_{d,\delta}^{I,res}$ which we name as the *differential soft-collinear operator for threshold resummation*, embeds the $\delta(1 - z_i)$ contributions from the soft distribution function $\Phi_{d,\text{sv}}^I$ and from $\Gamma_{I,\text{fin}}$ in the following way:

$$S_{d,\delta}^{I,res}(q^2, \mu_R^2, \mu_F^2) = \exp\left(2\Phi_{d,\delta}^I(q^2, \mu_R^2, \mu_F^2) - 2\ln\Gamma_{I,\delta}(\mu_F^2)\right). \quad (5.37)$$

The subscript δ indicates $\delta(1 - z_1)\delta(1 - z_2)$ coefficients of the aforementioned quantities. Expanding in powers of $a_s(\mu_R^2)$, it takes the form in z -space with $q^2 = \mu_R^2 = \mu_F^2$:

$$S_{d,\delta}^{I,res}(q^2, \mu_R^2, \mu_F^2) = 1 + \sum_{i=1}^{\infty} a_s^i(\mu_R^2) S_{d,\delta,i}^{I,res}(q^2, \mu_R^2, \mu_F^2). \quad (5.38)$$

with

$$\begin{aligned} S_{d,\delta,1}^{I,res} &= 2\tilde{\mathcal{G}}_{d,1}^{I,1}, \\ S_{d,\delta,2}^{I,res} &= \tilde{\mathcal{G}}_{d,2}^{I,1} + 2(\tilde{\mathcal{G}}_{d,1}^{I,1})^2 + 2\beta_0\tilde{\mathcal{G}}_{d,1}^{I,2}, \\ S_{d,\delta,3}^{I,res} &= \frac{2}{3}\tilde{\mathcal{G}}_{d,3}^{I,1} + 2\tilde{\mathcal{G}}_{d,1}^{I,1}\tilde{\mathcal{G}}_{d,2}^{I,1} + \frac{4}{3}(\tilde{\mathcal{G}}_{d,1}^{I,1})^3 + \frac{4}{3}\beta_1\tilde{\mathcal{G}}_{d,1}^{I,2} + \frac{4}{3}\beta_0\tilde{\mathcal{G}}_{d,2}^{I,2} + 4\beta_0\tilde{\mathcal{G}}_{d,1}^{I,1}\tilde{\mathcal{G}}_{d,1}^{I,2} + \frac{8}{3}\beta_0^2\tilde{\mathcal{G}}_{d,1}^{I,3}, \\ S_{d,\delta,4}^{I,res} &= \frac{1}{2}\tilde{\mathcal{G}}_{d,4}^{I,1} + \frac{1}{2}(\tilde{\mathcal{G}}_{d,2}^{I,1})^2 + \frac{4}{3}\tilde{\mathcal{G}}_{d,1}^{I,1}\tilde{\mathcal{G}}_{d,3}^{I,1} + 2(\tilde{\mathcal{G}}_{d,1}^{I,1})^2\tilde{\mathcal{G}}_{d,2}^{I,1} + \frac{2}{3}(\tilde{\mathcal{G}}_{d,1}^{I,1})^4 + \beta_2\tilde{\mathcal{G}}_{d,1}^{I,2} + \beta_1\tilde{\mathcal{G}}_{d,2}^{I,2} \\ &\quad + \frac{8}{3}\beta_1\tilde{\mathcal{G}}_{d,1}^{I,1}\tilde{\mathcal{G}}_{d,1}^{I,2} + \beta_0\tilde{\mathcal{G}}_{d,3}^{I,2} + 2\beta_0\tilde{\mathcal{G}}_{d,1}^{I,2}\tilde{\mathcal{G}}_{d,2}^{I,1} + \frac{8}{3}\beta_0\tilde{\mathcal{G}}_{d,1}^{I,1}\tilde{\mathcal{G}}_{d,2}^{I,2} + 4\beta_0(\tilde{\mathcal{G}}_{d,1}^{I,1})^2\tilde{\mathcal{G}}_{d,1}^{I,2} \\ &\quad + 4\beta_0\beta_1\tilde{\mathcal{G}}_{d,1}^{I,3} + 2\beta_0^2\tilde{\mathcal{G}}_{d,2}^{I,3} + 2\beta_0^2(\tilde{\mathcal{G}}_{d,1}^{I,2})^2 + \frac{16}{3}\beta_0^2\tilde{\mathcal{G}}_{d,1}^{I,1}\tilde{\mathcal{G}}_{d,1}^{I,3} + 4\beta_0^3\tilde{\mathcal{G}}_{d,1}^{I,4}. \end{aligned} \quad (5.39)$$

where $\tilde{\mathcal{G}}_{d,i}^{I,k}$ are given in Appendix C.

In a similar way, we denote the process independent contributions to $\Delta_{d,I}^{\text{sv}}$ as $\Phi_d^{I,res}$ which comprises of the terms proportional to plus distributions from $\Phi_{d,\text{sv}}^I$ and $\Gamma_{I,\text{fin}}$. Mathemat-

ically it can be written as,

$$\begin{aligned}\Phi_d^{I,res}(z_1, z_2, q^2, \mu_F^2) &= 2\Phi_{d,\mathcal{D}}^I(z_1, z_2, q^2) - C \ln \Gamma_{I,\mathcal{D}}(z_1, \mu_F^2) \delta(1 - z_2) \\ &\quad - C \ln \Gamma_{I,\mathcal{D}}(z_2, \mu_F^2) \delta(1 - z_1),\end{aligned}\quad (5.40)$$

where the subscript \mathcal{D} indicates the terms proportional to plus distribution which includes, $\mathcal{D}_i(z_1)\delta(1 - z_2)$, $\mathcal{D}_i(z_2)\delta(1 - z_1)$, and $\mathcal{D}_i(z_1)\mathcal{D}_j(z_2)$. Similar to the inclusive case, following the approach given in [5], $\Phi_d^{I,res}$ can be expressed in an integral form given as,

$$\begin{aligned}\Phi_d^{I,res}(z_1, z_2, q^2, \mu_F^2) &= \left[\delta(\bar{z}_2) \left(\frac{1}{\bar{z}_1} \left\{ \int_{\mu_F^2}^{q^2 \bar{z}_1} \frac{d\lambda^2}{\lambda^2} A^I(a_s(\lambda^2)) + \mathbf{D}_d^I(a_s(q^2 \bar{z}_1)) \right\} \right)_+ \right. \\ &\quad \left. + \frac{1}{2} \left(\frac{1}{\bar{z}_1 \bar{z}_2} \left\{ A^I(a_s(z_{12})) + \frac{d\mathbf{D}_d^I(a_s(z_{12}))}{d \ln z_{12}} \right\} \right)_+ + (z_1 \leftrightarrow z_2) \right],\end{aligned}\quad (5.41)$$

here the subscript $+$ indicates the standard plus distribution and the other constants are defined as $\bar{z}_i = (1 - z_i)$ and $z_{12} = q^2 \bar{z}_1 \bar{z}_2$. The finite functions, $\mathbf{D}_d^I = \sum_{i=1}^{\infty} a_s^i \mathbf{D}_{d,i}^I$, are related to the threshold exponent \mathbf{D}_i^I of inclusive cross section owing to the relation given in (5.20) (See Eq.(2.87) and [5, 189] for more details). For completeness, we provide the coefficients A_i^I and $\mathbf{D}_{d,i}^I$ in the Appendix B and C respectively.

Consequently the SV differential cross-section decomposes into a process dependent and a process independent way and can be re-written in the following form:

$$\begin{aligned}\Delta_{d,I}^{\text{sv}}(\{p_j \cdot q_k\}, z_1, z_2, q^2, \mu_F^2) &= C_{d,0}^I(\{p_j \cdot q_k\}, q^2, \mu_F^2) \delta(1 - z_1) \delta(1 - z_2) \\ &\quad \otimes C \exp(\Phi_d^{I,res}(z_1, z_2, q^2, \mu_F^2)) \otimes \mathbf{I}_{d,I}^{\text{sv}}.\end{aligned}\quad (5.42)$$

Substituting (5.42) in (5.35) and after doing the two dimensional Mellin transformation systematically, we obtain

$$\tilde{\Delta}_{d,I}^{\text{sv}}(\bar{N}_1, \bar{N}_2) = C_{d,0}^I(\{p_j \cdot q_k\}, q^2, \mu_F^2) \exp\left(\ln g_{d,0}^I(q^2, \mu_F^2) + G_{d,\bar{N}}^I(q^2, \mu_F^2, \omega)\right),\quad (5.43)$$

with $\omega = \beta_0 a_s(\mu_R^2) \ln(\bar{N}_1 \bar{N}_2)$. The first coefficient of QCD β -function is denoted by $\beta_0 \equiv (11C_A - 2n_f)/3$, n_f is the number of active light quark flavours. Here, the decomposition in the exponent is done in such a way that the coefficient $G_{d,\bar{N}}^I$ contains $N_{1(2)}$ dependent terms, and the remaining ones are embedded in $(\ln g_{d,0}^I)$. Besides this, $G_{d,\bar{N}}^I(q^2, \mu_F^2, \omega)$ also vanishes in the limit $\omega \rightarrow 1$. Needless to say that both of these coefficients has a universal structure in terms of the anomalous dimensions A^I and process independent coefficients \mathbf{D}^I and thus are dependent only on the incoming partons. Further we combine the $N_{1(2)}$ independent coefficients $g_{d,0}^I$ with $C_{d,0}^I$ from (5.43) and define,

$$\bar{g}_{d,0}^I(\{p_j \cdot q_k\}, q^2, \mu_F^2) = C_{d,0}^I(\{p_j \cdot q_k\}, q^2, \mu_F^2) g_{d,0}^I(q^2, \mu_F^2) \quad (5.44)$$

which can be expanded in terms of $a_s(\mu_R^2)$ as,

$$\bar{g}_{d,0}^I(\{p_j \cdot q_k\}, q^2, \mu_F^2) = \sum_{i=0}^{\infty} a_s^i(\mu_R^2) \bar{g}_{d,0}^{I,i}(\{p_j \cdot q_k\}, q^2, \mu_F^2, \mu_R^2). \quad (5.45)$$

From (5.44) it can be seen, that the coefficient $\bar{g}_{d,0}^I$ contains finite contribution from virtual corrections, *differential soft-collinear operator for threshold resummation* and N independent terms coming from Mellin transformation of plus distribution. Consequently, (5.43) gets modified as,

$$\tilde{Z}_{d,I}^{\text{sv}}(\bar{N}_1, \bar{N}_2) = \bar{g}_{d,0}^I(\{p_j \cdot q_k\}, q^2, \mu_F^2) \exp\left(G_{d,\bar{N}}^I(q^2, \mu_F^2, \omega)\right). \quad (5.46)$$

where the exponent $G_{d,\bar{N}}^I$ can be organized as a resummed perturbation series in Mellin space as,

$$G_{d,\bar{N}}^I(q^2, \mu_F^2, \omega) = g_{d,1}^I(\omega) \ln(\bar{N}_1 \bar{N}_2) + \sum_{i=0}^{\infty} a_s^i(\mu_R^2) g_{d,i+2}^I(\omega, q^2, \mu_F^2, \mu_R^2). \quad (5.47)$$

The explicit form in (5.46) when expanded till k -th order in powers of $a_s(\mu_R^2)$, gives the logarithmically enhanced contributions to the fixed order results $\tilde{Z}_{d,I}^{\text{sv}}(\bar{N}_1, \bar{N}_2)$ up to the

same order. The successive terms in the above series given in (5.47) along with the corresponding terms in (5.45) define the resummed accuracy as LL, NLL, NNLL, N³LL and so on. In general for N^kLL accuracy, terms up to $g_{d,k+1}^I$ must be included along with $\bar{g}_{d,0}^I$ up to order $a_s^k(\mu_R^2)$. The general expression for the coefficients $\bar{g}_{d,0}^{I,i}$ and $g_{d,i}^I$ up to N³LL are provided in the Appendix E.

The coefficients $G_{d,\bar{N}}^I$ remains unaltered even for $2 \rightarrow n$ scattering process owing to its universality. However, the process dependent coefficient function $\bar{g}_{d,0}^I$ changes for the production of n -colorless particles due to the inclusion of process specific form factor via (5.36) and (5.44). The results of these coefficients appear as a product of N_1 and N_2 in the Mellin space, and all those terms which are only function of N_1 or N_2 cancel internally.

We have also observed that the coefficients $\bar{g}_{d,0}^I$ and $G_{d,\bar{N}}^I$ coincides with their inclusive counterparts \bar{g}_0^I and $G_{\bar{N}}^I$ respectively in the limit $N_1 \rightarrow N_2 \rightarrow N$, provided the coefficients \mathbf{D}_d^I in (5.41) is expressed in terms of \mathbf{D}^I of inclusive soft distribution function (See Eq.(2.87)) using the relation (5.20). Hence we infer that all the above observations which hold true for $2 \rightarrow 1$ scattering processes are further extended and verified for any generic system of n -colorless particles in the final state.

5.5 Summary

To summarize, through this chapter we presented a systematic framework for the study of soft-plus-virtual corrections to the differential distribution with respect to the rapidity variable y , for the production of n -colorless particles in the hadron collider. The infrared structure of rapidity distribution which was earlier studied in ref. [5] for Sudakov type processes is further extended to the case of $2 \rightarrow n$ scattering. We employ the universality of the soft enhancements associated with the real emission diagrams. The main deviation from the Sudakov type formalism comes from the virtual corrections where the kinematic dependence is much more involved. The rest of the formalism relies on the collinear

factorization of the differential cross section, the renormalization group invariance, universality of perturbative infrared structure of the scattering amplitudes, and the process independence of the soft-collinear distribution. Besides this, we also use an additional fact that the N -th Mellin moment of the differential distribution has a relation with its inclusive counterpart in the limit $N \rightarrow \infty$. The mere use of this fact enables us to get an all order relation between the soft-collinear distribution of inclusive cross-section and that of rapidity.

6 On next to soft corrections to Drell-Yan and Higgs Boson production

Till this point, our center of discussion was on computing higher order corrections at the threshold approximation, the resulting contributions are the threshold corrections. In the last chapter, we go beyond the threshold, and look into the structure of next-to-threshold logarithms. We address not only the next-to-threshold corrections, but also attempt to study the structure of next-to-leading power resummation. The materials presented in this chapter are the result of original research done in collaboration with Pooja Mukherjee and V. Ravindran and are based on the article [198]

6.1 Prologue

Before going to the discussion on next-to-threshold formalism, let us briefly summarize the details of threshold framework that we discussed in previous chapters.

The higher order quantum effects from QCD and EW theory provide theoretical laboratory to understand the ultraviolet and infrared structure of the underlying quantum field theory. This is due to certain factorisation properties of scattering amplitudes in UV and IR regions. The consequence of the factorisation is the RG invariance which demonstrates the structure of logarithms of the renormalisation scale μ_R from UV and of the factorisation scale μ_F from IR to all orders in perturbation theory. The renormalisation

scale separates UV divergent part from the finite part of the Green's function or on-shell amplitudes, quantifying the arbitrariness in the finite part. While the parameters of the renormalised version of the theory are functions of the renormalisation scale, the physical observables are expected to be independent of this scale. This is the consequence of RG invariance. The anomalous dimensions of the RG equations govern the structure of the logarithms of renormalisation scale in the perturbation theory to all orders.

Like UV sector, the infrared sectors of both SM and QCD are also very rich. Massless gauge fields such as photons in QED and gluons in QCD and light matter particles at high energies give soft and collinear divergences, collectively called IR divergences, in scattering amplitudes. The IR divergences are shown to factorise from on-shell amplitudes and from certain cross sections respectively in a process independent way at an arbitrary factorisation scale. The resulting IR renormalisation group equations are governed by IR anomalous dimensions. The IR renormalisation group equations are peculiar in the sense that the resulting evolution is not only controlled by the factorisation scale but also by the energy scale(s) in the amplitude or in the scattering process. Unlike the UV divergences which are removed by appropriate renormalisation constants, the IR divergences do not require any such renormalisation procedure as they add up to zero for infrared safe observables thanks to KLN theorem [31, 32]. The structure of resulting IR logarithms at every order in the perturbation theory is governed by the IR anomalous dimensions. Hence, most of the logarithms present at higher orders are due to UV and IR divergences present at the intermediate stages of the computations.

The logarithms of renormalisation and factorisation scales present in the perturbative expansions often play important role to estimate the error that results due to the truncation of the perturbative series. Lesser the dependence on these scales, more the reliability of the truncated results. Note that there are also logarithms that are functions of physical scales or the corresponding scaling variables in the observables. In certain kinematical regions, these logarithms that are present at every order can be large enough to spoil the reliability

of the truncated perturbative series. Since the structure of these logarithms at every order is controlled by anomalous dimensions of IR renormalisation group equations, they can be systematically summed up to all orders. This procedure is called resummation. There are classic examples in QCD. For example, the threshold logarithms of the kind

$$\mathcal{D}_i(z) = \left(\frac{\ln^i(1-z)}{1-z} \right)_+ \quad (6.1)$$

are present in the perturbative results of invariant mass distribution of pair of leptons in Drell-Yan process. The scaling variable for the DY is $z = M_{l+l-}^2/\hat{s}$. The invariants \hat{s} and M_{l+l-}^2 denote the center of mass energy of incoming partons and invariant mass of final state leptons respectively. The distributions $\mathcal{D}_i(z)$ are often called *threshold logarithms* as they dominate in the threshold region namely z approaches 1. In this limit, the entire energy of the incoming particles in the scattering event goes into producing a set of hard particles along with infinite number of soft gluons each carrying almost zero momentum. In particular, the logarithms of the form $\ln^i(1-z)/(1-z)$ result from the processes involving real radiations of soft gluons and collinear particles. While these contributions are ill defined in 4 space-time dimensions in the limit $z \rightarrow 1$, the inclusion of pure virtual contributions gives distributions $\mathcal{D}_i(z)$ and $\delta(1-z)$. The terms that constitute these distributions and $\delta(1-z)$ are called the SV contributions. (For SV results up to third order, see [39, 40, 60–63, 65–67]).

The threshold logarithms in the perturbative results when convoluted with appropriate parton distribution functions to obtain hadronic cross section can not only dominate over other contributions but also give large contributions at every order. Presence of these large corrections at every order spoil the reliability of the predictions from the truncated series. The seminal works by Sterman [69] and Catani and Trentedue [68] provide resolution to this problem through reorganisation of the perturbative series called *threshold resummation*. Since z -space results involve convolutions of these distributions, Mellin space approach using the conjugate variable N is used for resummation. The large logarithms

of the kind $\mathcal{D}_i(z)$ become functions of $\ln^{j+1}(N)$, $j \leq i$ with $O(1/N)$ suppressed terms in the corresponding N -space threshold limit, namely $N \rightarrow \infty$. Threshold resummation allows one to resum $\omega = 2a_s(\mu_R^2)\beta_0 \ln(N)$ terms to all orders in ω and then to organise the resulting perturbative result in powers of coupling constant $a_s(\mu_R^2) = g_s^2(\mu_R^2)/16\pi^2$, where g_s is the strong coupling constant. Here, β_0 is the leading coefficient of QCD beta function. If O_N is an observable in Mellin N -space, with N being the conjugate variable to z of the observable $O(z)$ in z -space, then the resummation of threshold logarithms gives

$$\ln(O_N) = \ln(N) g_1^O(\omega) + \sum_{i=0}^{\infty} a_s^i(\mu_R^2) g_{i+2}^O(\omega) + g_0^O(a_s(\mu_R^2)), \quad (6.2)$$

where $g_0^O(a_s(\mu_R^2))$ is N independent and is given by

$$g_0^O(a_s(\mu_R^2)) = \sum_{i=0}^{\infty} a_s^i(\mu_R^2) g_{0,i}^O. \quad (6.3)$$

Inclusion of more and more terms in Eq.(6.2) predicts the LL, NLL etc logarithms of O to all orders in a_s . The functions $g_i^O(\omega)$ are functions of process independent universal IR anomalous dimensions while g_0^O depend on the hard process. For the invariant mass distribution of lepton pairs in DY, Higgs boson productions in various channels, all the ingredients to perform the resummation of threshold logarithms in N -space up to N³LL accuracy are available.

While the resummed results provide reliable predictions that can be compared against the experimental data, it is important to find out the role of sub leading terms namely $\ln^i(1-z)$, $i = 0, 1, \dots$, We call them by next-to-SV (NSV) contributions. In literature they are also known in names of *next-to-threshold* or *next-to-leading-power corrections*. In addition to understand the role of NSV terms, the question on weather these terms can also be resummed systematically to all orders exactly like the way the leading SV terms are resummed remains unanswered satisfactorily. These questions have already been addressed in great detail and remarkable progress has been made in recent times leading to a

better understanding of NSV terms. (See, [6–8, 199–208] for more other works on NSV in the literature). Motivating from the parallel works, in this chapter, we make an attempt to study the structure of NSV logarithms by exploiting collinear factorisation, RG invariance and with an understanding on the logarithmic structure of higher order perturbative results coming from Feynman and phase space integrals. Through the formalism, we propose an all order result both in z -space and in N -space, which can predict NSV terms for DY and Higgs boson production to all orders in perturbation theory.

6.2 Next to SV in z -space

In the following, we study the inclusive cross-sections for the production of a pair of leptons in DY and the production of a single scalar Higgs boson in gluon fusion as well as in bottom quark annihilation. Let us denote the corresponding inclusive cross sections generically by $\sigma(q^2, \tau)$. In the QCD improved parton model, σ is written in terms of parton level coefficient functions (CF) denoted by $\Delta_{ab}(q^2, \mu_R^2, \mu_F^2, z)$ convoluted with appropriate pdfs, $f_c(x_i, \mu_F^2)$, of incoming partons:

$$\sigma(q^2, \tau) = \sigma_B(\mu_R^2) \sum_{ab} \int dx_1 dx_2 f_a(x_1, \mu_F^2) f_b(x_2, \mu_F^2) \Delta_{ab}(q^2, \mu_R^2, \mu_F^2, z), \quad (6.4)$$

where σ_B is the born level cross section. The scaling variable τ is defined by $\tau = q^2/S$, S is hadronic center of mass energy. For DY, $q^2 = M_{l^+l^-}^2$, the invariant mass of the final state leptons and $q^2 = m_h^2$ for the Higgs boson productions, with m_h being the mass of the Higgs boson. The subscripts a, b in Δ_{ab} and c in f_c collectively denote the type of parton (quark, antiquark and gluon), their flavour etc. The scaling variable x_i is the momentum fraction of the incoming partons. In the CF, $z = q^2/\hat{s}$ is the partonic scaling variable and \hat{s} is the partonic center of mass energy and is related to hadronic S by $\hat{s} = x_1 x_2 S$ which implies $z = \tau/x_1 x_2$. The factorisation scale μ_F results from mass factorisation and the renormalisation scale μ_R from UV renormalisation of the theory. Both σ_B and Δ_{ab}

depend on the renormalisation scale, however their product is independent of the scale if we include Δ_{ab} to all orders in perturbation theory.

The partonic cross section is computable order by order in QCD perturbation theory. Beyond leading order, one encounters UV, soft and collinear divergences at the intermediate stages of the computation. If we use dimensional regularisation to regulate all these divergences, the partonic cross sections depend on the space time dimension $n = 4 + \epsilon$ and the divergences show up as poles in ϵ . The UV divergences are removed by QCD renormalisation constants in modified minimal subtraction (\overline{MS}) scheme. The soft divergences from the gluons and the collinear divergence resulting from final state partons cancel independently when we perform the sum over all the degenerate states. Since the hadronic observables under study are infrared safe, these partonic cross sections are factorisable in terms of collinear singular Altarelli-Parisi [33] kernels Γ_{ab} and finite CFs at an arbitrary factorisation scale μ_F . The factorised formula that relates the collinear finite CFs Δ_{ab} and the parton level subprocesses is given by

$$\frac{1}{z} \hat{\sigma}_{ab}(q^2, z, \epsilon) = \sigma_B(\mu_R^2) \sum_{a'b'} \Gamma_{aa'}^T(z, \mu_F^2, \epsilon) \otimes \left(\frac{1}{z} \Delta_{a'b'}(q^2, \mu_R^2, \mu_F^2, z, \epsilon) \right) \otimes \Gamma_{b'b}(z, \mu_F^2, \epsilon). \quad (6.5)$$

These kernels are then absorbed into the bare pdfs to define collinear finite pdfs. Note that the singular AP kernels do not depend on the type of partonic reaction but depend only on the type of partons in addition to the scaling variable z and scale μ_F . The symbol \otimes refers to convolution, which is defined as in Eq.(2.43).

The partonic cross section in perturbation theory in QCD can be expressed in powers of strong coupling constant a_s :

$$\hat{\sigma}_{ab}(q^2, z, \epsilon) = \sum_{i=0}^{\infty} a_s^i(\mu_R^2) \hat{\sigma}_{ab}^{(i)}(q^2, \mu_R^2, z, \epsilon). \quad (6.6)$$

We restrict ourselves to $\Delta_{q\bar{q}}$ for DY, $\Delta_{b\bar{b}}$ for Higgs boson production in bottom quark an-

annihilation and Δ_{gg} for Higgs boson production in gluon fusion to investigate the structure of NSV terms. We call these CFs collectively by $\Delta_{c\bar{c}}$ with $c\bar{c} = q\bar{q}, b\bar{b}, gg$.

To obtain SV and NSV terms in $\Delta_{c\bar{c}}$ using the mass factorised result given in Eq.(6.5), it is sufficient to keep only those components of AP kernels Γ_{ab} s and of $\hat{\sigma}_{ab}$ that upon convolution gives SV and/or NSV terms. In the mass factorised result, if we express $\Delta_{q\bar{q}}$ for DY in terms of $\hat{\sigma}_{ab}$ s and Γ_{ab} s, we either have convolutions with terms involving *only diagonal terms/channels*, for example $\hat{\sigma}_{q\bar{q}} \otimes \Gamma_{qq} \otimes \Gamma_{\bar{q}\bar{q}}$ or with terms containing *one diagonal and a pair of non-diagonal ones/channels*, for example $\hat{\sigma}_{qg} \otimes \Gamma_{qq} \otimes \Gamma_{gq}$. The former gives SV plus NSV terms upon convolutions while the latter will give *only* beyond the NSV terms. The diagonal Γ_{cc} s also contain convolutions with only diagonal AP splitting functions, P_{cc} , or one diagonal and a pair of non-diagonal AP splitting functions P_{ab} , $a \neq b$. We again drop those terms in diagonal Γ_{cc} s that contain pair of non-diagonal P_{ab} s. This results in Γ_{cc} containing only diagonal P_{cc} s. Similar argument will go through for $\Delta_{b\bar{b}}$ and Δ_{gg} as well. This allows us to write mass factorised result given in Eq.(6.5) in terms of only diagonal terms $\hat{\sigma}_{c\bar{c}}$, $\Delta_{c\bar{c}}$ and AP kernels Γ_{cc} and the sum over ab is dropped.

In summary, since our main focus here is on SV and NSV terms resulting from quark initiated processes for DY and gluon or bottom quark initiated processes for Higgs boson production, we drop contributions from non-diagonal partonic channels in the mass factorised result of $\Delta_{c\bar{c}}$. In addition, gluon-gluon initiated channels which start contributing at NNLO onwards for DY and quark antiquark initiated channels for Higgs boson production are also dropped as they do not contribute to NSV of $\Delta_{c\bar{c}}$. Since our discussion is confined to only diagonal terms or channels, we collectively use the index I here after, where where $I = q, b, g$ respectively refers to Drell-Yan process, Higgs production via bottom quark annihilation and from gluon fusion channel:

$$\begin{aligned}\Delta_I(q^2, \mu_R^2, \mu_F^2, z) &= \Delta_{c\bar{c}}^{\text{sv+nsv}}(q^2, \mu_R^2, \mu_F^2, z). \\ \sigma_I(q^2, \mu_R^2, \mu_F^2, z) &= \sigma_{c\bar{c}}^{\text{sv+nsv}}(q^2, \mu_R^2, \mu_F^2, z).\end{aligned}\tag{6.7}$$

Beyond the leading order, the partonic channels that contribute to $\hat{\sigma}_I^{(i)}$ gets contributions from virtual corrections – denoted in terms of form factor (FF) – and the real emission contributions. In FFs, the entire partonic center of mass energy goes into producing a pair of leptons in DY or Higgs boson in Higgs boson production. While in real emission processes, the initial state energy is shared among all the final state particles. We denote FF of DY by $\hat{\mathcal{F}}^q$ and FF of Higgs boson productions by $\hat{\mathcal{F}}^b, \hat{\mathcal{F}}^g$.

Our next step is to factor out the square of the UV renormalised FF ($Z^I \hat{\mathcal{F}}^I$) from the partonic channels $\hat{\sigma}_I$ and write the resulting normalised real emission contribution as

$$\begin{aligned} \mathcal{S}^I(\hat{a}_s, \mu^2, q^2, z, \epsilon) &= \left(\sigma_B(\mu_R^2)\right)^{-1} \left(Z^I(\hat{a}_s, \mu_R^2, \mu^2, \epsilon)\right)^{-1} |\hat{\mathcal{F}}^I(\hat{a}_s, \mu^2, Q^2, \epsilon)|^{-1} \\ &\quad \times \delta(1-z) \otimes \hat{\sigma}_{c\bar{c}}^{\text{sv+nsv}}(q^2, z, \epsilon) \\ &= C \exp\left(2\Phi^I(\hat{a}_s, \mu^2, q^2, z, \epsilon)\right), \end{aligned} \quad (6.8)$$

where \hat{a}_s is the bare strong coupling constant, $Q^2 = -q^2$ and Z^I is overall renormalisation constant that is required for Higgs boson production from gluon fusion and bottom quark annihilation. Note that \mathcal{S}^I does not depend on μ_R^2 and hence, \mathcal{S}^I is RG invariant. The function \mathcal{S}^I is computable in perturbation theory in powers of a_s and it gets contribution from $c\bar{c}$ initiated processes containing at least one real radiation. The symbol ‘‘C’’ refers to convolution and are defined in Eq.(2.72).

Substituting for $\hat{\sigma}_I$ from Eq.(6.8) in terms of Φ^I in Eq.(6.5) and keeping only diagonal terms in AP kernels, we find

$$\Delta_I(q^2, \mu_R^2, \mu_F^2, z) = C \exp\left(\Psi^I(q^2, \mu_R^2, \mu_F^2, z, \epsilon)\right)\Big|_{\epsilon=0}, \quad (6.9)$$

where Ψ^I is a finite in the limit $\epsilon \rightarrow 0$ and is given by

$$\begin{aligned} \Psi^I(q^2, \mu_R^2, \mu_F^2, z, \epsilon) &= \left(\ln\left(Z^I(\hat{a}_s, \mu^2, \mu_R^2, \epsilon)\right)\right)^2 + \ln\left|\hat{\mathcal{F}}^I(\hat{a}_s, \mu^2, Q^2, \epsilon)\right|^2 \delta(1-z) \\ &\quad + 2\Phi^I(\hat{a}_s, \mu^2, q^2, z, \epsilon) - 2C \ln \Gamma_I(\hat{a}_s, \mu^2, \mu_F^2, z, \epsilon). \end{aligned} \quad (6.10)$$

It contains only the distributions and the logarithms of the form $\ln^i(1 - z)$, $i = 0, 1, \dots$. The all order result given in Eq.(6.9) is the master formula which can be used for obtaining SV+NSV contributions to Δ_I order by order in perturbation theory provided various functions that appear in Eq.(6.10) are known to desired accuracy. In particular, it can predict certain SV and NSV terms to all orders in a_s in terms of lower order terms. In the above formula, we keep the entire FF and overall renormalisation constant as they are proportional to only $\delta(1 - z)$. However, in the functions S^I and $\ln(\Gamma_I)$, we keep only SV and NSV terms.

In the master formula, Eq.(6.9), the form factor for the DY process is the matrix element of vector current $\bar{\psi}_q \gamma_\mu \psi_q$ between on-shell quark states and for the Higgs boson production in gluon fusion (bottom quark annihilation), it is the matrix element of $G_{\mu\nu}^a G^{\mu\nu a}$ ($\bar{\psi}_b \psi_b$) between on-shell gluon (bottom quark) states. Here ψ_c is the c type quark field operator and $G_{\mu\nu a}$ is the gluon field strength operator with a being the $SU(N_c)$ gauge group index in the adjoint representation. These FFs are known in QCD up to third order in perturbation theory, [2, 41, 42, 47, 53, 55, 58, 59, 209–213]. The overall renormalisation constant for the vector current is one to all orders in QCD while for the Higgs boson productions, Z^I s are non-zero. For $I = b$, see [164] and for $I = g$, it is expressed in terms of QCD beta function coefficients to all orders [214].

Perturbative results of FF in renormalisable quantum field theory demonstrate rich structure, in particular, one finds that they satisfy certain differential equations. The simplest one is the RG equation that FFs satisfy, namely $\mu_R^2 \frac{d\hat{\mathcal{F}}^I}{d\mu_R^2} = 0$, using which we can predict the logarithms resulting from the UV sector, i.e., the logarithms of the form $\ln^k(\mu_R^2)$, $k = 1, \dots$ at every order in perturbation theory. In addition, these FFs satisfy Sudakov differential equation [34, 37–39, 148, 215–217] which is used to study their IR structure in terms of certain IR anomalous dimensions such as cusp A^I , collinear B^I and soft f^I anomalous

dimensions. In dimensional regularisation, the equation takes the following form:

$$Q^2 \frac{d}{dQ^2} \ln \hat{\mathcal{F}}^I(\hat{a}_s, Q^2, \mu^2, \epsilon) = \frac{1}{2} \left[K^I\left(\hat{a}_s, \frac{\mu_R^2}{\mu^2}, \epsilon\right) + G^I\left(\hat{a}_s, \frac{Q^2}{\mu_R^2}, \frac{\mu_R^2}{\mu^2}, \epsilon\right) \right], \quad (6.11)$$

where $Q^2 = -q^2$. The unrenormalised FFs contain both UV and IR divergences. UV divergences go away after UV renormalisation. The IR divergences of the FFs can be shown to factorise. The divergence of FFs are such that the factorised IR divergent part is q^2 dependent. The consequence of these facts is that the right hand side of the differential equation can be expressed in terms of two functions K^I and G^I in such a way that K^I accounts for all the poles in ϵ whereas G^I is finite term in the limit $\epsilon \rightarrow 0$. The RG invariance of FFs implies, in the limit $\epsilon \rightarrow 0$,

$$\mu_R^2 \frac{d}{d\mu_R^2} K^I\left(\hat{a}_s, \frac{\mu_R^2}{\mu^2}, \epsilon\right) = -\mu_R^2 \frac{d}{d\mu_R^2} G^I\left(\hat{a}_s, \frac{Q^2}{\mu_R^2}, \frac{\mu_R^2}{\mu^2}, \epsilon\right) = -A^I(a_s(\mu_R^2)). \quad (6.12)$$

The solutions to Eq.(6.12) are given in Sec.[2.3.1]. Substituting these solutions in Eq.(6.11) one can find the structure of FF in terms of IR anomalous dimensions and the process dependent quantities. A more elaborate discussion on the structure of FF can be found in [39]. The IR anomalous dimensions are known to three loops in QCD, see [41, 42, 44, 45, 52, 55, 218, 219] and for beyond three loops, see [47].

The fact that the initial state collinear divergences in parton level cross sections factorises in terms of splitting kernels $\Gamma_{ab}(z, \mu_F^2, \epsilon)$ implies RG evolution equation with respect to the scale μ_F :

$$\mu_F^2 \frac{d}{d\mu_F^2} \Gamma_{ab}(z, \mu_F^2, \epsilon) = \frac{1}{2} \sum_{a'=q, \bar{q}, g} P_{aa'}(z, a_s(\mu_F^2)) \otimes \Gamma_{a'b}(z, \mu_F^2, \epsilon), \quad a, b = q, \bar{q}, g. \quad (6.13)$$

Since we are interested only in diagonal splitting kernels for our analysis, the corresponding splitting functions $P_{cc}(z, \mu_F^2)$ are expanded around $z = 1$ and all those terms that do not contribute to SV+NSV are dropped. The AP splitting functions near $z = 1$ take then

the following form:

$$P_I(z, a_s(\mu_F^2)) = 2B^I(a_s(\mu_F^2)) \delta(1-z) + P'_I(z, a_s(\mu_F^2)), \quad (6.14)$$

where,

$$P'_I(z, a_s(\mu_F^2)) = 2 \left[A^I(a_s(\mu_F^2)) \mathcal{D}_0(z) + C^I(a_s(\mu_F^2)) \ln(1-z) + D^I(a_s(\mu_F^2)) \right] + \mathcal{O}((1-z)). \quad (6.15)$$

The above equation limited to only SV part is identical to the one given in Eq.(2.65). In the rest of this chapter, we drop the terms in P'_I proportional to $\mathcal{O}((1-z))$ for our study. The constants C^I and D^I can be obtained from the the splitting functions P'_I which are known to three loops in QCD [44, 45] (see [44, 45, 204, 220–226] for the lower order ones). Similar to the cusp and the collinear anomalous dimensions, the constants C^I and D^I are also expanded in powers of $a_s(\mu_F^2)$ as:

$$C^I(a_s(\mu_F^2)) = \sum_{i=1}^{\infty} a_s^i(\mu_F^2) C_i^I, \quad D^I(a_s(\mu_F^2)) = \sum_{i=1}^{\infty} a_s^i(\mu_F^2) D_i^I, \quad (6.16)$$

where C_i^I and D_i^I to third order are available in [44, 45]. Our next task is to study the function \mathcal{S}^I defined in Eq.(6.8) order by order in QCD perturbation theory. It should contain right IR divergences to cancel those resulting from FF and AP kernels to give IR finite Δ_I . Recall the IR structure of \mathcal{S}^I in the SV limit that we discussed in previous chapters. It was found that the function \mathcal{S}^I 's demonstrate rich infrared structure in the SV approximation. It provides framework to obtain SV contribution order by order in perturbation theory. We have also seen that it demonstrate an all order result in z -space which allows one to write the integral representation suitable for studying resummation in Mellin N -space. In the following, we proceed along this direction to study NSV contributions in z -space to all orders in perturbation theory and to provide an integral representation that can be used for performing Mellin N -space resummation. Using Eqs.(6.9),(6.10) and the K+G

equation of FFs as given in Eq. (6.11), it is straightforward to show that the functions \mathcal{S}^I equivalently, Φ^I satisfy K+G type of first order differential equation:

$$q^2 \frac{d}{dq^2} \Phi^I = \frac{1}{2} \left[\overline{K}^I \left(\hat{a}_s, \frac{\mu_R^2}{\mu^2}, \epsilon, z \right) + \overline{G}^I \left(\hat{a}_s, \frac{q^2}{\mu_R^2}, \frac{\mu_R^2}{\mu^2}, \epsilon, z \right) \right], \quad (6.17)$$

where the right hand side of the above equation is written as a sum of \overline{K}^I which accounts for all the divergent terms and \overline{G}^I which is a finite function of (z, ϵ) . In addition, Φ^I s satisfy renormalisation group invariance namely $\mu_R^2 \frac{d\Phi^I}{d\mu_R^2} = 0$ which implies

$$\mu_R^2 \frac{d}{d\mu_R^2} \overline{K}^I(a_s(\mu_R^2), z) = -\mu_R^2 \frac{d}{d\mu_R^2} \overline{G}^I(a_s(\mu_R^2), z) = -\overline{A}^I(a_s(\mu_R^2)) \delta(1-z), \quad (6.18)$$

where \overline{A}^I is analogous of cusp anomalous dimension that appears in K+G equation of FFs. Integrating Eq.(6.17) after substituting the solutions of RGs for \overline{K}^I and \overline{G}^I , the solution Φ^I takes the most general form¹

$$\Phi^I(\hat{a}_s, q^2, \mu^2, z, \epsilon) = \sum_{i=1}^{\infty} \hat{a}_s^i \left(\frac{q^2(1-z)^2}{\mu^2 z} \right)^{i \frac{\epsilon}{2}} S_\epsilon^i \left(\frac{i\epsilon}{1-z} \right) \tilde{\phi}_i^I(z, \epsilon). \quad (6.19)$$

where $S_\epsilon = \exp(\frac{\epsilon}{2}[\gamma_E - \ln(4\pi)])$ with γ_E being the Euler Mascheroni constant. The form of the solution given in Eq.(6.19) is inspired by the result for the production of a pair of leptons in quark antiquark channel or Higgs boson in gluon fusion at next to leading order in a_s . The term $\left(\frac{q^2(1-z)^2}{\mu^2 z} \right)^{\frac{\epsilon}{2}}$ in the parenthesis results from two body phase space while $\tilde{\phi}_i^I(z, \epsilon)/(1-z)$ comes from the square of the matrix elements for corresponding amplitudes. In general, the term $q^2(1-z)^2/z$ inside the parenthesis is the hard scale in the problem and it controls the evolution of Φ^I at every order. The function $\tilde{\phi}_i^I(z, \epsilon)$ is regular as $z \rightarrow 0$ but contains poles in ϵ . We have factored out $1/(1-z)$ explicitly so that it generates all the distributions $\mathcal{D}_j(z)$ and $\delta(1-z)$ and NSV terms $\ln^k(1-z)$, $k = 0, \dots$ when combined with the factor $((1-z)^2)^{i\epsilon/2}$ and $\tilde{\phi}_i^I(z, \epsilon)$ at each order in \hat{a}_s . Note that the

¹Note here that the solution (6.19) is different from the one given in Eq.(2.71) in the context of threshold framework. Here, $\tilde{\phi}_i^I(z, \epsilon)$ is a general function which depends on (z, ϵ) , while the latter, $\hat{\phi}_i^I$ contains only SV coefficients.

term $z^{-i\epsilon/2}$ inside the parenthesis does not give distributions $\mathcal{D}_j(z)$ and $\delta(1-z)$, however they can contribute to NSV terms $\ln^j(1-z)$, $j = 0, 1, \dots$ when we expand around $z = 1$. In addition the terms proportional to $(1-z)$ in $\tilde{\phi}_i^I$ near $z = 1$ also give NSV terms for Φ^I . We rewrite the solution of Φ^I in a convenient form which separates SV terms from the NSV in Φ^I . Hence, we decompose Φ^I as $\Phi^I = \Phi_{\text{sv}}^I + \Phi_{\text{nsv}}^I$ in such a way that Φ_{sv}^I contains only SV terms and the remaining Φ_{nsv}^I contains next to soft-virtual terms in the limit $z \rightarrow 1$. The distribution Φ_{sv}^I satisfies K+G equation given in (2.68), also see [39, 40] for details. An all order solution for Φ_{sv}^I in powers of \hat{a}_s in dimensional regularisation is given Eq.(2.71). For convenience, we present it here:

$$\Phi_{\text{sv}}^I(\hat{a}_s, q^2, \mu^2, \epsilon, z) = \sum_{i=1}^{\infty} \hat{a}_s^i \left(\frac{q^2(1-z)^2}{\mu^2} \right)^{i\frac{\epsilon}{2}} S_{\epsilon}^i \left(\frac{i\epsilon}{1-z} \right) \hat{\phi}_i^I(\epsilon), \quad (6.20)$$

where,

$$\hat{\phi}_i^I(\epsilon) = \frac{1}{i\epsilon} \left[\bar{K}_i^I(\epsilon) + \bar{G}_{\text{sv},i}^I(\epsilon) \right], \quad (6.21)$$

the result of which are presented in Eq.(2.74). Similarly the integral representation for Φ_{sv}^I as given in Eq.(2.82) is:

$$\begin{aligned} \Phi_{\text{sv}}^I(\hat{a}_s, q^2, \mu^2, z, \epsilon) &= \left(\frac{1}{1-z} \left\{ \int_{\mu_R^2}^{q^2(1-z)^2} \frac{d\lambda^2}{\lambda^2} A^I(a_s(\lambda^2)) + \bar{G}_{\text{sv}}^I(a_s(q^2(1-z)^2), \epsilon) \right\} \right)_+ \\ &+ \delta(1-z) \sum_{i=1}^{\infty} \hat{a}_s^i \left(\frac{q^2}{\mu^2} \right)^{i\frac{\epsilon}{2}} S_{\epsilon}^i \hat{\phi}_i^I(\epsilon) \\ &+ \left(\frac{1}{1-z} \right)_+ \sum_{i=1}^{\infty} \hat{a}_s^i \left(\frac{\mu_R^2}{\mu^2} \right)^{i\frac{\epsilon}{2}} S_{\epsilon}^i \bar{K}_i^I(\epsilon) \end{aligned} \quad (6.22)$$

Having all the information about the SV coefficients, let us now study in detail the structure of Φ_{nsv}^I using Eq.(6.17). Subtracting out the K+G equation for the SV part Φ_{sv}^I from

(6.17), we find that Φ_{nsv}^I satisfies

$$q^2 \frac{d}{dq^2} \Phi_{\text{nsv}}^I(q^2, z, \epsilon) = \frac{1}{2} \left[G_L^I(\hat{a}_s, \frac{q^2}{\mu_R^2}, \frac{\mu_R^2}{\mu^2}, \epsilon, z) \right], \quad (6.23)$$

where $G_L^I = \bar{G}^I - \bar{G}_{\text{sv}}^I$,

$$G_L^I(\hat{a}_s, \frac{q^2}{\mu_R^2}, \frac{\mu_R^2}{\mu^2}, z, \epsilon) = \sum_{i=1}^{\infty} a_s^i(q^2(1-z)^2) \mathcal{G}_{L,i}^I(z, \epsilon) \quad (6.24)$$

Now integrating Eq.(6.23) we obtain the following structure for Φ_{nsv}^I :

$$\Phi_{\text{nsv}}^I(\hat{a}_s, \mu^2, q^2, z, \epsilon) = \sum_{i=1}^{\infty} \hat{a}_s^i \left(\frac{q^2(1-z)^2}{\mu^2} \right)^{i\frac{\epsilon}{2}} S_{\epsilon}^i \varphi_i^I(z, \epsilon). \quad (6.25)$$

The coefficients $\varphi_i^I(z, \epsilon)$ in Eq.(6.25) can be expressed as a sum of singular and finite part in ϵ given by,

$$\varphi_i^I(z, \epsilon) = \varphi_{s,i}^I(z, \epsilon) + \varphi_{f,i}^I(z, \epsilon), \quad (6.26)$$

where the singular coefficients $\varphi_{s,i}^I$ has an analogous structure to Eq.(2.50) with the substitution:

$$\varphi_{s,i}^I(z, \epsilon) = K_i^I(\epsilon) \Big|_{A^I \rightarrow -L^I(z)}, \quad (6.27)$$

where $L^I(a_s(\mu_R^2), z)$ can be expanded in powers of $a_s(\mu_R^2)$ as

$$L^I(a_s(\mu_R^2), z) = \sum_{i=1}^{\infty} a_s^i(\mu_R^2) L_i^I(z). \quad (6.28)$$

The coefficients $\varphi_{f,i}^I(z, \epsilon)$ are finite in the limit $\epsilon \rightarrow 0$ and can be written in terms of the finite coefficients $\mathcal{G}_{L,i}^I(z, \epsilon)$ as,

$$\begin{aligned} \varphi_{f,1}^I(z, \epsilon) &= \frac{1}{\epsilon} \mathcal{G}_{L,1}^I(z, \epsilon), \\ \varphi_{f,2}^I(z, \epsilon) &= \frac{1}{\epsilon^2} (-\beta_0 \mathcal{G}_{L,1}^I(z, \epsilon)) + \frac{1}{2\epsilon} \mathcal{G}_{L,2}^I(z, \epsilon), \end{aligned}$$

$$\begin{aligned}
\varphi_{f,3}^I(z, \epsilon) &= \frac{1}{\epsilon^3} \left(\frac{4}{3} \beta_0^2 \mathcal{G}_{L,1}^I(z, \epsilon) \right) + \frac{1}{\epsilon^2} \left(-\frac{1}{3} \beta_1 \mathcal{G}_{L,1}^I(z, \epsilon) - \frac{4}{3} \beta_0 \mathcal{G}_{L,2}^I(z, \epsilon) \right) + \frac{1}{3\epsilon} \mathcal{G}_{L,3}^I(z, \epsilon), \\
\varphi_{f,4}^I(z, \epsilon) &= \frac{1}{\epsilon^4} (-2\beta_0^3 \mathcal{G}_{L,1}^I(z, \epsilon)) + \frac{1}{\epsilon^3} \left(\frac{4}{3} \beta_0 \beta_1 \mathcal{G}_{L,1}^I(z, \epsilon) + 3\beta_0^2 \mathcal{G}_{L,2}^I(z, \epsilon) \right) \\
&\quad + \frac{1}{\epsilon^2} \left(-\frac{1}{6} \beta_2 \mathcal{G}_{L,1}^I(z, \epsilon) - \frac{1}{2} \beta_1 \mathcal{G}_{L,2}^I(z, \epsilon) - \frac{3}{2} \beta_0 \mathcal{G}_{L,3}^I(z, \epsilon) \right) + \frac{1}{4\epsilon} \mathcal{G}_{L,4}^I(z, \epsilon), \quad (6.29)
\end{aligned}$$

with

$$\mathcal{G}_{L,i}^I(z, \epsilon) = \chi_{L,i}^I(z) + \sum_{j=1}^{\infty} \epsilon^j \mathcal{G}_{L,i}^{I,j}(z) \quad (6.30)$$

where the coefficients $\chi_{L,i}^I(z)$ are:

$$\begin{aligned}
\chi_{L,1}^I(z) &= 0, \\
\chi_{L,2}^I(z) &= -2\beta_0 \mathcal{G}_{L,1}^{I,1}(z), \\
\chi_{L,3}^I(z) &= -2\beta_1 \mathcal{G}_{L,1}^{I,1}(z) - 2\beta_0 \left(\mathcal{G}_{L,2}^{I,1}(z) + 2\beta_0 \mathcal{G}_{L,1}^{I,2}(z) \right), \\
\chi_{L,4}^I(z) &= -2\beta_2 \mathcal{G}_{L,1}^{I,1}(z) - 2\beta_1 \left(\mathcal{G}_{L,1}^{I,2}(z) + 4\beta_0 \mathcal{G}_{L,2}^{I,1}(z) \right) \\
&\quad - 2\beta_0 \left(\mathcal{G}_{L,1}^{I,3}(z) + 2\beta_0 \mathcal{G}_{L,2}^{I,2}(z) + 4\beta_0^2 \mathcal{G}_{L,3}^{I,1}(z) \right). \quad (6.31)
\end{aligned}$$

The coefficients $\mathcal{G}_{L,i}^{I,j}(z)$ in the above equations are parametrised in terms of $\ln^k(1-z)$, $k = 0, 1, \dots$ and all the terms that vanish as $z \rightarrow 1$ are dropped

$$\mathcal{G}_{L,i}^{I,j}(z) = \sum_{k=0}^{i+j-1} \mathcal{G}_{L,i}^{I,(j,k)} \ln^k(1-z). \quad (6.32)$$

The highest power of the $\ln(1-z)$ at every order depends on the order of the perturbation, namely the power of a_s and also the power of ϵ at each order in a_s . Hence the summation runs from 0 to $i+j-1$.

Decomposing into divergent and finite part, the Φ_{nsv}^I in Eq.(6.25) can be rewrite as:

$$\begin{aligned}
\Phi_{\text{nsv}}^I(\hat{a}_s, \mu^2, q^2, z, \epsilon) &= \int_{\mu_F^2}^{q^2(1-z)^2} \frac{d\lambda^2}{\lambda^2} L^I(a_s(\lambda^2), z) + \varphi_f^I(a_s(q^2(1-z)^2), z, \epsilon) \Big|_{\epsilon=0} \\
&\quad + \varphi_s^I(a_s(\mu_F^2), z, \epsilon), \quad (6.33)
\end{aligned}$$

with,

$$\varphi_a^I(a_s(\lambda^2), z) = \sum_{i=1}^{\infty} \hat{a}_s^i \left(\frac{\lambda^2}{\mu^2} \right)^{i\frac{\epsilon}{2}} S_{\epsilon}^i \varphi_{a,i}^I(z, \epsilon). \quad a = f, s \quad (6.34)$$

Here the first line of (6.33) is finite when $\epsilon \rightarrow 0$ while φ_s^I in the second line is a divergent term.

The fact that Φ_{nsv}^I is RG invariant implies, from Eq.(6.33):

$$\mu_F^2 \frac{d}{d\mu_F^2} \varphi_s^I(a_s(\mu_F^2), z) = L^I(a_s(\mu_F^2), z). \quad (6.35)$$

The fact that Ψ^I in Eq.(6.10) is finite at every order in a_s in the limit $\epsilon \rightarrow 0$ allows us to determine the coefficients L_i^I :

$$L_i^I = C_i^I \ln(1-z) + D_i^I, \quad (6.36)$$

which is nothing but the NSV part of AP splitting function at every order in perturbation theory. This completely fix the divergent piece of Φ_{nsv}^I . These coefficients are related to the cusp A_i^I and collinear B_i^I anomalous dimensions in the following way up to third order:

$$\begin{aligned} D_1^I &= -A_1^I, & D_2^I &= -A_2^I + A_1^I (B_1^I - \beta_0), \\ D_3^I &= -A_3^I - A_1^I (-B_2^I + \beta_1) - A_2^I (-B_1^I + \beta_0), \\ C_1^I &= 0, & C_2^I &= (A_1^I)^2, & C_3^I &= 2A_1^I A_2^I. \end{aligned} \quad (6.37)$$

To see the structure of finite piece φ_f^I , we first expand them in powers of renormalised coupling a_s :

$$\begin{aligned} \varphi_f^I(a_s(q^2(1-z)^2), z) &= \sum_{i=1}^{\infty} a_s^i (q^2(1-z)^2)^i \bar{\varphi}_i^I \\ &= \sum_{i=1}^{\infty} a_s^i (q^2(1-z)^2)^i \sum_{k=0}^i \bar{\varphi}_i^{I,(k)} \ln^k(1-z), \end{aligned} \quad (6.38)$$

where the highest power of $\ln(1-z)$ are in accord with the same in Eq.(6.30). We will discuss more on this structure in subsequent sections. The coefficients $\bar{\varphi}_i^{I,(k)}$ can be expressed in terms of their unrenormalized counter part $\mathcal{G}_{L,i}^{I,(j,k)}$'s as:

$$\begin{aligned}
\bar{\varphi}_1^{I,(k)} &= \mathcal{G}_{L,1}^{I,(1,k)}, \quad k = 0, 1 \\
\bar{\varphi}_2^{I,(k)} &= \left(\frac{1}{2} \mathcal{G}_{L,2}^{I,(1,k)} + \beta_0 \mathcal{G}_{L,1}^{I,(2,k)} \right), \quad k = 0, 1, 2 \\
\bar{\varphi}_3^{I,(k)} &= \left(\frac{1}{3} \mathcal{G}_{L,3}^{I,(1,k)} + \frac{2}{3} \beta_1 \mathcal{G}_{L,1}^{I,(2,k)} + \frac{2}{3} \beta_0 \mathcal{G}_{L,2}^{I,(2,k)} + \frac{4}{3} \beta_0^2 \mathcal{G}_{L,1}^{I,(3,k)} \right), \quad k = 0, 1, 2, 3 \\
\bar{\varphi}_4^{I,(k)} &= \left(\frac{1}{4} \mathcal{G}_{L,4}^{I,(1,k)} + \frac{1}{2} \beta_2 \mathcal{G}_{L,1}^{I,(2,k)} + \frac{1}{2} \beta_1 \mathcal{G}_{L,2}^{I,(2,k)} + \frac{1}{2} \beta_0 \mathcal{G}_{L,3}^{I,(2,k)} + 2\beta_0 \beta_1 \mathcal{G}_{L,1}^{I,(3,k)} + \beta_0^2 \mathcal{G}_{L,2}^{I,(3,k)} \right. \\
&\quad \left. + 2\beta_0^3 \mathcal{G}_{L,1}^{I,(4,k)} \right), \quad k = 0, 1, 2, 3, 4
\end{aligned} \tag{6.39}$$

with $\mathcal{G}_{L,1}^{I,(2,3)}$, $\mathcal{G}_{L,1}^{I,(2,4)}$, $\mathcal{G}_{L,2}^{I,(2,4)}$, $\mathcal{G}_{L,1}^{I,(3,4)}$ are all zero.

Knowing the structure of divergent and finite pieces of Φ_{nsv}^I , let us see how to obtain the unknown coefficients $\mathcal{G}_{L,i}^{I,(j,k)}(z)$. At every order a_s^i , the coefficients $\mathcal{G}_{L,i}^{I,(j,k)}$ for various values of k, j can be determine from Δ_I , $\hat{\mathcal{F}}^I$, Z^I , Φ_{sv}^I , and Γ_I known to order a_s^i expanded in double series expansion of $\epsilon^j \ln^k(1-z)$. In order to do this we use the available information up to two loop level.

The explicit results for $\mathcal{G}_{L,i}^{I,(j,k)}$ for bottom quark annihilation is found to be same as of Drell-Yan till second order in \hat{a}_s , which are given by:

$$\begin{aligned}
\mathcal{G}_{L,1}^{b,(1,0)} &= 4C_F, \quad \mathcal{G}_{L,1}^{b,(2,0)} = 3C_F \zeta_2, \quad \mathcal{G}_{L,1}^{b,(3,0)} = -C_F \left(\frac{3}{2} \zeta_2 + \frac{7}{3} \zeta_3 \right), \\
\mathcal{G}_{L,2}^{b,(1,0)} &= C_A C_F \left(\frac{2804}{27} - \frac{290}{3} \zeta_2 - 56 \zeta_3 \right) + C_F n_f \left(-\frac{656}{27} + \frac{44}{3} \zeta_2 \right) - 64 C_F^2 \zeta_2, \\
\mathcal{G}_{L,2}^{b,(1,1)} &= 20C_F (C_A - C_F), \quad \mathcal{G}_{L,2}^{b,(1,2)} = -8C_F^2,
\end{aligned} \tag{6.40}$$

and for the Higgs boson production in gluon fusion:

$$\begin{aligned}
\mathcal{G}_{L,1}^{g,(1,0)} &= 4C_A, \quad \mathcal{G}_{L,1}^{g,(2,0)} = 3C_A \zeta_2, \quad \mathcal{G}_{L,1}^{g,(3,0)} = -C_A \left(\frac{3}{2} \zeta_2 + \frac{7}{3} \zeta_3 \right), \\
\mathcal{G}_{L,2}^{g,(1,0)} &= C_A^2 \left(\frac{2612}{27} - \frac{482}{3} \zeta_2 - 56 \zeta_3 \right) + C_A n_f \left(-\frac{392}{27} + \frac{44}{3} \zeta_2 \right),
\end{aligned}$$

$$\mathcal{G}_{L,2}^{g,(1,1)} = \frac{4}{3}C_A(C_A - n_f), \quad \mathcal{G}_{L,2}^{g,(1,2)} = -8C_A^2. \quad (6.41)$$

The remaining coefficients up to second order are identically zero. Unlike the SV finite coefficients $\overline{\mathcal{G}}_i^{I,j}$ that appear in Φ_{sv}^I (see Eq.(C.17) and more details in Sec.[2.3.1]), the quark and gluon coefficients $\mathcal{G}_{L,i}^{q,(j,k)}$ do not satisfy maximal non-abelian relation beyond one loop. Recall that $\overline{\mathcal{G}}_i^{I,j}$ satisfy $\overline{\mathcal{G}}_i^{q,j} = (C_F/C_A)\overline{\mathcal{G}}_i^{g,j}$, confirmed up to third order in a_s as shown in [39, 40].

Third order contributions to Δ_I for DY became available very recently in [16] and for the Higgs boson productions in gluon fusion as well as in bottom quark annihilation the third order results were presented in [4, 227, 228]. The analytical results for FFs, over all renormalisation constants, the functions Φ_{sv}^I and Γ_I are all available up to third order in the literature. Using these results, we can in principle extract the relevant coefficients $\mathcal{G}_{L,i}^{q,(j,k)}$ to third order. In the absence of analytical results for second order corrections to Δ_q for positive powers of ϵ , we can not determine the coefficients $\mathcal{G}_{L,i}^{q,(j,k)}$ at the third order. However, the combination of these coefficients namely φ_f^I can be extracted for $I = q$ (DY) and $I = b$ ($b\bar{b}H$) and $I = g$ (ggH) up to third order using the available results to third order. We find for DY:

$$\begin{aligned} \bar{\varphi}_1^{q,(0)} &= 4C_F, \quad \bar{\varphi}_1^{q,(1)} = 0, \\ \bar{\varphi}_2^{q,(0)} &= C_F C_A \left(\frac{1402}{27} - 28\zeta_3 - \frac{112}{3}\zeta_2 \right) + C_F^2 (-32\zeta_2) + n_f C_F \left(-\frac{328}{27} + \frac{16}{3}\zeta_2 \right), \\ \bar{\varphi}_2^{q,(1)} &= 10C_F C_A - 10C_F^2, \quad \bar{\varphi}_{q,2}^{(2)} = -4C_F^2, \\ \bar{\varphi}_3^{q,(0)} &= C_F C_A^2 \left(\frac{727211}{729} + 192\zeta_5 - \frac{29876}{27}\zeta_3 - \frac{82868}{81}\zeta_2 + \frac{176}{3}\zeta_2\zeta_3 + 120\zeta_2^2 \right) \\ &\quad + C_F^2 C_A \left(-\frac{5143}{27} - \frac{2180}{9}\zeta_3 - \frac{11584}{27}\zeta_2 + \frac{2272}{15}\zeta_2^2 \right) + C_F^3 \left(23 + 48\zeta_3 \right. \\ &\quad \left. - \frac{32}{3}\zeta_2 - \frac{448}{15}\zeta_2^2 \right) + n_f C_F C_A \left(-\frac{155902}{729} + \frac{1292}{9}\zeta_3 + \frac{26312}{81}\zeta_2 - \frac{368}{15}\zeta_2^2 \right) \\ &\quad + n_f C_F^2 \left(-\frac{1309}{9} + \frac{496}{3}\zeta_3 + \frac{2536}{27}\zeta_2 + \frac{32}{5}\zeta_2^2 \right) + n_f^2 C_F \left(\frac{12656}{729} \right. \\ &\quad \left. - \frac{160}{27}\zeta_3 - \frac{704}{27}\zeta_2 \right), \end{aligned}$$

$$\begin{aligned}
\bar{\varphi}_3^{q,(1)} &= C_F C_A^2 \left(\frac{244}{9} + 24\zeta_3 - \frac{8}{9}\zeta_2 \right) + C_F^2 C_A \left(-\frac{18436}{81} + \frac{544}{3}\zeta_3 + \frac{964}{9}\zeta_2 \right) \\
&\quad + C_F^3 \left(-\frac{64}{3} - 64\zeta_3 + \frac{80}{3}\zeta_2 \right) + n_f C_F C_A \left(-\frac{256}{9} - \frac{28}{9}\zeta_2 \right) \\
&\quad + n_f C_F^2 \left(\frac{3952}{81} - \frac{160}{9}\zeta_2 \right), \\
\bar{\varphi}_3^{q,(2)} &= C_F C_A^2 \left(34 - \frac{10}{3}\zeta_2 \right) + C_F^2 C_A \left(-96 + \frac{52}{3}\zeta_2 \right) + C_F^3 \left(\frac{16}{3} \right) \\
&\quad + n_f C_F C_A \left(-\frac{10}{3} \right) + n_f C_F^2 \left(\frac{40}{3} \right), \\
\bar{\varphi}_3^{q,(3)} &= C_F^2 C_A \left(-\frac{176}{27} \right) + n_f C_F^2 \left(\frac{32}{27} \right), \tag{6.42}
\end{aligned}$$

and for the Higgs boson production:

$$\begin{aligned}
\bar{\varphi}_1^{g,(0)} &= 4C_A, \quad \bar{\varphi}_1^{g,(1)} = 0, \\
\bar{\varphi}_2^{g,(0)} &= C_A^2 \left(\frac{1306}{27} - 28\zeta_3 - \frac{208}{3}\zeta_2 \right) + n_f C_A \left(-\frac{196}{27} + \frac{16}{3}\zeta_2 \right), \\
\bar{\varphi}_2^{g,(1)} &= C_A^2 \left(\frac{2}{3} \right) + n_f C_A \left(-\frac{2}{3} \right), \quad \bar{\varphi}_{g,2}^{g,(2)} = -4C_A^2, \\
\bar{\varphi}_3^{g,(0)} &= C_A^3 \left(\frac{563231}{729} + 192\zeta_5 - \frac{34292}{27}\zeta_3 - \frac{113600}{81}\zeta_2 + \frac{176}{3}\zeta_2\zeta_3 + \frac{3488}{15}\zeta_2^2 \right) \\
&\quad + n_f C_A^2 \left(-\frac{117778}{729} + \frac{1888}{9}\zeta_3 + \frac{26780}{81}\zeta_2 - \frac{232}{15}\zeta_2^2 \right) \\
&\quad + n_f C_F C_A \left(-\frac{2653}{27} + \frac{616}{9}\zeta_3 + \frac{40}{3}\zeta_2 + \frac{32}{5}\zeta_2^2 \right) + n_f^2 C_A \left(\frac{1568}{729} - \frac{160}{27}\zeta_3 - \frac{152}{9}\zeta_2 \right), \\
\bar{\varphi}_3^{g,(1)} &= C_A^3 \left(-\frac{18988}{81} + \frac{448}{3}\zeta_3 + \frac{1280}{9}\zeta_2 \right) + n_f C_A^2 \left(\frac{1528}{81} - 8\zeta_3 - \frac{248}{9}\zeta_2 \right) \\
&\quad + n_f C_F C_A \left(4 - \frac{8}{3}\zeta_2 \right) + n_f^2 C_A \left(\frac{56}{27} \right), \\
\bar{\varphi}_3^{g,(2)} &= C_A^3 \left(-\frac{1432}{27} + \frac{40}{3}\zeta_2 \right) + n_f C_A^2 \left(\frac{164}{27} + \frac{2}{3}\zeta_2 \right) + n_f^2 C_A \left(\frac{8}{27} \right), \\
\bar{\varphi}_3^{g,(3)} &= C_A^3 \left(-\frac{176}{27} \right) + n_f C_A^2 \left(\frac{32}{27} \right). \tag{6.43}
\end{aligned}$$

While the NSV function Φ_{nsv}^l for quarks and gluon are not related, they are found to be universal up to second order in the sense that they do not depend on the hard process. For example, to second order in a_s , Φ_{nsv}^q of DY is found to be identical to that of Higgs boson production in bottom quark annihilation [130]. In addition, we find that they agree with that of Graviton (G) production in quark annihilation processes [229–234]. In terms of

$\bar{\varphi}_i^{q,(k)}$ it translates to

$$\bar{\varphi}_i^{q,(k)} \Big|_{q+\bar{q} \rightarrow l+l'+X} = \bar{\varphi}_i^{q,(k)} \Big|_{b+\bar{b} \rightarrow H+X} = \bar{\varphi}_i^{q,(k)} \Big|_{q+\bar{q} \rightarrow G+X} \quad i = 1, 2, k = 0, i \quad (6.44)$$

Similarly, to second order in a_s , Φ_{NSV}^g from Higgs boson production in gluon fusion is found to be identical to that of graviton production in gluon fusion channel and pseudo scalar Higgs boson production [235–240] in gluon fusion. That is,

$$\bar{\varphi}_i^{g,(k)} \Big|_{g+g \rightarrow H+X} = \bar{\varphi}_i^{g,(k)} \Big|_{g+g \rightarrow A+X} = \bar{\varphi}_i^{g,(k)} \Big|_{g+g \rightarrow G+X} \quad i = 1, 2, k = 0, i \quad (6.45)$$

However, the universality breaks at third order, namely, we find that the $\bar{\varphi}_3^{b,(k)}$ for $k = 0, 1$ differs from that of DY production while for $k = 2, 3$ they agree.

$$\begin{aligned} \bar{\varphi}_3^{b,(0)} &= \bar{\varphi}_3^{q,(0)} - 16C_A C_F (C_A - 2C_F), \\ \bar{\varphi}_3^{b,(1)} &= \bar{\varphi}_3^{q,(1)} + 8C_A C_F (C_A - 2C_F), \\ \bar{\varphi}_3^{b,(k)} &= \bar{\varphi}_3^{q,(k)} \quad k = 2, 3. \end{aligned} \quad (6.46)$$

The origin of this violation for $k = 0, 1$ at third order, which has been evaluated using the state-of-art results [4, 16, 227, 228], needs to be understood within the framework of factorisation.

6.3 All order predictions for Δ_I

In this section, we discuss the predictive power of the master formula (6.9). In other words, given $Z^I, \hat{\mathcal{F}}^I, \Phi^I$ and the Γ_I up to a certain order in perturbation theory, we show that the master formula can predict certain SV and NSV terms to all orders in perturbation theory. The partonic coefficient function Δ_I can be expanded order by order in

perturbation theory in powers of $a_s(\mu_R^2)$ as

$$\Delta_I(q^2, \mu_R^2, \mu_F^2, z) = \sum_{i=0}^{\infty} a_s^i(\mu_R^2) \Delta_I^{(i)}(q^2, \mu_R^2, \mu_F^2, z), \quad (6.47)$$

where the coefficient $\Delta_I^{(i)}$ can be obtained by first expanding the exponential given in (6.10) in powers of $a_s(\mu_R^2)$ and then performing all the resulting convolutions in z -space. Note that $\Delta_I^{(0)} = \delta(1-z)$. We have dropped all those terms that are of order $\mathcal{O}((1-z)^\alpha)$, $\alpha > 0$. Finally, we write the following decomposition ,

$$\Delta_I^{(i)}(q^2, \mu_R^2, \mu_F^2, z) = \Delta_I^{\text{sv},(i)}(q^2, \mu_R^2, \mu_F^2, z) + \Delta_I^{\text{nsv},(i)}(q^2, \mu_R^2, \mu_F^2, z). \quad (6.48)$$

Here $\Delta_I^{\text{sv},(i)}$ contains only SV terms, such as the distributions $\mathcal{D}_i(z)$, ($i = 0, 1, \dots$) and $\delta(1-z)$ and next-to-SV terms, i.e., the logarithms $\ln^i(1-z)$, ($i = 0, 1, \dots$) are embedded within $\Delta_I^{\text{nsv},(i)}$. Now given the distribution function Φ^I , upto a certain order in a_s , there are several SV and NSV logarithms which can be predicted to all orders in a_s . For example, we observe that if Ψ^I is known at leading order in a_s , we can predict all the leading distributions $\mathcal{D}_i(z)$ and leading NSV terms $\ln^i(1-z)$ to all orders in a_s . In the following, we elaborate on this by comparing our predictions with the available N³LO results and also predict N⁴LO and some higher order results for few observables.

Given Ψ^I at order a_s , by expanding the master formula given in Eq.(6.9) in powers of strong coupling constant, we obtain the leading SV terms such as $(\mathcal{D}_3(z), \mathcal{D}_2(z))$, $(\mathcal{D}_5(z), \mathcal{D}_4(z)), \dots, (\mathcal{D}_{2i-1}(z), \mathcal{D}_{2i-2}(z))$ and the leading NSV terms $\ln^3(1-z), \ln^5(1-z), \dots, \ln^{2i-1}(1-z)$ at $a_s^2, a_s^3, \dots, a_s^i$ respectively for all i . Since C_1^I is identically zero, $\ln^{2i}(1-z)$ terms do not contribute for all i . Hence we predict,

$$\begin{aligned} \Delta_I^{\text{nsv}} &= a_s \Delta_I^{\text{nsv},(1)} + a_s^2 \left[-128 C_R^2 L_z^3 + \mathcal{O}(L_z^2) \right] + a_s^3 \left[-512 C_R^3 L_z^5 + \mathcal{O}(L_z^4) \right] \\ &+ a_s^4 \left[-\frac{4096}{3} C_R^4 L_z^7 + \mathcal{O}(L_z^6) \right] + \mathcal{O}(a_s^5) \end{aligned} \quad (6.49)$$

Here we write $\ln^i(1-z) \equiv L_z^i$ for brevity. Also $C_R = C_F$ for $I = \{q, b\}$ i.e. for DY and Higgs

production through bottom quark annihilation. And for Higgs production through gluon fusion i.e. $I = g$, we have $C_R = C_A$. Thus with the knowledge of one loop anomalous dimensions $\{C_1^I, D_1^I, A_1^I, B_1^I, f_1^I\}$ and one-loop $\bar{\varphi}_1^{I,(k)}$, we predicted the above NSV logarithms and the known NNLO, N³LO results [4, 227, 228] for DY and Higgs boson productions confirm this.

Similarly from Ψ^I to order a_s^2 , we can predict the tower consisting of $(\mathcal{D}_3, \mathcal{D}_2)$, $(\mathcal{D}_5, \mathcal{D}_4)$, $\dots, (\mathcal{D}_{2i-3}(z), \mathcal{D}_{2i-4}(z))$ and of $L_z^4, L_z^6, \dots, L_z^{2i-2}$ at $a_s^3, a_s^4, \dots, a_s^i$ respectively for all i . For the DY and Higgs production in bottom quark annihilation, our prediction reads as:

$$\begin{aligned} \Delta_{q(b)}^{\text{nsv}} = & a_s \Delta_{q(b)}^{\text{nsv,(1)}} + a_s^2 \Delta_{q(b)}^{\text{nsv,(2)}} + a_s^3 \left[-512 C_F^3 L_z^5 + \left(\frac{7040}{9} C_F^2 C_A - \frac{1280}{9} n_f C_F^2 \right. \right. \\ & \left. \left. + 1728 C_F^3 \right) L_z^4 + \mathcal{O}(L_z^3) \right] + a_s^4 \left[-\frac{4096}{3} C_F^4 L_z^7 + \left(\frac{39424}{9} C_F^3 C_A + \frac{19712}{3} C_F^4 \right. \right. \\ & \left. \left. - \frac{7168}{9} n_f C_F^3 \right) L_z^6 + \mathcal{O}(L_z^5) \right] + \mathcal{O}(a_s^5) \end{aligned} \quad (6.50)$$

and for the Higgs production in gluon fusion,

$$\begin{aligned} \Delta_g^{\text{nsv}} = & a_s \Delta_g^{\text{nsv,(1)}} + a_s^2 \Delta_g^{\text{nsv,(2)}} + a_s^3 \left[-512 C_A^3 L_z^5 + \left(\frac{22592}{9} C_A^3 - \frac{1280}{9} n_f C_A^2 \right) L_z^4 \right. \\ & \left. + \mathcal{O}(L_z^3) \right] + a_s^4 \left[-\frac{4096}{3} C_A^4 L_z^7 + \left(\frac{98560}{9} C_A^4 - \frac{7168}{9} n_f C_A^3 \right) L_z^6 + \mathcal{O}(L_z^5) \right] + \mathcal{O}(a_s^5) \end{aligned} \quad (6.51)$$

Our predictions for $L_z^i, i = 5, 4$ agree with the those obtained by explicit computation [4, 241]. For the comparison purpose, we have presented the logarithms only upto order a_s^4 , however, the master formula can predict such logarithms to all orders in a_s . Thanks to [4, 16, 241], the third order results are now available for all these processes allowing us to determine φ_f^I for $I = q, b, g$ till third order. Using this, we can predict a tower of $(\mathcal{D}_3(z), \mathcal{D}_2(z))$, $(\mathcal{D}_5(z), \mathcal{D}_4(z)) \dots, (\mathcal{D}_{2i-5}(z), \mathcal{D}_{2i-6}(z))$ and of L_z^5, \dots, L_z^{2i-3} at $a_s^4, a_s^5, \dots, a_s^i$ respectively for all i . In the following for the illustrative purpose, we have presented the NSV terms L_z till seventh order in a_s . For DY, we find

$$\Delta_q^{\text{nsv}} = a_s \Delta_q^{\text{nsv,(1)}} + a_s^2 \Delta_q^{\text{nsv,(2)}} + a_s^3 \Delta_q^{\text{nsv,(3)}} + a_s^4 \left[\left\{ -\frac{4096}{3} C_F^4 \right\} L_z^7 + \left\{ \frac{39424}{9} C_F^3 C_A + \frac{19712}{3} C_F^4 \right\} \right]$$

$$\begin{aligned}
& -\frac{7168}{9}n_f C_F^3 \Big\} L_z^6 + \left\{ -\frac{123904}{27}C_F^2 C_A^2 - \left(\frac{805376}{27} - 3072\zeta_2\right)C_F^3 C_A + \left(9088 + 20480\zeta_2\right)C_F^4 \right. \\
& + \left. \frac{45056}{27}n_f C_F^2 C_A + \frac{139520}{27}n_f C_F^3 - \frac{4096}{27}n_f^2 C_F^2 \right\} L_z^5 + \mathcal{O}(L_z^4) \Big] \\
& + a_s^5 \left[\left\{ -\frac{8192}{3}C_F^5 \right\} L_z^9 + \left\{ \frac{51200}{3}C_F^5 - \frac{8192}{3}C_F^4 n_f + \frac{45056}{3}C_F^4 C_A \right\} L_z^8 \right. \\
& + \left. \left\{ \left(\frac{72704}{3} + \frac{229376}{3}\zeta_2\right)C_F^5 - \left(\frac{1120256}{9} - \frac{32768}{3}\zeta_2\right)C_F^4 C_A - \frac{81920}{81}C_F^3 n_f^2 \right. \right. \\
& + \left. \left. \frac{194560}{9}C_F^4 n_f + \frac{901120}{81}C_F^3 C_A n_f - \frac{2478080}{81}C_F^3 C_A^2 \right\} L_z^7 + \mathcal{O}(L_z^6) \right] \\
& + a_s^6 \left[\left\{ -\frac{65536}{15}C_F^6 \right\} L_z^{11} + \left\{ \frac{167936}{5}C_F^6 - \frac{180224}{27}C_F^5 n_f + \frac{991232}{27}C_F^5 C_A \right\} L_z^{10} \right. \\
& + \left. \left\{ \left(\frac{145408}{3} + 196608\zeta_2\right)C_F^6 + \frac{5054464}{81}C_F^5 n_f - \frac{327680}{81}C_F^4 n_f^2 - \left(\frac{28997632}{81} \right. \right. \right. \\
& - \left. \left. \frac{81920}{3}\zeta_2\right)C_F^5 C_A + \frac{3604480}{81}C_F^4 C_A n_f - \frac{9912320}{81}C_F^4 C_A^2 \right\} L_z^9 + \mathcal{O}(L_z^8) \right] \\
& + a_s^7 \left[\left\{ -\frac{262144}{45}C_F^7 \right\} L_z^{13} + \left\{ \frac{2392064}{45}C_F^7 - \frac{1703936}{135}C_F^6 n_f + \frac{9371648}{135}C_F^6 C_A \right\} L_z^{12} \right. \\
& + \left. \left\{ \left(\frac{1163264}{15} + \frac{5767168}{15}\zeta_2\right)C_F^7 + \frac{55115776}{405}C_F^6 n_f - \left(\frac{315080704}{405} - \frac{262144}{5}\zeta_2\right)C_F^6 C_A \right. \right. \\
& - \left. \left. \frac{917504}{81}C_F^5 n_f^2 + \frac{10092544}{81}C_F^5 C_A n_f - \frac{27754496}{81}C_F^5 C_A^2 \right\} L_z^{11} + \mathcal{O}(L_z^{10}) \right] + \mathcal{O}(a_s^8), \quad (6.52)
\end{aligned}$$

for the Higgs production in bottom quark annihilation,

$$\begin{aligned}
\Delta_b^{\text{nsv}} &= a_s \Delta_b^{\text{nsv},(1)} + a_s^2 \Delta_b^{\text{nsv},(2)} + a_s^3 \Delta_b^{\text{nsv},(3)} + a_s^4 \left[\Delta_q^{\text{nsv},(4)} - 6144C_F^4 L_z^5 + \mathcal{O}(L_z^4) \right] \\
&+ a_s^5 \left[\Delta_q^{\text{nsv},(5)} - 16384C_F^5 L_z^7 + \mathcal{O}(L_z^6) \right] + a_s^6 \left[\Delta_q^{\text{nsv},(6)} - 32768C_F^6 L_z^9 + \mathcal{O}(L_z^8) \right] \\
&+ a_s^7 \left[\Delta_q^{\text{nsv},(7)} - \frac{262144}{5}C_F^7 L_z^{11} + \mathcal{O}(L_z^{10}) \right] + \mathcal{O}(a_s^8), \quad (6.53)
\end{aligned}$$

and for the Higgs production in gluon fusion,

$$\begin{aligned}
\Delta_g^{\text{nsv}} &= a_s \Delta_g^{\text{nsv},(1)} + a_s^2 \Delta_g^{\text{nsv},(2)} + a_s^3 \Delta_g^{\text{nsv},(3)} \\
&+ a_s^4 \left[\left\{ -\frac{4096}{3}C_A^4 \right\} L_z^7 + \left\{ \frac{98560}{9}C_A^4 - \frac{7168}{9}n_f C_A^3 \right\} L_z^6 + \left\{ \left(-\frac{298240}{9} + 23552\zeta_2\right)C_A^4 \right. \right. \\
&+ \left. \left. \frac{174208}{27}n_f C_A^3 - \frac{4096}{27}n_f^2 C_A^2 \right\} L_z^5 + \mathcal{O}(L_z^4) \right] + a_s^5 \left[\left\{ -\frac{8192}{3}C_A^5 \right\} L_z^9 + \left\{ \frac{96256}{3}C_A^5 \right. \right. \\
&- \left. \left. \frac{8192}{3}C_A^4 n_f \right\} L_z^8 + \left\{ \left(-\frac{12283904}{81} + \frac{262144}{3}\zeta_2\right)C_A^5 + \frac{2569216}{81}C_A^4 n_f - \frac{81920}{81}n_f^2 C_A^3 \right\} L_z^7 \right. \\
&+ \left. \mathcal{O}(L_z^6) \right] + a_s^6 \left[\left\{ -\frac{65536}{15}C_A^6 \right\} L_z^{11} + \left\{ \frac{9490432}{135}C_A^6 - \frac{180224}{27}C_A^5 n_f \right\} L_z^{10} + \left\{ \left(\frac{671744}{3}\zeta_2 \right. \right. \right. \\
&- \left. \left. \frac{4261888}{9}\right)C_A^6 + \frac{8493056}{81}C_A^5 n_f - \frac{327680}{81}n_f^2 C_A^4 \right\} L_z^9 + \mathcal{O}(L_z^8) \right]
\end{aligned}$$

$$\begin{aligned}
& + a_s^7 \left[\left\{ -\frac{262144}{45} C_A^7 \right\} L_z^{13} + \left\{ \frac{3309568}{27} C_A^7 - \frac{1703936}{135} C_A^6 n_f \right\} L_z^{12} + \left\{ \left(-\frac{449429504}{405} \right. \right. \right. \\
& \left. \left. \left. + \frac{1310720}{3} \zeta_2 \right) C_A^7 + \frac{11583488}{45} C_A^6 n_f - \frac{917504}{81} n_f^2 C_A^5 \right\} L_z^{11} + \mathcal{O}(L_z^{10}) \right] + \mathcal{O}(a_s^8). \quad (6.54)
\end{aligned}$$

Our predictions for L_z^7, L_z^6 and L_z^5 terms at fourth order for Δ_I agree with those of [8, 52, 204, 205] predicted using physical evolution equations. As can be seen from Eqs.(6.52-6.54), given the third order results, our master formula can predict three highest logarithms for fifth order onwards in a_s . For instance at a_s^5 , we can predict L_z^9, L^8, L_z^7 . Generalising this, if we know Ψ^I up to n th order, we can predict $(\mathcal{D}_{2i-2n+1}(z), \mathcal{D}_{2i-2n}(z))$ and L_z^{2i-n} at every order in a_s^i for all i . Table[6.1] is devoted to summarise the predictions from the master formula for any given order of a_s . The explicit structure of Δ_I till four loop are presented in the ancillary files submitted with the arXiv submission [198]. The predictive power of the master formula to all orders in a_s in terms of distributions and $\ln(1-z)$ terms in Δ_I is due to the all order structure of the exponent Ψ^I and this can be further exploited to resum them. We devote a separate section for this.

GIVEN				PREDICTIONS		
$\Psi^{I,(1)}$	$\Psi^{I,(2)}$	$\Psi^{I,(3)}$	$\Psi^{I,(n)}$	$\Delta_I^{(2)}$	$\Delta_I^{(3)}$	$\Delta_I^{(i)}$
$\mathcal{D}_0, \mathcal{D}_1, \delta$ L_z^1, L_z^0				$\mathcal{D}_3, \mathcal{D}_2$ L_z^3	$\mathcal{D}_5, \mathcal{D}_4$ L_z^5	$\mathcal{D}_{(2i-1)}, \mathcal{D}_{(2i-2)}$ $L_z^{(2i-1)}$
	$\mathcal{D}_0, \mathcal{D}_1, \delta$ L_z^2, L_z^1, L_z^0				$\mathcal{D}_3, \mathcal{D}_2$ L_z^4	$\mathcal{D}_{(2i-3)}, \mathcal{D}_{(2i-4)}$ $L_z^{(2i-2)}$
		$\mathcal{D}_0, \mathcal{D}_1, \delta$ L_z^3, \dots, L_z^0				$\mathcal{D}_{(2i-5)}, \mathcal{D}_{(2i-6)}$ $L_z^{(2i-3)}$
			$\mathcal{D}_0, \mathcal{D}_1, \delta$ L_z^n, \dots, L_z^0			$\mathcal{D}_{(2i-(2n-1))}, \mathcal{D}_{(2i-2n)}$ $L_z^{(2i-n)}$

Table 6.1: Towers of Distributions ($\mathcal{D}_i \equiv \mathcal{D}_i(z)$) and NSV logarithms ($L_z^i \equiv \ln^i(1-z)$) that can be predicted for Δ_I using Eq.(6.9). Here $\Psi^{I,(i)}$ and $\Delta_I^{(i)}$ denotes Ψ^I and Δ_I at order a_s^i respectively.

So far, we have compared our higher predictions for SV and NSV logarithms obtained using the lower order results against those available in the literature and found that our all order master formula correctly predicts these logarithms. For example, from the knowl-

	$gg \rightarrow H$			Drell-Yan (DY)		$b\bar{b} \rightarrow H$	
C_A^3	$\frac{-111008}{27} + 3584\zeta_2$	$\frac{-110656}{27} + 3584\zeta_2 + \eta_1$	C_F^3	$2272 + 3072\zeta_2$	$2272 + 3072\zeta_2$	$736 + 3072\zeta_2$	$736 + 3072\zeta_2$
$C_A^2 n_f$	$\frac{6560}{9}$	$\frac{19616}{27} + \eta_2$	$C_F^2 n_f$	$\frac{19456}{27}$	$\frac{6464}{9} + \eta_3$	$\frac{19456}{27}$	$\frac{6464}{9} + \eta_3$
$C_A n_f^2$	$\frac{-256}{27}$	$\frac{-256}{27}$	$C_A C_F^2$	$\frac{-111904}{27} + 512\zeta_2$	$\frac{-37184}{9} + 512\zeta_2 + \eta_4$	$\frac{-111904}{27} + 512\zeta_2$	$\frac{-37184}{9} + 512\zeta_2 + \eta_4$
			$C_F n_f^2$	$\frac{-256}{27}$	$\frac{-256}{27}$	$\frac{-256}{27}$	$\frac{-256}{27}$
			$C_A C_F n_f$	$\frac{2816}{27}$	$\frac{2816}{27}$	$\frac{2816}{27}$	$\frac{2816}{27}$
			$C_A^2 C_F$	$\frac{-7744}{27}$	$\frac{-7744}{27}$	$\frac{-7744}{27}$	$\frac{-7744}{27}$

Table 6.2: Comparison of $\ln^3(1-z)$ coefficients at the third order against exact results. The left column stands for the exact results and the right column gives the respective contributions when Ψ^l is taken till two loop.

edge of the second order result for Ψ^l , we can correctly predict $\ln^5(1-z)$ and $\ln^4(1-z)$ terms at third order. Even though this second order information is not sufficient to predict the lower order NSV logarithms, namely $\ln^k(1-z)$ for $k = 3, 2, 1, 0$ at α_s^3 level, we observe that our predictions for these logarithms agree with the known results for several color factors. In Table [6.2] we compare our predictions for $\ln^3(1-z)$ terms at the third order, which are obtained using Ψ^l considered till α_s^2 , against the known results for the DY production, Higgs productions in bottom quark annihilation and gluon fusion. As can be seen from the table, the master formula correctly predicts the results for many color factors. For instance, for DY, the predictions for color factors $C_F^3, C_F n_f^2, C_A C_F n_f$ and $C_A^2 C_F$ are matching with the exact results. However for the other color factors, certain third order information are required, which is represented as η_i which when taken into account will reproduce the exact $\ln^3(1-z)$ terms at third order.

6.4 More on the z -space NSV Solution $\Phi_{\text{NSV}}^{\text{I}}$

6.4.1 On the form of the solution

In this section, we discuss in detail the peculiar structure of SV and NSV solutions given in Eq.(6.20) and Eq.(6.25) respectively, that satisfy the K+G equation (6.17). Both of them contain divergent as well as finite terms at every order. For example, the SV part of the solution, $\Phi_{\text{sv}}^{\text{I}}$, contains the right soft and collinear divergences proportional to distributions $\delta(1-z)$ and $\mathcal{D}_0(z)$ to cancel those from the FF entirely and from the AP kernels partially and the z dependent finite terms to correctly reproduce all the distributions in the SV part of CFs Δ_I . The NSV part, $\Phi_{\text{NSV}}^{\text{I}}$, removes the remaining collinear divergences of the AP kernels. The finite part of it when combined with SV counterpart of $\Phi_{\text{sv}}^{\text{I}}$ contributes to next-to-SV terms to CFs Δ_I . As we mentioned in the previous section, the z dependence of the solution is inspired from the structure of various contributions that constitute the next to leading order contributions to variety of inclusive reactions, namely production of a pair of leptons in quark anti-quark annihilation, a Higgs boson in gluon fusion or in bottom quark annihilation at hadron colliders. In addition, the renormalisation group equation, Eq.(6.35), brings in additional z dependent logarithmic structure through the anomalous dimensions $C^I(a_s)$ and $D^I(a_s)$.

Note that the solution given in (6.19) is organised in such a way that the term $\Phi_{\text{sv}}^{\text{I}}$ contains only leading contributions namely the distributions such as $\delta(1-z)$ and $\mathcal{D}_j(z)$, the so called SV terms and the term $\Phi_{\text{NSV}}^{\text{I}}$, the sub-leading terms, i.e., the NSV logarithms $\ln^k(1-z)$. Even though $\Phi_{\text{sv}}^{\text{I}}$ does not contain next-to-SV terms, they contribute to next-to-SV terms to Δ_I , when the exponential is expanded in powers of a_s . Not only do distributions result from the convolutions of two or more distributions, they also give next-to-SV logarithms. In addition, the convolution of distributions with next-to-SV terms in turn give pure NSV logarithms. Hence, the leading solution $\Phi_{\text{sv}}^{\text{I}}$ plays an important role for generating next-

to-SV terms for the CFs Δ_I at every order in perturbation theory.

The solution Φ_{sv}^I (see Eq.(6.20)) at every order in \hat{a}_s is found to factorise into z dependent piece, $((1-z)^m)^{i\epsilon/2} \frac{1}{1-z}$ with $m = 2$, and the z independent coefficients $\hat{\phi}_i^I(\epsilon)$. The peculiarity of this solution is that we can retain the independence of $\hat{\phi}_i^I(\epsilon)$ with respect to the variable z at every order in \hat{a}_s , thanks to presence of the factor $((1-z)^m)^{i\epsilon/2} \frac{1}{1-z}$ which not only ensures the finiteness of SV part of CFs Δ_I but also gives right distributions at every order. The factor m takes the value $m = 2$ for DY and Higgs productions as observed in Eq.(6.20) and the origin of it can be traced to the number of external legs that require mass factorisation [40]. It was observed in [40, 242] that the parameter m takes the value $m = 1$ for the SV part of the solutions to CFs of structure functions of Deep Inelastic Scattering (DIS) and of Semi-Inclusive Annihilation (SIA) of hadron production and the reason is that only one of the external legs requires mass factorisation. The uniqueness of the structure of $\hat{\phi}_i^I$ may be attributed to the fact that the entire z dependence of the solution factorises at every order as $((1-z)^m)^{i\epsilon/2} \frac{1}{1-z}$ leaving $\hat{\phi}_i^I(\epsilon)$ z -independent.

Like SV part, the NSV part of the solution is also determined by demanding that it should contain the right divergences to cancel those present in AP kernels. The structure of the finite part of the solution is determined by Eq.(6.33), which when combined with SV part of the solution, reproduces the correct NSV terms for Δ_I . The perturbative structure of higher order results allows only certain powers of logarithms at every order in perturbation theory thanks to inherent transcendentality structure of Feynman integrals that appear at every order in a_s and in ϵ in the dimensionally regularised theory. We find that the coefficients $\varphi_i^I(z, \epsilon)$ are consistent with this expectation. In addition, the solution demonstrates an interesting structure that deserves a mention. We find that the K+G equation allows us to construct not just one solution but a class of solutions, a minimal class, satisfying the right divergent structure as well as the dependence on $\ln^k(1-z)$, $k = 0, 1, \dots$:

$$\Phi_{\text{nsv},\alpha}^I = \sum_{i=1}^{\infty} \hat{a}_s^i \left(\frac{q^2(1-z)^\alpha}{\mu^2} \right)^{\frac{i\epsilon}{2}} S_\epsilon^i \varphi_{\alpha,i}^I(z, \epsilon). \quad (6.55)$$

The predictions from the solutions $\Phi_{\text{nsv},\alpha}^I$ are found to be independent of choice of α owing to the explicit z -dependence of the coefficients $\varphi_{\alpha,i}^I(z, \epsilon)$ at every order in \hat{a}_s and in ϵ . It is straightforward to show that any variation of α in the factor $(1-z)^{i\alpha\epsilon}$ can always be compensated by suitably adjusting the z independent coefficients of $\ln(1-z)$ terms in $\varphi_{\alpha,i}^I(z, \epsilon)$ at every order in \hat{a}_s . The reason for this is the invariance of the solution under certain ‘‘gauge like’’ transformations on both $(1-z)^{i\alpha\epsilon}$ and $\varphi_{f,\alpha}^I(z, \epsilon)$ at every order in \hat{a}_s . Note that the logarithmic structure of $\varphi_{\alpha,i}^I(z, \epsilon)$ plays an important role. Because of this invariance, these transformations neither affect the divergent structure nor the finite parts of $\Phi_{\text{nsv},\alpha}^I$. We find that the invariance can be realised through the renormalisation group equation of strong coupling constant. To end, the solution given in Eq.(6.55) takes the following integral form:

$$\Phi_{\text{nsv},\alpha}^I = \int_{\mu_F^2}^{q^2(1-z)^\alpha} \frac{d\lambda^2}{\lambda^2} L^I(a_s(\lambda^2), z) + \varphi_{f,\alpha}^I(a_s(q^2(1-z)^\alpha), z, \epsilon)|_{\epsilon=0} + \varphi_s^I(a_s(\mu_F^2), z, \epsilon), \quad (6.56)$$

The finite part $\varphi_{f,\alpha}^I$ can be expanded as

$$\varphi_{f,\alpha}^I(a_s(q^2(1-z)^\alpha), z) = \sum_{i=1}^{\infty} a_s^i(q^2(1-z)^\alpha) \sum_{k=0}^i \bar{\varphi}_{\alpha,i}^{I,(k)} \ln^k(1-z). \quad (6.57)$$

The fact that the predictions are insensitive to α relates the coefficient $\bar{\varphi}_{\alpha,i}^{I,(k)}$ to $\bar{\varphi}_i^{I,(k)}$, the solution corresponding to $\alpha = 2$, through

$$\begin{aligned} \bar{\varphi}_{\alpha,1}^{I,(0)} &= \bar{\varphi}_1^{I,(0)}, & \bar{\varphi}_{\alpha,1}^{I,(1)} &= -D_1^I \tilde{\alpha} + \bar{\varphi}_1^{I,(1)}, & \bar{\varphi}_{\alpha,2}^{I,(0)} &= \bar{\varphi}_2^{I,(0)} \\ \bar{\varphi}_{\alpha,2}^{I,(1)} &= -\tilde{\alpha} (D_2^I - \beta_0 \bar{\varphi}_1^{I,(0)}) + \bar{\varphi}_2^{I,(1)}, \\ \bar{\varphi}_{\alpha,2}^{I,(2)} &= -\frac{1}{2} \tilde{\alpha}^2 \beta_0 D_1^I - \tilde{\alpha} (C_2^I - \beta_0 \bar{\varphi}_1^{I,(1)}) + \bar{\varphi}_2^{I,(2)} \\ \bar{\varphi}_{\alpha,3}^{I,(0)} &= \bar{\varphi}_3^{I,(0)}, & \bar{\varphi}_{\alpha,3}^{I,(1)} &= -\tilde{\alpha} (D_3^I - \beta_1 \bar{\varphi}_1^{I,(0)} - 2\beta_0 \bar{\varphi}_2^{I,(0)}) + \bar{\varphi}_3^{I,(1)} \\ \bar{\varphi}_{\alpha,3}^{I,(2)} &= -\tilde{\alpha}^2 \left(\frac{1}{2} \beta_1 D_1^I + \beta_0 D_2^I - \beta_0^2 \bar{\varphi}_1^{I,(0)} \right) - \tilde{\alpha} (C_3^I \tilde{\alpha} - \beta_1 \bar{\varphi}_1^{I,(1)} - 2\beta_0 \bar{\varphi}_2^{I,(1)}) + \bar{\varphi}_3^{I,(2)} \\ \bar{\varphi}_{\alpha,3}^{I,(3)} &= \beta_0^2 \left(-\frac{1}{3} D_1^I \tilde{\alpha}^3 + \tilde{\alpha}^2 \bar{\varphi}_1^{I,(1)} \right) + \beta_0 \tilde{\alpha} \left(-C_2^I \tilde{\alpha} + 2\bar{\varphi}_2^{I,(2)} \right) + \bar{\varphi}_3^{I,(3)} \end{aligned}$$

$$\begin{aligned}
\bar{\varphi}_{\alpha,4}^{I,(0)} &= \bar{\varphi}_4^{I,(0)}, & \bar{\varphi}_{\alpha,4}^{I,(1)} &= -D_4^I \tilde{\alpha} + \beta_2 \tilde{\alpha} \bar{\varphi}_1^{I,(0)} + 2\beta_1 \tilde{\alpha} \bar{\varphi}_2^{I,(0)} + 3\beta_0 \tilde{\alpha} \bar{\varphi}_3^{I,(0)} + \bar{\varphi}_4^{I,(1)} \\
\bar{\varphi}_{\alpha,4}^{I,(2)} &= -C_4^I \tilde{\alpha} - \frac{1}{2} \beta_2 D_1^I \tilde{\alpha}^2 - \beta_1 D_2^I \tilde{\alpha}^2 - \frac{3}{2} \beta_0 D_3^I \tilde{\alpha}^2 + \frac{5}{2} \beta_0 \beta_1 \tilde{\alpha}^2 \bar{\varphi}_1^{I,(0)} \\
&\quad + \beta_2 \tilde{\alpha} \bar{\varphi}_1^{I,(1)} + 3\beta_0^2 \tilde{\alpha}^2 \bar{\varphi}_2^{I,(0)} + 2\beta_1 \tilde{\alpha} \bar{\varphi}_2^{I,(1)} + 3\beta_0 \tilde{\alpha} \bar{\varphi}_3^{I,(1)} + \bar{\varphi}_4^{I,(2)} \\
\bar{\varphi}_{\alpha,4}^{I,(3)} &= \beta_0^3 \tilde{\alpha}^3 \bar{\varphi}_1^{I,(0)} + \beta_0^2 \tilde{\alpha}^2 \left(-D_2^I \tilde{\alpha} + 3\bar{\varphi}_2^{I,(1)} \right) - \frac{1}{6} \beta_1 \tilde{\alpha} \left(6C_2^I \tilde{\alpha} + 5\beta_0 \tilde{\alpha} \left(D_1^I \tilde{\alpha} - 3\bar{\varphi}_1^{I,(1)} \right) \right. \\
&\quad \left. - 12\bar{\varphi}_2^{I,(2)} \right) - \frac{3}{2} \beta_0 \tilde{\alpha} \left(C_3^I \tilde{\alpha} - 2\bar{\varphi}_3^{I,(2)} \right) + \bar{\varphi}_4^{I,(3)} \\
\bar{\varphi}_{\alpha,4}^{I,(4)} &= \beta_0^3 \left(-\frac{1}{4} D_1^I \tilde{\alpha}^4 + \tilde{\alpha}^3 \bar{\varphi}_1^{I,(1)} \right) + \beta_0^2 \tilde{\alpha}^2 \left(-C_2^I \tilde{\alpha} + 3\bar{\varphi}_2^{I,(2)} \right) + 3\beta_0 \tilde{\alpha} \bar{\varphi}_3^{I,(3)} + \bar{\varphi}_4^{I,(4)} \quad (6.58)
\end{aligned}$$

where $\tilde{\alpha} = \alpha - 2$. The above relations are the transformations for $\bar{\varphi}_{\alpha,i}^{I,(k)}$ that are required to compensate the contributions resulting from the change in the exponent of $(1-z)$ from $i\epsilon$ to $i\alpha\epsilon$. This invariance property with respect to the parameter α makes the solution a peculiar one compared to SV counter part.

We would like to point out that the class of solutions parametrized by α is not the only one that satisfies K+G equation. For example, if we do not restrict z -dependence, we can obtain different kinds of solution. Then for such solution, we need to add more terms on the right hand side of (6.55) in such a way that all the requirements are fulfilled. In other words if we assume the following form for the solution,

$$\tilde{\Phi}_{\text{nsv}}^I = \sum_{\alpha} \sum_{i=1}^{\infty} \hat{\alpha}_s^i \left(\frac{q^2(1-z)^\alpha}{\mu^2} \right)^{\frac{i\epsilon}{2}} S_{\epsilon}^i \mathfrak{N}_{\alpha,i}^I(\epsilon) \quad (6.59)$$

with various $\mathfrak{N}_{\alpha,i}^I(\epsilon)$'s to containing right divergent as well as finite terms and then sum them up over α s, we can obtain Δ_I that agrees with the known result.

In the present work, we use the minimal solution with the choice $\alpha = 2$ in Eq.(6.55) so that the solution resembles more like the SV part. Thanks to the invariance property of the solution, the different choices for α neither alter the qualitative behaviour nor the quantitative predictions for Δ_I to all orders. For example, an alternate choice, say $\alpha = 1$ can only change the coefficients of $\ln^k(1-z)$ in the φ_f^I without affecting the all order structure and the predictions for Δ_I . With our choice of $\alpha = 2$, the all order solution,

equivalently integral representation resembles that of SV part. We will see later that this choice will allow us to study N -space resummation for both SV and NSV terms with single order one term namely $\omega = 2a_s\beta_0 \ln N$.

6.4.2 On the Logarithmic Structure

In the last section, we derived z space result that can correctly predict certain SV and NSV terms to all orders from the knowledge of previous orders. This was possible due to a peculiar logarithm structure of the solution to K+G equation at every order in \hat{a}_s and ϵ , see Eq. (6.32). In this sub section, we present an explicit result for Φ^c , $c = b$ to second order in perturbation theory in order to explain the structure of SV and NSV logarithms at a given order in \hat{a}_s with an accuracy of ϵ^n . We have used inclusive cross section for the production of Higgs boson in bottom quark annihilation for this purpose. The conclusions remain unchanged as long as color neutral production in diagonal channels are considered. To order \hat{a}_s^2 , the inclusive cross section for the production of Higgs boson in bottom quark annihilation receives contributions from a) pure real emissions

$$b + \bar{b} \rightarrow H + g, \quad b + \bar{b} \rightarrow H + g + g, \quad b + \bar{b} \rightarrow H + b + \bar{b}, \quad b + \bar{b} \rightarrow H + q + \bar{q},$$

b) pure virtual corrections through one and two loop corrections to leading order $b + \bar{b} \rightarrow H$ and c) interference of pure real emission process $b + \bar{b} \rightarrow H + g$ with the loop corrected process $b + \bar{b} \rightarrow H + g$. Here, q refers light quarks leaving t - and b -quarks. We compute these parton level sub processes using the standard Feynman diagram approach. Beyond the leading order in strong coupling, all these sub processes develop UV and IR divergences and they are regulated in dimensional regularisation. As we encounter large number of Feynman diagrams, we use QGRAF to generate them and an in-house FORM routine to perform all the symbolic manipulations, e.g. for Dirac, $SU(N)$ color and Lorentz algebra. We use the integration-by-parts identities through a *Mathematica* based package, LiteRed, to reduce Feynman integrals to a minimum set of master integrals. In

addition, for real emission and real-virtual processes the method of reverse unitarity is used along with IBP identities to reduce the resulting phase-space integrals to a set of few master integrals. The master integrals for the virtual processes can be found in [59, 157] and for the real emission in [157] up to desired accuracy in ϵ . While individual sub processes contain UV, soft and collinear divergences, after renormalising the strong coupling constant \hat{a}_s and the Yukawa coupling λ , the sum becomes UV finite. In addition, the soft and final state collinear divergences cancel in real and virtual sub processes leaving only initial state collinear divergences in $\hat{\sigma}_{b\bar{b}}$.

Since we are interested only in those terms that are proportional to distributions and NSV logarithms $\ln^k(1-z)$, we expand $\hat{\sigma}_{b\bar{b}}$ around $z = 1$ and drop those terms that vanish when $z \rightarrow 1$. In order to extract Φ^c from the latter, we follow (6.8), where the virtual contributions are factored out from $\hat{\sigma}_I$ giving rise to the function \mathcal{S}^I . Owing to (6.17), \mathcal{S}^I has an exponential structure

$$\mathcal{S}^b(z, q^2, \epsilon) = C \exp\left(2\Phi^b(z, q^2, \epsilon)\right) \quad (6.60)$$

where $\Phi^b = \Phi_{\text{sv}}^b + \Phi_{\text{nsv}}^b$. Expanding Φ_{nsv}^b in powers of \hat{a}_s as

$$\begin{aligned} \Phi_{\text{nsv}}^b(\hat{a}_s, \mu^2, q^2, z, \epsilon) &= \sum_{i=1}^{\infty} \hat{a}_s^i \left(\frac{q^2(1-z)^2}{\mu^2} \right)^{i\frac{\epsilon}{2}} S_{\epsilon}^i \varphi_i^b(z, \epsilon) \\ &= \sum_{i=1}^{\infty} \hat{a}_s^i \left(\frac{q^2}{\mu^2} \right)^{i\frac{\epsilon}{2}} S_{\epsilon}^i \hat{\Phi}_{\text{nsv},i}^b(z, \epsilon), \end{aligned} \quad (6.61)$$

and using explicit results for $\hat{\sigma}_{b\bar{b}}^{\text{sv+nsv}}$, Z_b and $\hat{\mathcal{F}}^b$, we obtain $\hat{\Phi}_{\text{nsv},b}^{(i)}$ for $i = 1, 2$ in powers of ϵ . They are given by

$$\begin{aligned} \hat{\Phi}_{\text{nsv},1}^b &= C_F \left\{ \frac{1}{\epsilon} \left(-8 \right) + \left(-8L_z + 4 \right) + \epsilon \left(-4L_z^2 + 4L_z + 3\zeta_2 \right) + \epsilon^2 \left(-\frac{4}{3}L_z^3 + 2L_z^2 \right. \right. \\ &\quad \left. \left. + 3\zeta_2 L_z - \left(\frac{7}{3}\zeta_3 + \frac{3}{2}\zeta_2 \right) \right) + \epsilon^3 \left(-\frac{1}{3}L_z^4 + \frac{2}{3}L_z^3 + \frac{3}{2}\zeta_2 L_z^2 - \left(\frac{7}{3}\zeta_3 + \frac{3}{2}\zeta_2 \right) L_z \right. \right. \\ &\quad \left. \left. + \left(\frac{7}{6}\zeta_3 + \frac{3}{16}\zeta_2^2 \right) \right) \right\} \end{aligned}$$

$$\begin{aligned}
\hat{\Phi}_{\text{nsv},2}^b = & C_F C_A \left\{ \frac{1}{\epsilon^2} \left(\frac{88}{3} \right) + \frac{1}{\epsilon} \left(\frac{176}{3} L_z + 8\zeta_2 - \frac{664}{9} \right) + \left(\frac{176}{3} L_z^2 + \left(16\zeta_2 - \frac{1238}{9} \right) L_z \right. \right. \\
& + \frac{1402}{27} - 28\zeta_3 - \frac{178}{3} \zeta_2 \left. \right) + \epsilon \left(\frac{352}{9} L_z^3 + \left(16\zeta_2 - \frac{2341}{18} \right) L_z^2 + \left(\frac{2750}{27} \right. \right. \\
& - 56\zeta_3 - \frac{356}{3} \zeta_2 \left. \right) L_z + \frac{934}{9} \zeta_3 - \frac{4021}{81} + \frac{982}{9} \zeta_2 - 4\zeta_2^2 \left. \right\} + C_F^2 \left\{ \frac{1}{\epsilon} \left(16L_z \right. \right. \\
& + 12 \left. \right) + \left(28L_z^2 + 14L_z - 32\zeta_2 \right) + \epsilon \left(\frac{74}{3} L_z^3 + \frac{13}{2} L_z^2 + \left(6 - 76\zeta_2 \right) L_z \right. \\
& - 8 + 48\zeta_3 - \zeta_2 \left. \right\} + C_F n_f \left\{ \frac{1}{\epsilon^2} \left(\frac{-16}{3} \right) + \frac{1}{\epsilon} \left(\frac{-32}{3} L_z + \frac{112}{9} \right) + \left(\frac{-32}{3} L_z^2 \right. \right. \\
& + \left(\frac{224}{9} \right) L_z + \frac{28}{3} \zeta_2 - \frac{328}{27} \left. \right) + \epsilon \left(\frac{-64}{9} L_z^3 + \frac{224}{9} L_z^2 + \left(\frac{56}{3} \zeta_2 - \frac{656}{27} \right) L_z \right. \\
& \left. \left. + \frac{1030}{81} - \frac{124}{9} \zeta_3 - \frac{196}{9} \zeta_2 \right) \right\}. \tag{6.62}
\end{aligned}$$

As can be seen from the above results, at order \hat{a}_s , the leading pole in ϵ is of order one and it is two at \hat{a}_s^2 and the increment of one unit for the leading poles is expected to continue with the order of perturbation. However, the pole structure for $\hat{\sigma}_{b\bar{b}}$ shows an increment of two units. In addition, at every order in \hat{a}_s , for a given color factor, the combination of ϵ and the leading logarithm shows uniform transcendentality weight. In other words, if we assign n_ϵ weight for ϵ^{-n_ϵ} and n_L for $\ln^{n_L}(1-z)$, then the highest weight at every order in ϵ shows uniform transcendentality $w = n_\epsilon + n_L$. For instance, at one loop, we find $w = 1$ at every order of ϵ and at two loops it is two ($w = 2$). This clearly explains that the highest power of $\ln(1-z)$ at every order in ϵ is constrained by the order of \hat{a}_s and the accuracy in ϵ and is found to be $i + j$ for the term $\hat{a}_s^i \epsilon^j$. This translates to $i + j - 1$ for $\mathcal{G}_{L,i}^{l,j}$ in Eq.(6.32) as the latter is the coefficient of ϵ^{j-1} . This exercise provides an explanation for the logarithmic structure given in Eq.(6.32), in particular the upper limit of the summation. This logarithmic structure determines the structure of φ_f^l given in Eq.(6.38).

Precisely because of the logarithmic structure of the exponents, namely, increment by one unit, we get logarithms in CFs with increment of two units. It is easy to understand this structure if we observe that when we expand the exponents containing $\mathcal{D}_k(z)$ and $\ln^k(1-z)$ to obtain CFs, the resulting convolutions between various orders in a_s will be of the form $\mathcal{D}_k(z) \otimes \mathcal{D}_l(z)$ and/or $\mathcal{D}_k(z) \otimes \ln^l(1-z)$ which will result in leading distributions $\mathcal{D}_{k+l+1}(z)$ and leading NSV logarithms $\ln^{k+l+1}(1-z)$.

6.5 Resummation of next-to-SV in N -space

To study all order behavior of Δ_I in Mellin space, it is convenient to use the integral representations of both Φ_{sv}^I and Φ_{nsv}^I given in (2.71) and (6.33) respectively. Substituting the solutions for $\hat{\mathcal{F}}^I$, Z^I and $\ln \Gamma_I$ along with the integral representations for Φ_{sv}^I and Φ_{nsv}^I in (6.9), we find

$$\Delta_I(q^2, \mu_R^2, \mu_F^2, z) = C_0^I(q^2, \mu_R^2, \mu_F^2) C \exp\left(2\Psi_{\mathcal{D}}^I(q^2, \mu_F^2, z)\right), \quad (6.63)$$

where

$$\Psi_{\mathcal{D}}^I(q^2, \mu_F^2, z) = \frac{1}{2} \int_{\mu_F^2}^{q^2(1-z)^2} \frac{d\lambda^2}{\lambda^2} P_I'(a_s(\lambda^2), z) + \mathcal{Q}^I(a_s(q^2(1-z)^2), z), \quad (6.64)$$

with

$$\mathcal{Q}^I(a_s(q^2(1-z)^2), z) = \left(\frac{1}{1-z} \bar{G}_{\text{sv}}^I(a_s(q^2(1-z)^2)) \right)_+ + \varphi_f^I(a_s(q^2(1-z)^2), z). \quad (6.65)$$

The coefficient C_0^I is z independent coefficient and is expanded in powers of $a_s(\mu_R^2)$ as

$$C_0^I(q^2, \mu_R^2, \mu_F^2) = \sum_{i=0}^{\infty} a_s^i(\mu_R^2) C_{0,i}^I(q^2, \mu_R^2, \mu_F^2), \quad (6.66)$$

The C_0^I , being z -independent, is identical to the one in threshold limit and can find C_0^I for DY and Higgs production in [62]. The Eq.(6.63) is our z -space resummed result for Δ_I in integral representation which can be used to predict SV and NSV terms to all orders in perturbation theory in terms of universal anomalous dimensions, A^I, B^I, C^I, D^I, f^I , SV coefficients $\bar{\mathcal{G}}_i^{I,j}$, NSV coefficients $\mathcal{G}_{L,i}^{I,(j,k)}$ and process dependent $C_{0,i}^I$. We have few comments in order. The next-to-SV corrections to various inclusive processes were studied in a series of papers [6, 199–201, 207, 208, 243] and lot of progress have been made which lead to better understanding of the underlying physics. Our result has close resemblance with the one which was conjectured in [6] and indeed there are few terms which are common in both the results. Our result, (6.64) differs from Eq.(31) in [6], in the upper limit of the integral, the presence of extra term φ_f^I and the dependence on the variable z . These differences do not alter the SV predictions but will give NSV terms different from those

obtained using Eq.(31) of [6].

The Mellin moment of Δ_I is now straight forward to compute using the integral representation given in Eq.(6.64). Note that the (6.64) is suitable for obtaining only SV and NSV terms while the predictions beyond NSV terms such as those proportional to $\mathcal{O}((1-z)^n \ln^j(1-z))$; $n, j \geq 0$ in z -space and terms of $\mathcal{O}(1/N^2)$ in N -space will not be correct! Hence, we compute the Mellin moment of (6.63) in the appropriate limit of N such that the resulting expression in N -space correctly predicts all the SV and NSV terms. The limit $z \rightarrow 1$ translates to $N \rightarrow \infty$ and if one is interested to include NSV terms, we need to keep $\mathcal{O}(1/N)$ corrections in the large N limit. The Mellin moment of Δ_I is given by

$$\Delta_N^I(q^2, \mu_R^2, \mu_F^2) = C_0^I(q^2, \mu_R^2, \mu_F^2) \exp\left(\Psi_N^I(q^2, \mu_F^2)\right), \quad (6.67)$$

where

$$\Psi_N^I(q^2, \mu_F^2) = 2 \int_0^1 dz z^{N-1} \Psi_{\mathcal{D}}^I(q^2, \mu_F^2, z). \quad (6.68)$$

The computation of Mellin moment in the large N limit which retains SV and NSV terms involves two major steps: (1) Following [6] and we replace $\int dz(z^{N-1} - 1)/(1-z)$ and $\int dz z^{N-1}$ by a theta function $\theta(1-z-1/N)$ and apply the operators $\Gamma_A(N \frac{d}{dN})$ and $\Gamma_B(N \frac{d}{dN})$ on the integrals respectively; (2) We perform the integrals over λ^2 after expressing $a_s(\lambda^2)$ in terms of $a_s(\mu_R^2)$ obtained using resummed solution to RG equation of a_s in (F.5). Step 1 makes sure that we retain only $\ln^j(N)$ and $(1/N) \ln^j(N)$ terms and step 2 guarantees the resummation of $2\beta_0 a_s(\mu_R^2) \ln(N)$ terms to all orders and also the organisation of the result in powers of $a_s(\mu_R^2)$. The details of the computation are described in the Appendix F. The Mellin moment of the exponent takes the following form:

$$\Psi_N^I = \Psi_{sv,N}^I + \Psi_{nsv,N}^I \quad (6.69)$$

where we have split Ψ_N^I in such a way that all those terms that are functions of $\ln^j(N)$, $j = 0, 1, \dots$ are kept in $\Psi_{sv,N}^I$ and the remaining terms that are proportional to $(1/N) \ln^j(N)$, $j = 0, 1, \dots$ are

contained in $\Psi_{\text{nsv},N}^I$. Hence,

$$\Psi_{\text{sv},N}^I = \ln(g_0^I(a_s(\mu_R^2))) + g_1^I(\omega) \ln(N) + \sum_{i=0}^{\infty} a_s^i(\mu_R^2) g_{i+2}^I(\omega), \quad (6.70)$$

where $g_i^I(\omega)$ are identical to those in [68, 155, 244] obtained from the resummed formula for SV terms. For completeness, we present them in Appendix E. It is to be noted that $g_i^I(\omega)$ vanishes in the limit $\omega \rightarrow 0$. The coefficients $g_0^I(a_s)$ is expanded in powers of a_s as (see [244])

$$\ln(g_0^I(a_s(\mu_R^2))) = \sum_{i=1}^{\infty} a_s^i(\mu_R^2) g_{0,i}^I. \quad (6.71)$$

The N -independent coefficients C_0^I and g_0^I are related to the coefficients \bar{g}_0^I given in the paper [155, 245] using the following relation,

$$\bar{g}_0^I(q^2, \mu_R^2, \mu_F^2) = C_0^I(q^2, \mu_R^2, \mu_F^2) g_0^I(a_s(\mu_R^2)) \quad (6.72)$$

which can be expanded in terms of $a_s(\mu_R^2)$ as,

$$\bar{g}_0^I(a_s(\mu_R^2)) = \sum_{i=0}^{\infty} a_s^i(\mu_R^2) \bar{g}_{0,i}^I. \quad (6.73)$$

The coefficient $\bar{g}_{0,i}^I$ are presented in the Appendix E, which are solely coming from the SV part.

Now let us discuss NSV piece. The function $\Psi_{\text{nsv},N}^I$ is given by

$$\Psi_{\text{nsv},N}^I = \frac{1}{N} \sum_{i=0}^{\infty} a_s^i(\mu_R^2) \left(\bar{g}_{i+1}^I(\omega) + h_i^I(\omega, N) \right), \quad (6.74)$$

with

$$h_i^I(\omega, N) = \sum_{k=0}^i h_{ik}^I(\omega) \ln^k(N). \quad (6.75)$$

where $\bar{g}_i^I(\omega)$ are given by ²:

$$\begin{aligned}
\bar{g}_1^I(\omega) &= \frac{A_1^I}{\beta_0} \bar{L}_w, \\
\bar{g}_2^I(\omega) &= \frac{1}{(1-\omega)} \left[\frac{\mathbf{D}_1^I}{2} - \frac{A_2^I}{\beta_0} \omega + \frac{A_1^I \beta_1}{\beta_0^2} (\omega + \bar{L}_w) - A_1^I (2 + 2\gamma_E - L_{qr} + L_{fr}(1-\omega)) \right], \\
\bar{g}_3^I(\omega) &= \frac{1}{(1-\omega)^2} \left[\mathbf{D}_2^I \left\{ \frac{1}{2} \right\} + \mathbf{D}_1^I \left\{ -\frac{\bar{L}_w \beta_1}{2\beta_0} + \beta_0 \left(1 + \gamma_E - \frac{1}{2} L_{qr} \right) \right\} - \frac{A_3^I}{\beta_0} \left\{ 1 - \frac{\omega}{2} \right\} \omega \right. \\
&\quad + A_2^I \left\{ + \frac{\beta_1}{\beta_0^2} (\omega - \frac{1}{2} \omega^2 + \bar{L}_w) - (2 + 2\gamma_E - L_{qr} + L_{fr}(1-\omega)^2) \right\} - \frac{\beta_2 A_1^I}{\beta_0^2} \frac{\omega^2}{2} \\
&\quad + A_1^I \left\{ \frac{\beta_1^2}{2\beta_0^3} (\omega^2 - \bar{L}_w^2) + \frac{\beta_1}{\beta_0} (2 + 2\gamma_E - L_{qr}) \bar{L}_w - 2\beta_0 (2\gamma_E + \gamma_E^2 + \zeta_2 - L_{qr} \right. \\
&\quad \left. - L_{qr} \gamma_E + \frac{1}{4} L_{qr}^2 - \frac{1}{4} L_{fr}^2 (1-\omega)^2) \right\} \left. \right], \\
\bar{g}_4^I(\omega) &= \frac{1}{(1-\omega)^3} \left[\mathbf{D}_1^I \left\{ \frac{\beta_1^2}{2\beta_0^2} (-\omega - \bar{L}_w + \bar{L}_w^2) + \frac{\omega \beta_2}{2\beta_0} + \beta_1 (1 + \gamma_E - \frac{1}{2} L_{qr}) (1 - 2\bar{L}_w) \right. \right. \\
&\quad + 2\beta_0^2 (2\gamma_E + \gamma_E^2 + \zeta_2 - L_{qr} - L_{qr} \gamma_E + \frac{1}{4} L_{qr}^2) \left. \right\} + \mathbf{D}_2^I \left\{ -\frac{\beta_1}{\beta_0} \bar{L}_w + \beta_0 (2 + 2\gamma_E \right. \\
&\quad \left. - L_{qr}) \right\} + \frac{1}{2} \mathbf{D}_3^I - \frac{A_4^I}{\beta_0} \omega \left\{ 1 - \omega + \frac{1}{3} \omega^2 \right\} + A_3^I \left\{ \frac{\beta_1}{\beta_0^2} (\omega - \omega^2 + \frac{1}{3} \omega^3 + \bar{L}_w) - 2 \right. \\
&\quad \left. - 2\gamma_E + L_{qr} - L_{fr} + 3L_{fr} (1 - \omega + \frac{\omega^2}{3}) \omega \right\} + A_2^I \left\{ \frac{\beta_1^2}{\beta_0^3} (\omega^2 - \frac{1}{3} \omega^3 - \bar{L}_w^2) - \frac{\beta_2}{\beta_0^2} \right. \\
&\quad \left. (1 - \frac{1}{3} \omega) \omega^2 + 2\frac{\beta_1}{\beta_0} (2 + 2\gamma_E - L_{qr}) \bar{L}_w - \beta_0 (8\gamma_E + 4\gamma_E^2 + 4\zeta_2 - 4L_{qr}(1 + \gamma_E)) \right. \\
&\quad \left. + L_{qr}^2 - L_{fr}^2 + 3L_{fr}^2 (1 - \omega + \frac{\omega^2}{3}) \omega \right\} + A_1^I \left\{ -\frac{\beta_1^3}{\beta_0^4} (\frac{1}{2} \omega^2 - \frac{1}{3} \omega^3 + \bar{L}_w \omega + \frac{1}{2} \bar{L}_w^2 \right. \\
&\quad \left. - \frac{1}{3} \bar{L}_w^3) + \frac{\beta_1 \beta_2}{\beta_0^3} (\omega - \frac{2}{3} \omega^2 + \bar{L}_w) \omega - \frac{\beta_3}{\beta_0^2} \omega^2 (\frac{1}{2} - \frac{1}{3} \omega) + 2\frac{\beta_1^2}{\beta_0^2} (\omega + \bar{L}_w - \bar{L}_w^2) (1 \right. \\
&\quad \left. + \gamma_E - \frac{L_{qr}}{2}) + \frac{\beta_2}{\beta_0} (-2 - 2\gamma_E + L_{qr}) \omega + \beta_1 (-4\gamma_E - 2\gamma_E^2 - 2\zeta_2 + 2L_{qr} - \frac{1}{2} L_{qr}^2 \right. \\
&\quad \left. + 2L_{qr} \gamma_E) (1 - 2\bar{L}_w) + \frac{\beta_1}{2} L_{fr}^2 (1-\omega)^3 - \beta_0^2 (8\gamma_E^2 + \frac{8}{3} \gamma_E^3 + \frac{16}{3} \zeta_3 + 2(4\zeta_2 + L_{qr}^2) \right. \\
&\quad \left. (1 + \gamma_E) - 4L_{qr} \gamma_E (2 + \gamma_E) - 4L_{qr} \zeta_2 - \frac{1}{3} L_{qr}^3 + \frac{1}{3} L_{fr}^3 (1-\omega)^3) \right\} \left. \right]. \tag{6.76}
\end{aligned}$$

Here $\bar{L}_\omega = \ln(1 - \omega)$, $L_{qr} = \ln(\frac{q^2}{\mu_R^2})$, $L_{fr} = \ln(\frac{\mu_E^2}{\mu_R^2})$ and $\omega = 2\beta_0 a_s (\mu_R^2) \ln(N)$. Also, \mathbf{D}_i^I are the threshold exponent defined in terms of \bar{G}_{SV}^c :

$$\mathbf{D}^I(a_s(q^2(1-z)^2)) = \sum_{i=1}^{\infty} a_s^i(q^2(1-z)^2) \mathbf{D}_i^I$$

² $\bar{g}_5^I(\omega)$ are given in the ancillary files submitted with the arXiv submission [198]

$$= 2 \bar{G}_{sv}^I(a_s(q^2(1-z)^2), \epsilon) \Big|_{\epsilon=0} \quad (6.77)$$

Also the resummation constants $h_{ik}^I(\omega)$ are given by ³:

$$h_{00}^I(\omega) = \frac{2}{\beta_0} \bar{L}_\omega \left[-\gamma_2^B C_1^I + \gamma_1^B D_1^I \right],$$

$$h_{01}^I(\omega) = \frac{2}{\beta_0} \bar{L}_\omega \left[-\gamma_1^B C_1^I \right],$$

$$h_{10}^I(\omega) = \frac{1}{(1-\omega)} \left[\frac{2\beta_1 D_1^I}{\beta_0^2} \left\{ \gamma_1^B \omega + \gamma_1^B \bar{L}_\omega \right\} - \frac{2\beta_1}{\beta_0^2} C_1^I \left\{ \gamma_2^B \omega + \gamma_2^B \bar{L}_\omega \right\} - 2 \frac{D_2^I}{\beta_0} \gamma_1^B \omega + 2 \frac{C_2^I}{\beta_0} \gamma_2^B \omega \right. \\ \left. - 2\bar{\varphi}_1^{I,(1)} \gamma_2^B + 2\bar{\varphi}_1^{I,(0)} \gamma_1^B + 2D_1^I \left\{ L_{qr} \gamma_1^B - L_{fr} \gamma_1^B + L_{fr} \gamma_1^B \omega - 2\gamma_2^B \right\} - 2C_1^I \left\{ L_{qr} \gamma_2^B - L_{fr} \gamma_2^B \right. \right. \\ \left. \left. + L_{fr} \gamma_2^B \omega - 4\gamma_3^B \right\} \right],$$

$$h_{11}^I(\omega) = \frac{1}{(1-\omega)} \left[\frac{\beta_1}{\beta_0^2} C_1^I \left\{ -2\gamma_1^B \omega - 2\gamma_1^B \bar{L}_\omega \right\} + 2 \frac{C_2^I}{\beta_0} \gamma_1^B \omega - 2\bar{\varphi}_1^{I,(1)} \gamma_1^B + C_1^I \left\{ -2L_{qr} \gamma_1^B + 2L_{fr} \gamma_1^B \right. \right. \\ \left. \left. - 2L_{fr} \gamma_1^B \omega + 4\gamma_2^B \right\} + \frac{\omega}{(1-\omega)} \left\{ \frac{\bar{\varphi}_2^{I,(2)}}{\beta_0} \gamma_1^B \right\} \right],$$

$$h_{21}^I(\omega) = \frac{1}{(1-\omega)^2} \left[\frac{\beta_1^2 C_1^I}{\beta_0^3} \left\{ -\gamma_1^B \omega^2 + \gamma_1^B \bar{L}_\omega^2 \right\} + \frac{\beta_2 C_1^I}{\beta_0^2} \gamma_1^B \omega^2 + \frac{\beta_1 C_2^I}{\beta_0^2} \left\{ -2\omega + \omega^2 - 2\bar{L}_\omega \right\} \gamma_1^B \right. \\ \left. + \frac{C_3^I}{\beta_0} \left\{ 2\gamma_1^B \omega - \gamma_1^B \omega^2 \right\} + 2 \frac{\beta_1 \bar{\varphi}_1^{I,(1)}}{\beta_0} \gamma_1^B \bar{L}_\omega + \frac{\beta_1 C_1^I}{\beta_0} \left\{ 2L_{qr} \gamma_1^B - 4\gamma_2^B \right\} \bar{L}_\omega + 4\bar{\varphi}_2^{I,(2)} \gamma_2^B \right. \\ \left. - 2\bar{\varphi}_2^{I,(1)} \gamma_1^B + C_2^I \left\{ -2L_{qr} \gamma_1^B + 2L_{fr} \gamma_1^B (1-\omega)^2 + 4\gamma_2^B \right\} + 2\beta_0 \bar{\varphi}_1^{I,(1)} \left\{ L_{qr} \gamma_1^B - 2\gamma_2^B \right\} \right. \\ \left. + \beta_0 C_1^I \left\{ L_{qr}^2 \gamma_1^B - 4L_{qr} \gamma_2^B - L_{fr}^2 \gamma_1^B + 2L_{fr}^2 \gamma_1^B \omega + 8\gamma_3^B - L_{fr}^2 \gamma_1^B \omega^2 \right\} \right],$$

$$h_{22}^I(\omega) = \frac{\omega}{(1-\omega)^3} \left[\frac{-\bar{\varphi}_3^{I,(3)}}{\beta_0} \gamma_1^B \right],$$

$$h_{32}^I(\omega) = \frac{1}{(1-\omega)^3} \left[-4\gamma_1^B \bar{L}_\omega \left\{ \frac{\beta_1 \bar{\varphi}_2^{I,(2)}}{\beta_0} \right\} - 6\bar{\varphi}_3^{I,(3)} \gamma_2^B + 2\bar{\varphi}_3^{I,(2)} \gamma_1^B - 4\beta_0 \bar{\varphi}_2^{I,(2)} \left\{ L_{qr} \gamma_1^B - 2\gamma_2^B \right\} \right],$$

$$h_{33}^I(\omega) = \frac{\omega}{(1-\omega)^4} \left[\frac{\bar{\varphi}_4^{I,(4)}}{\beta_0} \gamma_1^B \right],$$

$$h_{42}^I(\omega) = \frac{1}{(1-\omega)^4} \left[\frac{2\beta_1^2}{\beta_0^2} \bar{\varphi}_2^{I,(2)} \left\{ 3\bar{L}_\omega^2 - 2\omega - 2\bar{L}_\omega \right\} \gamma_1^B + \frac{4\beta_2}{\beta_0} \bar{\varphi}_2^{I,(2)} \gamma_1^B \omega + \frac{18\beta_1}{\beta_0} \bar{\varphi}_3^{I,(3)} \gamma_2^B \bar{L}_\omega + 24\bar{\varphi}_4^{I,(4)} \gamma_3^B \right. \\ \left. - \frac{6\beta_1}{\beta_0} \bar{\varphi}_3^{I,(2)} \gamma_1^B \bar{L}_\omega - 6\bar{\varphi}_4^{I,(3)} \gamma_2^B + 2\bar{\varphi}_4^{I,(2)} \gamma_1^B - 4\beta_1 \bar{\varphi}_2^{I,(2)} \left\{ L_{qr} \gamma_1^B - 3L_{qr} \gamma_1^B \bar{L}_\omega - 2\gamma_2^B + 6\gamma_2^B \bar{L}_\omega \right\} \right. \\ \left. + 18\beta_0 \bar{\varphi}_3^{I,(3)} \left\{ L_{qr} \gamma_2^B - 4\gamma_3^B \right\} - 6\beta_0 \bar{\varphi}_3^{I,(2)} \left\{ L_{qr} \gamma_1^B - 2\gamma_2^B \right\} + 6\beta_0^2 \bar{\varphi}_2^{I,(2)} \left\{ L_{qr}^2 \gamma_1^B - 4L_{qr} \gamma_2^B \right. \right. \\ \left. \left. - 4\gamma_3^B \right\} \right]$$

³The results of $(h_{20}^I(\omega), h_{30}^I(\omega), h_{31}^I(\omega), h_{40}^I(\omega), h_{41}^I(\omega))$ are provided in the ancillary files of [198].

$$\begin{aligned}
& + 8\gamma_3^B \Big] \Big], \\
h_{43}^I(\omega) &= \frac{2}{(1-\omega)^4} \left[\frac{3\beta_1}{\beta_0} \bar{\varphi}_3^{I,(3)} \gamma_1^B \bar{L}_w + 4\bar{\varphi}_4^{I,(4)} \gamma_2^B - \bar{\varphi}_4^{I,(3)} \gamma_1^B + 3\beta_0 \bar{\varphi}_3^{I,(3)} \{L_{qr} \gamma_1^B - 2\gamma_2^B\} \right], \\
h_{44}^I(\omega) &= \frac{\omega}{(1-\omega)^5} \left[\frac{-\bar{\varphi}_5^{I,(5)}}{\beta_0} \gamma_1^B \right], \tag{6.78}
\end{aligned}$$

We can see that in each coefficient, say $g_i^I(\omega), \bar{g}_i^I(\omega), h_{ik}^I(\omega)$ from the SV as well as the NSV, we are resumming in Mellin space “order one” term ω to all orders in perturbation theory. This is the consequence of the argument in the coupling constant $a_s(q^2(1-z)^2)$ resulting from the integral over λ and the function Q^I . The peculiarity of the series is that the SV $g_1^I(\omega)$ comes with $\ln N$ and hence it starts with a double logarithm. This extra $\ln N$ arises from the Mellin moment of the factor $1/(1-z)_+$ appearing in the exponent. Similarly for $\Psi_{\text{nsv},N}^I$ we note that it is proportional to $1/N$ at every order as expected. Explicit $\ln N$ that appear with $h_{ik}^I(\omega)$ results from the explicit $\ln(1-x)$ appearing in the exponent. The sum containing $\bar{g}_i^I, i = 1, 2, \dots$ results entirely from A^I coefficients of P_I' and from the function \bar{G}_{sv}^I of (6.65). We find that none of the coefficients $\bar{g}_i^I(\omega)$ contains explicit $\ln(N)$. The second sum comes from C^I, D^I coefficients of P_I' and from φ_f^I and each term in this expansion contains explicit $\ln^k(N), k = 0, \dots, i$. We find that coefficient of h_{01}^I is proportional to C_1^I which is identically zero. Hence, at order a_s^0 , there is no $(1/N) \ln(N)$ term.

Summarising, we find that in Mellin N -space one obtains compact expression for the exponent in terms of quantities that are functions of $\omega = 2a_s(\mu_R^2)\beta_0 \ln(N)$ as we use resummed a_s to perform the integral. In addition, the resummed a_s allows us to organise the N -space perturbative expansion in such a way that ω is treated as order one at every order in $a_s(\mu_R^2)$. Both integral representation in z -space and Mellin moment of the integral in N -space contain exactly same information and hence predict SV and NSV logarithms to all orders in perturbation theory. The all order structure is more transparent in N -space compared to z -space result and it is technically easy to use resummed result in N -space for any phenomenological studies.

Let us first consider $\Psi_{\text{sv},N}^I$ given in (6.70). If we keep only $\bar{g}_{0,0}$ and g_1 terms in (6.70) and expand the exponent in powers of $a_s = a_s(\mu_R^2)$, we can predict leading $a_s^i \ln^{2i}(N)$ terms for all $i > 1$. This happens because of the all order structure of Φ_{sv}^I in z -space. For example if we know Φ_{sv}^I to order a_s , we can predict rest of the other terms of the form $a_s^i \mathcal{D}_{2i-1}(z)$ in Φ_{sv}^I for all $i > 1$. If

we further include $\bar{g}_{0,1}$ and g_2 terms, then we can predict next to leading $a_s^i \ln^{2i-1}(N)$ terms for all $i > 2$. Again this is due to the fact that in z -space, knowing Φ_{sv}^I to second order one can predict $a_s^i \mathcal{D}_{2i-2}(z)$ terms for all $i > 3$. In general, resummed result with terms $\bar{g}_{0,0}^I, \dots, \bar{g}_{0,n-1}^I$ and g_1^I, \dots, g_n^I can predict $a_s^i \ln^{2i-n+1}(N)$ or $a_s^i \mathcal{D}_{2i-n}(z)$ terms for $i > n$.

The inclusion of sub leading terms through $\exp(\Psi_{nsv,N}^I)$ gives additional $(1/N) \ln^j(N)$ terms in N -space or $\ln^j(1-z)$ terms in z -space. In perturbative QCD, $C_1^I = 0$, where $I = q, g$ and we use this in the rest of our analysis. Like the $\Psi_{sv,N}^I$ exponent, $\Psi_{nsv,N}^I$ also organises the perturbation theory by keeping $2a_s(\mu_R^2)\beta_0 \ln(N)$ terms as order one at every order in a_s . However these terms are suppressed by $1/N$ factor at every order in a_s .

We find that if we keep $\{\bar{g}_{0,0}^I, g_1^I\}$ in $\Psi_{sv,N}^I$ and $\{\bar{g}_1^I, h_0^I\}$ in $\Psi_{nsv,N}^I$ and drop the rest, one can predict $(a_s^i/N) \ln^{2i-1}(N)$ terms for CFs for all $i > 1$. We call this tower of logarithms by NSV-Leading Logarithm (NSV-LL). Similarly, knowing, along with the previous ones, $\{\bar{g}_{0,1}^I, g_2^I\}$ in $\Psi_{sv,N}^I$ and $\{\bar{g}_2^I, h_1^I\}$ in $\Psi_{nsv,N}^I$, one can predict $(a_s^i/N) \ln^{2i-2}(N)$ for CFs for all $i > 2$. This belongs to NSV-Next-to-Leading Logarithm (NSV-NLL). In general, resummed result with $\bar{g}_1^I, \dots, \bar{g}_{n+1}^I$ and h_0^I, \dots, h_n^I in $\Psi_{nsv,N}^I$ along with $\bar{g}_{0,0}^I, \dots, \bar{g}_{0,n}^I$ and g_1^I, \dots, g_{n+1}^I in $\Psi_{sv,N}^I$ can predict $(a_s^i/N) \ln^{2i-(n+1)}(N)$ for all $i > n$ in Mellin space N and it is NSV- N^n LL. We summarise our findings in the Table [6.3] below.

GIVEN		PREDICTIONS		
Logarithmic Accuracy	Resummed Exponents	$\Delta_{I,N}^{(2)}$	$\Delta_{I,N}^{(3)}$	$\Delta_{I,N}^{(i)}$
NSV-LL	$\bar{g}_{0,0}^I, g_1^I, \bar{g}_1^I, h_0^I$	L_N^3	L_N^5	L_N^{2i-1}
NSV-NLL	$\bar{g}_{0,1}^I, g_2^I, \bar{g}_2^I, h_1^I$		L_N^4	L_N^{2i-2}
NSV- N^2 LL	$\bar{g}_{0,2}^I, g_3^I, \bar{g}_3^I, h_2^I$			L_N^{2i-3}
NSV- N^n LL	$\bar{g}_{0,n}^I, g_{n+1}^I, \bar{g}_{n+1}^I, h_n^I$			$L_N^{2i-(n+1)}$

Table 6.3: The all order predictions for $1/N$ coefficients of Δ_N^I for a given set of resummation coefficients $\{\bar{g}_{0,i}^I, g_i^I(\omega), \bar{g}_i^I(\omega), h_i^I(\omega)\}$ at a given order. Here $L_N^i = \frac{1}{N} \ln^i(N)$

We find that unlike SV resummed terms, which result from only $\mathcal{D}_0(z)$ and $a_s(q^2(1-z)^2)$, the resummation of NSV terms is controlled in addition by $\ln(1-z)$ at each order in a_s as can be seen

from (6.64). This logarithmic dependence in Φ_{nsv}^I at each order along with resummed $a_s(q^2(1-z)^2)$, allows one to reorganize order one terms differently from SV case. Hence, the resulting NSV resummed result has different logarithmic structure in terms of order one ω compared to that of SV.

Few remarks on the resummed result are in order in the light of previous section. Note that we considered a particular solution Φ_{nsv}^I that corresponds to the case $\alpha = 2$ and summed up order one terms ω in Mellin N -space using the resummed solution to RGE of a_s . While the SV part is insensitive to α , the NSV terms, namely the resummation exponents $h^I(\omega)$ depend on α ($\alpha = 2$) through ω resulting from $a_s(q^2/N^\alpha)$ and the coefficients $\bar{\varphi}_{\alpha,i}^{I,(k)}$. We had already seen how $\bar{\varphi}_{\alpha,i}^{I,(k)}$ transforms with respect to α . The resummed result in the N -space for arbitrary α will be function of $a_s(q^2/N^\alpha)$. This will lead to resummation of order one $\omega_\alpha = \alpha\beta_0 a_s(\mu_R^2) \ln N$ to all orders in a_s . Hence, the summation of order one ω_α terms with α dependent coefficients $\varphi_{\alpha,i}^{I,(k)}$ leads variety of resummed predictions each depending on the choice of α . However, the fixed order predictions for the CFs Δ_I will be unaffected, thanks to the invariance in NSV solution. This invariance has allowed us to choose $\alpha = 2$ to resum order one ω terms analogous to SV counterpart.

There have been several attempts [7, 203, 206–208] in the past to understand the structure of NSV logarithms of inclusive cross sections and its all order structure and in this context, we compare our prediction at LL level for CF of DY, $\Delta_N^{q,LL}$ against that of [206]. Note that the [206] contains NSV terms only to LL accuracy. In [206], within the framework of soft-collinear effective theory (SCET), the authors have obtained leading logarithmic terms at NSV for the quark-antiquark production channel of the DY process to all orders in a_s . This was achieved by extending the factorisation properties of the cross section to NSV level and using renormalisation group equations of NSV operators and soft functions. Using our N -space result, in the LL approximation, that is for DY

$$\Delta_N^{I,LL} = \bar{g}_{0,0}^I \exp \left[\ln N g_1^I(\omega) + \frac{1}{N} \left(\bar{g}_1^I(\omega) + h_0^I(\omega, N) \right) \right] \Big|_{LL} \quad (6.79)$$

we obtain,

$$\Delta_N^{I,LL} = \exp \left[8C_F a_s \left(\ln^2 N + \frac{\ln N}{N} \right) \right] \quad (6.80)$$

where we have expanded the exponents in powers of a_s and kept only terms of $O(1/N)$. The above N -space result can be Mellin transformed to z -space and it reads as

$$\Delta_N^{I,LL} = \Delta_{N,SV}^{I,LL} - 16C_F a_s \exp\left[8C_F a_s \ln^2(1-z)\right] \ln(1-z) \quad (6.81)$$

The above result agrees exactly with Eq.(4.2) of [206] for $\mu = Q$. Our result given in (6.69) contains terms that can in principle resum N^n LL, $n \geq 0$ provided the universal anomalous dimensions and process dependent coefficients are available to desired accuracy in a_s . Hence given three loop results, which are available for several observables, we can perform N^2 LL resummation taking into account NSV logarithms.

The numerical effects of the SV+NSV logarithms have been studied in [?] for the invariant mass distribution of a pair of leptons in DY process at the LHC. The numerical significance of these contributions for fixed order calculations in QCD till N^3 LO is shown in [241] for Drell-Yan process. We find the similar trend for the SV+NSV resummed results as well, wherein a significant enhancement could be observed when the resummed NSV corrections are taken into account. This is illustrated in Table 6.4 where we quote the SV and SV+NSV resummed results along with the fixed order ones for the central scales $Q = \mu_R = \mu_F = 1000$ and 2000 GeV.

$Q = \mu_R = \mu_F$	NNLO	NNLO +NNLL	NNLO+ $\overline{\text{NNLL}}$
1000	$3.2876^{+0.20\%}_{-0.31\%}$	$3.2993^{+0.36\%}_{-0.29\%}$	$3.3191^{+1.13\%}_{-0.86\%}$
2000	$0.0684^{+0.37\%}_{-0.62\%}$	$0.0687^{+0.32\%}_{-0.27\%}$	$0.0692^{+0.89\%}_{-0.78\%}$

Table 6.4: Values of SV and SV+NSV resummed cross section in 10^{-5} pb/GeV at second logarithmic accuracy in comparison to the fixed order results at different central scales .

Here NNLO+NNLL denotes the SV resummed cross section, while NNLO + $\overline{\text{NNLL}}$ refers to the SV+NSV resummed results. Also, the uncertainty arising from renormalization, μ_R , and factorization, μ_F , scales are depicted in terms of percentage errors, which are calculated using 7-point scale variation approach. From these values, it can be observed that the uncertainty band starts widening when we include the NSV corrections. A detailed investigation on this leads to the fact that these large variations are mostly arising due to the μ_F uncertainty. Note that we

have not included resummed contributions from other channels such as qg which are numerically comparable to the diagonal channel. The inclusion of them can reduce the μ_F dependence because different partonic channels mix under μ_F variations when they are convoluted with the appropriate PDFs. However, for the case of renormalization scale variations, the partonic channels do not mix, leading to less sensitivity of our predictions to this scale. This is evident from the Table 6.5 where we depict the μ_R variations of SV+NSV resummed results focusing only the contribution coming from $q\bar{q}$ -channel.

$Q = \mu_R = \mu_F$	NNLO $_{q\bar{q}}$	NNLO $_{q\bar{q}}$ + NNLL	NNLO $_{q\bar{q}}$ + $\overline{\text{NNLL}}$
1000	3.5260 $^{+0.49\%}_{-0.58\%}$	3.5376 $^{+0.25\%}_{-0.39\%}$	3.5576 $^{+0.006\%}_{-0.20\%}$
2000	0.0717 $^{+0.54\%}_{-0.62\%}$	0.0721 $^{+0.19\%}_{-0.33\%}$	0.0725 $^{+0.0\%}_{-0.15\%}$

Table 6.5: Comparison of SV and SV+NSV resummed cross section in 10^{-5} pb/GeV for $q\bar{q}$ -channel at different central scales.

6.6 Physical Evolution Kernel

In the past, in [246], the scheme invariant approach through physical evolution equation was explored to understand the structure of NSV terms for the coefficient functions of DIS cross section. The physical evolution kernel that controls the evolution of the physical observables with respect to external scale q^2 is invariant under scheme transformations with respect to renormalisation and factorisation. This property can be exploited to understand certain universal structure of perturbative predictions. By suitably modifying physical evolution kernel (PEK) [246] with the help of scales in the strong coupling constant and using the renormalisation group invariance, predictions at second and third orders for the CFs of DIS structure functions were made, given the known lower order results for CFs. Even though, the predictions did not agree for some of the color factors, it was found that they were very close to the known results. Using the second order results for DIS, semi-inclusive e^+e^- annihilation and DY, a striking observation was made by Moch and Vogt in [8] (and [52,205]) on the PEK namely the enhancement of a single-logarithms at large z to

all order in $1 - z$. It was found that if one conjectures that it will hold true at every order in a_s , the structure of corresponding leading $\ln(1 - z)$ terms in the kernel can be constrained. This allowed them to predict certain next-to-SV logarithms at higher orders in a_s which are in agreement with the known results up to third order.

Motivated by this approach, we use our formulation that describes next-to-SV logarithms both in z and N -spaces to study the structure of physical evolution equation and present our findings on the structure of leading logarithms in the PEK. For convenience we work in Mellin space. The Mellin moment of hadronic cross section $\sigma(q^2, \tau)$ is given by

$$\sigma_N(q^2) = \int_0^1 d\tau \tau^{N-1} \sigma(q^2, \tau) \quad (6.82)$$

The hadronic observable $\sigma(q^2, \tau)$ is renormalisation scheme (RS) independent namely it does not depend on the scheme in which CFs Δ_{ab} and the structure functions f_c are defined. The fact that f_c is independent of q^2 , the first derivative of σ with respect to q^2 will not depend on f_c . Restricting ourselves to SV and NSV terms, we can define physical evolution kernel \mathcal{K}^I by

$$\begin{aligned} \mathcal{K}^I(a_s(\mu_R^2), N) &= q^2 \frac{d}{dq^2} \ln \left(\frac{\sigma_N(q^2)}{\sigma_B(q^2)} \right) \Big|_{\text{sv+nsv}}, \\ &= q^2 \frac{d}{dq^2} \ln \Delta_N^I(q^2). \end{aligned} \quad (6.83)$$

which is independent of any renormalisation scheme. The kernel $\mathcal{K}^I(a_s(\mu_R^2), N)$ can be computed order by order in perturbation theory using $\ln \Delta_N^I$.

$$\mathcal{K}^I(a_s(\mu_R^2), N) = \sum_{i=1}^{\infty} a_s^i(\mu_R^2) \mathcal{K}_{i-1}^I(N) \quad (6.84)$$

As in [8], the leading $(1/N) \ln^i(N)$ terms at every order defined by \mathcal{K}^I :

$$\overline{\mathcal{K}}_i^I = \mathcal{K}_i^I \Big|_{(1/N) \ln^i(N)} \quad (6.85)$$

can be obtained. Using (6.67), we find that these terms can be obtained directly from $\Psi_{\text{nsv}, N}^I$ alone

and are given by

$$\begin{aligned}
\overline{\mathcal{K}}_0^I &= A_1^I + 2D_1^I, \\
\overline{\mathcal{K}}_1^I &= 2A_1^I\beta_0 - 2C_2^I + 4\beta_0 D_1^I + 2\beta_0 \overline{\varphi}_1^{I,(1)}, \\
\overline{\mathcal{K}}_2^I &= 4A_1^I\beta_0^2 - 8\beta_0 C_2^I + 8\beta_0^2 D_1^I + 8\beta_0^2 \overline{\varphi}_1^{I,(1)} - 4\beta_0 \overline{\varphi}_2^{I,(2)}, \\
\overline{\mathcal{K}}_3^I &= 8A_1^I\beta_0^3 - 24\beta_0^3 C_2^I + 16\beta_0^3 D_1^I + 24\beta_0^3 \overline{\varphi}_1^{I,(1)} - 24\beta_0^2 \overline{\varphi}_2^{I,(2)} + 6\beta_0 \overline{\varphi}_3^{I,(3)}, \\
\overline{\mathcal{K}}_4^I &= 16A_1^I\beta_0^4 - 64\beta_0^4 C_2^I + 32\beta_0^4 D_1^I + 64\beta_0^4 \overline{\varphi}_1^{I,(1)} - 96\beta_0^3 \overline{\varphi}_2^{I,(2)} + 48\beta_0^2 \overline{\varphi}_3^{I,(3)} - 8\beta_0 \overline{\varphi}_4^{I,(4)}. \quad (6.86)
\end{aligned}$$

We find that the structure of $\overline{\mathcal{K}}_i^I$ resembles very much like that of [8]. Interestingly, the leading logarithms at every order depends only on the universal anomalous dimensions A_1^I , D_1^I and C_2^I , and the diagonal coefficients $\overline{\varphi}_k^{I,(k)}$ with $k < i$, where i is the order of the perturbation. In addition, if we substitute the known values for these quantities in the (6.86), we obtain

$$\begin{aligned}
\overline{\mathcal{K}}_1^I &= -8\beta_0 C_R - 32C_R^2 \\
\overline{\mathcal{K}}_2^I &= -16\beta_0^2 C_R - 112\beta_0 C_R^2 \\
\overline{\mathcal{K}}_3^I &= -32\beta_0^3 C_R - \frac{896}{3}\beta_0^2 C_R^2 \\
\overline{\mathcal{K}}_4^I &= -64\beta_0^4 C_R - \frac{2176}{3}\beta_0^3 C_R^2 - 8\beta_0 \overline{\varphi}_4^{I,(4)} \quad (6.87)
\end{aligned}$$

where $C_R = C_F$ for $I = q, b$ and $C_R = C_A$ for $I = g$.

The reason for the agreement of our predictions for PEK to third order with those of [8] is simply because of the K+G equation that Φ^I satisfies. In fact, K+G equation is partonic version of the physical evolution equation and the partonic PEK given by $\overline{K}^I + \overline{G}^I$. The logarithm structure of PEK is controlled by the upper limit i in the summation over the index k in (6.38). In N -space, the highest power of corresponding $\ln(N)$ in the $1/N$ coefficient of \mathcal{K}^I is in turn controlled by the upper limit on the summation in (6.32). Our predictions based on the inherent transcendentality structure of perturbative results are in complete agreement with the logarithmic structure of CFs or PEKs obtained from explicit results. Note that the structure of PEK (6.86) expressed in terms of A_1^I , C_2^I , D_1^I and $\overline{\varphi}_i^{I,(i)}$ is straightforward to understand from K+G equations and renormalisation group invariance. However, as was already noted in [8], the coefficient of the leading logarithms

contains peculiar structure containing only β_0^i and β_0^{i-1} at every order in a_s^i . In addition, if the structure continues to be true at every order, the coefficients $\bar{\varphi}_i^{I,(i)}$ has to be proportional to β_0^{i-2} for every i which can be tested when results beyond third order become available.

6.7 Summary

To summarise, in this chapter, we discussed in detail the structure of SV and next-to-SV logarithms that arises in the inclusive cross section for $2 \rightarrow 1$ processes, focusing on the diagonal partonic channels. The NSV contributions are as important as the SV ones for any precision studies, as they give rise to numerically sizeable corrections. Using IR factorisation and UV renormalisation group invariance, we show that SV+NSV contributions satisfy Sudakov differential equation whose solution provides an all order perturbative result in strong coupling constant. We show that like SV contributions, next-to-SV contributions also demonstrate IR structure in terms of certain infrared anomalous dimensions. However, NSV terms depend, in addition, on certain process dependent functions. The underlying universal IR structure of NSV terms can be further unravelled when results for variety of inclusive reactions become available. In z -space, we show that the next-to-SV contributions do exponentiate allowing us to predict the corresponding next-to-SV logarithms to all orders. We also develop an integral representation for the exponent in the z -space, which can further use to study these threshold logarithms in Mellin N -space. This in turn give rise a framework for resumming the NSV logarithms in N -space. Unlike the SV part of the resummed result, the resummation coefficients for NSV terms are found to be controlled not only by process independent anomalous dimensions but also by process dependent $\bar{\varphi}_i^{I,(k)}$.

The master formula that we obtain in z -space demonstrates a perturbative structure which can predict certain SV and NSV logarithms to all orders in strong coupling constant a_s , given the lower order results. From the available results at a_s and at a_s^2 for the CFs, our predictions for third order NSV logarithms are in complete agreement with the known results available for variety of inclusive reactions, namely DY production and Higgs productions in bottom quark annihilation and gluon fusion. Using the corresponding CFs that are known to third order, our formalism allows us to predict three leading NSV logarithms to all orders starting from fourth order, of

which, we reported here the results to order a_s^7 . We have studied the logarithmic structure of physical evolution kernel, in particular the leading logarithms, and found that they are controlled only by process independent anomalous dimensions $\beta_0, A_1^I, C_2^I, D_1^I$ and diagonal coefficients $\bar{\varphi}_i^{I,(i)}$ at every order a_s^i . We conclude by noting that the structure of NSV logarithms demonstrates a rich perturbative structure that need to be explored further.

A QCD Feynman rules

The QCD Feynman rules derived from quantised Lagrangian Eq.(2.1) is given below. The solid, curly and dotted lines refers to quarks, gluons and ghosts respectively. The ξ denotes the gauge fixing parameter. Note that, symmetry factor is multiplied appropriately and also quark and ghost loops are multiplied by a factor of (-1).

- quark propagator

$$\begin{array}{ccc}
 j, \beta & & i, \alpha \\
 \xrightarrow{\hspace{2cm}} & & \\
 \leftarrow p_2 & & \rightarrow p_1
 \end{array}
 \quad
 i (2\pi)^4 \delta^{(4)}(p_1 + p_2) \delta_{ij} \left(\frac{1}{\not{p}_1 - m_f + i\epsilon} \right)_{\alpha\beta}$$

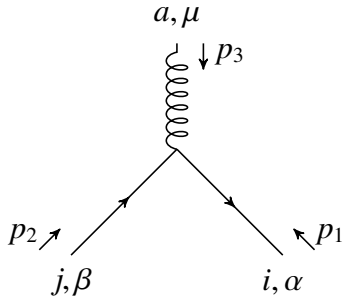
- gluon propagator

$$\begin{array}{ccc}
 b, \nu & & a, \mu \\
 \text{~~~~~} & & \\
 \leftarrow p_2 & & \rightarrow p_1
 \end{array}
 \quad
 i (2\pi)^4 \delta^{(4)}(p_1 + p_2) \delta_{ab} \frac{1}{p_1^2} \left[-g_{\mu\nu} + (1 - \xi) \frac{p_{1\mu} p_{1\nu}}{p_1^2} \right]$$

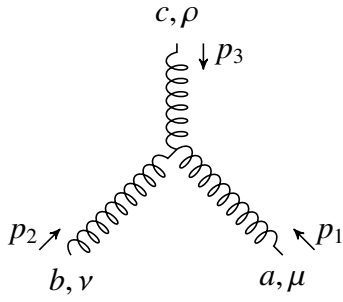
- ghost propagator

$$\begin{array}{ccc}
 b & & a \\
 \text{-----} & & \\
 \leftarrow p_2 & & \rightarrow p_1
 \end{array}
 \quad
 i (2\pi)^4 \delta^{(4)}(p_1 + p_2) \delta_{ab} \frac{1}{p_1^2}$$

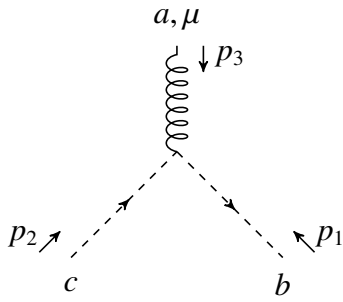
- The interacting vertices:



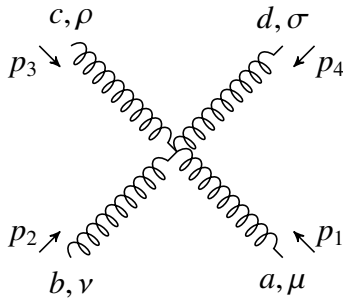
$$i\hat{g}_s (2\pi)^4 \delta^{(4)}(p_1 + p_2 + p_3) T_{ij}^a (\gamma^\mu)_{\alpha\beta}$$



$$\frac{1}{3!} \hat{g}_s (2\pi)^4 \delta^{(4)}(p_1 + p_2 + p_3) f^{abc} \\ \times [g^{\mu\nu}(p_1 - p_2)^\rho + g^{\nu\rho}(p_2 - p_3)^\mu + g^{\rho\mu}(p_3 - p_1)^\nu]$$



$$-g_s (2\pi)^4 \delta^{(4)}(p_1 + p_2 + p_3) f^{abc} p_1^\mu$$



$$-\frac{1}{4!} \hat{g}_s^2 (2\pi)^4 \delta^{(4)}(p_1 + p_2 + p_3 + p_4) \\ \left\{ (f^{acx} f^{bdx} - f^{adx} f^{cbx}) g^{\mu\nu} g^{\rho\sigma} \right. \\ + (f^{abx} f^{cdx} - f^{adx} f^{bcx}) g^{\mu\rho} g^{\nu\sigma} \\ \left. + (f^{acx} f^{dbx} - f^{abx} f^{cdx}) g^{\mu\sigma} g^{\nu\rho} \right\}$$

B Anomalous dimensions

Here we present available cusp A^I , collinear B^I , soft f^I and mass γ^I anomalous dimensions.

Cusp anomalous dimension

The cusp anomalous dimensions are available to four loop. Since they exhibit *generalised Casimir scaling principle*, we can write them together with: $C_R = C_A$ for $I = g$ and $C_R = C_f$ for $I = q, b$.

$$\begin{aligned}
A_1^I &= C_R \{4\}, \\
A_2^I &= C_R C_A \left\{ \frac{268}{9} - 8\zeta_2 \right\} + C_R n_f \left\{ -\frac{40}{9} \right\}, \\
A_3^I &= C_R C_A^2 \left\{ \frac{490}{3} - \frac{1072\zeta_2}{9} + \frac{88\zeta_3}{3} + \frac{176\zeta_2^2}{5} \right\} + C_R C_F n_f \left\{ -\frac{110}{3} + 32\zeta_3 \right\} \\
&\quad + C_R C_A n_f \left\{ -\frac{836}{27} + \frac{160\zeta_2}{9} - \frac{112\zeta_3}{3} \right\} + C_A n_f^2 \left\{ -\frac{16}{27} \right\} \\
A_4^I &= \frac{d_A^{abcd} d_R^{abcd}}{N_R} \left(\frac{3520}{3} \zeta_5 + \frac{128}{3} \zeta_3 - 384\zeta_3^2 - 128\zeta_2 - \frac{7936}{35} \zeta_2^3 \right) \\
&\quad + n_f \frac{d_F^{abcd} d_R^{abcd}}{N_R} \left(-\frac{1280}{3} \zeta_5 - \frac{256}{3} \zeta_3 + 256\zeta_2 \right) + C_R n_f^3 \left(-\frac{32}{81} + \frac{64}{27} \zeta_3 \right) \\
&\quad + C_F C_R n_f^2 \left(\frac{2392}{81} - \frac{640}{9} \zeta_3 + \frac{64}{5} \zeta_2^2 \right) + C_F^2 C_R n_f \left(\frac{572}{9} - 320\zeta_5 + \frac{592}{3} \zeta_3 \right) \\
&\quad + C_A C_R n_f^2 \left(\frac{923}{81} + \frac{2240}{27} \zeta_3 - \frac{608}{81} \zeta_2 - \frac{224}{15} \zeta_2^2 \right) + C_A C_F C_R n_f \left(-\frac{34066}{81} + 160\zeta_5 + \frac{3712}{9} \zeta_3 \right) \\
&\quad + \frac{440}{3} \zeta_2 - 128\zeta_2 \zeta_3 - \frac{352}{5} \zeta_2^2 \right) + C_A^2 C_R n_f \left(-\frac{24137}{81} + \frac{2096}{9} \zeta_5 - \frac{23104}{27} \zeta_3 + \frac{20320}{81} \zeta_2 \right) \\
&\quad + \frac{448}{3} \zeta_2 \zeta_3 - \frac{352}{15} \zeta_2^2 \right) + C_A^3 C_R \left(\frac{84278}{81} - \frac{3608}{9} \zeta_5 + \frac{20944}{27} \zeta_3 - 16\zeta_3^2 - \frac{88400}{81} \zeta_2 \right. \\
&\quad \left. - \frac{352}{3} \zeta_2 \zeta_3 + \frac{3608}{5} \zeta_2^2 - \frac{20032}{105} \zeta_2^3 \right). \tag{B.1}
\end{aligned}$$

where the quartic casimirs are given by

$$\frac{d_F^{abcd} d_A^{abcd}}{N_A} = \frac{N_c(N_c^2 + 6)}{48}, \quad \frac{d_F^{abcd} d_F^{abcd}}{N_A} = \frac{(N_c^4 - 6N_c^2 + 18)}{96N_c^2}, \quad (\text{B.2})$$

with $N_A = N_c^2 - 1$ and $N_F = N_c$ where $N_c = 3$ for QCD.

Soft anomalous dimension

The soft anomalous dimensions f^I 's are obtained as follows. They also satisfy Casimir scaling.

Hence, below we denote $C_R = C_A$ for $I = g$ and $C_R = C_f$ for $I = q, b$.

$$\begin{aligned} f_1^I &= 0, \\ f_2^I &= C_A C_R \left\{ -\frac{22}{3} \zeta_2 - 28 \zeta_3 + \frac{808}{27} \right\} + C_R n_f \left\{ \frac{4}{3} \zeta_2 - \frac{112}{27} \right\}, \\ f_3^I &= C_A^2 C_R \left\{ \frac{352}{5} \zeta_2^2 + \frac{176}{3} \zeta_2 \zeta_3 - \frac{12650}{81} \zeta_2 - \frac{1316}{3} \zeta_3 + 192 \zeta_5 + \frac{136781}{729} \right\} \\ &+ C_A C_R n_f \left\{ -\frac{96}{5} \zeta_2^2 + \frac{2828}{81} \zeta_2 + \frac{728}{27} \zeta_3 - \frac{11842}{729} \right\} \\ &+ C_R C_F n_f \left\{ \frac{32}{5} \zeta_2^2 + 4 \zeta_2 + \frac{304}{9} \zeta_3 - \frac{1711}{27} \right\} + C_R n_f^2 \left\{ -\frac{40}{27} \zeta_2 + \frac{112}{27} \zeta_3 - \frac{2080}{729} \right\}. \end{aligned} \quad (\text{B.3})$$

Collinear anomalous dimension

Similarly, the collinear anomalous dimension (B^I)'s are given as follows. They do not satisfy Casimir scaling. However, they depends only on the incoming partons, hence $B_i^a = B_i^b$.

$$\begin{aligned} B_1^g &= C_A \left\{ \frac{11}{3} \right\} - n_f \left\{ \frac{2}{3} \right\}, \\ B_2^g &= C_A^2 \left\{ \frac{32}{3} + 12 \zeta_3 \right\} - n_f C_A \left\{ \frac{8}{3} \right\} - n_f C_F \{2\}, \\ B_3^g &= C_A C_F n_f \left\{ -\frac{241}{18} \right\} + C_A n_f^2 \left\{ \frac{29}{18} \right\} - C_A^2 n_f \left\{ \frac{233}{18} + \frac{8}{3} \zeta_2 + \frac{4}{3} \zeta_2^2 + \frac{80}{3} \zeta_3 \right\} \\ &+ C_A^3 \left\{ \frac{79}{2} - 16 \zeta_2 \zeta_3 + \frac{8}{3} \zeta_2 + \frac{22}{3} \zeta_2^2 + \frac{536}{3} \zeta_3 - 80 \zeta_5 \right\} + C_F n_f^2 \left\{ \frac{11}{9} \right\} + C_F^2 n_f \{1\}, \end{aligned} \quad (\text{B.4})$$

$$\begin{aligned}
B_1^q &= C_F \{3\}, \\
B_2^q &= C_F^2 \left\{ \frac{3}{2} - 12\zeta_2 + 24\zeta_3 \right\} + C_A C_F \left\{ \frac{17}{34} + \frac{88}{6}\zeta_2 - 12\zeta_3 \right\} + n_f C_F T_F \left\{ -\frac{2}{3} - \frac{16}{3}\zeta_2 \right\}, \\
B_3^q &= C_A^2 C_F \left\{ -2\zeta_2^2 + \frac{4496}{27}\zeta_2 - \frac{1552}{9}\zeta_3 + 40\zeta_5 - \frac{1657}{36} \right\} + C_A C_F^2 \left\{ -\frac{988}{15}\zeta_2^2 \right. \\
&\quad \left. + 16\zeta_2\zeta_3 - \frac{410}{3}\zeta_2 + \frac{844}{3}\zeta_3 + 120\zeta_5 + \frac{151}{4} \right\} + C_A C_F n_f \left\{ \frac{4}{5}\zeta_2^2 - \frac{1336}{27}\zeta_2 + \frac{200}{9}\zeta_3 \right. \\
&\quad \left. + 20 \right\} + C_F^3 \left\{ \frac{288}{5}\zeta_2^2 - 32\zeta_2\zeta_3 + 18\zeta_2 + 68\zeta_3 - 240\zeta_5 + \frac{29}{2} \right\} \\
&\quad + C_F^2 n_f \left\{ \frac{232}{15}\zeta_2^2 + \frac{20}{3}\zeta_2 - \frac{136}{3}\zeta_3 - 23 \right\} + C_F n_f^2 \left\{ \frac{80}{27}\zeta_2 - \frac{16}{9}\zeta_3 - \frac{17}{9} \right\}, \tag{B.5}
\end{aligned}$$

Mass or UV anomalous dimension

The process dependent UV anomalous dimension γ 's are obtained as:

$$\begin{aligned}
\gamma_{b,1}^H &= 3C_F, \\
\gamma_{b,2}^H &= \frac{3}{2}C_F^2 + \frac{97}{6}C_F C_A - \frac{5}{3}C_F n_f, \\
\gamma_{b,3}^H &= \frac{129}{2}C_F^3 - \frac{129}{4}C_F^2 C_A + \frac{11413}{108}C_F C_A^2 + (-23 + 24\zeta_3)C_F^2 n_f \\
&\quad + \left(-\frac{278}{27} - 24\zeta_3 \right) C_F C_A n_f - \frac{35}{27}C_F n_f^2 \tag{B.6}
\end{aligned}$$

$$\gamma_{q,1}^H = 0, \quad \gamma_{q,2}^H = 0, \quad \gamma_{q,3}^H = 0 \tag{B.7}$$

$$\gamma_{g,1}^H = \beta_0, \quad \gamma_{g,2}^H = 2\beta_1, \quad \gamma_{g,3}^H = 3\beta_2 \tag{B.8}$$

C The relevant coefficients for form factor and Soft-collinear distributions

Here, we present the relevant coefficients required for form factor and soft-collinear distributions, which are extracted from the available explicit results. In the following, $C_R = C_F$ for $I = q, b$ and $C_R = C_A$ for $I = g$, where $C_A \equiv N_c$ and $C_F \equiv \frac{N_c^2 - 1}{2N_c}$ are the Casimirs of adjoint and fundamental representations.

Inclusive

Coefficients $g_i^{I,j}$'s :

The finite coefficients $g_i^{I,j}$'s coming from the explicit calculation of the form factor are given as below. For the gluon form factor:

$$g_1^{g,1} = C_A \left\{ \zeta_2 \right\}, \quad g_1^{g,2} = C_A \left\{ 1 - \frac{7}{3} \zeta_3 \right\}, \quad g_1^{g,3} = C_A \left\{ -\frac{3}{2} + \frac{47}{80} \zeta_2^2 \right\}, \quad (\text{C.1})$$

$$g_2^{g,1} = C_F n_f \left\{ -\frac{67}{3} + 16 \zeta_3 \right\} + C_A n_f \left\{ -\frac{1724}{81} - \frac{40}{3} \zeta_3 - \frac{10}{3} \zeta_2 \right\} + C_A^2 \left\{ \frac{4511}{81} - \frac{44}{3} \zeta_3 + \frac{67}{3} \zeta_2 \right\}, \quad (\text{C.2})$$

$$g_2^{g,2} = C_F n_f \left\{ \frac{2027}{36} - \frac{92}{3} \zeta_3 - \frac{7}{3} \zeta_2 - \frac{16}{3} \zeta_2^2 \right\} + C_A n_f \left\{ \frac{24103}{486} + \frac{604}{27} \zeta_3 + \frac{16}{9} \zeta_2 + \frac{259}{60} \zeta_2^2 \right\} + C_A^2 \left\{ -\frac{141677}{972} - 39 \zeta_5 + \frac{1139}{27} \zeta_3 - \frac{142}{9} \zeta_2 + \frac{5}{3} \zeta_2 \zeta_3 + \frac{671}{120} \zeta_2^2 \right\}, \quad (\text{C.3})$$

$$g_3^{g,1} = C_F n_f^2 \left\{ \frac{6508}{27} - \frac{1376}{9} \zeta_3 - \frac{88}{9} \zeta_2 - \frac{368}{45} \zeta_2^2 \right\} + C_F^2 n_f \left\{ \frac{304}{3} - 480 \zeta_5 + 296 \zeta_3 \right\}$$

$$\begin{aligned}
& + C_A n_f^2 \left\{ \frac{912301}{4374} + \frac{6992}{81} \zeta_3 + \frac{100}{27} \zeta_2 + \frac{232}{45} \zeta_2^2 \right\} \\
& + C_A C_F n_f \left\{ -\frac{473705}{324} + \frac{608}{3} \zeta_5 + \frac{20384}{27} \zeta_3 + \frac{503}{18} \zeta_2 + 40 \zeta_2 \zeta_3 + \frac{1568}{45} \zeta_2^2 \right\} \\
& + C_A^2 n_f \left\{ -\frac{5035009}{2187} + \frac{272}{3} \zeta_5 - \frac{11372}{81} \zeta_3 - \frac{14225}{243} \zeta_2 - \frac{88}{9} \zeta_2 \zeta_3 - \frac{128}{45} \zeta_2^2 \right\} \\
& + C_A^3 \left\{ +\frac{39497339}{8748} + \frac{3080}{3} \zeta_5 - \frac{57830}{27} \zeta_3 - \frac{104}{3} \zeta_3^2 + \frac{221521}{486} \zeta_2 - \frac{1496}{9} \zeta_2 \zeta_3 \right. \\
& \left. - \frac{5744}{45} \zeta_2^2 - \frac{12352}{315} \zeta_2^3 \right\}. \tag{C.4}
\end{aligned}$$

For the quark form factor in Drell-Yan:

$$g_1^{q,1} = C_F \{ \zeta_2 - 8 \}, \quad g_1^{q,2} = C_F \left\{ 8 - \frac{7}{3} \zeta_3 - \frac{3}{4} \zeta_2 \right\}, \quad g_1^{q,3} = C_F \left\{ \frac{7}{4} \zeta_3 + \zeta_2 + \frac{47}{80} \zeta_2^2 - 8 \right\}, \tag{C.5}$$

$$\begin{aligned}
g_2^{q,1} &= C_F n_f \left\{ \frac{5813}{162} - \frac{8}{3} \zeta_3 + \frac{37}{9} \zeta_2 \right\} + C_A C_F \left\{ -\frac{70165}{324} + \frac{260}{3} \zeta_3 - \frac{575}{18} \zeta_2 + \frac{88}{5} \zeta_2^2 \right\} \\
& + C_F^2 \left\{ -\frac{1}{4} - 60 \zeta_3 + 58 \zeta_2 - \frac{88}{5} \zeta_2^2 \right\}, \tag{C.6}
\end{aligned}$$

$$\begin{aligned}
g_2^{q,2} &= C_F n_f \left\{ -\frac{129389}{1944} + \frac{301}{27} \zeta_3 - \frac{425}{54} \zeta_2 + \frac{7}{12} \zeta_2^2 \right\} \\
& + C_F^2 \left\{ -\frac{109}{16} + 12 \zeta_5 + 184 \zeta_3 - \frac{437}{4} \zeta_2 - 28 \zeta_2 \zeta_3 + \frac{108}{5} \zeta_2^2 \right\} \\
& + C_A C_F \left\{ \frac{1547797}{3888} - 51 \zeta_5 - \frac{12479}{54} \zeta_3 + \frac{7297}{108} \zeta_2 + \frac{89}{3} \zeta_2 \zeta_3 - \frac{653}{24} \zeta_2^2 \right\}, \tag{C.7}
\end{aligned}$$

$$\begin{aligned}
g_3^{q,1} &= C_F N_4 n_{fv} \left\{ 12 - 80 \zeta_5 + 14 \zeta_3 + 30 \zeta_2 - \frac{6}{5} \zeta_2^2 \right\} + C_F n_f^2 \left\{ \frac{536}{81} \zeta_3 - \frac{258445}{2187} - \frac{3466}{81} \zeta_2 - \frac{40}{9} \zeta_2^2 \right\} \\
& + C_F^2 n_f \left\{ \frac{73271}{162} - \frac{368}{3} \zeta_5 + \frac{19700}{27} \zeta_3 - \frac{7541}{18} \zeta_2 - \frac{152}{3} \zeta_2 \zeta_3 - \frac{704}{45} \zeta_2^2 \right\} \\
& + C_F^3 \left\{ -\frac{1527}{4} + 1992 \zeta_5 - 2130 \zeta_3 + 48 \zeta_3^2 - 206 \zeta_2 + 840 \zeta_2 \zeta_3 - 534 \zeta_2^2 + \frac{21584}{105} \zeta_2^3 \right\} \\
& + C_A C_F n_f \left\{ \frac{3702974}{2187} - 72 \zeta_5 - \frac{68660}{81} \zeta_3 + \frac{155008}{243} \zeta_2 + \frac{392}{9} \zeta_2 \zeta_3 - \frac{1298}{45} \zeta_2^2 \right\} \\
& + C_A C_F^2 \left\{ \frac{230}{3} - \frac{3020}{3} \zeta_5 - \frac{23402}{9} \zeta_3 + 296 \zeta_3^2 + \frac{55499}{18} \zeta_2 - \frac{3448}{3} \zeta_2 \zeta_3 \right. \\
& + \frac{2432}{45} \zeta_2^2 - \frac{15448}{105} \zeta_2^3 \left. \right\} + C_A^2 C_F \left\{ -\frac{48902713}{8748} + \frac{688}{3} \zeta_5 + \frac{85883}{18} \zeta_3 - \frac{1136}{3} \zeta_3^2 \right. \\
& \left. - \frac{1083305}{486} \zeta_2 + \frac{1786}{9} \zeta_2 \zeta_3 + \frac{37271}{90} \zeta_2^2 - \frac{6152}{63} \zeta_2^3 \right\}. \tag{C.8}
\end{aligned}$$

Here $N_4 = (N_c^2 - 4)/N_c$ and n_{fv} is proportional to the charge weighted sum of the quark flavors [58].

For the bottom quark form factor in $b\bar{b} \rightarrow H$ process:

$$g_1^{b,1} = C_F \left\{ -2 + \zeta_2 \right\}, \quad g_1^{b,2} = C_F \left\{ 2 - \frac{7}{3} \zeta_3 \right\}, \quad g_1^{b,3} = C_F \left\{ -2 + \frac{1}{4} \zeta_2 + \frac{47}{80} \zeta_2^2 \right\}, \quad (\text{C.9})$$

$$g_2^{b,1} = C_{Fnf} \left\{ \frac{616}{81} - \frac{8}{3} \zeta_3 + \frac{10}{9} \zeta_2 \right\} + C_F^2 \left\{ 8 - 60 \zeta_3 + 32 \zeta_2 - \frac{88}{5} \zeta_2^2 \right\} \\ + C_A C_F \left\{ -\frac{2122}{81} + \frac{152}{3} \zeta_3 - \frac{103}{9} \zeta_2 + \frac{88}{5} \zeta_2^2 \right\}, \quad (\text{C.10})$$

$$g_2^{b,2} = C_{Fnf} \left\{ \frac{130}{27} \zeta_3 - \frac{3100}{243} - \frac{55}{27} \zeta_2 + \frac{7}{12} \zeta_2^2 \right\} - C_F^2 \left\{ 24 - 12 \zeta_5 - 116 \zeta_3 + 44 \zeta_2 + 28 \zeta_2 \zeta_3 - \frac{96}{5} \zeta_2^2 \right\} \\ + C_A C_F \left\{ \frac{9142}{243} - 51 \zeta_5 - \frac{2923}{27} \zeta_3 + \frac{1079}{54} \zeta_2 + \frac{89}{3} \zeta_2 \zeta_3 - \frac{365}{24} \zeta_2^2 \right\}, \quad (\text{C.11})$$

$$g_3^{b,1} = C_{Fnf}^2 \left\{ -\frac{27352}{2187} + \frac{320}{81} \zeta_3 - \frac{892}{81} \zeta_2 - \frac{40}{9} \zeta_2^2 \right\} \\ + C_{Fnf}^2 \left\{ \frac{32899}{324} - \frac{368}{3} \zeta_5 + \frac{15956}{27} \zeta_3 - \frac{3173}{18} \zeta_2 - \frac{152}{3} \zeta_2 \zeta_3 + \frac{772}{45} \zeta_2^2 \right\} \\ + C_F^3 \left\{ 603 + 1272 \zeta_5 - 2142 \zeta_3 + 48 \zeta_3^2 - 275 \zeta_2 + 624 \zeta_2 \zeta_3 - \frac{1644}{5} \zeta_2^2 + \frac{21584}{105} \zeta_2^3 \right\} \\ + C_A C_{Fnf} \left\{ -\frac{6119}{4374} - 72 \zeta_5 - \frac{41552}{81} \zeta_3 + \frac{44551}{243} \zeta_2 + \frac{392}{9} \zeta_2 \zeta_3 - \frac{1064}{45} \zeta_2^2 \right\} \\ + C_A C_F^2 \left\{ -\frac{613}{3} - \frac{1940}{3} \zeta_5 - \frac{11570}{9} \zeta_3 + 296 \zeta_3^2 + \frac{13357}{9} \zeta_2 - \frac{2584}{3} \zeta_2 \zeta_3 - \frac{3634}{45} \zeta_2^2 \right. \\ \left. - \frac{15448}{105} \zeta_2^3 \right\} + C_A^2 C_F \left\{ \frac{4095263}{8748} + \frac{1228}{3} \zeta_5 + \frac{19582}{9} \zeta_3 - \frac{1136}{3} \zeta_3^2 - \frac{342263}{486} \zeta_2 + \frac{976}{9} \zeta_2 \zeta_3 \right. \\ \left. + \frac{2738}{9} \zeta_2^2 - \frac{6152}{63} \zeta_2^3 \right\}. \quad (\text{C.12})$$

The coefficients $\bar{\mathcal{G}}_i^{I,k}$ s:

The SV coefficients $\bar{\mathcal{G}}_i^{I,k}$ that appear in soft-collinear distributions in Eq.(2.77) are found to be:

$$\bar{\mathcal{G}}_1^{I,1} = C_R \left(-3 \zeta_2 \right), \quad \bar{\mathcal{G}}_1^{I,2} = C_R \left(\frac{7}{3} \zeta_3 \right), \quad (\text{C.13})$$

$$\bar{\mathcal{G}}_1^{I,3} = C_R \left(-\frac{3}{16} \zeta_2^2 \right), \quad \bar{\mathcal{G}}_1^{I,4} = C_R \left(-\frac{7}{8} \zeta_2 \zeta_3 + \frac{31}{20} \zeta_5 \right), \quad (\text{C.14})$$

$$\bar{\mathcal{G}}_2^{I,1} = C_R C_A \left(\frac{2428}{81} - \frac{469}{9} \zeta_2 + 4 \zeta_2^2 - \frac{176}{3} \zeta_3 \right) + C_{Rnf} \left(-\frac{328}{81} + \frac{70}{9} \zeta_2 + \frac{32}{3} \zeta_3 \right), \quad (\text{C.15})$$

$$\bar{\mathcal{G}}_2^{I,2} = C_{Rnf} \left(\frac{976}{243} - \frac{196}{27} \zeta_2 - \frac{1}{20} \zeta_2^2 - \frac{310}{27} \zeta_3 \right) \\ + C_R C_A \left(-\frac{7288}{243} + \frac{1414}{27} \zeta_2 + \frac{11}{40} \zeta_2^2 + \frac{2077}{27} \zeta_3 - \frac{203}{3} \zeta_2 \zeta_3 + 43 \zeta_5 \right), \quad (\text{C.16})$$

$$\begin{aligned}
\bar{\mathcal{G}}_3^{I,1} = & C_R C_A^2 \left(\frac{152}{63} \zeta_2^3 + \frac{1964}{9} \zeta_2^2 + \frac{11000}{9} \zeta_2 \zeta_3 - \frac{765127}{486} \zeta_2 + \frac{536}{3} \zeta_3^2 - \frac{59648}{27} \zeta_3 \right. \\
& - \left. \frac{1430}{3} \zeta_5 + \frac{7135981}{8748} \right) + C_R C_{A n_f} \left(-\frac{532}{9} \zeta_2^2 - \frac{1208}{9} \zeta_2 \zeta_3 + \frac{105059}{243} \zeta_2 \right. \\
& + \left. \frac{45956}{81} \zeta_3 + \frac{148}{3} \zeta_5 - \frac{716509}{4374} \right) + C_R C_{F n_f} \left(\frac{152}{15} \zeta_2^2 - 88 \zeta_2 \zeta_3 + \frac{605}{6} \zeta_2 + \frac{2536}{27} \zeta_3 \right. \\
& + \left. \frac{112}{3} \zeta_5 - \frac{42727}{324} \right) + C_R n_f^2 \left(\frac{32}{9} \zeta_2^2 - \frac{1996}{81} \zeta_2 - \frac{2720}{81} \zeta_3 + \frac{11584}{2187} \right). \tag{C.17}
\end{aligned}$$

Rapidity

The coefficients $\tilde{\mathcal{G}}_{d,i}^{I,(k)}$ that appear in soft-collinear operator in Eq.(D.1) of differential rapidity distributions is given by:

$$\tilde{\mathcal{G}}_{d,1}^{I,1} = -\zeta_2 C_R, \quad \tilde{\mathcal{G}}_{d,1}^{I,2} = \frac{1}{3} C_R \zeta_3, \quad \tilde{\mathcal{G}}_{d,1}^{I,3} = \frac{1}{80} C_R \zeta_2^2, \quad \tilde{\mathcal{G}}_{d,1}^{I,4} = \frac{1}{20} \zeta_5 C_R - \frac{1}{24} \zeta_2 \zeta_3 C_R, \tag{C.18}$$

$$\tilde{\mathcal{G}}_{d,2}^{I,1} = C_R C_A \left(\frac{2428}{81} - \frac{67}{3} \zeta_2 - 4 \zeta_2^2 - \frac{44}{3} \zeta_3 \right) + C_R n_f \left(\frac{-328}{81} + \frac{10}{3} \zeta_2 + \frac{8}{3} \zeta_3 \right), \tag{C.19}$$

$$\begin{aligned}
\tilde{\mathcal{G}}_{d,2}^{I,2} = & C_R n_f \left(\frac{976}{243} - \frac{70}{27} \zeta_3 - \frac{28}{9} \zeta_2 + \frac{29}{60} \zeta_2^2 \right) \\
& + C_A C_R \left(-\frac{7288}{243} + 43 \zeta_5 + \frac{469}{27} \zeta_3 + \frac{202}{9} \zeta_2 - \frac{71}{3} \zeta_2 \zeta_3 - \frac{319}{120} \zeta_2^2 \right), \tag{C.20}
\end{aligned}$$

$$\begin{aligned}
\tilde{\mathcal{G}}_{d,2}^{I,3} = & C_R n_f \left(-\frac{2920}{729} + 2 \zeta_5 + \frac{196}{81} \zeta_3 + \frac{82}{27} \zeta_2 - \frac{41}{18} \zeta_2 \zeta_3 - \frac{5}{12} \zeta_2^2 \right) \\
& + C_A C_R \left(\frac{21868}{729} - 11 \zeta_5 - \frac{1414}{81} \zeta_3 + \frac{77}{6} \zeta_3^2 - \frac{607}{27} \zeta_2 + \frac{451}{36} \zeta_2 \zeta_3 + \frac{67}{24} \zeta_2^2 - \frac{1129}{420} \zeta_2^3 \right), \tag{C.21}
\end{aligned}$$

$$\begin{aligned}
\tilde{\mathcal{G}}_{d,3}^{I,1} = & C_R n_f^2 \left(\frac{11584}{2187} - \frac{320}{81} \zeta_3 - \frac{316}{27} \zeta_2 + \frac{152}{45} \zeta_2^2 \right) \\
& + C_R C_{F n_f} \left(-\frac{42727}{324} + \frac{112}{3} \zeta_5 + \frac{1672}{27} \zeta_3 + \frac{275}{6} \zeta_2 - 40 \zeta_2 \zeta_3 + \frac{152}{15} \zeta_2^2 \right) \\
& + C_R C_{A n_f} \left(-\frac{716509}{4374} + \frac{148}{3} \zeta_5 + \frac{12356}{81} \zeta_3 + \frac{51053}{243} \zeta_2 - \frac{392}{9} \zeta_2 \zeta_3 - \frac{1372}{45} \zeta_2^2 \right) \\
& + C_A^2 C_R \left(\frac{7135981}{8748} - \frac{1430}{3} \zeta_5 - 936 \zeta_3 + \frac{536}{3} \zeta_3^2 - \frac{379417}{486} \zeta_2 + \frac{4136}{9} \zeta_2 \zeta_3 + \frac{1538}{15} \zeta_2^2 + \frac{17392}{315} \zeta_2^3 \right). \tag{C.22}
\end{aligned}$$

Threshold exponents \mathbf{D}'_d s:

The threshold exponent \mathbf{D}'_d that appear in the rapidity resummation formula as given in Eq.(5.41)

$$\mathbf{D}'_{d,1} = 0 \quad , \mathbf{D}'_{d,2} = C_R n_f \left(\frac{112}{27} - \frac{8\zeta_2}{3} \right) + C_R C_A \left(-\frac{808}{27} + \frac{44\zeta_2}{3} + 28\zeta_3 \right) \quad (\text{C.23})$$

$$\begin{aligned} \mathbf{D}'_{d,3} = & C_R C_A n_f \left(\frac{62626}{729} - \frac{7760\zeta_2}{81} + \frac{208\zeta_2^2}{15} - \frac{536\zeta_3}{9} \right) + C_R C_F n_f \left(\frac{1711}{27} - 8\zeta_2 - \frac{32\zeta_2^2}{5} - \frac{304\zeta_3}{9} \right) \\ & + C_R n_f^2 \left(-\frac{1856}{729} + \frac{160\zeta_2}{27} - \frac{32\zeta_3}{27} \right) \\ & + C_R C_A^2 \left(-\frac{297029}{729} + \frac{27752\zeta_2}{81} - \frac{616\zeta_2^2}{15} + \frac{14264\zeta_3}{27} - \frac{176\zeta_2\zeta_3}{3} - 192\zeta_5 \right) \end{aligned} \quad (\text{C.24})$$

D Soft-collinear distribution for rapidity distribution

In this section, we present soft-collinear distribution $\mathbf{S}_{d,I}$, as defined in (5.25), in powers of $a_s(\mu_R^2)$ up to N⁴LO. Expanding the quantity in powers of a_s as

$$\mathbf{S}_{d,I}(z_1, z_2, q^2, \mu_R^2, \mu_F^2) = \delta(1 - z_1)\delta(1 - z_2) + \sum_{i=1}^{\infty} a_s^i(\mu_R^2) \mathbf{S}_{d,i}^I(z_1, z_2, q^2, \mu_R^2, \mu_F^2), \quad (\text{D.1})$$

we present the results for $\mu_R^2 = \mu_F^2 = q^2$.

$$\begin{aligned} \mathbf{S}_{d,1}^I &= \mathcal{D}_0 \overline{\mathcal{D}}_0 \left\{ \frac{1}{2} A_1^I \right\} + \delta(1 - z_1) \overline{\mathcal{D}}_1 \left\{ A_1^I \right\} + \delta(1 - z_1) \overline{\mathcal{D}}_0 \left\{ -f_1^I \right\} \\ &\quad + \delta(1 - z_1) \delta(1 - z_2) \left\{ \tilde{\mathcal{G}}_{d,1}^{I,1} \right\} + (z_1 \leftrightarrow z_2), \\ \mathbf{S}_{d,2}^I &= \mathcal{D}_1 \overline{\mathcal{D}}_1 \left\{ \frac{3}{2} (A_1^I)^2 \right\} + \mathcal{D}_0 \overline{\mathcal{D}}_2 \left\{ \frac{3}{2} (A_1^I)^2 \right\} + \mathcal{D}_0 \overline{\mathcal{D}}_1 \left\{ -3A_1^I f_1^I - \beta_0 A_1^I \right\} + \mathcal{D}_0 \overline{\mathcal{D}}_0 \left\{ \frac{1}{2} (f_1^I)^2 + \frac{1}{2} A_2^I \right. \\ &\quad \left. + A_1^I \tilde{\mathcal{G}}_{d,1}^{I,1} - (A_1^I)^2 \zeta_2 + \frac{1}{2} \beta_0 f_1^I \right\} + \delta(1 - z_1) \overline{\mathcal{D}}_3 \left\{ \frac{1}{2} (A_1^I)^2 \right\} + \delta(1 - z_1) \overline{\mathcal{D}}_2 \left\{ -\frac{3}{2} A_1^I f_1^I - \frac{1}{2} \beta_0 A_1^I \right\} \\ &\quad + \delta(1 - z_1) \overline{\mathcal{D}}_1 \left\{ (f_1^I)^2 + A_2^I + 2A_1^I \tilde{\mathcal{G}}_{d,1}^{I,1} - 2(A_1^I)^2 \zeta_2 + \beta_0 f_1^I \right\} + \delta(1 - z_1) \overline{\mathcal{D}}_0 \left\{ -f_2^I - 2f_1^I \tilde{\mathcal{G}}_{d,1}^{I,1} \right. \\ &\quad \left. + 2A_1^I \zeta_2 f_1^I + 2(A_1^I)^2 \zeta_3 - 2\beta_0 \tilde{\mathcal{G}}_{d,1}^{I,1} \right\} + \delta(1 - z_1) \delta(1 - z_2) \left\{ \frac{1}{2} \tilde{\mathcal{G}}_{d,2}^{I,1} + (\tilde{\mathcal{G}}_{d,1}^{I,1})^2 - \frac{1}{2} \zeta_2 (f_1^I)^2 \right. \\ &\quad \left. - A_1^I \zeta_3 f_1^I + \frac{1}{5} (A_1^I)^2 \zeta_2^2 + \beta_0 \tilde{\mathcal{G}}_{d,1}^{I,2} \right\} + (z_1 \leftrightarrow z_2), \\ \mathbf{S}_{d,3}^I &= \mathcal{D}_2 \overline{\mathcal{D}}_2 \left\{ \frac{15}{8} (A_1^I)^3 \right\} + \mathcal{D}_1 \overline{\mathcal{D}}_3 \left\{ \frac{5}{2} (A_1^I)^3 \right\} + \mathcal{D}_1 \overline{\mathcal{D}}_2 \left\{ -\frac{15}{2} (A_1^I)^2 f_1^I - 5\beta_0 (A_1^I)^2 \right\} + \mathcal{D}_1 \overline{\mathcal{D}}_1 \left\{ 3A_1^I (f_1^I)^2 \right. \\ &\quad \left. + 3A_1^I A_2^I + 3(A_1^I)^2 \tilde{\mathcal{G}}_{d,1}^{I,1} - 6(A_1^I)^3 \zeta_2 + 5\beta_0 A_1^I f_1^I + \beta_0^2 A_1^I \right\} + \mathcal{D}_0 \overline{\mathcal{D}}_4 \left\{ \frac{5}{8} (A_1^I)^3 \right\} + \mathcal{D}_0 \overline{\mathcal{D}}_3 \left\{ \right. \\ &\quad \left. -\frac{5}{2} (A_1^I)^2 f_1^I - \frac{5}{3} \beta_0 (A_1^I)^2 \right\} + \mathcal{D}_0 \overline{\mathcal{D}}_2 \left\{ 3A_1^I (f_1^I)^2 + 3A_1^I A_2^I + 3(A_1^I)^2 \tilde{\mathcal{G}}_{d,1}^{I,1} - 6(A_1^I)^3 \zeta_2 + 5\beta_0 A_1^I f_1^I \right. \end{aligned}$$

$$\begin{aligned}
& + \beta_0^2 A_1^I \Big\} + \mathcal{D}_0 \overline{\mathcal{D}}_1 \Big\{ - (f_1^I)^3 - 3A_2^I f_1^I - 3A_1^I f_2^I - 6A_1^I f_1^I \tilde{\mathcal{G}}_{d,1}^{I,1} + 12(A_1^I)^2 \zeta_2 f_1^I + 10(A_1^I)^3 \zeta_3 \\
& - \beta_1 A_1^I - 3\beta_0 (f_1^I)^2 - 2\beta_0 A_2^I - 8\beta_0 A_1^I \tilde{\mathcal{G}}_{d,1}^{I,1} + 6\beta_0 (A_1^I)^2 \zeta_2 - 2\beta_0^2 f_1^I \Big\} + \mathcal{D}_0 \overline{\mathcal{D}}_0 \Big\{ f_1^I f_2^I \\
& + (f_1^I)^2 \tilde{\mathcal{G}}_{d,1}^{I,1} + \frac{1}{2} A_3^I + A_2^I \tilde{\mathcal{G}}_{d,1}^{I,1} + \frac{1}{2} A_1^I \tilde{\mathcal{G}}_{d,2}^{I,1} + A_1^I (\tilde{\mathcal{G}}_{d,1}^{I,1})^2 - \frac{5}{2} A_1^I \zeta_2 (f_1^I)^2 - 2A_1^I A_2^I \zeta_2 \\
& - 5(A_1^I)^2 \zeta_3 f_1^I - 2(A_1^I)^2 \zeta_2 \tilde{\mathcal{G}}_{d,1}^{I,1} + (A_1^I)^3 \zeta_2^2 + \frac{1}{2} \beta_1 f_1^I + \beta_0 f_2^I + 3\beta_0 f_1^I \tilde{\mathcal{G}}_{d,1}^{I,1} + \beta_0 A_1^I \tilde{\mathcal{G}}_{d,1}^{I,2} \\
& - 3\beta_0 A_1^I \zeta_2 f_1^I - 3\beta_0 (A_1^I)^2 \zeta_3 + 2\beta_0^2 \tilde{\mathcal{G}}_{d,1}^{I,1} \Big\} + \delta(1 - z_1) \overline{\mathcal{D}}_5 \Big\{ \frac{1}{8} (A_1^I)^3 \Big\} \\
& + \delta(1 - z_1) \overline{\mathcal{D}}_4 \Big\{ - \frac{5}{8} (A_1^I)^2 f_1^I - \frac{5}{12} \beta_0 (A_1^I)^2 \Big\} + \delta(1 - z_1) \overline{\mathcal{D}}_3 \Big\{ A_1^I (f_1^I)^2 + A_1^I A_2^I + (A_1^I)^2 \tilde{\mathcal{G}}_{d,1}^{I,1} \\
& - 2(A_1^I)^3 \zeta_2 + \frac{5}{3} \beta_0 A_1^I f_1^I + \frac{1}{3} \beta_0^2 A_1^I \Big\} + \delta(1 - z_1) \overline{\mathcal{D}}_2 \Big\{ - \frac{1}{2} (f_1^I)^3 - \frac{3}{2} A_2^I f_1^I - \frac{3}{2} A_1^I f_2^I \\
& - 3A_1^I f_1^I \tilde{\mathcal{G}}_{d,1}^{I,1} + 6(A_1^I)^2 \zeta_2 f_1^I + 5(A_1^I)^3 \zeta_3 - \frac{1}{2} \beta_1 A_1^I - \frac{3}{2} \beta_0 (f_1^I)^2 - \beta_0 A_2^I - 4\beta_0 A_1^I \tilde{\mathcal{G}}_{d,1}^{I,1} \\
& + 3\beta_0 (A_1^I)^2 \zeta_2 - \beta_0^2 f_1^I \Big\} + \delta(1 - z_1) \overline{\mathcal{D}}_1 \Big\{ 2f_1^I f_2^I + 2(f_1^I)^2 \tilde{\mathcal{G}}_{d,1}^{I,1} + A_3^I + 2A_2^I \tilde{\mathcal{G}}_{d,1}^{I,1} + A_1^I \tilde{\mathcal{G}}_{d,2}^{I,1} \\
& + 2A_1^I (\tilde{\mathcal{G}}_{d,1}^{I,1})^2 - 5A_1^I \zeta_2 (f_1^I)^2 - 4A_1^I A_2^I \zeta_2 - 10(A_1^I)^2 \zeta_3 f_1^I - 4(A_1^I)^2 \zeta_2 \tilde{\mathcal{G}}_{d,1}^{I,1} + 2(A_1^I)^3 \zeta_2^2 + \beta_1 f_1^I \\
& + 2\beta_0 f_2^I + 6\beta_0 f_1^I \tilde{\mathcal{G}}_{d,1}^{I,1} + 2\beta_0 A_1^I \tilde{\mathcal{G}}_{d,1}^{I,2} - 6\beta_0 A_1^I \zeta_2 f_1^I - 6\beta_0 (A_1^I)^2 \zeta_3 + 4\beta_0^2 \tilde{\mathcal{G}}_{d,1}^{I,1} \Big\} + \delta(1 - z_1) \overline{\mathcal{D}}_0 \Big\{ \\
& - f_3^I - 2f_2^I \tilde{\mathcal{G}}_{d,1}^{I,1} - f_1^I \tilde{\mathcal{G}}_{d,2}^{I,1} - 2f_1^I (\tilde{\mathcal{G}}_{d,1}^{I,1})^2 + \zeta_2 (f_1^I)^3 + 2A_2^I \zeta_2 f_1^I + 4A_1^I \zeta_3 (f_1^I)^2 + 2A_1^I \zeta_2 f_2^I \\
& + 4A_1^I \zeta_2 f_1^I \tilde{\mathcal{G}}_{d,1}^{I,1} + 4A_1^I A_2^I \zeta_3 + 4(A_1^I)^2 \zeta_3 \tilde{\mathcal{G}}_{d,1}^{I,1} - 2(A_1^I)^2 \zeta_2^2 f_1^I + 6(A_1^I)^3 \zeta_5 - 8(A_1^I)^3 \zeta_2 \zeta_3 \\
& - 2\beta_1 \tilde{\mathcal{G}}_{d,1}^{I,1} - 2\beta_0 \tilde{\mathcal{G}}_{d,2}^{I,1} - 4\beta_0 (\tilde{\mathcal{G}}_{d,1}^{I,1})^2 - 2\beta_0 f_1^I \tilde{\mathcal{G}}_{d,1}^{I,2} + 2\beta_0 \zeta_2 (f_1^I)^2 + 6\beta_0 A_1^I \zeta_3 f_1^I + 4\beta_0 A_1^I \zeta_2 \tilde{\mathcal{G}}_{d,1}^{I,1} \\
& - 4\beta_0^2 \tilde{\mathcal{G}}_{d,1}^{I,1} \Big\} + \delta(1 - z_1) \delta(1 - z_2) \Big\{ \frac{1}{3} \tilde{\mathcal{G}}_{d,3}^{I,1} + \tilde{\mathcal{G}}_{d,1}^{I,1} \tilde{\mathcal{G}}_{d,2}^{I,1} + \frac{2}{3} (\tilde{\mathcal{G}}_{d,1}^{I,1})^3 - \frac{1}{3} \zeta_3 (f_1^I)^3 - \zeta_2 f_1^I f_2^I \\
& - \zeta_2 (f_1^I)^2 \tilde{\mathcal{G}}_{d,1}^{I,1} - A_2^I \zeta_3 f_1^I - A_1^I \zeta_3 f_2^I - 2A_1^I \zeta_3 f_1^I \tilde{\mathcal{G}}_{d,1}^{I,1} + \frac{2}{5} A_1^I \zeta_2^2 (f_1^I)^2 + \frac{2}{5} A_1^I A_2^I \zeta_2^2 - 3(A_1^I)^2 \zeta_5 f_1^I \\
& + 4(A_1^I)^2 \zeta_2 \zeta_3 f_1^I + \frac{2}{5} (A_1^I)^2 \zeta_2^2 \tilde{\mathcal{G}}_{d,1}^{I,1} + \frac{5}{3} (A_1^I)^3 \zeta_3^2 - \frac{4}{105} (A_1^I)^3 \zeta_2^3 + \frac{2}{3} \beta_1 \tilde{\mathcal{G}}_{d,1}^{I,2} + \frac{2}{3} \beta_0 \tilde{\mathcal{G}}_{d,2}^{I,2} \\
& + 2\beta_0 \tilde{\mathcal{G}}_{d,1}^{I,1} \tilde{\mathcal{G}}_{d,1}^{I,2} - \beta_0 \zeta_3 (f_1^I)^2 - 2\beta_0 \zeta_2 f_1^I \tilde{\mathcal{G}}_{d,1}^{I,1} - 2\beta_0 A_1^I \zeta_3 \tilde{\mathcal{G}}_{d,1}^{I,1} - 2\beta_0 (A_1^I)^2 \zeta_5 + 2\beta_0 (A_1^I)^2 \zeta_2 \zeta_3 \\
& + \frac{4}{3} \beta_0^2 \tilde{\mathcal{G}}_{d,1}^{I,3} \Big\} + (z_1 \leftrightarrow z_2), \\
\mathbf{S}_{d,4}^I & = \mathcal{D}_3 \overline{\mathcal{D}}_3 \Big\{ \frac{35}{24} (A_1^I)^4 \Big\} + \mathcal{D}_2 \overline{\mathcal{D}}_4 \Big\{ \frac{35}{16} (A_1^I)^4 \Big\} + \mathcal{D}_2 \overline{\mathcal{D}}_3 \Big\{ - \frac{35}{4} (A_1^I)^3 f_1^I - \frac{35}{4} \beta_0 (A_1^I)^3 \Big\} + \mathcal{D}_2 \overline{\mathcal{D}}_2 \Big\{ \\
& \frac{45}{8} (A_1^I)^2 (f_1^I)^2 + \frac{45}{8} (A_1^I)^2 A_2^I + \frac{15}{4} (A_1^I)^3 \tilde{\mathcal{G}}_{d,1}^{I,1} - \frac{45}{4} (A_1^I)^4 \zeta_2 + \frac{105}{8} \beta_0 (A_1^I)^2 f_1^I + 5\beta_0^2 (A_1^I)^2 \Big\} \\
& + \mathcal{D}_1 \overline{\mathcal{D}}_5 \Big\{ \frac{7}{8} (A_1^I)^4 \Big\} + \mathcal{D}_1 \overline{\mathcal{D}}_4 \Big\{ - \frac{35}{8} (A_1^I)^3 f_1^I - \frac{35}{8} \beta_0 (A_1^I)^3 \Big\} + \mathcal{D}_1 \overline{\mathcal{D}}_3 \Big\{ \frac{15}{2} (A_1^I)^2 (f_1^I)^2 \\
& + \frac{15}{2} (A_1^I)^2 A_2^I + 5(A_1^I)^3 \tilde{\mathcal{G}}_{d,1}^{I,1} - 15(A_1^I)^4 \zeta_2 + \frac{35}{2} \beta_0 (A_1^I)^2 f_1^I + \frac{20}{3} \beta_0^2 (A_1^I)^2 \Big\} + \mathcal{D}_1 \overline{\mathcal{D}}_2 \Big\{ \\
& - 5A_1^I (f_1^I)^3 - 15A_1^I A_2^I f_1^I - \frac{15}{2} (A_1^I)^2 f_2^I - 15(A_1^I)^2 f_1^I \tilde{\mathcal{G}}_{d,1}^{I,1} + 45(A_1^I)^3 \zeta_2 f_1^I + 35(A_1^I)^4 \zeta_3 \\
& - 5\beta_1 (A_1^I)^2 - 20\beta_0 A_1^I (f_1^I)^2 - 15\beta_0 A_1^I A_2^I - 25\beta_0 (A_1^I)^2 \tilde{\mathcal{G}}_{d,1}^{I,1} + 40\beta_0 (A_1^I)^3 \zeta_2 - 20\beta_0^2 A_1^I f_1^I
\end{aligned}$$

$$\begin{aligned}
& -3\beta_0^3 A_1^I \Big\} + \mathcal{D}_1 \overline{\mathcal{D}}_1 \left\{ \frac{1}{2} (f_1^I)^4 + 3A_2^I (f_1^I)^2 + \frac{3}{2} (A_2^I)^2 + 6A_1^I f_1^I f_2^I + 6A_1^I (f_1^I)^2 \tilde{\mathcal{G}}_{d,1}^{I,1} + 3A_1^I A_3^I \right. \\
& + 6A_1^I A_2^I \tilde{\mathcal{G}}_{d,1}^{I,1} + \frac{3}{2} (A_1^I)^2 \tilde{\mathcal{G}}_{d,2}^{I,1} + 3(A_1^I)^2 (\tilde{\mathcal{G}}_{d,1}^{I,1})^2 - \frac{39}{2} (A_1^I)^2 \zeta_2 (f_1^I)^2 - 18(A_1^I)^2 A_2^I \zeta_2 \\
& - 35(A_1^I)^3 \zeta_3 f_1^I - 12(A_1^I)^3 \zeta_2 \tilde{\mathcal{G}}_{d,1}^{I,1} + 9(A_1^I)^4 \zeta_2^2 + 5\beta_1 A_1^I f_1^I + 3\beta_0 (f_1^I)^3 + 7\beta_0 A_2^I f_1^I \\
& + 8\beta_0 A_1^I f_2^I + 22\beta_0 A_1^I f_1^I \tilde{\mathcal{G}}_{d,1}^{I,1} + 3\beta_0 (A_1^I)^2 \tilde{\mathcal{G}}_{d,1}^{I,2} - 40\beta_0 (A_1^I)^2 \zeta_2 f_1^I - 34\beta_0 (A_1^I)^3 \zeta_3 \\
& + \frac{5}{2} \beta_0 \beta_1 A_1^I + \frac{11}{2} \beta_0^2 (f_1^I)^2 + 3\beta_0^2 A_2^I + 18\beta_0^2 A_1^I \tilde{\mathcal{G}}_{d,1}^{I,1} - 11\beta_0^2 (A_1^I)^2 \zeta_2 + 3\beta_0^3 f_1^I \Big\} + \mathcal{D}_0 \overline{\mathcal{D}}_6 \left\{ \right. \\
& \frac{7}{48} (A_1^I)^4 \Big\} + \mathcal{D}_0 \overline{\mathcal{D}}_5 \left\{ -\frac{7}{8} (A_1^I)^3 f_1^I - \frac{7}{8} \beta_0 (A_1^I)^3 \right\} + \mathcal{D}_0 \overline{\mathcal{D}}_4 \left\{ \frac{15}{8} (A_1^I)^2 (f_1^I)^2 + \frac{15}{8} (A_1^I)^2 A_2^I \right. \\
& + \frac{5}{4} (A_1^I)^3 \tilde{\mathcal{G}}_{d,1}^{I,1} - \frac{15}{4} (A_1^I)^4 \zeta_2 + \frac{35}{8} \beta_0 (A_1^I)^2 f_1^I + \frac{5}{3} \beta_0^2 (A_1^I)^2 \Big\} + \mathcal{D}_0 \overline{\mathcal{D}}_3 \left\{ -\frac{5}{3} A_1^I (f_1^I)^3 - 5A_1^I A_2^I f_1^I \right. \\
& - \frac{5}{2} (A_1^I)^2 f_2^I - 5(A_1^I)^2 f_1^I \tilde{\mathcal{G}}_{d,1}^{I,1} + 15(A_1^I)^3 \zeta_2 f_1^I + \frac{35}{3} (A_1^I)^4 \zeta_3 - \frac{5}{3} \beta_1 (A_1^I)^2 - \frac{20}{3} \beta_0 A_1^I (f_1^I)^2 \\
& - 5\beta_0 A_1^I A_2^I - \frac{25}{3} \beta_0 (A_1^I)^2 \tilde{\mathcal{G}}_{d,1}^{I,1} + \frac{40}{3} \beta_0 (A_1^I)^3 \zeta_2 - \frac{20}{3} \beta_0^2 A_1^I f_1^I - \beta_0^3 A_1^I \Big\} + \mathcal{D}_0 \overline{\mathcal{D}}_2 \left\{ \frac{1}{2} (f_1^I)^4 \right. \\
& + 3A_2^I (f_1^I)^2 + \frac{3}{2} (A_2^I)^2 + 6A_1^I f_1^I f_2^I + 6A_1^I (f_1^I)^2 \tilde{\mathcal{G}}_{d,1}^{I,1} + 3A_1^I A_3^I + 6A_1^I A_2^I \tilde{\mathcal{G}}_{d,1}^{I,1} + \frac{3}{2} (A_1^I)^2 \tilde{\mathcal{G}}_{d,2}^{I,1} \\
& + 3(A_1^I)^2 (\tilde{\mathcal{G}}_{d,1}^{I,1})^2 - \frac{39}{2} (A_1^I)^2 \zeta_2 (f_1^I)^2 - 18(A_1^I)^2 A_2^I \zeta_2 - 35(A_1^I)^3 \zeta_3 f_1^I - 12(A_1^I)^3 \zeta_2 \tilde{\mathcal{G}}_{d,1}^{I,1} \\
& + 9(A_1^I)^4 \zeta_2^2 + 5\beta_1 A_1^I f_1^I + 3\beta_0 (f_1^I)^3 + 7\beta_0 A_2^I f_1^I + 8\beta_0 A_1^I f_2^I + 22\beta_0 A_1^I f_1^I \tilde{\mathcal{G}}_{d,1}^{I,1} + 3\beta_0 (A_1^I)^2 \tilde{\mathcal{G}}_{d,1}^{I,2} \\
& - 40\beta_0 (A_1^I)^2 \zeta_2 f_1^I - 34\beta_0 (A_1^I)^3 \zeta_3 + \frac{5}{2} \beta_0 \beta_1 A_1^I + \frac{11}{2} \beta_0^2 (f_1^I)^2 + 3\beta_0^2 A_2^I + 18\beta_0^2 A_1^I \tilde{\mathcal{G}}_{d,1}^{I,1} \\
& - 11\beta_0^2 (A_1^I)^2 \zeta_2 + 3\beta_0^3 f_1^I \Big\} + \mathcal{D}_0 \overline{\mathcal{D}}_1 \left\{ -3(f_1^I)^2 f_2^I - 2(f_1^I)^3 \tilde{\mathcal{G}}_{d,1}^{I,1} - 3A_3^I f_1^I - 3A_2^I f_2^I - 6A_2^I f_1^I \tilde{\mathcal{G}}_{d,1}^{I,1} \right. \\
& - 3A_1^I f_3^I - 6A_1^I f_2^I \tilde{\mathcal{G}}_{d,1}^{I,1} - 3A_1^I f_1^I \tilde{\mathcal{G}}_{d,2}^{I,1} - 6A_1^I f_1^I (\tilde{\mathcal{G}}_{d,1}^{I,1})^2 + 9A_1^I \zeta_2 (f_1^I)^3 + 24A_1^I A_2^I \zeta_2 f_1^I \\
& + 30(A_1^I)^2 \zeta_3 (f_1^I)^2 + 12(A_1^I)^2 \zeta_2 f_2^I + 24(A_1^I)^2 \zeta_2 f_1^I \tilde{\mathcal{G}}_{d,1}^{I,1} + 30(A_1^I)^2 A_2^I \zeta_3 + 20(A_1^I)^3 \zeta_3 \tilde{\mathcal{G}}_{d,1}^{I,1} \\
& - 18(A_1^I)^3 \zeta_2^2 f_1^I + 42(A_1^I)^4 \zeta_5 - 60(A_1^I)^4 \zeta_2 \zeta_3 - \beta_2 A_1^I - 3\beta_1 (f_1^I)^2 - 2\beta_1 A_2^I - 8\beta_1 A_1^I \tilde{\mathcal{G}}_{d,1}^{I,1} \\
& + 6\beta_1 (A_1^I)^2 \zeta_2 - 9\beta_0 f_1^I f_2^I - 12\beta_0 (f_1^I)^2 \tilde{\mathcal{G}}_{d,1}^{I,1} - 3\beta_0 A_3^I - 10\beta_0 A_2^I \tilde{\mathcal{G}}_{d,1}^{I,1} - 7\beta_0 A_1^I \tilde{\mathcal{G}}_{d,2}^{I,1} \\
& - 14\beta_0 A_1^I (\tilde{\mathcal{G}}_{d,1}^{I,1})^2 - 6\beta_0 A_1^I f_1^I \tilde{\mathcal{G}}_{d,1}^{I,2} + 31\beta_0 A_1^I \zeta_2 (f_1^I)^2 + 18\beta_0 A_1^I A_2^I \zeta_2 + 68\beta_0 (A_1^I)^2 \zeta_3 f_1^I \\
& + 36\beta_0 (A_1^I)^2 \zeta_2 \tilde{\mathcal{G}}_{d,1}^{I,1} - 10\beta_0 (A_1^I)^3 \zeta_2^2 - 5\beta_0 \beta_1 f_1^I - 6\beta_0^2 f_2^I - 22\beta_0^2 f_1^I \tilde{\mathcal{G}}_{d,1}^{I,1} - 14\beta_0^2 A_1^I \tilde{\mathcal{G}}_{d,1}^{I,2} \\
& + 22\beta_0^2 A_1^I \zeta_2 f_1^I + 22\beta_0^2 (A_1^I)^2 \zeta_3 - 12\beta_0^3 \tilde{\mathcal{G}}_{d,1}^{I,1} \Big\} + \mathcal{D}_0 \overline{\mathcal{D}}_0 \left\{ \frac{1}{2} (f_2^I)^2 + f_1^I f_3^I + 2f_1^I f_2^I \tilde{\mathcal{G}}_{d,1}^{I,1} \right. \\
& + \frac{1}{2} (f_1^I)^2 \tilde{\mathcal{G}}_{d,2}^{I,1} + (f_1^I)^2 (\tilde{\mathcal{G}}_{d,1}^{I,1})^2 - \frac{1}{2} \zeta_2 (f_1^I)^4 + \frac{1}{2} A_4^I + A_3^I \tilde{\mathcal{G}}_{d,1}^{I,1} + \frac{1}{2} A_2^I \tilde{\mathcal{G}}_{d,2}^{I,1} + A_2^I (\tilde{\mathcal{G}}_{d,1}^{I,1})^2 \\
& - \frac{5}{2} A_2^I \zeta_2 (f_1^I)^2 - (A_2^I)^2 \zeta_2 + \frac{1}{3} A_1^I \tilde{\mathcal{G}}_{d,3}^{I,1} + A_1^I \tilde{\mathcal{G}}_{d,1}^{I,1} \tilde{\mathcal{G}}_{d,2}^{I,1} + \frac{2}{3} A_1^I (\tilde{\mathcal{G}}_{d,1}^{I,1})^3 - \frac{10}{3} A_1^I \zeta_3 (f_1^I)^3 \\
& - 5A_1^I \zeta_2 f_1^I f_2^I - 5A_1^I \zeta_2 (f_1^I)^2 \tilde{\mathcal{G}}_{d,1}^{I,1} - 2A_1^I A_3^I \zeta_2 - 10A_1^I A_2^I \zeta_3 f_1^I - 4A_1^I A_2^I \zeta_2 \tilde{\mathcal{G}}_{d,1}^{I,1} - 5(A_1^I)^2 \zeta_3 f_2^I \\
& - 10(A_1^I)^2 \zeta_3 f_1^I \tilde{\mathcal{G}}_{d,1}^{I,1} - (A_1^I)^2 \zeta_2 \tilde{\mathcal{G}}_{d,2}^{I,1} - 2(A_1^I)^2 \zeta_2 (\tilde{\mathcal{G}}_{d,1}^{I,1})^2 + 4(A_1^I)^2 \zeta_2^2 (f_1^I)^2 + 3(A_1^I)^2 A_2^I \zeta_2^2 \\
\end{aligned}$$

$$\begin{aligned}
& -21(A_1^I)^3 \zeta_5 f_1^I + 30(A_1^I)^3 \zeta_2 \zeta_3 f_1^I + 2(A_1^I)^3 \zeta_2^2 \tilde{\mathcal{G}}_{d,1}^{I,1} + \frac{35}{3}(A_1^I)^4 \zeta_3^2 - \frac{2}{3}(A_1^I)^4 \zeta_3^3 + \frac{1}{2}\beta_2 f_1^I + \beta_1 f_1^I \\
& + 3\beta_1 f_1^I \tilde{\mathcal{G}}_{d,1}^{I,1} + \frac{2}{3}\beta_1 A_1^I \tilde{\mathcal{G}}_{d,1}^{I,2} - 3\beta_1 A_1^I \zeta_2 f_1^I - 3\beta_1 (A_1^I)^2 \zeta_3 + \frac{3}{2}\beta_0 f_3^I + 4\beta_0 f_2^I \tilde{\mathcal{G}}_{d,1}^{I,1} + \frac{5}{2}\beta_0 f_1^I \tilde{\mathcal{G}}_{d,2}^{I,1} \\
& + 5\beta_0 f_1^I (\tilde{\mathcal{G}}_{d,1}^{I,1})^2 + \beta_0 (f_1^I)^2 \tilde{\mathcal{G}}_{d,1}^{I,2} - \frac{5}{2}\beta_0 \zeta_2 (f_1^I)^3 + \beta_0 A_2^I \tilde{\mathcal{G}}_{d,1}^{I,2} - 4\beta_0 A_2^I \zeta_2 f_1^I + \frac{2}{3}\beta_0 A_1^I \tilde{\mathcal{G}}_{d,2}^{I,2} \\
& + 2\beta_0 A_1^I \tilde{\mathcal{G}}_{d,1}^{I,1} \tilde{\mathcal{G}}_{d,1}^{I,2} - 13\beta_0 A_1^I \zeta_3 (f_1^I)^2 - 5\beta_0 A_1^I \zeta_2 f_2^I - 16\beta_0 A_1^I \zeta_2 f_1^I \tilde{\mathcal{G}}_{d,1}^{I,1} - 9\beta_0 A_1^I A_2^I \zeta_3 \\
& - 16\beta_0 (A_1^I)^2 \zeta_3 \tilde{\mathcal{G}}_{d,1}^{I,1} - 2\beta_0 (A_1^I)^2 \zeta_2 \tilde{\mathcal{G}}_{d,1}^{I,2} + 5\beta_0 (A_1^I)^2 \zeta_2^2 f_1^I - 21\beta_0 (A_1^I)^3 \zeta_5 + 26\beta_0 (A_1^I)^3 \zeta_2 \zeta_3 \\
& + 5\beta_0 \beta_1 \tilde{\mathcal{G}}_{d,1}^{I,1} + 3\beta_0^2 \tilde{\mathcal{G}}_{d,2}^{I,1} + 6\beta_0^2 (\tilde{\mathcal{G}}_{d,1}^{I,1})^2 + 5\beta_0^2 f_1^I \tilde{\mathcal{G}}_{d,1}^{I,2} - 3\beta_0^2 \zeta_2 (f_1^I)^2 + \frac{4}{3}\beta_0^2 A_1^I \tilde{\mathcal{G}}_{d,1}^{I,3} - 11\beta_0^2 A_1^I \zeta_3 f_1^I \\
& - 10\beta_0^2 A_1^I \zeta_2 \tilde{\mathcal{G}}_{d,1}^{I,1} - \frac{4}{5}\beta_0^2 (A_1^I)^2 \zeta_2^2 + 6\beta_0^3 \tilde{\mathcal{G}}_{d,1}^{I,2} \} + \delta(1-z_1) \overline{\mathcal{D}}_7 \left\{ \frac{1}{48} (A_1^I)^4 \right\} + \delta(1-z_1) \overline{\mathcal{D}}_6 \left\{ \right. \\
& - \frac{7}{48} (A_1^I)^3 f_1^I - \frac{7}{48} \beta_0 (A_1^I)^3 \} + \delta(1-z_1) \overline{\mathcal{D}}_5 \left\{ \frac{3}{8} (A_1^I)^2 (f_1^I)^2 + \frac{3}{8} (A_1^I)^2 A_2^I + \frac{1}{4} (A_1^I)^3 \tilde{\mathcal{G}}_{d,1}^{I,1} \right. \\
& - \frac{3}{4} (A_1^I)^4 \zeta_2 + \frac{7}{8} \beta_0 (A_1^I)^2 f_1^I + \frac{1}{3} \beta_0^2 (A_1^I)^2 \} + \delta(1-z_1) \overline{\mathcal{D}}_4 \left\{ -\frac{5}{12} A_1^I (f_1^I)^3 - \frac{5}{4} A_1^I A_2^I f_1^I \right. \\
& - \frac{5}{8} (A_1^I)^2 f_2^I - \frac{5}{4} (A_1^I)^2 f_1^I \tilde{\mathcal{G}}_{d,1}^{I,1} + \frac{15}{4} (A_1^I)^3 \zeta_2 f_1^I + \frac{35}{12} (A_1^I)^4 \zeta_3 - \frac{5}{12} \beta_1 (A_1^I)^2 - \frac{5}{3} \beta_0 A_1^I (f_1^I)^2 \\
& - \frac{5}{4} \beta_0 A_1^I A_2^I - \frac{25}{12} \beta_0 (A_1^I)^2 \tilde{\mathcal{G}}_{d,1}^{I,1} + \frac{10}{3} \beta_0 (A_1^I)^3 \zeta_2 - \frac{5}{3} \beta_0^2 A_1^I f_1^I - \frac{1}{4} \beta_0^3 A_1^I \} + \delta(1-z_1) \overline{\mathcal{D}}_3 \left\{ \frac{1}{6} (f_1^I)^4 \right. \\
& + A_2^I (f_1^I)^2 + \frac{1}{2} (A_2^I)^2 + 2A_1^I f_1^I f_2^I + 2A_1^I (f_1^I)^2 \tilde{\mathcal{G}}_{d,1}^{I,1} + A_1^I A_3^I + 2A_1^I A_2^I \tilde{\mathcal{G}}_{d,1}^{I,1} + \frac{1}{2} (A_1^I)^2 \tilde{\mathcal{G}}_{d,2}^{I,1} \\
& + (A_1^I)^2 (\tilde{\mathcal{G}}_{d,1}^{I,1})^2 - \frac{13}{2} (A_1^I)^2 \zeta_2 (f_1^I)^2 - 6(A_1^I)^2 A_2^I \zeta_2 - \frac{35}{3} (A_1^I)^3 \zeta_3 f_1^I - 4(A_1^I)^3 \zeta_2 \tilde{\mathcal{G}}_{d,1}^{I,1} + 3(A_1^I)^4 \zeta_2^2 \\
& + \frac{5}{3} \beta_1 A_1^I f_1^I + \beta_0 (f_1^I)^3 + \frac{7}{3} \beta_0 A_2^I f_1^I + \frac{8}{3} \beta_0 A_1^I f_2^I + \frac{22}{3} \beta_0 A_1^I f_1^I \tilde{\mathcal{G}}_{d,1}^{I,1} + \beta_0 (A_1^I)^2 \tilde{\mathcal{G}}_{d,1}^{I,2} \\
& - \frac{40}{3} \beta_0 (A_1^I)^2 \zeta_2 f_1^I - \frac{34}{3} \beta_0 (A_1^I)^3 \zeta_3 + \frac{5}{6} \beta_0 \beta_1 A_1^I + \frac{11}{6} \beta_0^2 (f_1^I)^2 + \beta_0^2 A_2^I + 6\beta_0^2 A_1^I \tilde{\mathcal{G}}_{d,1}^{I,1} \\
& - \frac{11}{3} \beta_0^2 (A_1^I)^2 \zeta_2 + \beta_0^3 f_1^I \} + \delta(1-z_1) \overline{\mathcal{D}}_2 \left\{ -\frac{3}{2} (f_1^I)^2 f_2^I - (f_1^I)^3 \tilde{\mathcal{G}}_{d,1}^{I,1} - \frac{3}{2} A_3^I f_1^I - \frac{3}{2} A_2^I f_2^I \right. \\
& - 3A_2^I f_1^I \tilde{\mathcal{G}}_{d,1}^{I,1} - \frac{3}{2} A_1^I f_3^I - 3A_1^I f_2^I \tilde{\mathcal{G}}_{d,1}^{I,1} - \frac{3}{2} A_1^I f_1^I \tilde{\mathcal{G}}_{d,2}^{I,1} - 3A_1^I f_1^I (\tilde{\mathcal{G}}_{d,1}^{I,1})^2 + \frac{9}{2} A_1^I \zeta_2 (f_1^I)^3 \\
& + 12A_1^I A_2^I \zeta_2 f_1^I + 15(A_1^I)^2 \zeta_3 (f_1^I)^2 + 6(A_1^I)^2 \zeta_2 f_2^I + 12(A_1^I)^2 \zeta_2 f_1^I \tilde{\mathcal{G}}_{d,1}^{I,1} + 15(A_1^I)^2 A_2^I \zeta_3 \\
& + 10(A_1^I)^3 \zeta_3 \tilde{\mathcal{G}}_{d,1}^{I,1} - 9(A_1^I)^3 \zeta_2^2 f_1^I + 21(A_1^I)^4 \zeta_5 - 30(A_1^I)^4 \zeta_2 \zeta_3 - \frac{1}{2} \beta_2 A_1^I - \frac{3}{2} \beta_1 (f_1^I)^2 - \beta_1 A_2^I \\
& - 4\beta_1 A_1^I \tilde{\mathcal{G}}_{d,1}^{I,1} + 3\beta_1 (A_1^I)^2 \zeta_2 - \frac{9}{2} \beta_0 f_1^I f_2^I - 6\beta_0 (f_1^I)^2 \tilde{\mathcal{G}}_{d,1}^{I,1} - \frac{3}{2} \beta_0 A_3^I - 5\beta_0 A_2^I \tilde{\mathcal{G}}_{d,1}^{I,1} - \frac{7}{2} \beta_0 A_1^I \tilde{\mathcal{G}}_{d,2}^{I,1} \\
& - 7\beta_0 A_1^I (\tilde{\mathcal{G}}_{d,1}^{I,1})^2 - 3\beta_0 A_1^I f_1^I \tilde{\mathcal{G}}_{d,1}^{I,2} + \frac{31}{2} \beta_0 A_1^I \zeta_2 (f_1^I)^2 + 9\beta_0 A_1^I A_2^I \zeta_2 + 34\beta_0 (A_1^I)^2 \zeta_3 f_1^I \\
& + 18\beta_0 (A_1^I)^2 \zeta_2 \tilde{\mathcal{G}}_{d,1}^{I,1} - 5\beta_0 (A_1^I)^3 \zeta_2^2 - \frac{5}{2} \beta_0 \beta_1 f_1^I - 3\beta_0^2 f_2^I - 11\beta_0^2 f_1^I \tilde{\mathcal{G}}_{d,1}^{I,1} - 7\beta_0^2 A_1^I \tilde{\mathcal{G}}_{d,1}^{I,2} \\
& + 11\beta_0^2 A_1^I \zeta_2 f_1^I + 11\beta_0^2 (A_1^I)^2 \zeta_3 - 6\beta_0^3 \tilde{\mathcal{G}}_{d,1}^{I,1} \} + \delta(1-z_1) \overline{\mathcal{D}}_1 \left\{ (f_2^I)^2 + 2f_1^I f_3^I + 4f_1^I f_2^I \tilde{\mathcal{G}}_{d,1}^{I,1} \right. \\
& + (f_1^I)^2 \tilde{\mathcal{G}}_{d,2}^{I,1} + 2(f_1^I)^2 (\tilde{\mathcal{G}}_{d,1}^{I,1})^2 - \zeta_2 (f_1^I)^4 + A_4^I + 2A_3^I \tilde{\mathcal{G}}_{d,1}^{I,1} + A_2^I \tilde{\mathcal{G}}_{d,2}^{I,1} + 2A_2^I (\tilde{\mathcal{G}}_{d,1}^{I,1})^2 - 5A_2^I \zeta_2 (f_1^I)^2 \\
& - 2(A_2^I)^2 \zeta_2 + \frac{2}{3} A_1^I \tilde{\mathcal{G}}_{d,3}^{I,1} + 2A_1^I \tilde{\mathcal{G}}_{d,1}^{I,1} \tilde{\mathcal{G}}_{d,2}^{I,1} + \frac{4}{3} A_1^I (\tilde{\mathcal{G}}_{d,1}^{I,1})^3 - \frac{20}{3} A_1^I \zeta_3 (f_1^I)^3 - 10A_1^I \zeta_2 f_1^I f_2^I
\end{aligned}$$

$$\begin{aligned}
& -10A_1^I \zeta_2 (f_1^I)^2 \tilde{\mathcal{G}}_{d,1}^{I,1} - 4A_1^I A_3^I \zeta_2 - 20A_1^I A_2^I \zeta_3 f_1^I - 8A_1^I A_2^I \zeta_2 \tilde{\mathcal{G}}_{d,1}^{I,1} - 10(A_1^I)^2 \zeta_3 f_2^I \\
& - 20(A_1^I)^2 \zeta_3 f_1^I \tilde{\mathcal{G}}_{d,1}^{I,1} - 2(A_1^I)^2 \zeta_2 \tilde{\mathcal{G}}_{d,2}^{I,1} - 4(A_1^I)^2 \zeta_2 (\tilde{\mathcal{G}}_{d,1}^{I,1})^2 + 8(A_1^I)^2 \zeta_2^2 (f_1^I)^2 + 6(A_1^I)^2 A_2^I \zeta_2^2 \\
& - 42(A_1^I)^3 \zeta_5 f_1^I + 60(A_1^I)^3 \zeta_2 \zeta_3 f_1^I + 4(A_1^I)^3 \zeta_2^2 \tilde{\mathcal{G}}_{d,1}^{I,1} + \frac{70}{3}(A_1^I)^4 \zeta_3^2 - \frac{4}{3}(A_1^I)^4 \zeta_3^3 + \beta_2 f_1^I + 2\beta_1 f_2^I \\
& + 6\beta_1 f_1^I \tilde{\mathcal{G}}_{d,1}^{I,1} + \frac{4}{3}\beta_1 A_1^I \tilde{\mathcal{G}}_{d,1}^{I,2} - 6\beta_1 A_1^I \zeta_2 f_1^I - 6\beta_1 (A_1^I)^2 \zeta_3 + 3\beta_0 f_3^I + 8\beta_0 f_2^I \tilde{\mathcal{G}}_{d,1}^{I,1} + 5\beta_0 f_1^I \tilde{\mathcal{G}}_{d,2}^{I,1} \\
& + 10\beta_0 f_1^I (\tilde{\mathcal{G}}_{d,1}^{I,1})^2 + 2\beta_0 (f_1^I)^2 \tilde{\mathcal{G}}_{d,1}^{I,2} - 5\beta_0 \zeta_2 (f_1^I)^3 + 2\beta_0 A_2^I \tilde{\mathcal{G}}_{d,1}^{I,2} - 8\beta_0 A_2^I \zeta_2 f_1^I + \frac{4}{3}\beta_0 A_1^I \tilde{\mathcal{G}}_{d,2}^{I,2} \\
& + 4\beta_0 A_1^I \tilde{\mathcal{G}}_{d,1}^{I,1} \tilde{\mathcal{G}}_{d,1}^{I,2} - 26\beta_0 A_1^I \zeta_3 (f_1^I)^2 - 10\beta_0 A_1^I \zeta_2 f_2^I - 32\beta_0 A_1^I \zeta_2 f_1^I \tilde{\mathcal{G}}_{d,1}^{I,1} - 18\beta_0 A_1^I A_2^I \zeta_3 \\
& - 32\beta_0 (A_1^I)^2 \zeta_3 \tilde{\mathcal{G}}_{d,1}^{I,1} - 4\beta_0 (A_1^I)^2 \zeta_2 \tilde{\mathcal{G}}_{d,1}^{I,2} + 10\beta_0 (A_1^I)^2 \zeta_2^2 f_1^I - 42\beta_0 (A_1^I)^3 \zeta_5 + 52\beta_0 (A_1^I)^3 \zeta_2 \zeta_3 \\
& + 10\beta_0 \beta_1 \tilde{\mathcal{G}}_{d,1}^{I,1} + 6\beta_0^2 \tilde{\mathcal{G}}_{d,2}^{I,1} + 12\beta_0^2 (\tilde{\mathcal{G}}_{d,1}^{I,1})^2 + 10\beta_0^2 f_1^I \tilde{\mathcal{G}}_{d,1}^{I,2} - 6\beta_0^2 \zeta_2 (f_1^I)^2 + \frac{8}{3}\beta_0^2 A_1^I \tilde{\mathcal{G}}_{d,1}^{I,3} \\
& - 22\beta_0^2 A_1^I \zeta_3 f_1^I - 20\beta_0^2 A_1^I \zeta_2 \tilde{\mathcal{G}}_{d,1}^{I,1} - \frac{8}{5}\beta_0^2 (A_1^I)^2 \zeta_2^2 + 12\beta_0^3 \tilde{\mathcal{G}}_{d,1}^{I,1} \Big\} + \delta(1 - z_1) \bar{\mathcal{D}}_0 \Big\{ -f_4 - 2f_3^I \tilde{\mathcal{G}}_{d,1}^{I,1} \\
& - f_2^I \tilde{\mathcal{G}}_{d,2}^{I,1} - 2f_2^I (\tilde{\mathcal{G}}_{d,1}^{I,1})^2 - \frac{2}{3}f_1^I \tilde{\mathcal{G}}_{d,3}^{I,1} - 2f_1^I \tilde{\mathcal{G}}_{d,1}^{I,1} \tilde{\mathcal{G}}_{d,2}^{I,1} - \frac{4}{3}f_1^I (\tilde{\mathcal{G}}_{d,1}^{I,1})^3 + \frac{2}{3}\zeta_3 (f_1^I)^4 + 3\zeta_2 (f_1^I)^2 f_2^I \\
& + 2\zeta_2 (f_1^I)^3 \tilde{\mathcal{G}}_{d,1}^{I,1} + 2A_3^I \zeta_2 f_1^I + 4A_2^I \zeta_3 (f_1^I)^2 + 2A_2^I \zeta_2 f_2^I + 4A_2^I \zeta_2 f_1^I \tilde{\mathcal{G}}_{d,1}^{I,1} + 2(A_2^I)^2 \zeta_3 + 8A_1^I \zeta_3 f_1^I f_2^I \\
& + 8A_1^I \zeta_3 (f_1^I)^2 \tilde{\mathcal{G}}_{d,1}^{I,1} + 2A_1^I \zeta_2 f_3^I + 4A_1^I \zeta_2 f_2^I \tilde{\mathcal{G}}_{d,1}^{I,1} + 2A_1^I \zeta_2 f_1^I \tilde{\mathcal{G}}_{d,2}^{I,1} + 4A_1^I \zeta_2 f_1^I (\tilde{\mathcal{G}}_{d,1}^{I,1})^2 \\
& - 2A_1^I \zeta_2^2 (f_1^I)^3 + 4A_1^I A_3^I \zeta_3 + 8A_1^I A_2^I \zeta_3 \tilde{\mathcal{G}}_{d,1}^{I,1} - 4A_1^I A_2^I \zeta_2^2 f_1^I + 18(A_1^I)^2 \zeta_5 (f_1^I)^2 + 2(A_1^I)^2 \zeta_3 \tilde{\mathcal{G}}_{d,2}^{I,1} \\
& + 4(A_1^I)^2 \zeta_3 (\tilde{\mathcal{G}}_{d,1}^{I,1})^2 - 26(A_1^I)^2 \zeta_2 \zeta_3 (f_1^I)^2 - 2(A_1^I)^2 \zeta_2^2 f_2^I - 4(A_1^I)^2 \zeta_2^2 f_1^I \tilde{\mathcal{G}}_{d,1}^{I,1} + 18(A_1^I)^2 A_2^I \zeta_5 \\
& - 24(A_1^I)^2 A_2^I \zeta_2 \zeta_3 + 12(A_1^I)^3 \zeta_5 \tilde{\mathcal{G}}_{d,1}^{I,1} - \frac{70}{3}(A_1^I)^3 \zeta_3^2 f_1^I - 16(A_1^I)^3 \zeta_2 \zeta_3 \tilde{\mathcal{G}}_{d,1}^{I,1} + \frac{4}{3}(A_1^I)^3 \zeta_2^3 f_1^I \\
& + 30(A_1^I)^4 \zeta_7 - 36(A_1^I)^4 \zeta_2 \zeta_5 + 12(A_1^I)^4 \zeta_2^2 \zeta_3 - 2\beta_2 \tilde{\mathcal{G}}_{d,1}^{I,1} - 2\beta_1 \tilde{\mathcal{G}}_{d,2}^{I,1} - 4\beta_1 (\tilde{\mathcal{G}}_{d,1}^{I,1})^2 - \frac{4}{3}\beta_1 f_1^I \tilde{\mathcal{G}}_{d,1}^{I,2} \\
& + 2\beta_1 \zeta_2 (f_1^I)^2 + 6\beta_1 A_1^I \zeta_3 f_1^I + 4\beta_1 A_1^I \zeta_2 \tilde{\mathcal{G}}_{d,1}^{I,1} - 2\beta_0 \tilde{\mathcal{G}}_{d,3}^{I,1} - 6\beta_0 \tilde{\mathcal{G}}_{d,1}^{I,1} \tilde{\mathcal{G}}_{d,2}^{I,1} - 4\beta_0 (\tilde{\mathcal{G}}_{d,1}^{I,1})^3 \\
& - 2\beta_0 f_2^I \tilde{\mathcal{G}}_{d,1}^{I,2} - \frac{4}{3}\beta_0 f_1^I \tilde{\mathcal{G}}_{d,2}^{I,2} - 4\beta_0 f_1^I \tilde{\mathcal{G}}_{d,1}^{I,1} \tilde{\mathcal{G}}_{d,1}^{I,2} + 4\beta_0 \zeta_3 (f_1^I)^3 + 6\beta_0 \zeta_2 f_1^I f_2^I + 10\beta_0 \zeta_2 (f_1^I)^2 \tilde{\mathcal{G}}_{d,1}^{I,1} \\
& + 8\beta_0 A_2^I \zeta_3 f_1^I + 4\beta_0 A_2^I \zeta_2 \tilde{\mathcal{G}}_{d,1}^{I,1} + 10\beta_0 A_1^I \zeta_3 f_2^I + 28\beta_0 A_1^I \zeta_3 f_1^I \tilde{\mathcal{G}}_{d,1}^{I,1} + 4\beta_0 A_1^I \zeta_2 \tilde{\mathcal{G}}_{d,2}^{I,1} \\
& + 8\beta_0 A_1^I \zeta_2 (\tilde{\mathcal{G}}_{d,1}^{I,1})^2 + 4\beta_0 A_1^I \zeta_2 f_1^I \tilde{\mathcal{G}}_{d,1}^{I,2} - 4\beta_0 A_1^I \zeta_2^2 (f_1^I)^2 + 42\beta_0 (A_1^I)^2 \zeta_5 f_1^I + 4\beta_0 (A_1^I)^2 \zeta_3 \tilde{\mathcal{G}}_{d,1}^{I,2} \\
& - 52\beta_0 (A_1^I)^2 \zeta_2 \zeta_3 f_1^I - 4\beta_0 (A_1^I)^2 \zeta_2^2 \tilde{\mathcal{G}}_{d,1}^{I,1} - 22\beta_0 (A_1^I)^3 \zeta_3^2 - 8\beta_0 \beta_1 \tilde{\mathcal{G}}_{d,1}^{I,2} - 4\beta_0^2 \tilde{\mathcal{G}}_{d,2}^{I,2} \\
& - 12\beta_0^2 \tilde{\mathcal{G}}_{d,1}^{I,1} \tilde{\mathcal{G}}_{d,1}^{I,2} - \frac{8}{3}\beta_0^2 f_1^I \tilde{\mathcal{G}}_{d,1}^{I,3} + 6\beta_0^2 \zeta_3 (f_1^I)^2 + 12\beta_0^2 \zeta_2 f_1^I \tilde{\mathcal{G}}_{d,1}^{I,1} + 20\beta_0^2 A_1^I \zeta_3 \tilde{\mathcal{G}}_{d,1}^{I,1} + 8\beta_0^2 A_1^I \zeta_2 \tilde{\mathcal{G}}_{d,1}^{I,2} \\
& + \frac{8}{5}\beta_0^2 A_1^I \zeta_2^2 f_1^I + 16\beta_0^2 (A_1^I)^2 \zeta_5 - 12\beta_0^2 (A_1^I)^2 \zeta_2 \zeta_3 - 8\beta_0^3 \tilde{\mathcal{G}}_{d,1}^{I,3} \Big\} + \delta(1 - z_1) \delta(1 - z_2) \Big\{ \frac{1}{4} \tilde{\mathcal{G}}_{d,4}^{I,1} \\
& + \frac{1}{4} (\tilde{\mathcal{G}}_{d,2}^{I,1})^2 + \frac{2}{3} \tilde{\mathcal{G}}_{d,1}^{I,1} \tilde{\mathcal{G}}_{d,3}^{I,1} + (\tilde{\mathcal{G}}_{d,1}^{I,1})^2 \tilde{\mathcal{G}}_{d,2}^{I,1} + \frac{1}{3} (\tilde{\mathcal{G}}_{d,1}^{I,1})^4 - \zeta_3 (f_1^I)^2 f_2^I - \frac{2}{3} \zeta_3 (f_1^I)^3 \tilde{\mathcal{G}}_{d,1}^{I,1} - \frac{1}{2} \zeta_2 (f_2^I)^2 \\
& - \zeta_2 f_1^I f_3^I - 2\zeta_2 f_1^I f_2^I \tilde{\mathcal{G}}_{d,1}^{I,1} - \frac{1}{2} \zeta_2 (f_1^I)^2 \tilde{\mathcal{G}}_{d,2}^{I,1} - \zeta_2 (f_1^I)^2 (\tilde{\mathcal{G}}_{d,1}^{I,1})^2 + \frac{3}{20} \zeta_2^2 (f_1^I)^4 - A_3^I \zeta_3 f_1^I - A_2^I \zeta_3 f_2^I
\end{aligned}$$

$$\begin{aligned}
& -2A_2^I \zeta_3 f_1^I \tilde{\mathcal{G}}_{d,1}^{I,1} + \frac{2}{5} A_2^I \zeta_2^2 (f_1^I)^2 + \frac{1}{5} (A_2^I)^2 \zeta_2^2 - 2A_1^I \zeta_5 (f_1^I)^3 - A_1^I \zeta_3 f_1^I - 2A_1^I \zeta_3 f_2^I \tilde{\mathcal{G}}_{d,1}^{I,1} \\
& - A_1^I \zeta_3 f_1^I \tilde{\mathcal{G}}_{d,2}^{I,1} - 2A_1^I \zeta_3 f_1^I (\tilde{\mathcal{G}}_{d,1}^{I,1})^2 + 3A_1^I \zeta_2 \zeta_3 (f_1^I)^3 + \frac{4}{5} A_1^I \zeta_2^2 f_1^I f_2^I + \frac{4}{5} A_1^I \zeta_2^2 (f_1^I)^2 \tilde{\mathcal{G}}_{d,1}^{I,1} \\
& + \frac{2}{5} A_1^I A_3^I \zeta_2^2 - 6A_1^I A_2^I \zeta_5 f_1^I + 8A_1^I A_2^I \zeta_2 \zeta_3 f_1^I + \frac{4}{5} A_1^I A_2^I \zeta_2^2 \tilde{\mathcal{G}}_{d,1}^{I,1} - 3(A_1^I)^2 \zeta_5 f_2^I - 6(A_1^I)^2 \zeta_5 f_1^I \tilde{\mathcal{G}}_{d,1}^{I,1} \\
& + 5(A_1^I)^2 \zeta_3^2 (f_1^I)^2 + 4(A_1^I)^2 \zeta_2 \zeta_3 f_2^I + 8(A_1^I)^2 \zeta_2 \zeta_3 f_1^I \tilde{\mathcal{G}}_{d,1}^{I,1} + \frac{1}{5} (A_1^I)^2 \zeta_2^2 \tilde{\mathcal{G}}_{d,2}^{I,1} + \frac{2}{5} (A_1^I)^2 \zeta_2^2 (\tilde{\mathcal{G}}_{d,1}^{I,1})^2 \\
& - \frac{11}{35} (A_1^I)^2 \zeta_2^3 (f_1^I)^2 + 5(A_1^I)^2 A_2^I \zeta_3^2 - \frac{4}{35} (A_1^I)^2 A_2^I \zeta_3^2 - 15(A_1^I)^3 \zeta_7 f_1^I + \frac{10}{3} (A_1^I)^3 \zeta_3^2 \tilde{\mathcal{G}}_{d,1}^{I,1} \\
& + 18(A_1^I)^3 \zeta_2 \zeta_5 f_1^I - 6(A_1^I)^3 \zeta_2 \zeta_3 f_1^I - \frac{8}{105} (A_1^I)^3 \zeta_2^3 \tilde{\mathcal{G}}_{d,1}^{I,1} + 14(A_1^I)^4 \zeta_3 \zeta_5 - 10(A_1^I)^4 \zeta_2 \zeta_3^2 \\
& + \frac{1}{35} (A_1^I)^4 \zeta_2^4 + \frac{1}{2} \beta_2 \tilde{\mathcal{G}}_{d,1}^{I,2} + \frac{1}{2} \beta_1 \tilde{\mathcal{G}}_{d,2}^{I,2} + \frac{4}{3} \beta_1 \tilde{\mathcal{G}}_{d,1}^{I,1} \tilde{\mathcal{G}}_{d,1}^{I,2} - \beta_1 \zeta_3 (f_1^I)^2 - 2\beta_1 \zeta_2 f_1^I \tilde{\mathcal{G}}_{d,1}^{I,1} \\
& - 2\beta_1 A_1^I \zeta_3 \tilde{\mathcal{G}}_{d,1}^{I,1} - 2\beta_1 (A_1^I)^2 \zeta_5 + 2\beta_1 (A_1^I)^2 \zeta_2 \zeta_3 + \frac{1}{2} \beta_0 \tilde{\mathcal{G}}_{d,3}^{I,2} + \beta_0 \tilde{\mathcal{G}}_{d,1}^{I,2} \tilde{\mathcal{G}}_{d,2}^{I,1} + \frac{4}{3} \beta_0 \tilde{\mathcal{G}}_{d,1}^{I,1} \tilde{\mathcal{G}}_{d,2}^{I,2} \\
& + 2\beta_0 (\tilde{\mathcal{G}}_{d,1}^{I,1})^2 \tilde{\mathcal{G}}_{d,1}^{I,2} - 3\beta_0 \zeta_3 f_1^I f_2^I - 4\beta_0 \zeta_3 (f_1^I)^2 \tilde{\mathcal{G}}_{d,1}^{I,1} - 2\beta_0 \zeta_2 f_2^I \tilde{\mathcal{G}}_{d,1}^{I,1} - 2\beta_0 \zeta_2 f_1^I \tilde{\mathcal{G}}_{d,2}^{I,1} \\
& - 4\beta_0 \zeta_2 f_1^I (\tilde{\mathcal{G}}_{d,1}^{I,1})^2 - \beta_0 \zeta_2 (f_1^I)^2 \tilde{\mathcal{G}}_{d,1}^{I,2} + \frac{2}{5} \beta_0 \zeta_2^2 (f_1^I)^3 - 2\beta_0 A_2^I \zeta_3 \tilde{\mathcal{G}}_{d,1}^{I,1} - \frac{2}{5} \beta_0 A_2^I \zeta_2^2 f_1^I \\
& - 8\beta_0 A_1^I \zeta_5 (f_1^I)^2 - 2\beta_0 A_1^I \zeta_3 \tilde{\mathcal{G}}_{d,2}^{I,1} - 4\beta_0 A_1^I \zeta_3 (\tilde{\mathcal{G}}_{d,1}^{I,1})^2 - 2\beta_0 A_1^I \zeta_3 f_1^I \tilde{\mathcal{G}}_{d,1}^{I,2} + 10\beta_0 A_1^I \zeta_2 \zeta_3 (f_1^I)^2 \\
& + \frac{2}{5} \beta_0 A_1^I \zeta_2^2 f_2^I + \frac{8}{5} \beta_0 A_1^I \zeta_2^2 f_1^I \tilde{\mathcal{G}}_{d,1}^{I,1} - 6\beta_0 A_1^I A_2^I \zeta_5 + 6\beta_0 A_1^I A_2^I \zeta_2 \zeta_3 - 10\beta_0 (A_1^I)^2 \zeta_5 \tilde{\mathcal{G}}_{d,1}^{I,1} \\
& + 11\beta_0 (A_1^I)^2 \zeta_3^2 f_1^I + 12\beta_0 (A_1^I)^2 \zeta_2 \zeta_3 \tilde{\mathcal{G}}_{d,1}^{I,1} + \frac{2}{5} \beta_0 (A_1^I)^2 \zeta_2^2 \tilde{\mathcal{G}}_{d,1}^{I,2} - 15\beta_0 (A_1^I)^3 \zeta_7 + 16\beta_0 (A_1^I)^3 \zeta_2 \zeta_5 \\
& - \frac{16}{5} \beta_0 (A_1^I)^3 \zeta_2 \zeta_3 + 2\beta_0 \beta_1 \tilde{\mathcal{G}}_{d,1}^{I,3} + \beta_0^2 \tilde{\mathcal{G}}_{d,2}^{I,3} + \beta_0^2 (\tilde{\mathcal{G}}_{d,1}^{I,2})^2 + \frac{8}{3} \beta_0^2 \tilde{\mathcal{G}}_{d,1}^{I,1} \tilde{\mathcal{G}}_{d,1}^{I,3} - 6\beta_0^2 \zeta_3 f_1^I \tilde{\mathcal{G}}_{d,1}^{I,1} \\
& - 2\beta_0^2 \zeta_2 (\tilde{\mathcal{G}}_{d,1}^{I,1})^2 - 4\beta_0^2 \zeta_2 f_1^I \tilde{\mathcal{G}}_{d,1}^{I,2} - \frac{3}{5} \beta_0^2 \zeta_2^2 (f_1^I)^2 - 8\beta_0^2 A_1^I \zeta_5 f_1^I - 4\beta_0^2 A_1^I \zeta_3 \tilde{\mathcal{G}}_{d,1}^{I,2} + 6\beta_0^2 A_1^I \zeta_2 \zeta_3 f_1^I \\
& + \frac{4}{5} \beta_0^2 A_1^I \zeta_2^2 \tilde{\mathcal{G}}_{d,1}^{I,1} + 3\beta_0^2 (A_1^I)^2 \zeta_3^2 + \frac{12}{35} \beta_0^2 (A_1^I)^2 \zeta_2^3 + 2\beta_0^3 \tilde{\mathcal{G}}_{d,1}^{I,4} \} + (z_1 \leftrightarrow z_2).
\end{aligned} \tag{D.2}$$

where

$$\mathcal{D}_i \equiv \mathcal{D}_i(z_1) = \left[\frac{\ln^i(1-z_1)}{(1-z_1)} \right]_+, \quad \bar{\mathcal{D}}_i \equiv \mathcal{D}_i(z_2) = \left[\frac{\ln^i(1-z_2)}{(1-z_2)} \right]_+. \tag{D.3}$$

In the aforementioned equations, we define

$$\mathcal{M}_{I,\text{fin}}^{(m,n)} \equiv \text{Real} \left(\langle \mathcal{M}_I^{(m)} | \mathcal{M}_I^{(n)} \rangle_{\text{fin}} \right), \tag{D.4}$$

where $|\mathcal{M}_I^{(n)}\rangle$ is the UV renormalized pure virtual amplitude at n -th order in a_s , as introduced in (5.12). Also, $\tilde{\mathcal{G}}_{d,i}^{l,k}$ are the finite coefficients coming from soft-collinear distribution, whose values are given in Appendix C.

E Resummation coefficients

Inclusive

Here we present the relevant resummation coefficients for the threshold resummation in the context of inclusive corrections. For the N -space resummation formula:

$$\ln \Delta_N^I = \bar{g}_0^I \exp(G_N^I) \quad (\text{E.1})$$

$$\text{with } \bar{g}_0^I = \sum_{i=0} a_s^i \bar{g}_0^{I,i} \quad G_N = \ln N g_1^I + \sum_{i=0} a_s^i g_{i+2}^I \quad (\text{E.2})$$

For standard $\bar{N} = N \exp(\gamma_E)$, the general expressions for these resummation coefficients in terms of anomalous dimensions and process dependent constants ($g_i^{I,j}$ s) and β -functions are given below.

$$\bar{g}_{01} = \left[\bar{\mathcal{G}}_1^{I,1} (2) + g_1^{I,1} (2) + B_1^I (2 L_{qr} - 2 L_{fr}) + A_1^I (5 \zeta_2) \right], \quad (\text{E.3})$$

$$\begin{aligned} \bar{g}_{02} = & \left[\bar{\mathcal{G}}_2^{I,1} (1) + \bar{\mathcal{G}}_1^{I,2} (2 \beta_0) + \bar{\mathcal{G}}_1^{I,1} (-2 \beta_0 L_{qr}) + (\bar{\mathcal{G}}_1^{I,1})^2 (2) + g_2^{I,1} (1) + g_1^{I,2} (2 \beta_0) + g_1^{I,1} (\right. \\ & - 2 \beta_0 L_{qr}) + g_1^{I,1} \bar{\mathcal{G}}_1^{I,1} (4) + (g_1^{I,1})^2 (2) + f_1^1 (5 \beta_0 \zeta_2) + B_2^I (2 L_{qr} - 2 L_{fr}) + B_1^I (-\beta_0 L_{qr}^2 \\ & + \beta_0 L_{fr}^2 + 6 \beta_0 \zeta_2) + B_1^I \bar{\mathcal{G}}_1^{I,1} (4 L_{qr} - 4 L_{fr}) + B_1^I g_1^{I,1} (4 L_{qr} - 4 L_{fr}) + (B_1^I)^2 (2 L_{qr}^2 \\ & - 4 L_{fr} L_{qr} + 2 L_{fr}^2) + A_2^I (5 \zeta_2) + A_1^I \left(\frac{8}{3} \beta_0 \zeta_3 - 5 \beta_0 \zeta_2 L_{qr} \right) + A_1^I \bar{\mathcal{G}}_1^{I,1} (10 \zeta_2) \\ & \left. + A_1^I g_1^{I,1} (10 \zeta_2) + A_1^I B_1^I (10 \zeta_2 L_{qr} - 10 \zeta_2 L_{fr}) + (A_1^I)^2 \left(\frac{25}{2} \zeta_2^2 \right) \right], \quad (\text{E.4}) \end{aligned}$$

$$\begin{aligned} \bar{g}_{03} = & \left[\bar{\mathcal{G}}_3^{I,1} \left(\frac{2}{3} \right) + \bar{\mathcal{G}}_2^{I,2} \left(\frac{4}{3} \beta_0 \right) + \bar{\mathcal{G}}_2^{I,1} (-2 \beta_0 L_{qr}) + \bar{\mathcal{G}}_1^{I,3} \left(\frac{8}{3} \beta_0^2 \right) + \bar{\mathcal{G}}_1^{I,2} \left(\frac{4}{3} \beta_1 - 4 \beta_0^2 L_{qr} \right) + \bar{\mathcal{G}}_1^{I,1} (\right. \\ & - 2 \beta_1 L_{qr} + 2 \beta_0^2 L_{qr}^2 + 8 \beta_0^2 \zeta_2) + \bar{\mathcal{G}}_1^{I,1} \bar{\mathcal{G}}_2^{I,1} (2) + \bar{\mathcal{G}}_1^{I,1} \bar{\mathcal{G}}_1^{I,2} (4 \beta_0) + (\bar{\mathcal{G}}_1^{I,1})^2 (-4 \beta_0 L_{qr}) \end{aligned}$$

$$\begin{aligned}
& + (\overline{\mathcal{G}}_1^{I,1})^3 \left(\frac{4}{3}\right) + g_3^{I,1} \left(\frac{2}{3}\right) + g_2^{I,2} \left(\frac{4}{3} \beta_0\right) + g_2^{I,1} \left(-2 \beta_0 L_{qr}\right) + g_2^{I,1} \overline{\mathcal{G}}_1^{I,1} \left(2\right) + g_1^{I,3} \left(\frac{8}{3} \beta_0^2\right) \\
& + g_1^{I,2} \left(\frac{4}{3} \beta_1 - 4 \beta_0^2 L_{qr}\right) + g_1^{I,2} \overline{\mathcal{G}}_1^{I,1} \left(4 \beta_0\right) + g_1^{I,1} \left(-2 \beta_1 L_{qr} + 2 \beta_0^2 L_{qr}^2 - 12 \beta_0^2 \zeta_2\right) \\
& + g_1^{I,1} \overline{\mathcal{G}}_2^{I,1} \left(2\right) + g_1^{I,1} \overline{\mathcal{G}}_1^{I,2} \left(4 \beta_0\right) + g_1^{I,1} \overline{\mathcal{G}}_1^{I,1} \left(-8 \beta_0 L_{qr}\right) + g_1^{I,1} \left(\overline{\mathcal{G}}_1^{I,1}\right)^2 \left(4\right) + g_1^{I,1} g_2^{I,1} \left(2\right) \\
& + g_1^{I,1} g_1^{I,2} \left(4 \beta_0\right) + \left(g_1^{I,1}\right)^2 \left(-4 \beta_0 L_{qr}\right) + \left(g_1^{I,1}\right)^2 \overline{\mathcal{G}}_1^{I,1} \left(4\right) + \left(g_1^{I,1}\right)^3 \left(\frac{4}{3}\right) + f_2^I \left(10 \beta_0 \zeta_2\right) \\
& + f_1^I \left(5 \beta_1 \zeta_2 + \frac{16}{3} \beta_0^2 \zeta_3 - 10 \beta_0^2 \zeta_2 L_{qr}\right) + f_1^I \overline{\mathcal{G}}_1^{I,1} \left(10 \beta_0 \zeta_2\right) + f_1^I g_1^{I,1} \left(10 \beta_0 \zeta_2\right) \\
& + B_3^I \left(2 L_{qr} - 2 L_{fr}\right) + B_2^I \left(-2 \beta_0 L_{qr}^2 + 2 \beta_0 L_{fr}^2 + 12 \beta_0 \zeta_2\right) + B_2^I \overline{\mathcal{G}}_1^{I,1} \left(4 L_{qr} - 4 L_{fr}\right) \\
& + B_2^I g_1^{I,1} \left(4 L_{qr} - 4 L_{fr}\right) + B_1^I \left(-\beta_1 L_{qr}^2 + \beta_1 L_{fr}^2 + 6 \beta_1 \zeta_2 + \frac{2}{3} \beta_0^2 L_{qr}^3 - \frac{2}{3} \beta_0^2 L_{fr}^3 \right. \\
& \left. - 12 \beta_0^2 \zeta_2 L_{qr}\right) + B_1^I \overline{\mathcal{G}}_2^{I,1} \left(2 L_{qr} - 2 L_{fr}\right) + B_1^I \overline{\mathcal{G}}_1^{I,2} \left(4 \beta_0 L_{qr} - 4 \beta_0 L_{fr}\right) + B_1^I \overline{\mathcal{G}}_1^{I,1} \left(\right. \\
& \left. - 6 \beta_0 L_{qr}^2 + 4 \beta_0 L_{fr} L_{qr} + 2 \beta_0 L_{fr}^2 + 12 \beta_0 \zeta_2\right) + B_1^I \left(\overline{\mathcal{G}}_1^{I,1}\right)^2 \left(4 L_{qr} - 4 L_{fr}\right) \\
& + B_1^I g_2^{I,1} \left(2 L_{qr} - 2 L_{fr}\right) + B_1^I g_1^{I,2} \left(4 \beta_0 L_{qr} - 4 \beta_0 L_{fr}\right) + B_1^I g_1^{I,1} \left(-6 \beta_0 L_{qr}^2 \right. \\
& \left. + 4 \beta_0 L_{fr} L_{qr} + 2 \beta_0 L_{fr}^2 + 12 \beta_0 \zeta_2\right) + B_1^I g_1^{I,1} \overline{\mathcal{G}}_1^{I,1} \left(8 L_{qr} - 8 L_{fr}\right) + B_1^I \left(g_1^{I,1}\right)^2 \left(4 L_{qr} \right. \\
& \left. - 4 L_{fr}\right) + B_1^I f_1^I \left(10 \beta_0 \zeta_2 L_{qr} - 10 \beta_0 \zeta_2 L_{fr}\right) + B_1^I B_2^I \left(4 L_{qr}^2 - 8 L_{fr} L_{qr} + 4 L_{fr}^2\right) \\
& + \left(B_1^I\right)^2 \left(-2 \beta_0 L_{qr}^3 + 2 \beta_0 L_{fr} L_{qr}^2 + 2 \beta_0 L_{fr}^2 L_{qr} - 2 \beta_0 L_{fr}^3 + 12 \beta_0 \zeta_2 L_{qr} - 12 \beta_0 \zeta_2 L_{fr}\right) \\
& + \left(B_1^I\right)^2 \overline{\mathcal{G}}_1^{I,1} \left(4 L_{qr}^2 - 8 L_{fr} L_{qr} + 4 L_{fr}^2\right) + \left(B_1^I\right)^2 g_1^{I,1} \left(4 L_{qr}^2 - 8 L_{fr} L_{qr} + 4 L_{fr}^2\right) \\
& + \left(B_1^I\right)^3 \left(\frac{4}{3} L_{qr}^3 - 4 L_{fr} L_{qr}^2 + 4 L_{fr}^2 L_{qr} - \frac{4}{3} L_{fr}^3\right) + A_3^I \left(5 \zeta_2\right) + A_2^I \left(\frac{16}{3} \beta_0 \zeta_3 - 10 \beta_0 \zeta_2 L_{qr}\right) \\
& + A_2^I \overline{\mathcal{G}}_1^{I,1} \left(10 \zeta_2\right) + A_2^I g_1^{I,1} \left(10 \zeta_2\right) + A_2^I B_1^I \left(10 \zeta_2 L_{qr} - 10 \zeta_2 L_{fr}\right) + A_1^I \left(\frac{8}{3} \beta_1 \zeta_3 \right. \\
& \left. - 5 \beta_1 \zeta_2 L_{qr} - \frac{16}{3} \beta_0^2 \zeta_3 L_{qr} + 5 \beta_0^2 \zeta_2 L_{qr}^2 + \frac{21}{5} \beta_0^2 \zeta_2^2\right) + A_1^I \overline{\mathcal{G}}_2^{I,1} \left(5 \zeta_2\right) \\
& + A_1^I \overline{\mathcal{G}}_1^{I,2} \left(10 \beta_0 \zeta_2\right) + A_1^I \overline{\mathcal{G}}_1^{I,1} \left(\frac{16}{3} \beta_0 \zeta_3 - 20 \beta_0 \zeta_2 L_{qr}\right) + A_1^I \left(\overline{\mathcal{G}}_1^{I,1}\right)^2 \left(10 \zeta_2\right) \\
& + A_1^I g_2^{I,1} \left(5 \zeta_2\right) + A_1^I g_1^{I,2} \left(10 \beta_0 \zeta_2\right) + A_1^I g_1^{I,1} \left(\frac{16}{3} \beta_0 \zeta_3 - 20 \beta_0 \zeta_2 L_{qr}\right) \\
& + A_1^I g_1^{I,1} \overline{\mathcal{G}}_1^{I,1} \left(20 \zeta_2\right) + A_1^I \left(g_1^{I,1}\right)^2 \left(10 \zeta_2\right) + A_1^I f_1^I \left(25 \beta_0 \zeta_2^2\right) + A_1^I B_2^I \left(10 \zeta_2 L_{qr} \right. \\
& \left. - 10 \zeta_2 L_{fr}\right) + A_1^I B_1^I \left(\frac{16}{3} \beta_0 \zeta_3 L_{qr} - \frac{16}{3} \beta_0 \zeta_3 L_{fr} - 15 \beta_0 \zeta_2 L_{qr}^2 + 10 \beta_0 \zeta_2 L_{fr} L_{qr} \right. \\
& \left. + 5 \beta_0 \zeta_2 L_{fr}^2 + 30 \beta_0 \zeta_2^2\right) + A_1^I B_1^I \overline{\mathcal{G}}_1^{I,1} \left(20 \zeta_2 L_{qr} - 20 \zeta_2 L_{fr}\right) + A_1^I B_1^I g_1^{I,1} \left(20 \zeta_2 L_{qr} \right. \\
& \left. - 20 \zeta_2 L_{fr}\right) + A_1^I \left(B_1^I\right)^2 \left(10 \zeta_2 L_{qr}^2 - 20 \zeta_2 L_{fr} L_{qr} + 10 \zeta_2 L_{fr}^2\right) + A_1^I A_2^I \left(25 \zeta_2^2\right) \\
& + \left(A_1^I\right)^2 \left(\frac{40}{3} \beta_0 \zeta_2 \zeta_3 - 25 \beta_0 \zeta_2^2 L_{qr}\right) + \left(A_1^I\right)^2 \overline{\mathcal{G}}_1^{I,1} \left(25 \zeta_2^2\right) + \left(A_1^I\right)^2 g_1^{I,1} \left(25 \zeta_2^2\right)
\end{aligned}$$

$$+ (A_1^I)^2 B_1^I \left(25 \zeta_2^2 L_{qr} - 25 \zeta_2^2 L_{fr} \right) + (A_1^I)^3 \left(\frac{125}{6} \zeta_3^3 \right) \Big]. \quad (\text{E.5})$$

Similarly, the universal N -dependent resummation coefficients have following structure.

$$g_1^I = \left[\frac{A_1^I}{\beta_0} \left\{ 2 - 2 \ln(1 - \omega) + 2 \ln(1 - \omega) \omega^{-1} \right\} \right], \quad (\text{E.6})$$

$$g_2^I = \left[\frac{\mathbf{D}_1^I}{\beta_0} \left\{ \frac{1}{2} \ln(1 - \omega) \right\} + \frac{A_2^I}{\beta_0^2} \left\{ - \ln(1 - \omega) - \omega \right\} + \frac{A_1^I}{\beta_0} \left\{ \left(\ln(1 - \omega) + \frac{1}{2} \ln(1 - \omega)^2 + \omega \right) \left(\frac{\beta_1}{\beta_0^2} \right) \right. \right. \\ \left. \left. + \left(\omega \right) L_{fr} + \left(\ln(1 - \omega) \right) L_{qr} \right\} \right], \quad (\text{E.7})$$

$$g_3^I = \left[\frac{A_3^I}{\beta_0^2} \left\{ \frac{1}{2} \frac{\omega}{(1 - \omega)} - \frac{1}{2} \omega \right\} + \frac{A_2^I}{\beta_0} \left\{ \left(- \frac{3}{2} \frac{\omega}{(1 - \omega)} - \frac{\ln(1 - \omega)}{(1 - \omega)} + \frac{1}{2} \omega \right) \left(\frac{\beta_1}{\beta_0^2} \right) + \left(- \frac{\omega}{(1 - \omega)} \right) L_{qr} \right. \right. \\ \left. \left. + \left(\omega \right) L_{fr} \right\} + A_1^I \left\{ 2 \zeta_2 \frac{\omega}{(1 - \omega)} + \left(\frac{1}{2} \frac{\ln(1 - \omega)^2}{(1 - \omega)} + \frac{1}{2} \frac{\omega}{(1 - \omega)} + \frac{\ln(1 - \omega)}{(1 - \omega)} - \ln(1 - \omega) \right. \right. \\ \left. \left. - \frac{1}{2} \omega \right) \left(\frac{\beta_1}{\beta_0^2} \right)^2 + \left(\frac{1}{2} \frac{\omega}{(1 - \omega)} \right) L_{qr}^2 + \left(\frac{1}{2} \frac{\omega}{(1 - \omega)} + \ln(1 - \omega) + \frac{1}{2} \omega \right) \left(\frac{\beta_2}{\beta_0^3} \right) + \left(- \frac{1}{2} \omega \right) L_{fr}^2 \right. \\ \left. + \left(\left(\frac{\omega}{(1 - \omega)} + \frac{\ln(1 - \omega)}{(1 - \omega)} \right) \left(\frac{\beta_1}{\beta_0^2} \right) \right) L_{qr} \right\} + \frac{\mathbf{D}_2^I}{\beta_0} \left\{ - \frac{1}{2} \frac{\omega}{(1 - \omega)} \right\} + \mathbf{D}_1^I \left\{ \left(\frac{1}{2} \frac{\omega}{(1 - \omega)} \right) L_{qr} \right. \right. \\ \left. \left. + \left(\frac{1}{2} \frac{\omega}{(1 - \omega)} + \frac{1}{2} \frac{\ln(1 - \omega)}{(1 - \omega)} \right) \left(\frac{\beta_1}{\beta_0^2} \right) \right\} \right], \quad (\text{E.8})$$

$$g_4^I = \left[\frac{A_4^I}{\beta_0^3} \left\{ \frac{1}{6} \frac{\omega(2 - \omega)}{(1 - \omega)^2} - \frac{1}{3} \omega \right\} + \frac{A_3^I}{\beta_0} \left\{ \left(- \frac{1}{2} \frac{\omega(2 - \omega)}{(1 - \omega)^2} \right) L_{qr} + \left(- \frac{5}{12} \frac{\omega(2 - \omega)}{(1 - \omega)^2} - \frac{1}{2} \frac{\ln(1 - \omega)}{(1 - \omega)^2} \right. \right. \right. \\ \left. \left. + \frac{1}{3} \omega \right) \left(\frac{\beta_1}{\beta_0^2} \right) + \left(\omega \right) L_{fr} \right\} + A_2^I \left\{ 2 \zeta_2 \frac{\omega(2 - \omega)}{(1 - \omega)^2} + \left(\frac{1}{2} \frac{\ln(1 - \omega)^2}{(1 - \omega)^2} - \frac{1}{12} \frac{\omega^2}{(1 - \omega)^2} + \frac{5}{6} \frac{\omega}{(1 - \omega)} \right. \right. \\ \left. \left. + \frac{1}{2} \frac{\ln(1 - \omega)}{(1 - \omega)^2} - \frac{1}{3} \omega \right) \left(\frac{\beta_1}{\beta_0^2} \right)^2 + \left(\frac{1}{2} \frac{\omega(2 - \omega)}{(1 - \omega)^2} \right) L_{qr}^2 + \left(\frac{1}{3} \frac{\omega^2}{(1 - \omega)^2} - \frac{1}{3} \frac{\omega}{(1 - \omega)} + \frac{1}{3} \omega \right) \left(\frac{\beta_2}{\beta_0^3} \right) \right. \\ \left. + \left(- \omega \right) L_{fr}^2 + \left(\left(\frac{1}{2} \frac{\omega(2 - \omega)}{(1 - \omega)^2} + \frac{\ln(1 - \omega)}{(1 - \omega)^2} \right) \left(\frac{\beta_1}{\beta_0^2} \right) \right) L_{qr} \right\} + \beta_0 A_1^I \left\{ \frac{8}{3} \zeta_3 \frac{\omega(2 - \omega)}{(1 - \omega)^2} + \left(\right. \right. \\ \left. \left. - \frac{1}{6} \frac{\ln(1 - \omega)^3}{(1 - \omega)^2} + \frac{1}{3} \frac{\omega^2}{(1 - \omega)^2} - \frac{1}{3} \frac{\omega}{(1 - \omega)} + \frac{1}{2} \frac{\ln(1 - \omega)}{(1 - \omega)^2} - \frac{\ln(1 - \omega)}{(1 - \omega)} + \frac{1}{2} \ln(1 - \omega) \right. \right. \\ \left. \left. + \frac{1}{3} \omega \right) \left(\frac{\beta_1}{\beta_0^2} \right)^3 + \left(- \frac{1}{6} \frac{\omega(2 - \omega)}{(1 - \omega)^2} \right) L_{qr}^3 + \left(\frac{1}{12} \frac{\omega(2 - \omega)}{(1 - \omega)^2} + \frac{1}{2} \ln(1 - \omega) + \frac{1}{3} \omega \right) \left(\frac{\beta_3}{\beta_0^4} \right) + \left(\right. \right. \\ \left. \left. - \frac{5}{12} \frac{\omega^2}{(1 - \omega)^2} + \frac{1}{6} \frac{\omega}{(1 - \omega)} - \frac{1}{2} \frac{\ln(1 - \omega)}{(1 - \omega)^2} + \frac{\ln(1 - \omega)}{(1 - \omega)} - \ln(1 - \omega) - \frac{2}{3} \omega \right) \frac{\beta_1 \beta_2}{\beta_0^5} \right. \\ \left. + \left(\frac{1}{3} \omega \right) L_{fr}^3 + \left(- 2 \zeta_2 \frac{\omega(2 - \omega)}{(1 - \omega)^2} + \left(- \frac{1}{2} \frac{\ln(1 - \omega)^2}{(1 - \omega)^2} + \frac{1}{2} \frac{\omega^2}{(1 - \omega)^2} \right) \left(\frac{\beta_1}{\beta_0^2} \right)^2 + \left(\right. \right. \\ \left. \left. - \frac{1}{2} \frac{\omega^2}{(1 - \omega)^2} \right) \left(\frac{\beta_2}{\beta_0^3} \right) \right) L_{qr} + \left(- 2 \zeta_2 \frac{\ln(1 - \omega)}{(1 - \omega)^2} \right) \left(\frac{\beta_1}{\beta_0^2} \right) + \left(\left(- \frac{1}{2} \frac{\ln(1 - \omega)}{(1 - \omega)^2} \right) \left(\frac{\beta_1}{\beta_0^2} \right) \right) L_{qr}^2 + \left(\left(\right. \right. \\ \left. \left. - \frac{1}{2} \omega \right) \left(\frac{\beta_1}{\beta_0^2} \right) \right) L_{fr}^2 \right\} + \frac{\mathbf{D}_3^I}{\beta_0} \left\{ - \frac{1}{4} \frac{\omega(2 - \omega)}{(1 - \omega)^2} \right\} + \mathbf{D}_2^I \left\{ \left(\frac{1}{4} \frac{\omega(2 - \omega)}{(1 - \omega)^2} + \frac{1}{2} \frac{\ln(1 - \omega)}{(1 - \omega)^2} \right) \left(\frac{\beta_1}{\beta_0^2} \right) \right. \right. \\ \left. \left. + \left(\frac{1}{4} \frac{\omega(2 - \omega)}{(1 - \omega)^2} + \frac{1}{2} \frac{\ln(1 - \omega)}{(1 - \omega)^2} \right) \left(\frac{\beta_1}{\beta_0^2} \right) \right\} \right]$$

$$\begin{aligned}
& + \left(\frac{1}{2} \frac{\omega(2-\omega)}{(1-\omega)^2} \right) L_{qr} \} + \beta_0 \mathbf{D}_1^I \left\{ -\zeta_2 \frac{\omega(2-\omega)}{(1-\omega)^2} + \left(-\frac{1}{4} \frac{\ln(1-\omega)^2}{(1-\omega)^2} + \frac{1}{4} \frac{\omega^2}{(1-\omega)^2} \right) \left(\frac{\beta_1}{\beta_0^2} \right)^2 + \left(-\frac{1}{4} \frac{\omega(2-\omega)}{(1-\omega)^2} \right) L_{qr}^2 + \left(-\frac{1}{4} \frac{\omega^2}{(1-\omega)^2} \right) \left(\frac{\beta_2}{\beta_0^3} \right) + \left(\left(-\frac{1}{2} \frac{\ln(1-\omega)}{(1-\omega)^2} \right) \left(\frac{\beta_1}{\beta_0^2} \right) \right) L_{qr} \right\}. \quad (\text{E.9})
\end{aligned}$$

where $L_{qr} = \ln\left(\frac{q^2}{\mu_r^2}\right)$, $L_{fr} = \ln\left(\frac{\mu_f^2}{\mu_r^2}\right)$.

Differential rapidity

Here we present the relevant resummation coefficients for the threshold resummation in the context of differential rapidity distributions till N³LL. The resummation formula is given by:

$$\ln A_{d,N}^I = \bar{g}_{d,0}^I \exp(G_{d,N}^I) \quad (\text{E.10})$$

$$\text{with } \bar{g}_{d,0}^I = \sum_{i=0} a_s^i \bar{g}_{d,0}^{I,i} \quad G_N = \ln N g_{d,1}^I + \sum_{i=0} a_s^i g_{d,i+2}^I \quad (\text{E.11})$$

The general expression for these coefficients in terms of universal anomalous dimensions and the process dependent matrix elements $\mathcal{M}_{I,fin}$ are given below.

$$\bar{g}_{d,0}^{I,0} = 1 \quad (\text{E.12})$$

$$\bar{g}_{d,0}^{I,1} = 2\tilde{\mathcal{G}}_{d,1}^{I,1} - 2B_1^I L_{fr} - f_1^I L_{qr} + A_1^I \frac{L_{qr}^2}{2} + 2\mathcal{M}_{I,fin}^{(0,1)} + A_1^I \zeta_2 \quad (\text{E.13})$$

$$\begin{aligned}
\bar{g}_{d,0}^{I,2} = & 2(\tilde{\mathcal{G}}_{d,1}^{I,1})^2 + 2\beta_0 \tilde{\mathcal{G}}_{d,1}^{I,2} + \tilde{\mathcal{G}}_{d,2}^{I,1} - 2B_2^I L_{fr} - 4B_1^I \tilde{\mathcal{G}}_{d,1}^{I,1} L_{fr} + 2(B_1^I)^2 L_{fr}^2 + B_1^I \beta_0 L_{fr}^2 - f_2^I L_{qr} \\
& - 2\beta_0 \tilde{\mathcal{G}}_{d,1}^{I,1} L_{qr} - 2f_1^I \tilde{\mathcal{G}}_{d,1}^{I,1} L_{qr} + 2B_1^I f_1^I L_{fr} L_{qr} + A_2^I \frac{L_{qr}^2}{2} + \beta_0 f_1^I \frac{L_{qr}^2}{2} + (f_1^I)^2 \frac{L_{qr}^2}{2} \\
& + A_1^I \tilde{\mathcal{G}}_{d,1}^{I,1} L_{qr}^2 - A_1^I B_1^I L_{fr} L_{qr}^2 - A_1^I \beta_0 \frac{L_{qr}^3}{6} - A_1^I f_1^I \frac{L_{qr}^3}{2} + (A_1^I)^2 \frac{L_{qr}^4}{8} + 4\tilde{\mathcal{G}}_{d,1}^{I,1} \mathcal{M}_{I,fin}^{(0,1)} \\
& - 4B_1^I L_{fr} \mathcal{M}_{I,fin}^{(0,1)} - 2f_1^I L_{qr} \mathcal{M}_{I,fin}^{(0,1)} + A_1^I L_{qr}^2 \mathcal{M}_{I,fin}^{(0,1)} + (\mathcal{M}_{I,fin}^{(0,1)})^2 + 2\mathcal{M}_{I,fin}^{(0,2)} + A_2^I \zeta_2 + \beta_0 f_1^I \zeta_2 \\
& + 2A_1^I \tilde{\mathcal{G}}_{d,1}^{I,1} \zeta_2 - 2A_1^I B_1^I L_{fr} \zeta_2 - A_1^I \beta_0 L_{qr} \zeta_2 - A_1^I f_1^I L_{qr} \zeta_2 + (A_1^I)^2 L_{qr}^2 \frac{\zeta_2}{2} + 2A_1^I \mathcal{M}_{I,fin}^{(0,1)} \zeta_2 \\
& + (A_1^I)^2 \frac{\zeta_2^2}{2} + 2A_1^I \beta_0 \frac{\zeta_3}{3} \quad (\text{E.14})
\end{aligned}$$

$$\begin{aligned}
\bar{g}_{d,0}^{I,3} = & 4 \frac{(\tilde{\mathcal{G}}_{d,1}^{I,1})^3}{3} + 4\beta_1 \frac{\tilde{\mathcal{G}}_{d,1}^{I,2}}{3} + 4\beta_0 \tilde{\mathcal{G}}_{d,1}^{I,1} \tilde{\mathcal{G}}_{d,1}^{I,2} + 8\beta_0^2 \frac{\tilde{\mathcal{G}}_{d,1}^{I,3}}{3} + 2\tilde{\mathcal{G}}_{d,1}^{I,1} \tilde{\mathcal{G}}_{d,2}^{I,1} + 4\beta_0 \frac{\tilde{\mathcal{G}}_{d,2}^{I,2}}{3} + 2 \frac{\tilde{\mathcal{G}}_{d,3}^{I,1}}{3} \\
& - 2B_3^I L_{fr} - 4B_2^I \tilde{\mathcal{G}}_{d,1}^{I,1} L_{fr} - 4B_1^I (\tilde{\mathcal{G}}_{d,1}^{I,1})^2 L_{fr} - 4B_1^I \beta_0 \tilde{\mathcal{G}}_{d,1}^{I,2} L_{fr} - 2B_1^I \tilde{\mathcal{G}}_{d,2}^{I,1} L_{fr}
\end{aligned}$$

$$\begin{aligned}
& + 4B_1^I B_2^I L_{fr}^2 + 2B_2^I \beta_0 L_{fr}^2 + B_1^I \beta_1 L_{fr}^2 + 4(B_1^I)^2 \tilde{\mathcal{G}}_{d,1}^{I,1} L_{fr}^2 + 2B_1^I \beta_0 \tilde{\mathcal{G}}_{d,1}^{I,1} L_{fr}^2 - 4(B_1^I)^3 \frac{L_{fr}^3}{3} \\
& - 2(B_1^I)^2 \beta_0 L_{fr}^3 - 2B_1^I \beta_0^2 \frac{L_{fr}^3}{3} - f_3^I L_{qr} - 2\beta_1 \tilde{\mathcal{G}}_{d,1}^{I,1} L_{qr} - 2f_2^I \tilde{\mathcal{G}}_{d,1}^{I,1} L_{qr} - 4\beta_0 (\tilde{\mathcal{G}}_{d,1}^{I,1})^2 L_{qr} \\
& - 2f_1^I (\tilde{\mathcal{G}}_{d,1}^{I,1})^2 L_{qr} - 4\beta_0^2 \tilde{\mathcal{G}}_{d,1}^{I,2} L_{qr} - 2\beta_0 f_1^I \tilde{\mathcal{G}}_{d,1}^{I,2} L_{qr} - 2\beta_0 \tilde{\mathcal{G}}_{d,2}^{I,1} L_{qr} - f_1^I \tilde{\mathcal{G}}_{d,2}^{I,1} L_{qr} \\
& + 2B_2^I f_1^I L_{fr} L_{qr} + 2B_1^I f_2^I L_{fr} L_{qr} + 4B_1^I \beta_0 \tilde{\mathcal{G}}_{d,1}^{I,1} L_{fr} L_{qr} + 4B_1^I f_1^I \tilde{\mathcal{G}}_{d,1}^{I,1} L_{fr} L_{qr} \\
& - 2(B_1^I)^2 f_1^I L_{fr}^2 L_{qr} - B_1^I \beta_0 f_1^I L_{fr}^2 L_{qr} + A_3^I \frac{L_{qr}^2}{2} + \beta_1 f_1^I \frac{L_{qr}^2}{2} + \beta_0 f_2^I L_{qr}^2 + f_1^I f_2^I L_{qr}^2 \\
& + A_2^I \tilde{\mathcal{G}}_{d,1}^{I,1} L_{qr}^2 + 2\beta_0^2 \tilde{\mathcal{G}}_{d,1}^{I,1} L_{qr}^2 + 3\beta_0 f_1^I \tilde{\mathcal{G}}_{d,1}^{I,1} L_{qr}^2 + (f_1^I)^2 \tilde{\mathcal{G}}_{d,1}^{I,1} L_{qr}^2 + A_1^I (\tilde{\mathcal{G}}_{d,1}^{I,1})^2 L_{qr}^2 \\
& + A_1^I \beta_0 \tilde{\mathcal{G}}_{d,1}^{I,2} L_{qr}^2 + A_1^I \tilde{\mathcal{G}}_{d,2}^{I,1} \frac{L_{qr}^2}{2} - A_2^I B_1^I L_{fr} L_{qr}^2 - A_1^I B_2^I L_{fr} L_{qr}^2 - B_1^I \beta_0 f_1^I L_{fr} L_{qr}^2 \\
& - B_1^I (f_1^I)^2 L_{fr} L_{qr}^2 - 2A_1^I B_1^I \tilde{\mathcal{G}}_{d,1}^{I,1} L_{fr} L_{qr}^2 + A_1^I (B_1^I)^2 L_{fr}^2 L_{qr}^2 + A_1^I B_1^I \beta_0 L_{fr}^2 \frac{L_{qr}^2}{2} - A_2^I \beta_0 \frac{L_{qr}^3}{3} \\
& - A_1^I \beta_1 \frac{L_{qr}^3}{6} - A_2^I f_1^I \frac{L_{qr}^3}{2} - \beta_0^2 f_1^I \frac{L_{qr}^3}{3} - \beta_0 (f_1^I)^2 \frac{L_{qr}^3}{2} - (f_1^I)^3 \frac{L_{qr}^3}{6} - A_1^I f_2^I \frac{L_{qr}^3}{2} \\
& - 4A_1^I \beta_0 \tilde{\mathcal{G}}_{d,1}^{I,1} \frac{L_{qr}^3}{3} - A_1^I f_1^I \tilde{\mathcal{G}}_{d,1}^{I,1} L_{qr}^3 + A_1^I B_1^I \beta_0 L_{fr} \frac{L_{qr}^3}{3} + A_1^I B_1^I f_1^I L_{fr} L_{qr}^3 + A_1^I A_2^I \frac{L_{qr}^4}{4} \\
& + A_1^I \beta_0^2 \frac{L_{qr}^4}{12} + 5A_1^I \beta_0 f_1^I \frac{L_{qr}^4}{12} + A_1^I (f_1^I)^2 \frac{L_{qr}^4}{4} + (A_1^I)^2 \tilde{\mathcal{G}}_{d,1}^{I,1} \frac{L_{qr}^4}{4} - (A_1^I)^2 B_1^I L_{fr} \frac{L_{qr}^4}{4} \\
& - (A_1^I)^2 \beta_0 \frac{L_{qr}^5}{12} - (A_1^I)^2 f_1^I \frac{L_{qr}^5}{8} + (A_1^I)^3 \frac{L_{qr}^6}{48} + 4(\tilde{\mathcal{G}}_{d,1}^{I,1})^2 \mathcal{M}_{I,fin}^{(0,1)} + 4\beta_0 \tilde{\mathcal{G}}_{d,1}^{I,2} \mathcal{M}_{I,fin}^{(0,1)} \\
& + 2\tilde{\mathcal{G}}_{d,2}^{I,1} \mathcal{M}_{I,fin}^{(0,1)} - 4B_2^I L_{fr} \mathcal{M}_{I,fin}^{(0,1)} - 8B_1^I \tilde{\mathcal{G}}_{d,1}^{I,1} L_{fr} \mathcal{M}_{I,fin}^{(0,1)} + 4(B_1^I)^2 L_{fr}^2 \mathcal{M}_{I,fin}^{(0,1)} \\
& + 2B_1^I \beta_0 L_{fr}^2 \mathcal{M}_{I,fin}^{(0,1)} - 2f_2^I L_{qr} \mathcal{M}_{I,fin}^{(0,1)} - 4\beta_0 \tilde{\mathcal{G}}_{d,1}^{I,1} L_{qr} \mathcal{M}_{I,fin}^{(0,1)} - 4f_1^I \tilde{\mathcal{G}}_{d,1}^{I,1} L_{qr} \mathcal{M}_{I,fin}^{(0,1)} \\
& + 4B_1^I f_1^I L_{fr} L_{qr} \mathcal{M}_{I,fin}^{(0,1)} + A_2^I L_{qr}^2 \mathcal{M}_{I,fin}^{(0,1)} + \beta_0 f_1^I L_{qr}^2 \mathcal{M}_{I,fin}^{(0,1)} + (f_1^I)^2 L_{qr}^2 \mathcal{M}_{I,fin}^{(0,1)} \\
& + 2A_1^I \tilde{\mathcal{G}}_{d,1}^{I,1} L_{qr}^2 \mathcal{M}_{I,fin}^{(0,1)} - 2A_1^I B_1^I L_{fr} L_{qr}^2 \mathcal{M}_{I,fin}^{(0,1)} - A_1^I \beta_0 L_{qr}^3 \frac{\mathcal{M}_{I,fin}^{(0,1)}}{3} - A_1^I f_1^I L_{qr}^3 \mathcal{M}_{I,fin}^{(0,1)} \\
& + (A_1^I)^2 L_{qr}^4 \frac{\mathcal{M}_{I,fin}^{(0,1)}}{4} + 2\tilde{\mathcal{G}}_{d,1}^{I,1} (\mathcal{M}_{I,fin}^{(0,1)})^2 - 2B_1^I L_{fr} (\mathcal{M}_{I,fin}^{(0,1)})^2 - f_1^I L_{qr} (\mathcal{M}_{I,fin}^{(0,1)})^2 \\
& + A_1^I L_{qr}^2 \frac{(\mathcal{M}_{I,fin}^{(0,1)})^2}{2} + 4\tilde{\mathcal{G}}_{d,1}^{I,1} \mathcal{M}_{I,fin}^{(0,2)} - 4B_1^I L_{fr} \mathcal{M}_{I,fin}^{(0,2)} - 2f_1^I L_{qr} \mathcal{M}_{I,fin}^{(0,2)} + A_1^I L_{qr}^2 \mathcal{M}_{I,fin}^{(0,2)} \\
& + 2\mathcal{M}_{I,fin}^{(0,1)} \mathcal{M}_{I,fin}^{(0,2)} + 2\mathcal{M}_{I,fin}^{(0,3)} + A_3^I \zeta_2 + \beta_1 f_1^I \zeta_2 + 2\beta_0 f_2^I \zeta_2 + 2A_2^I \tilde{\mathcal{G}}_{d,1}^{I,1} \zeta_2 + 4\beta_0^2 \tilde{\mathcal{G}}_{d,1}^{I,1} \zeta_2 \\
& + 2\beta_0 f_1^I \tilde{\mathcal{G}}_{d,1}^{I,1} \zeta_2 + 2A_1^I (\tilde{\mathcal{G}}_{d,1}^{I,1})^2 \zeta_2 + 2A_1^I \beta_0 \tilde{\mathcal{G}}_{d,1}^{I,2} \zeta_2 + A_1^I \tilde{\mathcal{G}}_{d,2}^{I,1} \zeta_2 - 2A_2^I B_1^I L_{fr} \zeta_2 \\
& - 2A_1^I B_2^I L_{fr} \zeta_2 - 2B_1^I \beta_0 f_1^I L_{fr} \zeta_2 - 4A_1^I B_1^I \tilde{\mathcal{G}}_{d,1}^{I,1} L_{fr} \zeta_2 + 2A_1^I (B_1^I)^2 L_{fr}^2 \zeta_2 + A_1^I B_1^I \beta_0 L_{fr}^2 \zeta_2 \\
& - 2A_2^I \beta_0 L_{qr} \zeta_2 - A_1^I \beta_1 L_{qr} \zeta_2 - A_2^I f_1^I L_{qr} \zeta_2 - 2\beta_0^2 f_1^I L_{qr} \zeta_2 - \beta_0 (f_1^I)^2 L_{qr} \zeta_2 - A_1^I f_2^I L_{qr} \zeta_2 \\
& - 4A_1^I \beta_0 \tilde{\mathcal{G}}_{d,1}^{I,1} L_{qr} \zeta_2 - 2A_1^I f_1^I \tilde{\mathcal{G}}_{d,1}^{I,1} L_{qr} \zeta_2 + 2A_1^I B_1^I \beta_0 L_{fr} L_{qr} \zeta_2 + 2A_1^I B_1^I f_1^I L_{fr} L_{qr} \zeta_2
\end{aligned}$$

$$\begin{aligned}
& + A_1^I A_2^I L_{qr}^2 \zeta_2 + A_1^I \beta_0^2 L_{qr}^2 \zeta_2 + 2A_1^I \beta_0 f_1^I L_{qr}^2 \zeta_2 + A_1^I (f_1^I)^2 L_{qr}^2 \frac{\zeta_2}{2} + (A_1^I)^2 \tilde{\mathcal{G}}_{d,1}^{I,1} L_{qr}^2 \zeta_2 \\
& - (A_1^I)^2 B_1^I L_{fr} L_{qr}^2 \zeta_2 - 2(A_1^I)^2 \beta_0 L_{qr}^3 \frac{\zeta_2}{3} - (A_1^I)^2 f_1^I L_{qr}^3 \frac{\zeta_2}{2} + (A_1^I)^3 L_{qr}^4 \frac{\zeta_2}{8} + 2A_2^I \mathcal{M}_{I,fin}^{(0,1)} \zeta_2 \\
& + 2\beta_0 f_1^I \mathcal{M}_{I,fin}^{(0,1)} \zeta_2 + 4A_1^I \tilde{\mathcal{G}}_{d,1}^{I,1} \mathcal{M}_{I,fin}^{(0,1)} \zeta_2 - 4A_1^I B_1^I L_{fr} \mathcal{M}_{I,fin}^{(0,1)} \zeta_2 - 2A_1^I \beta_0 L_{qr} \mathcal{M}_{I,fin}^{(0,1)} \zeta_2 \\
& - 2A_1^I f_1^I L_{qr} \mathcal{M}_{I,fin}^{(0,1)} \zeta_2 + (A_1^I)^2 L_{qr}^2 \mathcal{M}_{I,fin}^{(0,1)} \zeta_2 + A_1^I (\mathcal{M}_{I,fin}^{(0,1)})^2 \zeta_2 + 2A_1^I \mathcal{M}_{I,fin}^{(0,2)} \zeta_2 + A_1^I A_2^I \zeta_2^2 \\
& + 7A_1^I \beta_0^2 \frac{\zeta_2^2}{5} + A_1^I \beta_0 f_1^I \zeta_2^2 + (A_1^I)^2 \tilde{\mathcal{G}}_{d,1}^{I,1} \zeta_2^2 - (A_1^I)^2 B_1^I L_{fr} \zeta_2^2 - (A_1^I)^2 \beta_0 L_{qr} \zeta_2^2 \\
& - (A_1^I)^2 f_1^I L_{qr} \frac{\zeta_2^2}{2} + (A_1^I)^3 L_{qr}^2 \frac{\zeta_2^2}{4} + (A_1^I)^2 \mathcal{M}_{I,fin}^{(0,1)} \zeta_2^2 + (A_1^I)^3 \frac{\zeta_2^3}{6} + 4A_2^I \beta_0 \frac{\zeta_3}{3} + 2A_1^I \beta_1 \frac{\zeta_3}{3} \\
& + 4\beta_0^2 f_1^I \frac{\zeta_3}{3} + 4A_1^I \beta_0 \tilde{\mathcal{G}}_{d,1}^{I,1} \frac{\zeta_3}{3} - 4A_1^I B_1^I \beta_0 L_{fr} \frac{\zeta_3}{3} - 4A_1^I \beta_0^2 L_{qr} \frac{\zeta_3}{3} - 2A_1^I \beta_0 f_1^I L_{qr} \frac{\zeta_3}{3} \\
& + (A_1^I)^2 \beta_0 L_{qr}^2 \frac{\zeta_3}{3} + 4A_1^I \beta_0 \mathcal{M}_{I,fin}^{(0,1)} \frac{\zeta_3}{3} + 2(A_1^I)^2 \beta_0 \zeta_2 \frac{\zeta_3}{3} \tag{E.15}
\end{aligned}$$

In the above equations, $\tilde{\mathcal{G}}_{d,i}^{I,(k)}$ are the finite coefficients coming from soft distribution, whose values are given in Appendix C. Also $\mathcal{M}_{I,fin}^{(m,n)}$ is defined in Eq.(D.4).

Similarly, the universal N -dependent resummation coefficients have following structure. These coefficients are identical for any number of colorless productions. Rescaling them by appropriate β_i as $\bar{g}_{d,1}^I = g_{d,1}^I$, $\bar{g}_{d,2}^I = g_{d,2}^I$, $\bar{g}_{d,3}^I = g_{d,3}^I/\beta_0$, $\bar{A}_i^I = A_i^I/\beta_0^i$, $\bar{\mathbf{D}}_{d,i}^I = \mathbf{D}_{d,i}^I/\beta_0^i$ and $\bar{\beta}_i = \beta_i/\beta_0^{i+1}$, we find¹

$$\bar{g}_{d,1}^I = \frac{\bar{A}_1^I}{\omega} (\omega + (1-\omega) \ln(1-\omega)), \tag{E.16}$$

$$\begin{aligned}
\bar{g}_{d,2}^I &= \omega (\bar{A}_1^I \bar{\beta}_1 - \bar{A}_2^I) + \ln(1-\omega) (\bar{A}_1^I \bar{\beta}_1 + \bar{\mathbf{D}}_{d,1}^I - \bar{A}_2^I) + \frac{1}{2} \ln^2(1-\omega) \bar{A}_1^I \bar{\beta}_1 \\
&+ L_{qr} \ln(1-\omega) \bar{A}_1^I + L_{fr} \omega \bar{A}_1^I, \tag{E.17}
\end{aligned}$$

$$\begin{aligned}
\bar{g}_{d,3}^I &= -\frac{\omega \bar{A}_3^I}{2} - \frac{\omega}{2(1-\omega)} \left(-\bar{A}_3^I + (2+\omega) \bar{\beta}_1 \bar{A}_2^I + \{(w-2)\bar{\beta}_2 - \omega \bar{\beta}_1^2 - 2\zeta_2\} \bar{A}_1^I \right. \\
&+ 2\bar{\mathbf{D}}_{d,2}^I - 2\bar{\beta}_1 \bar{\mathbf{D}}_{d,1}^I \left. \right) - \ln(1-\omega) \left(\frac{\bar{\beta}_1}{1-\omega} \{ \bar{A}_2^I - \bar{\mathbf{D}}_{d,1}^I - \bar{A}_1^I \bar{\beta}_1 \omega \} - \bar{A}_1^I \bar{\beta}_2 \right) \\
&+ \frac{\ln^2(1-\omega)}{2(1-\omega)} \bar{A}_1^I \bar{\beta}_1^2 + L_{fr} \bar{A}_2^I \omega - \frac{1}{2} L_{fr}^2 \bar{A}_1^I \omega \\
&- L_{qr} \frac{1}{1-\omega} \left(\{ \bar{A}_2^I - \bar{\mathbf{D}}_{d,1}^I \} \omega - \bar{A}_1^I \bar{\beta}_1 \{ \omega + \ln(1-\omega) \} \right) + \frac{1}{2} L_{qr}^2 \frac{\omega}{1-\omega} \bar{A}_1^I \tag{E.18}
\end{aligned}$$

where $L_{qr} = \ln\left(\frac{q^2}{\mu_R^2}\right)$ and $L_{fr} = \ln\left(\frac{\mu_F^2}{\mu_R^2}\right)$.

¹ $\bar{g}_{d,4}^I$ is provided in the ancillary files supplemented with the arXiv submission [177].

F Deriving resummation formula for SV and NSV logarithms

In this section, we evaluate the Mellin moment of $\Psi_{I,\mathcal{D}}$ in the following way. At first, following Eq. (6.68) we decompose $\Psi_{I,N}$ into $\Sigma_{sv,N}^I$ and $\Sigma_{nsv,N}^I$. So, we begin with

$$\Sigma_{sv,N}^I = \int_0^1 dz \left(\frac{z^{N-1} - 1}{1-z} \right) \left(\int_{\mu_F^2}^{q^2(1-z)^2} \frac{d\lambda^2}{\lambda^2} 2A^I(a_s(\lambda^2)) + 2\bar{G}_{sv}^I(a_s(q^2(1-z)^2)) \right) \quad (\text{F.1})$$

We follow the method described in [6] to perform Mellin moment. In the large N , keeping $\frac{1}{N}$ corrections, we replace

$$\int_0^1 dz (z^{N-1} - 1) \rightarrow \Gamma_A \left(N \frac{d}{dN} \right) \int_0^1 dz \theta \left(1 - z - \frac{1}{N} \right) \quad (\text{F.2})$$

where $\Gamma_A(N \frac{d}{dN})$ is given in Appendix[G]. We expand Γ_A in powers of Nd/dN and apply on the integral. We then make appropriate change of variables and interchange of integrals to obtain

$$\begin{aligned} \Sigma_{sv,N}^I &= - \int_{q^2/N^2}^{q^2} \frac{d\lambda^2}{\lambda^2} \left\{ \left(\ln \frac{q^2}{\lambda^2 N^2} - 2\gamma_1^A \right) A^I(a_s(\lambda^2)) + \bar{G}_{sv}^I(a_s(\lambda^2)) \right. \\ &\quad \left. + \lambda^2 \frac{d}{d\lambda^2} \mathcal{F}_{sv}^I(a_s(\lambda^2)) \right\} + \mathcal{F}_{sv}^I(a_s(q^2)) \\ &\quad - 2 \left(\gamma_1^A + \ln(N) \right) \int_{\mu_F^2}^{q^2} \frac{d\lambda^2}{\lambda^2} A^I(a_s(\lambda^2)), \end{aligned} \quad (\text{F.3})$$

where

$$\mathcal{F}_{sv}^I(a_s(\lambda^2)) = -2\gamma_1^A \bar{G}_{sv}^I(a_s(\lambda^2)) + 4 \sum_{i=0}^{\infty} \gamma_{i+2}^A \left(-2\beta(a_s(\lambda^2)) \frac{\partial}{\partial a_s(\lambda^2)} \right)^i \left\{ A^I(a_s(\lambda^2)) \right\}$$

$$+\beta(a_s(\lambda^2))\frac{\partial}{\partial a_s(\lambda^2)}\bar{G}_{sv}^I(a_s(\lambda^2))\}. \quad (\text{F.4})$$

Here $\beta(a_s(\lambda^2))$ is defined as, $\beta(a_s(\lambda^2)) = -\sum_{i=0}^{\infty}\beta_i a_s^{i+2}(\lambda^2)$ (also see [247–249] for QCD).

Replacing $a_s(\lambda^2)$ by

$$\begin{aligned} a_s(\lambda^2) = & \left(\frac{a_s(\mu_R^2)}{l}\right)\left[1 - \frac{a_s(\mu_R^2)\beta_1}{l\beta_0}\ln(l) + \left(\frac{a_s(\mu_R^2)}{l}\right)^2\left(\frac{\beta_1^2}{\beta_0^2}(\ln^2(l) - \ln(l))\right.\right. \\ & \left.\left.+ l - 1\right) - \frac{\beta_2}{\beta_0}(l - 1)\right] + \left(\frac{a_s(\mu_R^2)}{l}\right)^3\left(\frac{\beta_1^3}{\beta_0^3}(2(1 - l)\ln(l) + \frac{5}{2}\ln^2(l))\right. \\ & \left.- \ln^3(l) - \frac{1}{2} + l - \frac{1}{2}l^2\right) + \frac{\beta_3}{2\beta_0}(1 - l^2) + \frac{\beta_1\beta_2}{\beta_0^2}(2l\ln(l) \\ & \left.- 3\ln(l) - l(1 - l))\right], \quad (\text{F.5}) \end{aligned}$$

where $l = 1 - \beta_0 a_s(\mu_R^2) \ln(\mu_R^2/\lambda^2)$ and performing the integrals over λ^2 we obtain the result. The entire result is decomposed into two parts. The one proportional to $\frac{1}{N}$, are expressed in terms of $\bar{g}_i^I(\omega)$ given in Eq. (6.74). And the remaining part is embedded in Eq. (6.70).

Similarly we define,

$$\Sigma_{\text{nsv},N}^I = 2 \int_0^1 dz z^{N-1} \left\{ \int_{\mu_F^2}^{q^2(1-z)^2} \frac{d\lambda^2}{\lambda^2} L^I(a_s(\lambda^2), z) + \varphi_f^I(a_s(q^2(1-z)^2), z) \right\}. \quad (\text{F.6})$$

Following [6], in the large N and keeping $\frac{1}{N}$ corrections, we replace

$$\int_0^1 dz z^{N-1} \rightarrow \Gamma_B\left(N\frac{d}{dN}\right) \int_0^1 \frac{dz}{1-z} \theta\left(1 - z - \frac{1}{N}\right), \quad (\text{F.7})$$

where $\Gamma_B(N\frac{d}{dN})$ is given in Appendix[G] and we replace Nd/dN by

$$N\frac{d}{dN} = N\frac{\partial}{\partial N} - 2\beta(a_s(\lambda^2))\frac{\partial}{\partial a_s(\lambda^2)}, \quad (\text{F.8})$$

to deal with N appearing in the argument of $a_s(q^2/N^2)$ and also the explicit ones present in φ_f^I .

After a little algebra, we obtain

$$\Sigma_{\text{nsv},N}^I = -\frac{1}{N} \int_{\frac{q^2}{N^2}}^{q^2} \frac{d\lambda^2}{\lambda^2} \left\{ \xi^I(a_s(\lambda^2), N) + \lambda^2 \frac{d}{d\lambda^2} \mathcal{F}_{\text{nsv}}^I(a_s(\lambda^2), N) \right\} + \frac{1}{N} \mathcal{F}_{\text{nsv}}^I(a_s(q^2), N)$$

$$+ \frac{1}{N} \int_{\mu_f^2}^{q^2} \frac{d\lambda^2}{\lambda^2} \xi^I(a_s(\lambda^2), N), \quad (\text{F.9})$$

where the functions ξ^I is defined as

$$\xi^I(a_s, N) = -2 \left(-\gamma_1^B (D^I(a_s) - C^I(a_s) \ln(N)) + \gamma_2^B C^I(a_s) \right), \quad (\text{F.10})$$

and

$$\begin{aligned} \mathcal{F}_{\text{nsv}}^I(a_s(\lambda^2), N) &= 2\gamma_1^B \varphi_f^I(a_s(\lambda^2), N) - 4\gamma_2^B \left(\lambda^2 \frac{d}{d\lambda^2} \varphi_f^I(a_s(\lambda^2), N) + \tilde{\xi}^I(a_s(\lambda^2), N) \right) \\ &\quad + 8 \left(\gamma_3^B + \tilde{\gamma}^B \right) \left(\lambda^2 \frac{d}{d\lambda^2} \left\{ \lambda^2 \frac{d}{d\lambda^2} \varphi_f^I(a_s(\lambda^2), N) + \tilde{\xi}^I(a_s(\lambda^2), N) \right\} \right. \\ &\quad \left. + \frac{1}{2} C^I(a_s(\lambda^2)) \right). \end{aligned} \quad (\text{F.11})$$

where

$$\begin{aligned} \tilde{\xi}^I(a_s, N) &= (D^I(a_s) - C^I(a_s) \ln(N)), \\ \varphi_f^I(a_s(\lambda^2), N) &= \sum_{i=1}^{\infty} \sum_{k=0}^i a_s^i(\lambda^2) \tilde{\varphi}_i^{I,(k)} (-\ln(N))^k, \quad \tilde{\gamma}^B = \sum_{i=4}^{\infty} \gamma_i^B \left(N \frac{d}{dN} \right)^{i-3}. \end{aligned} \quad (\text{F.12})$$

Using Eq.(F.5), we perform λ^2 integration to obtain the result in terms of $h_{ij}^I(\omega)$ given in Eq.(6.74).

G Expansion coefficients $\Gamma_A(x)$ and $\Gamma_B(x)$

In the section, we present the expansion coefficients of $\Gamma_A(x)$ and $\Gamma_B(x)$ used in the Eqs.(F.2,F.7) of the Appendix[F] . As in [6], the operators $\Gamma_A(x)$ and $\Gamma_B(x)$ are expanded in powers of x as

$$\Gamma_A(x) = \sum_{k=0} -\gamma_k^A x^k, \quad (\text{G.1})$$

where coefficients γ_k^A are given by [6]

$$\gamma_k^A = \frac{\Gamma_k(N)}{k!} (-1)^{k-1}, \quad (\text{G.2})$$

See Eq.(25) of [6] for the definition of $\Gamma_k(N)$. We find,

$$\begin{aligned} \gamma_0^A &= 1, \\ \gamma_1^A &= \gamma_E - \frac{1}{2N}, \\ \gamma_2^A &= \frac{1}{2}(\gamma_E^2 + \zeta_2) - \frac{1}{2N}(1 + \gamma_E), \\ \gamma_3^A &= \frac{1}{6}\gamma_E^3 + \frac{1}{2}(\gamma_E\zeta_2) + \frac{1}{3}\zeta_3 - \frac{1}{4N}(\gamma_E^2 + 2\gamma_E + \zeta_2), \\ \gamma_4^A &= \frac{1}{24}\gamma_E^4 + \frac{1}{4}(\gamma_E^2\zeta_2) + \frac{9}{40}\zeta_2^2 + \frac{1}{3}(\gamma_E\zeta_3) - \frac{1}{12N}(\gamma_E^3 + 3\gamma_E^2 + 3\zeta_2 + 3\gamma_E\zeta_2 + 2\zeta_3), \\ \gamma_5^A &= \frac{1}{120}\gamma_E^5 + \frac{1}{12}(\gamma_E^3\zeta_2) + \frac{1}{40}(9\gamma_E\zeta_2^2) + \frac{1}{6}(\gamma_E^2\zeta_3) + \frac{1}{6}(\zeta_2\zeta_3) + \frac{1}{5}\zeta_5 \\ &\quad - \frac{1}{240N}(20\gamma_E^3 + 5\gamma_E^4 + 30\gamma_E^2\zeta_2 + 27\zeta_2^2 + 40\zeta_3 + 20\gamma_E(3\zeta_2 + 2\zeta_3)), \\ \gamma_6^A &= \frac{1}{720}\gamma_E^6 + \frac{1}{48}(\gamma_E^4\zeta_2) + \frac{9}{80}(\gamma_E^2\zeta_2^2) + \frac{61}{560}\zeta_2^3 + \frac{1}{18}(\gamma_E^3\zeta_3) + \frac{1}{6}(\gamma_E\zeta_2\zeta_3) \end{aligned}$$

$$\begin{aligned}
& + \frac{1}{18}\zeta_3^2 + \frac{1}{5}\gamma_E\zeta_5 - \frac{1}{240N}\left(5\gamma_E^4 + \gamma_E^5 + 10\gamma_E^3\zeta_2 + 27\zeta_2^2 + 20\zeta_2\zeta_3 + 10\gamma_E^2(3\zeta_2 + 2\zeta_3)\right. \\
& \left. + \gamma_E(27\zeta_2^2 + 40\zeta_3) + 24\zeta_5\right), \\
\gamma_7^A & = \frac{1}{5040}\gamma_E^7 + \frac{1}{240}\left(\gamma_E^5\zeta_2\right) + \frac{3}{80}\left(\gamma_E^3\zeta_2^2\right) + \frac{61}{560}\left(\gamma_E\zeta_2^3\right) + \frac{1}{72}\left(\gamma_E^4\zeta_3\right) \\
& + \frac{1}{12}\left(\gamma_E^2\zeta_2\zeta_3\right) + \frac{3}{40}\left(\zeta_2^2\zeta_3\right) + \frac{1}{18}\left(\gamma_E\zeta_3^2\right) + \frac{1}{10}\left(\gamma_E^2\zeta_5\right) + \frac{1}{10}\left(\zeta_2\zeta_5\right) + \frac{1}{7}\zeta_7 \\
& - \frac{1}{10080N}\left(42\gamma_E^5 + 7\gamma_E^6 + 105\gamma_E^4\zeta_2 + 549\zeta_2^3 + 840\zeta_2\zeta_3 + 140\gamma_E^3(3\zeta_2 + 2\zeta_3)\right. \\
& \left. + 21\gamma_E^2(27\zeta_2^2 + 40\zeta_3) + 56(5\zeta_3^2 + 18\zeta_5) + 42\gamma_E(27\zeta_2^2 + 20\zeta_2\zeta_3 + 24\zeta_5)\right), \tag{G.3}
\end{aligned}$$

and similarly $\Gamma_B(x)$ is given by [6]

$$\Gamma_B(x) = \sum_{k=1} \gamma_k^B x^k, \tag{G.4}$$

where γ_{k+1}^B are given by [6]

$$\gamma_{k+1}^B = \frac{\Gamma^k(1)}{k!}(-1)^k, \tag{G.5}$$

explicitly we find,

$$\begin{aligned}
\gamma_1^B & = 1, \\
\gamma_2^B & = \gamma_E, \\
\gamma_3^B & = \frac{1}{2}\left(\gamma_E^2 + \zeta_2\right), \\
\gamma_4^B & = \frac{1}{6}\gamma_E^3 + \frac{1}{2}\left(\gamma_E\zeta_2\right) + \frac{1}{3}\zeta_3, \\
\gamma_5^B & = \frac{1}{24}\gamma_E^4 + \frac{1}{4}\left(\gamma_E^2\zeta_2\right) + \frac{9}{40}\zeta_2^2 + \frac{1}{3}\left(\gamma_E\zeta_3\right), \\
\gamma_6^B & = \frac{1}{120}\gamma_E^5 + \frac{1}{12}\left(\gamma_E^3\zeta_2\right) + \frac{1}{40}\left(9\gamma_E\zeta_2^2\right) + \frac{1}{6}\left(\gamma_E^2\zeta_3\right) + \frac{1}{6}\left(\zeta_2\zeta_3\right) + \frac{1}{5}\zeta_5, \\
\gamma_7^B & = \frac{1}{720}\gamma_E^6 + \frac{1}{48}\left(\gamma_E^4\zeta_2\right) + \frac{9}{80}\left(\gamma_E^2\zeta_2^2\right) + \frac{61}{560}\zeta_2^3 + \frac{1}{18}\left(\gamma_E^3\zeta_3\right) + \frac{1}{6}\left(\gamma_E\zeta_2\zeta_3\right) \\
& + \frac{1}{18}\zeta_3^2 + \frac{1}{5}\gamma_E\zeta_5, \\
\gamma_8^B & = \frac{1}{5040}\gamma_E^7 + \frac{1}{240}\left(\gamma_E^5\zeta_2\right) + \frac{3}{80}\left(\gamma_E^3\zeta_2^2\right) + \frac{61}{560}\left(\gamma_E\zeta_2^3\right) + \frac{1}{72}\left(\gamma_E^4\zeta_3\right) \\
& + \frac{1}{12}\left(\gamma_E^2\zeta_2\zeta_3\right) + \frac{3}{40}\left(\zeta_2^2\zeta_3\right) + \frac{1}{18}\left(\gamma_E\zeta_3^2\right) + \frac{1}{10}\left(\gamma_E^2\zeta_5\right) + \frac{1}{10}\left(\zeta_2\zeta_5\right) + \frac{1}{7}\zeta_7. \tag{G.6}
\end{aligned}$$

Bibliography

- [1] S. Dawson, C. Kao, Y. Wang, and P. Williams, “QCD Corrections to Higgs Pair Production in Bottom Quark Fusion,” *Phys. Rev.* **D75** (2007) 013007, [arXiv:hep-ph/0610284](#) [hep-ph].
- [2] T. Gehrmann and D. Kara, “The $Hb\bar{b}$ form factor to three loops in QCD,” *JHEP* **09** (2014) 174, [arXiv:1407.8114](#) [hep-ph].
- [3] S. Catani, “The Singular behavior of QCD amplitudes at two loop order,” *Phys. Lett.* **B427** (1998) 161–171, [arXiv:hep-ph/9802439](#) [hep-ph].
- [4] C. Duhr, F. Dulat, and B. Mistlberger, “Higgs Boson Production in Bottom-Quark Fusion to Third Order in the Strong Coupling,” *Phys. Rev. Lett.* **125** no. 5, (2020) 051804, [arXiv:1904.09990](#) [hep-ph].
- [5] V. Ravindran, J. Smith, and W. L. van Neerven, “QCD threshold corrections to di-lepton and Higgs rapidity distributions beyond N^2 LO,” *Nucl. Phys. B* **767** (2007) 100–129, [arXiv:hep-ph/0608308](#).
- [6] E. Laenen, L. Magnea, and G. Stavenga, “On next-to-eikonal corrections to threshold resummation for the Drell-Yan and DIS cross sections,” *Phys. Lett. B* **669** (2008) 173–179, [arXiv:0807.4412](#) [hep-ph].
- [7] N. Bahjat-Abbas, D. Bonocore, J. Sinninghe Damsté, E. Laenen, L. Magnea, L. Vernazza, and C. White, “Diagrammatic resummation of leading-logarithmic threshold effects at next-to-leading power,” *JHEP* **11** (2019) 002, [arXiv:1905.13710](#) [hep-ph].

- [8] S. Moch and A. Vogt, “On non-singlet physical evolution kernels and large- x coefficient functions in perturbative QCD,” *JHEP* **11** (2009) 099, [arXiv:0909.2124 \[hep-ph\]](#).
- [9] G. Sterman, “Summation of large corrections to short-distance hadronic cross sections,” *Nuclear Physics B* **281** no. 1, (1987) 310–364.
<https://www.sciencedirect.com/science/article/pii/0550321387902586>.
- [10] S. Catani and L. Trentadue, “Resummation of the qcd perturbative series for hard processes,” *Nuclear Physics B* **327** no. 2, (1989) 323–352.
<https://www.sciencedirect.com/science/article/pii/0550321389902733>.
- [11] P. W. Higgs, “Broken symmetries, massless particles and gauge fields,” *Phys. Lett.* **12** (1964) 132–133.
- [12] P. W. Higgs, “Broken Symmetries and the Masses of Gauge Bosons,” *Phys. Rev. Lett.* **13** (1964) 508–509.
- [13] P. W. Higgs, “Spontaneous Symmetry Breakdown without Massless Bosons,” *Phys. Rev.* **145** (1966) 1156–1163.
- [14] F. Englert and R. Brout, “Broken Symmetry and the Mass of Gauge Vector Mesons,” *Phys. Rev. Lett.* **13** (1964) 321–323.
- [15] G. S. Guralnik, C. R. Hagen, and T. W. B. Kibble, “Global Conservation Laws and Massless Particles,” *Phys. Rev. Lett.* **13** (1964) 585–587.
- [16] C. Duhr, F. Dulat, and B. Mistlberger, “The Drell-Yan cross section to third order in the strong coupling constant,” [arXiv:2001.07717 \[hep-ph\]](#).
- [17] C. Anastasiou, C. Duhr, F. Dulat, F. Herzog, and B. Mistlberger, “Higgs Boson Gluon-Fusion Production in QCD at Three Loops,” *Phys. Rev. Lett.* **114** (2015) 212001, [arXiv:1503.06056 \[hep-ph\]](#).
- [18] R. K. Ellis, W. J. Stirling, and B. R. Webber, *QCD and Collider Physics*. Cambridge Monographs on Particle Physics, Nuclear Physics and Cosmology. Cambridge University Press, 1996.

- [19] M. L. Mangano, “Introduction to QCD,” in *1998 European School of High-Energy Physics*. 1998.
- [20] G. P. Salam, “Elements of QCD for hadron colliders,” in *2009 European School of High-Energy Physics*. 11, 2010. [arXiv:1011.5131 \[hep-ph\]](#).
- [21] P. Nason, “Introduction to QCD,” *Conf. Proc. C* **9705251** (1997) 94–149.
- [22] G. ’t Hooft and M. J. G. Veltman, “Regularization and Renormalization of Gauge Fields,” *Nucl. Phys. B* **44** (1972) 189–213.
- [23] D. J. Gross and F. Wilczek, “Ultraviolet Behavior of Nonabelian Gauge Theories,” *Phys. Rev. Lett.* **30** (1973) 1343–1346. [,271(1973)].
- [24] H. D. Politzer, “Reliable Perturbative Results for Strong Interactions?,” *Phys. Rev. Lett.* **30** (1973) 1346–1349. [,274(1973)].
- [25] W. E. Caswell, “Asymptotic Behavior of Nonabelian Gauge Theories to Two Loop Order,” *Phys. Rev. Lett.* **33** (1974) 244.
- [26] D. R. T. Jones, “Two Loop Diagrams in Yang-Mills Theory,” *Nucl. Phys.* **B75** (1974) 531.
- [27] E. Egorian and O. V. Tarasov, “Two Loop Renormalization of the QCD in an Arbitrary Gauge,” *Teor. Mat. Fiz.* **41** (1979) 26–32. [Theor. Math. Phys.41,863(1979)].
- [28] O. Tarasov, A. Vladimirov, and A. Zharkov, “The Gell-Mann-Low Function of QCD in the Three Loop Approximation,” *Phys. Lett. B* **93** (1980) 429–432.
- [29] S. Larin and J. Vermaseren, “The Three loop QCD Beta function and anomalous dimensions,” *Phys. Lett. B* **303** (1993) 334–336, [arXiv:hep-ph/9302208](#).
- [30] T. van Ritbergen, J. A. M. Vermaseren, and S. A. Larin, “The Four loop beta function in quantum chromodynamics,” *Phys. Lett. B* **400** (1997) 379–384, [arXiv:hep-ph/9701390](#).
- [31] T. Kinoshita, “Mass singularities of Feynman amplitudes,” *J. Math. Phys.* **3** (1962) 650–677.
- [32] T. D. Lee and M. Nauenberg, “Degenerate Systems and Mass Singularities,” *Phys. Rev.* **133** (1964) B1549–B1562. [,25(1964)].

- [33] G. Altarelli and G. Parisi, “Asymptotic Freedom in Parton Language,” *Nucl. Phys. B* **126** (1977) 298–318.
- [34] V. Sudakov, “Vertex parts at very high-energies in quantum electrodynamics,” *Sov. Phys. JETP* **3** (1956) 65–71.
- [35] A. H. Mueller, “On the Asymptotic Behavior of the Sudakov Form-factor,” *Phys. Rev.* **D20** (1979) 2037.
- [36] J. C. Collins, “Algorithm to Compute Corrections to the Sudakov Form-factor,” *Phys. Rev.* **D22** (1980) 1478.
- [37] A. Sen, “Asymptotic Behavior of the Sudakov Form-Factor in QCD,” *Phys. Rev.* **D24** (1981) 3281.
- [38] L. Magnea and G. F. Sterman, “Analytic continuation of the Sudakov form-factor in QCD,” *Phys. Rev. D* **42** (1990) 4222–4227.
- [39] V. Ravindran, “On Sudakov and soft resummations in QCD,” *Nucl. Phys. B* **746** (2006) 58–76, [arXiv:hep-ph/0512249](#).
- [40] V. Ravindran, “Higher-order threshold effects to inclusive processes in QCD,” *Nucl. Phys.* **B752** (2006) 173–196, [arXiv:hep-ph/0603041](#) [hep-ph].
- [41] V. Ravindran, J. Smith, and W. L. van Neerven, “Two-loop corrections to Higgs boson production,” *Nucl. Phys. B* **704** (2005) 332–348, [arXiv:hep-ph/0408315](#).
- [42] S. Moch, J. A. M. Vermaseren, and A. Vogt, “Three-loop results for quark and gluon form-factors,” *Phys. Lett.* **B625** (2005) 245–252, [arXiv:hep-ph/0508055](#) [hep-ph].
- [43] G. Korchemsky and A. Radyushkin, “Renormalization of the Wilson Loops Beyond the Leading Order,” *Nucl. Phys. B* **283** (1987) 342–364.
- [44] S. Moch, J. A. M. Vermaseren, and A. Vogt, “The Three loop splitting functions in QCD: The Nonsinglet case,” *Nucl. Phys.* **B688** (2004) 101–134, [arXiv:hep-ph/0403192](#) [hep-ph].

- [45] A. Vogt, S. Moch, and J. A. M. Vermaseren, “The Three-loop splitting functions in QCD: The Singlet case,” *Nucl. Phys.* **B691** (2004) 129–181, [arXiv:hep-ph/0404111 \[hep-ph\]](#).
- [46] J. M. Henn, G. P. Korchemsky, and B. Mistlberger, “The full four-loop cusp anomalous dimension in $\mathcal{N} = 4$ super Yang-Mills and QCD,” *JHEP* **04** (2020) 018, [arXiv:1911.10174 \[hep-th\]](#).
- [47] A. von Manteuffel, E. Panzer, and R. M. Schabinger, “Analytic four-loop anomalous dimensions in massless QCD from form factors,” [arXiv:2002.04617 \[hep-ph\]](#).
- [48] T. Becher, M. Neubert, and B. D. Pecjak, “Factorization and Momentum-Space Resummation in Deep-Inelastic Scattering,” *JHEP* **01** (2007) 076, [arXiv:hep-ph/0607228](#).
- [49] T. Becher and M. Neubert, “On the Structure of Infrared Singularities of Gauge-Theory Amplitudes,” *JHEP* **06** (2009) 081, [arXiv:0903.1126 \[hep-ph\]](#). [Erratum: *JHEP*11,024(2013)].
- [50] J. Davies, A. Vogt, B. Ruijl, T. Ueda, and J. A. M. Vermaseren, “Large- n_f contributions to the four-loop splitting functions in QCD,” *Nucl. Phys.* **B915** (2017) 335–362, [arXiv:1610.07477 \[hep-ph\]](#).
- [51] G. Das, S.-O. Moch, and A. Vogt, “Soft corrections to inclusive deep-inelastic scattering at four loops and beyond,” [arXiv:1912.12920 \[hep-ph\]](#).
- [52] G. Das, S. Moch, and A. Vogt, “Approximate four-loop QCD corrections to the Higgs-boson production cross section,” [arXiv:2004.00563 \[hep-ph\]](#).
- [53] J. M. Henn, A. V. Smirnov, V. A. Smirnov, and M. Steinhauser, “A planar four-loop form factor and cusp anomalous dimension in QCD,” *JHEP* **05** (2016) 066, [arXiv:1604.03126 \[hep-ph\]](#).
- [54] J. Henn, A. V. Smirnov, V. A. Smirnov, M. Steinhauser, and R. N. Lee, “Four-loop photon quark form factor and cusp anomalous dimension in the large- N_c limit of QCD,” *JHEP* **03** (2017) 139, [arXiv:1612.04389 \[hep-ph\]](#).

- [55] A. von Manteuffel and R. M. Schabinger, “Quark and gluon form factors to four-loop order in QCD: the N_f^3 contributions,” *Phys. Rev. D* **95** no. 3, (2017) 034030, [arXiv:1611.00795 \[hep-ph\]](#).
- [56] R. N. Lee, A. V. Smirnov, V. A. Smirnov, and M. Steinhauser, “The n_f^2 contributions to fermionic four-loop form factors,” *Phys. Rev.* **D96** no. 1, (2017) 014008, [arXiv:1705.06862 \[hep-ph\]](#).
- [57] A. von Manteuffel and R. M. Schabinger, “Quark and gluon form factors in four loop QCD: The N_f^2 and $N_{q\gamma}N_f$ contributions,” *Phys. Rev. D* **99** no. 9, (2019) 094014, [arXiv:1902.08208 \[hep-ph\]](#).
- [58] T. Gehrmann, E. W. N. Glover, T. Huber, N. Ikizlerli, and C. Studerus, “Calculation of the quark and gluon form factors to three loops in QCD,” *JHEP* **06** (2010) 094, [arXiv:1004.3653 \[hep-ph\]](#).
- [59] T. Gehrmann, E. Glover, T. Huber, N. Ikizlerli, and C. Studerus, “The quark and gluon form factors to three loops in QCD through to $O(\epsilon^2)$,” *JHEP* **11** (2010) 102, [arXiv:1010.4478 \[hep-ph\]](#).
- [60] T. Ahmed, M. Mahakhud, N. Rana, and V. Ravindran, “Drell-Yan Production at Threshold to Third Order in QCD,” *Phys. Rev. Lett.* **113** no. 11, (2014) 112002, [arXiv:1404.0366 \[hep-ph\]](#).
- [61] Y. Li, A. von Manteuffel, R. M. Schabinger, and H. X. Zhu, “ N^3 LO Higgs boson and Drell-Yan production at threshold: The one-loop two-emission contribution,” *Phys. Rev.* **D90** no. 5, (2014) 053006, [arXiv:1404.5839 \[hep-ph\]](#).
- [62] S. Catani, L. Cieri, D. de Florian, G. Ferrera, and M. Grazzini, “Threshold resummation at N^3 LL accuracy and soft-virtual cross sections at N^3 LO,” *Nucl. Phys.* **B888** (2014) 75–91, [arXiv:1405.4827 \[hep-ph\]](#).
- [63] T. Ahmed, N. Rana, and V. Ravindran, “Higgs boson production through $b\bar{b}$ annihilation at threshold in N^3 LO QCD,” *JHEP* **10** (2014) 139, [arXiv:1408.0787 \[hep-ph\]](#).

- [64] S. Moch, B. Ruijl, T. Ueda, J. A. M. Vermaseren, and A. Vogt, “On quartic colour factors in splitting functions and the gluon cusp anomalous dimension,” *Phys. Lett.* **B782** (2018) 627–632, [arXiv:1805.09638 \[hep-ph\]](#).
- [65] S. Moch and A. Vogt, “Higher-order soft corrections to lepton pair and Higgs boson production,” *Phys. Lett. B* **631** (2005) 48–57, [arXiv:hep-ph/0508265](#).
- [66] D. de Florian and J. Mazzitelli, “A next-to-next-to-leading order calculation of soft-virtual cross sections,” *JHEP* **12** (2012) 088, [arXiv:1209.0673 \[hep-ph\]](#).
- [67] M. C. Kumar, M. K. Mandal, and V. Ravindran, “Associated production of Higgs boson with vector boson at threshold N³LO in QCD,” *JHEP* **03** (2015) 037, [arXiv:1412.3357 \[hep-ph\]](#).
- [68] S. Catani and L. Trentadue, “Resummation of the QCD Perturbative Series for Hard Processes,” *Nucl. Phys.* **B327** (1989) 323–352.
- [69] G. F. Sterman, “Summation of Large Corrections to Short Distance Hadronic Cross-Sections,” *Nucl. Phys.* **B281** (1987) 310–364.
- [70] A. H. Ajjath, P. Banerjee, A. Chakraborty, P. K. Dhani, P. Mukherjee, N. Rana, and V. Ravindran, “Higgs pair production from bottom quark annihilation to NNLO in QCD,” *JHEP* **05** (2019) 030, [arXiv:1811.01853 \[hep-ph\]](#).
- [71] ATLAS Collaboration, G. Aad *et al.*, “Observation of a new particle in the search for the Standard Model Higgs boson with the ATLAS detector at the LHC,” *Phys. Lett.* **B716** (2012) 1–29, [arXiv:1207.7214 \[hep-ex\]](#).
- [72] CMS Collaboration, S. Chatrchyan *et al.*, “Observation of a new boson at a mass of 125 GeV with the CMS experiment at the LHC,” *Phys. Lett.* **B716** (2012) 30–61, [arXiv:1207.7235 \[hep-ex\]](#).
- [73] R. P. Feynman and M. Gell-Mann, “Theory of the fermi interaction,” *Phys. Rev.* **109** (Jan, 1958) 193–198. <https://link.aps.org/doi/10.1103/PhysRev.109.193>.

- [74] S. L. Glashow, “Partial-symmetries of weak interactions,” *Nuclear Physics* **22** no. 4, (1961) 579–588.
<https://www.sciencedirect.com/science/article/pii/0029558261904692>.
- [75] M. Gell-Mann, “Symmetries of baryons and mesons,” *Phys. Rev.* **125** (Feb, 1962) 1067–1084. <https://link.aps.org/doi/10.1103/PhysRev.125.1067>.
- [76] J. Goldstone, A. Salam, and S. Weinberg, “Broken symmetries,” *Phys. Rev.* **127** (Aug, 1962) 965–970. <https://link.aps.org/doi/10.1103/PhysRev.127.965>.
- [77] P. Higgs, “Broken symmetries, massless particles and gauge fields,” *Physics Letters* **12** no. 2, (1964) 132–133.
<https://www.sciencedirect.com/science/article/pii/0031916364911369>.
- [78] F. Englert and R. Brout, “Broken symmetry and the mass of gauge vector mesons,” *Phys. Rev. Lett.* **13** (Aug, 1964) 321–323.
<https://link.aps.org/doi/10.1103/PhysRevLett.13.321>.
- [79] P. W. Higgs, “Broken symmetries and the masses of gauge bosons,” *Phys. Rev. Lett.* **13** (Oct, 1964) 508–509. <https://link.aps.org/doi/10.1103/PhysRevLett.13.508>.
- [80] G. S. Guralnik, C. R. Hagen, and T. W. B. Kibble, “Global conservation laws and massless particles,” *Phys. Rev. Lett.* **13** (Nov, 1964) 585–587.
<https://link.aps.org/doi/10.1103/PhysRevLett.13.585>.
- [81] P. W. Higgs, “Spontaneous symmetry breakdown without massless bosons,” *Phys. Rev.* **145** (May, 1966) 1156–1163. <https://link.aps.org/doi/10.1103/PhysRev.145.1156>.
- [82] S. Weinberg, “A model of leptons,” *Phys. Rev. Lett.* **19** (Nov, 1967) 1264–1266.
<https://link.aps.org/doi/10.1103/PhysRevLett.19.1264>.
- [83] H. Fritzsch, M. Gell-Mann, and H. Leutwyler, “Advantages of the color octet gluon picture,” *Physics Letters B* **47** no. 4, (1973) 365–368.
<https://www.sciencedirect.com/science/article/pii/0370269373906254>.
- [84] A. Salam, *Weak and electromagnetic interactions*, pp. 244–254.

- [85] CMS Collaboration, A. M. Sirunyan *et al.*, “A measurement of the Higgs boson mass in the diphoton decay channel,” *Phys. Lett. B* **805** (2020) 135425, [arXiv:2002.06398 \[hep-ex\]](#).
- [86] CMS Collaboration, A. M. Sirunyan *et al.*, “Combined measurements of Higgs boson couplings in proton–proton collisions at $\sqrt{s} = 13$ TeV,” *Eur. Phys. J. C* **79** no. 5, (2019) 421, [arXiv:1809.10733 \[hep-ex\]](#).
- [87] ATLAS Collaboration, G. Aad *et al.*, “Combined measurements of Higgs boson production and decay using up to 80 fb^{-1} of proton-proton collision data at $\sqrt{s} = 13$ TeV collected with the ATLAS experiment,” *Phys. Rev. D* **101** no. 1, (2020) 012002, [arXiv:1909.02845 \[hep-ex\]](#).
- [88] MuLan Collaboration, D. M. Webber *et al.*, “Measurement of the Positive Muon Lifetime and Determination of the Fermi Constant to Part-per-Million Precision,” *Phys. Rev. Lett.* **106** (2011) 041803, [arXiv:1010.0991 \[hep-ex\]](#).
- [89] T. Plehn and M. Rauch, “The quartic higgs coupling at hadron colliders,” *Phys. Rev. D* **72** (2005) 053008, [arXiv:hep-ph/0507321](#).
- [90] T. Binoth, S. Karg, N. Kauer, and R. Ruckl, “Multi-Higgs boson production in the Standard Model and beyond,” *Phys. Rev.* **D74** (2006) 113008, [arXiv:hep-ph/0608057 \[hep-ph\]](#).
- [91] U. Baur, T. Plehn, and D. L. Rainwater, “Probing the Higgs selfcoupling at hadron colliders using rare decays,” *Phys. Rev.* **D69** (2004) 053004, [arXiv:hep-ph/0310056 \[hep-ph\]](#).
- [92] J. Baglio, A. Djouadi, R. Gröber, M. M. Mühlleitner, J. Quevillon, and M. Spira, “The measurement of the Higgs self-coupling at the LHC: theoretical status,” *JHEP* **04** (2013) 151, [arXiv:1212.5581 \[hep-ph\]](#).
- [93] W. Yao, “Studies of measuring Higgs self-coupling with $HH \rightarrow b\bar{b}\gamma\gamma$ at the future hadron colliders,” in *Community Summer Study 2013: Snowmass on the Mississippi*. 8, 2013. [arXiv:1308.6302 \[hep-ph\]](#).

- [94] V. Barger, L. L. Everett, C. B. Jackson, and G. Shaughnessy, “Higgs-Pair Production and Measurement of the Triscalar Coupling at LHC(8,14),” *Phys. Lett. B* **728** (2014) 433–436, [arXiv:1311.2931 \[hep-ph\]](#).
- [95] A. Azatov, R. Contino, G. Panico, and M. Son, “Effective field theory analysis of double Higgs boson production via gluon fusion,” *Phys. Rev. D* **92** no. 3, (2015) 035001, [arXiv:1502.00539 \[hep-ph\]](#).
- [96] M. J. Dolan, C. Englert, and M. Spannowsky, “Higgs self-coupling measurements at the LHC,” *JHEP* **10** (2012) 112, [arXiv:1206.5001 \[hep-ph\]](#).
- [97] A. Papaefstathiou, L. L. Yang, and J. Zurita, “Higgs boson pair production at the LHC in the $b\bar{b}W^+W^-$ channel,” *Phys. Rev. D* **87** no. 1, (2013) 011301, [arXiv:1209.1489 \[hep-ph\]](#).
- [98] D. E. Ferreira de Lima, A. Papaefstathiou, and M. Spannowsky, “Standard model Higgs boson pair production in the $(b\bar{b})(b\bar{b})$ final state,” *JHEP* **08** (2014) 030, [arXiv:1404.7139 \[hep-ph\]](#).
- [99] J. Alison *et al.*, “Higgs boson potential at colliders: Status and perspectives,” *Rev. Phys.* **5** (2020) 100045, [arXiv:1910.00012 \[hep-ph\]](#).
- [100] E. W. N. Glover and J. J. van der Bij, “HIGGS BOSON PAIR PRODUCTION VIA GLUON FUSION,” *Nucl. Phys.* **B309** (1988) 282–294.
- [101] O. J. P. Eboli, G. C. Marques, S. F. Novaes, and A. A. Natale, “TWIN HIGGS BOSON PRODUCTION,” *Phys. Lett.* **B197** (1987) 269–272.
- [102] T. Plehn, M. Spira, and P. M. Zerwas, “Pair production of neutral Higgs particles in gluon-gluon collisions,” *Nucl. Phys.* **B479** (1996) 46–64, [arXiv:hep-ph/9603205 \[hep-ph\]](#). [Erratum: *Nucl. Phys.*B531,655(1998)].
- [103] S. Dawson, S. Dittmaier, and M. Spira, “Neutral Higgs boson pair production at hadron colliders: QCD corrections,” *Phys. Rev. D* **58** (1998) 115012, [arXiv:hep-ph/9805244 \[hep-ph\]](#).

- [104] J. Baglio, F. Campanario, S. Glaus, M. Mühlleitner, M. Spira, and J. Streicher, “Gluon fusion into Higgs pairs at NLO QCD and the top mass scheme,” *Eur. Phys. J. C* **79** no. 6, (2019) 459, [arXiv:1811.05692 \[hep-ph\]](#).
- [105] J. Davies, G. Heinrich, S. P. Jones, M. Kerner, G. Mishima, M. Steinhauser, and D. Wellmann, “Double Higgs boson production at NLO: combining the exact numerical result and high-energy expansion,” *JHEP* **11** (2019) 024, [arXiv:1907.06408 \[hep-ph\]](#).
- [106] D. de Florian and J. Mazzitelli, “Higgs Boson Pair Production at Next-to-Next-to-Leading Order in QCD,” *Phys. Rev. Lett.* **111** (2013) 201801, [arXiv:1309.6594 \[hep-ph\]](#).
- [107] D. de Florian and J. Mazzitelli, “Two-loop virtual corrections to Higgs pair production,” *Phys. Lett.* **B724** (2013) 306–309, [arXiv:1305.5206 \[hep-ph\]](#).
- [108] J. Grigo, J. Hoff, and M. Steinhauser, “Higgs boson pair production: top quark mass effects at NLO and NNLO,” *Nucl. Phys.* **B900** (2015) 412–430, [arXiv:1508.00909 \[hep-ph\]](#).
- [109] D. de Florian, M. Grazzini, C. Hanga, S. Kallweit, J. M. Lindert, P. Maierhöfner, J. Mazzitelli, and D. Rathlev, “Differential Higgs Boson Pair Production at Next-to-Next-to-Leading Order in QCD,” *JHEP* **09** (2016) 151, [arXiv:1606.09519 \[hep-ph\]](#).
- [110] L.-B. Chen, H. T. Li, H.-S. Shao, and J. Wang, “Higgs boson pair production via gluon fusion at N^3 LO in QCD,” *Phys. Lett. B* **803** (2020) 135292, [arXiv:1909.06808 \[hep-ph\]](#).
- [111] L.-B. Chen, H. T. Li, H.-S. Shao, and J. Wang, “The gluon-fusion production of Higgs boson pair: N^3 LO QCD corrections and top-quark mass effects,” *JHEP* **03** (2020) 072, [arXiv:1912.13001 \[hep-ph\]](#).
- [112] D. Y. Shao, C. S. Li, H. T. Li, and J. Wang, “Threshold resummation effects in Higgs boson pair production at the LHC,” *JHEP* **07** (2013) 169, [arXiv:1301.1245 \[hep-ph\]](#).
- [113] D. de Florian and J. Mazzitelli, “Higgs pair production at next-to-next-to-leading logarithmic accuracy at the LHC,” *JHEP* **09** (2015) 053, [arXiv:1505.07122 \[hep-ph\]](#).

- [114] D. De Florian and J. Mazzitelli, “Soft gluon resummation for Higgs boson pair production including finite M_t effects,” *JHEP* **08** (2018) 156, [arXiv:1807.03704 \[hep-ph\]](#).
- [115] M. Grazzini, G. Heinrich, S. Jones, S. Kallweit, M. Kerner, J. M. Lindert, and J. Mazzitelli, “Higgs boson pair production at NNLO with top quark mass effects,” *JHEP* **05** (2018) 059, [arXiv:1803.02463 \[hep-ph\]](#).
- [116] P. Banerjee, S. Borowka, P. K. Dhani, T. Gehrmann, and V. Ravindran, “Two-loop massless QCD corrections to the $g + g \rightarrow H + H$ four-point amplitude,” *Submitted to: JHEP* (2018), [arXiv:1809.05388 \[hep-ph\]](#).
- [117] H. P. Nilles, “Supersymmetry, Supergravity and Particle Physics,” *Phys. Rept.* **110** (1984) 1–162.
- [118] S. Dawson, C. Kao, and Y. Wang, “SUSY QCD Corrections to Higgs Pair Production from Bottom Quark Fusion,” *Phys. Rev.* **D77** (2008) 113005, [arXiv:0710.4331 \[hep-ph\]](#).
- [119] H.-S. Hou, W.-G. Ma, R.-Y. Zhang, Y. Jiang, L. Han, and L.-R. Xing, “Pair production of charged Higgs bosons from bottom-quark fusion,” *Phys. Rev.* **D71** (2005) 075014, [arXiv:hep-ph/0502214 \[hep-ph\]](#).
- [120] J.-J. Liu, W.-G. Ma, G. Li, R.-Y. Zhang, and H.-S. Hou, “Higgs boson pair production in the little Higgs model at hadron collider,” *Phys. Rev.* **D70** (2004) 015001, [arXiv:hep-ph/0404171 \[hep-ph\]](#).
- [121] M. A. G. Aivazis, J. C. Collins, F. I. Olness, and W.-K. Tung, “Leptoproduction of heavy quarks. 2. A Unified QCD formulation of charged and neutral current processes from fixed target to collider energies,” *Phys. Rev. D* **50** (1994) 3102–3118, [arXiv:hep-ph/9312319](#).
- [122] J. C. Collins, “Hard scattering factorization with heavy quarks: A General treatment,” *Phys. Rev.* **D58** (1998) 094002, [arXiv:hep-ph/9806259 \[hep-ph\]](#).
- [123] M. Krämer, F. I. Olness, and D. E. Soper, “Treatment of heavy quarks in deeply inelastic scattering,” *Phys. Rev. D* **62** (2000) 096007, [arXiv:hep-ph/0003035](#).
- [124] T. Gehrmann, L. Tancredi, and E. Weihs, “Two-loop master integrals for $q\bar{q} \rightarrow VV$: the planar topologies,” *JHEP* **08** (2013) 070, [arXiv:1306.6344](#).

- [125] D. A. Dicus and S. Willenbrock, “Higgs Boson Production from Heavy Quark Fusion,” *Phys. Rev.* **D39** (1989) 751.
- [126] D. Dicus, T. Stelzer, Z. Sullivan, and S. Willenbrock, “Higgs boson production in association with bottom quarks at next-to-leading order,” *Phys. Rev.* **D59** (1999) 094016, [arXiv:hep-ph/9811492](#) [hep-ph].
- [127] F. Maltoni, Z. Sullivan, and S. Willenbrock, “Higgs-Boson Production via Bottom-Quark Fusion,” *Phys. Rev. D* **67** (2003) 093005, [arXiv:hep-ph/0301033](#).
- [128] F. I. Olness and W.-K. Tung, “When Is a Heavy Quark Not a Parton? Charged Higgs Production and Heavy Quark Mass Effects in the QCD Based Parton Model,” *Nucl. Phys.* **B308** (1988) 813.
- [129] J. F. Gunion, H. E. Haber, F. E. Paige, W.-K. Tung, and S. S. D. Willenbrock, “Neutral and Charged Higgs Detection: Heavy Quark Fusion, Top Quark Mass Dependence and Rare Decays,” *Nucl. Phys.* **B294** (1987) 621.
- [130] R. V. Harlander and W. B. Kilgore, “Higgs boson production in bottom quark fusion at next-to-next-to leading order,” *Phys. Rev.* **D68** (2003) 013001, [arXiv:hep-ph/0304035](#) [hep-ph].
- [131] T. Ahmed, M. Mahakhud, P. Mathews, N. Rana, and V. Ravindran, “Two-loop QCD corrections to Higgs $\rightarrow b + \bar{b} + g$ amplitude,” *JHEP* **08** (2014) 075, [arXiv:1405.2324](#) [hep-ph].
- [132] T. Ahmed, M. K. Mandal, N. Rana, and V. Ravindran, “Higgs Rapidity Distribution in $b\bar{b}$ Annihilation at Threshold in N³LO QCD,” *JHEP* **02** (2015) 131, [arXiv:1411.5301](#) [hep-ph].
- [133] P. Nogueira, “Automatic Feynman graph generation,” *J. Comput. Phys.* **105** (1993) 279–289.
- [134] J. A. M. Vermaseren, “New features of FORM,” [arXiv:math-ph/0010025](#) [math-ph].
- [135] A. von Manteuffel and C. Studerus, “Reduze 2 - Distributed Feynman Integral Reduction,” [arXiv:1201.4330](#) [hep-ph].

- [136] F. V. Tkachov, “A Theorem on Analytical Calculability of Four Loop Renormalization Group Functions,” *Phys. Lett.* **100B** (1981) 65–68.
- [137] K. G. Chetyrkin and F. V. Tkachov, “Integration by Parts: The Algorithm to Calculate beta Functions in 4 Loops,” *Nucl. Phys.* **B192** (1981) 159–204.
- [138] T. Gehrmann and E. Remiddi, “Differential equations for two loop four point functions,” *Nucl. Phys.* **B580** (2000) 485–518, [arXiv:hep-ph/9912329](#) [hep-ph].
- [139] R. N. Lee, “LiteRed 1.4: a powerful tool for reduction of multiloop integrals,” *J. Phys. Conf. Ser.* **523** (2014) 012059, [arXiv:1310.1145](#) [hep-ph].
- [140] T. Gehrmann, A. von Manteuffel, L. Tancredi, and E. Weihs, “The two-loop master integrals for $q\bar{q} \rightarrow VV$,” *JHEP* **06** (2014) 032, [arXiv:1404.4853](#) [hep-ph].
- [141] N. Kidonakis, G. Oderda, and G. F. Sterman, “Evolution of color exchange in QCD hard scattering,” *Nucl. Phys.* **B531** (1998) 365–402, [arXiv:hep-ph/9803241](#) [hep-ph].
- [142] A. Sen, “Asymptotic Behavior of the Wide Angle On-Shell Quark Scattering Amplitudes in Nonabelian Gauge Theories,” *Phys. Rev.* **D28** (1983) 860.
- [143] L. W. Garland, T. Gehrmann, E. W. N. Glover, A. Koukoutsakis, and E. Remiddi, “The Two loop QCD matrix element for $e^+ e^- \rightarrow 3$ jets,” *Nucl. Phys.* **B627** (2002) 107–188, [arXiv:hep-ph/0112081](#) [hep-ph].
- [144] C. Anastasiou, E. W. N. Glover, C. Oleari, and M. E. Tejeda-Yeomans, “Two loop QCD corrections to massless quark gluon scattering,” *Nucl. Phys.* **B605** (2001) 486–516, [arXiv:hep-ph/0101304](#) [hep-ph].
- [145] E. W. N. Glover, C. Oleari, and M. E. Tejeda-Yeomans, “Two loop QCD corrections to gluon-gluon scattering,” *Nucl. Phys.* **B605** (2001) 467–485, [arXiv:hep-ph/0102201](#) [hep-ph].
- [146] Z. Bern, A. De Freitas, and L. J. Dixon, “Two loop helicity amplitudes for gluon-gluon scattering in QCD and supersymmetric Yang-Mills theory,” *JHEP* **03** (2002) 018, [arXiv:hep-ph/0201161](#) [hep-ph].

- [147] Z. Bern, L. J. Dixon, and D. A. Kosower, “Two-loop $g \rightarrow gg$ splitting amplitudes in QCD,” *JHEP* **08** (2004) 012, [arXiv:hep-ph/0404293](#) [[hep-ph](#)].
- [148] G. F. Sterman and M. E. Tejeda-Yeomans, “Multiloop amplitudes and resummation,” *Phys. Lett.* **B552** (2003) 48–56, [arXiv:hep-ph/0210130](#) [[hep-ph](#)].
- [149] S. M. Aybat, L. J. Dixon, and G. F. Sterman, “The Two-loop anomalous dimension matrix for soft gluon exchange,” *Phys. Rev. Lett.* **97** (2006) 072001, [arXiv:hep-ph/0606254](#) [[hep-ph](#)].
- [150] S. M. Aybat, L. J. Dixon, and G. F. Sterman, “The Two-loop soft anomalous dimension matrix and resummation at next-to-next-to leading pole,” *Phys. Rev.* **D74** (2006) 074004, [arXiv:hep-ph/0607309](#) [[hep-ph](#)].
- [151] B. W. Harris and J. F. Owens, “The Two cutoff phase space slicing method,” *Phys. Rev.* **D65** (2002) 094032, [arXiv:hep-ph/0102128](#) [[hep-ph](#)].
- [152] L. A. Harland-Lang, A. D. Martin, P. Motylinski, and R. S. Thorne, “Parton distributions in the LHC era: MMHT 2014 PDFs,” *Eur. Phys. J.* **C75** no. 5, (2015) 204, [arXiv:1412.3989](#) [[hep-ph](#)].
- [153] A. Buckley, J. Ferrando, S. Lloyd, K. Nordström, B. Page, M. RÃijfenacht, M. SchÃunherr, and G. Watt, “LHAPDF6: parton density access in the LHC precision era,” *Eur. Phys. J.* **C75** (2015) 132, [arXiv:1412.7420](#) [[hep-ph](#)].
- [154] A. Ajjath, P. Banerjee, A. Chakraborty, P. K. Dhani, P. Mukherjee, N. Rana, and V. Ravindran, “NNLO QCD \oplus QED corrections to Higgs production in bottom quark annihilation,” *Phys. Rev. D* **100** no. 11, (2019) 114016, [arXiv:1906.09028](#) [[hep-ph](#)].
- [155] A. H. Ajjath, A. Chakraborty, G. Das, P. Mukherjee, and V. Ravindran, “Resummed prediction for Higgs boson production through $b\bar{b}$ annihilation at N³LL,” *JHEP* **11** (2019) 006, [arXiv:1905.03771](#) [[hep-ph](#)].
- [156] D. de Florian, M. Der, and I. Fabre, “QCD \oplus QED NNLO corrections to Drell Yan production,” *Phys. Rev. D* **98** no. 9, (2018) 094008, [arXiv:1805.12214](#) [[hep-ph](#)].

- [157] C. Anastasiou, S. Buehler, C. Duhr, and F. Herzog, “NNLO phase space master integrals for two-to-one inclusive cross sections in dimensional regularization,” *JHEP* **11** (2012) 062, [arXiv:1208.3130 \[hep-ph\]](#).
- [158] T. Becher and M. Neubert, “Infrared singularities of scattering amplitudes in perturbative QCD,” *Phys. Rev. Lett.* **102** (2009) 162001, [arXiv:0901.0722 \[hep-ph\]](#). [Erratum: *Phys. Rev. Lett.* 111, no. 19, 199905 (2013)].
- [159] E. Gardi and L. Magnea, “Infrared singularities in QCD amplitudes,” *Nuovo Cim. C* **32N5-6** (2009) 137–157, [arXiv:0908.3273 \[hep-ph\]](#).
- [160] O. Almelid, C. Duhr, and E. Gardi, “Three-loop corrections to the soft anomalous dimension in multileg scattering,” *Phys. Rev. Lett.* **117** no. 17, (2016) 172002, [arXiv:1507.00047 \[hep-ph\]](#).
- [161] O. Almelid, C. Duhr, E. Gardi, A. McLeod, and C. D. White, “Bootstrapping the QCD soft anomalous dimension,” *JHEP* **09** (2017) 073, [arXiv:1706.10162 \[hep-ph\]](#).
- [162] A. Ajjath, P. Mukherjee, and V. Ravindran, “Infrared structure of $SU(N) \times U(1)$ gauge theory to three loops,” *JHEP* **08** (2020) 156, [arXiv:1912.13386 \[hep-ph\]](#).
- [163] L. Cieri, G. Ferrera, and G. F. R. Sborlini, “Combining QED and QCD transverse-momentum resummation for Z boson production at hadron colliders,” *JHEP* **08** (2018) 165, [arXiv:1805.11948 \[hep-ph\]](#).
- [164] J. A. M. Vermaseren, S. A. Larin, and T. van Ritbergen, “The four loop quark mass anomalous dimension and the invariant quark mass,” *Phys. Lett. B* **405** (1997) 327–333, [arXiv:hep-ph/9703284](#).
- [165] C. W. Bauer, S. Fleming, and M. E. Luke, “Summing Sudakov logarithms in $B \rightarrow X(s\gamma)$ in effective field theory,” *Phys. Rev. D* **63** (2000) 014006, [arXiv:hep-ph/0005275](#).
- [166] C. W. Bauer, S. Fleming, D. Pirjol, and I. W. Stewart, “An Effective field theory for collinear and soft gluons: Heavy to light decays,” *Phys. Rev. D* **63** (2001) 114020, [arXiv:hep-ph/0011336](#).

- [167] C. W. Bauer, D. Pirjol, and I. W. Stewart, “Soft collinear factorization in effective field theory,” *Phys. Rev. D* **65** (2002) 054022, [arXiv:hep-ph/0109045](#).
- [168] M. Beneke, A. P. Chapovsky, M. Diehl, and T. Feldmann, “Soft collinear effective theory and heavy to light currents beyond leading power,” *Nucl. Phys. B* **643** (2002) 431–476, [arXiv:hep-ph/0206152](#).
- [169] T. Becher, A. Broggio, and A. Ferroglia, *Introduction to Soft-Collinear Effective Theory*, vol. 896. Springer, 2015. [arXiv:1410.1892 \[hep-ph\]](#).
- [170] D. de Florian, G. F. R. Sborlini, and G. Rodrigo, “QED corrections to the Altarelli–Parisi splitting functions,” *Eur. Phys. J. C* **76** no. 5, (2016) 282, [arXiv:1512.00612 \[hep-ph\]](#).
- [171] S. Majhi, P. Mathews, and V. Ravindran, “NNLO QCD corrections to the resonant sneutrino/slepton production at Hadron Colliders,” *Nucl. Phys. B* **850** (2011) 287–320, [arXiv:1011.6027 \[hep-ph\]](#).
- [172] L. Lewin, *Dilogarithms and Associated Functions*. Macdonald, 1958.
<https://books.google.co.in/books?id=6KazAAAAIAAJ>.
- [173] L. Lewin, *Polylogarithms and Associated Functions*. North Holland, 1981.
<https://books.google.co.in/books?id=yETvAAAAIAAJ>.
- [174] **NNPDF** Collaboration, V. Bertone, S. Carrazza, N. P. Hartland, and J. Rojo, “Illuminating the photon content of the proton within a global PDF analysis,” *SciPost Phys.* **5** no. 1, (2018) 008, [arXiv:1712.07053 \[hep-ph\]](#).
- [175] A. D. Martin, R. G. Roberts, W. J. Stirling, and R. S. Thorne, “Parton distributions incorporating QED contributions,” *Eur. Phys. J. C* **39** (2005) 155–161, [arXiv:hep-ph/0411040](#).
- [176] C. Schmidt, J. Pumplin, D. Stump, and C. P. Yuan, “CT14QED parton distribution functions from isolated photon production in deep inelastic scattering,” *Phys. Rev. D* **93** no. 11, (2016) 114015, [arXiv:1509.02905 \[hep-ph\]](#).

- [177] T. Ahmed, A. A. H., P. Mukherjee, V. Ravindran, and A. Sankar, “Soft-virtual correction and threshold resummation for n -colorless particles to fourth order in QCD: Part II,” [arXiv:2010.02980 \[hep-ph\]](#).
- [178] C. Anastasiou, L. J. Dixon, K. Melnikov, and F. Petriello, “Dilepton rapidity distribution in the Drell-Yan process at NNLO in QCD,” *Phys. Rev. Lett.* **91** (2003) 182002, [arXiv:hep-ph/0306192 \[hep-ph\]](#).
- [179] C. Anastasiou, L. J. Dixon, K. Melnikov, and F. Petriello, “High precision QCD at hadron colliders: Electroweak gauge boson rapidity distributions at NNLO,” *Phys. Rev.* **D69** (2004) 094008, [arXiv:hep-ph/0312266 \[hep-ph\]](#).
- [180] C. Anastasiou, K. Melnikov, and F. Petriello, “Higgs boson production at hadron colliders: Differential cross sections through next-to-next-to-leading order,” *Phys. Rev. Lett.* **93** (2004) 262002, [arXiv:hep-ph/0409088 \[hep-ph\]](#).
- [181] F. Dulat, B. Mistlberger, and A. Pelloni, “Precision predictions at N³LO for the Higgs boson rapidity distribution at the LHC,” *Phys. Rev. D* **99** no. 3, (2019) 034004, [arXiv:1810.09462 \[hep-ph\]](#).
- [182] L. Cieri, X. Chen, T. Gehrmann, E. W. N. Glover, and A. Huss, “Higgs boson production at the LHC using the q_T subtraction formalism at N³LO QCD,” *JHEP* **02** (2019) 096, [arXiv:1807.11501 \[hep-ph\]](#).
- [183] S. BÄijhler, F. Herzog, A. Lazopoulos, and R. MÄijller, “The fully differential hadronic production of a Higgs boson via bottom quark fusion at NNLO,” *JHEP* **07** (2012) 115, [arXiv:1204.4415 \[hep-ph\]](#).
- [184] V. Ravindran and J. Smith, “Threshold corrections to rapidity distributions of Z and W[±] bosons beyond N² LO at hadron colliders,” *Phys. Rev.* **D76** (2007) 114004, [arXiv:0708.1689 \[hep-ph\]](#).
- [185] A. Mukherjee and W. Vogelsang, “Threshold resummation for W-boson production at RHIC,” *Phys. Rev. D* **73** (2006) 074005, [arXiv:hep-ph/0601162](#).

- [186] E. Laenen and G. F. Sterman, “Resummation for Drell-Yan differential distributions,” in *7th Meeting of the APS Division of Particles Fields*, pp. 987–989. 11, 1992.
- [187] P. Bolzoni, “Threshold resummation of Drell-Yan rapidity distributions,” *Phys. Lett. B* **643** (2006) 325–330, [arXiv:hep-ph/0609073](#).
- [188] M. Bonvini, S. Forte, and G. Ridolfi, “Soft gluon resummation of Drell-Yan rapidity distributions: Theory and phenomenology,” *Nucl. Phys.* **B847** (2011) 93–159, [arXiv:1009.5691 \[hep-ph\]](#).
- [189] P. Banerjee, G. Das, P. K. Dhani, and V. Ravindran, “Threshold resummation of the rapidity distribution for Higgs production at NNLO+NNLL,” *Phys. Rev.* **D97** no. 5, (2018) 054024, [arXiv:1708.05706 \[hep-ph\]](#).
- [190] G. Lustermsans, J. K. L. Michel, and F. J. Tackmann, “Generalized Threshold Factorization with Full Collinear Dynamics,” [arXiv:1908.00985 \[hep-ph\]](#).
- [191] C. Anastasiou, C. Duhr, F. Dulat, E. Furlan, T. Gehrmann, F. Herzog, and B. Mistlberger, “Higgs boson gluon fusion production at threshold in N³LO QCD,” *Phys. Lett.* **B737** (2014) 325–328, [arXiv:1403.4616 \[hep-ph\]](#).
- [192] L. J. Dixon, L. Magnea, and G. F. Sterman, “Universal structure of subleading infrared poles in gauge theory amplitudes,” *JHEP* **08** (2008) 022, [arXiv:0805.3515 \[hep-ph\]](#).
- [193] E. Gardi and L. Magnea, “Factorization constraints for soft anomalous dimensions in QCD scattering amplitudes,” *JHEP* **03** (2009) 079, [arXiv:0901.1091 \[hep-ph\]](#).
- [194] T. Ahmed, J. M. Henn, and M. Steinhauser, “High energy behaviour of form factors,” *JHEP* **06** (2017) 125, [arXiv:1704.07846 \[hep-ph\]](#).
- [195] T. Ahmed, M. K. Mandal, N. Rana, and V. Ravindran, “Rapidity Distributions in Drell-Yan and Higgs Productions at Threshold to Third Order in QCD,” *Phys. Rev. Lett.* **113** (2014) 212003, [arXiv:1404.6504 \[hep-ph\]](#).
- [196] T. Ahmed, A. A. H., G. Das, P. Mukherjee, V. Ravindran, and S. Tiwari, “Soft-virtual correction and threshold resummation for n -colorless particles to fourth order in QCD: Part I,” [arXiv:2010.02979 \[hep-ph\]](#).

- [197] P. Banerjee, G. Das, P. K. Dhani, and V. Ravindran, “Threshold resummation of the rapidity distribution for Drell-Yan production at NNLO+NNLL,” *Phys. Rev.* **D98** no. 5, (2018) 054018, [arXiv:1805.01186 \[hep-ph\]](#).
- [198] A. H. Ajjath, P. Mukherjee, and V. Ravindran, “On next to soft corrections to Drell-Yan and Higgs Boson productions,” [arXiv:2006.06726 \[hep-ph\]](#).
- [199] E. Laenen, L. Magnea, G. Stavenga, and C. D. White, “Next-to-Eikonal Corrections to Soft Gluon Radiation: A Diagrammatic Approach,” *JHEP* **01** (2011) 141, [arXiv:1010.1860 \[hep-ph\]](#).
- [200] D. Bonocore, E. Laenen, L. Magnea, L. Vernazza, and C. D. White, “The method of regions and next-to-soft corrections in Drell-Yan production,” *Phys. Lett. B* **742** (2015) 375–382, [arXiv:1410.6406 \[hep-ph\]](#).
- [201] D. Bonocore, E. Laenen, L. Magnea, S. Melville, L. Vernazza, and C. White, “A factorization approach to next-to-leading-power threshold logarithms,” *JHEP* **06** (2015) 008, [arXiv:1503.05156 \[hep-ph\]](#).
- [202] D. Bonocore, E. Laenen, L. Magnea, L. Vernazza, and C. White, “Non-abelian factorisation for next-to-leading-power threshold logarithms,” *JHEP* **12** (2016) 121, [arXiv:1610.06842 \[hep-ph\]](#).
- [203] V. Del Duca, E. Laenen, L. Magnea, L. Vernazza, and C. White, “Universality of next-to-leading power threshold effects for colourless final states in hadronic collisions,” *JHEP* **11** (2017) 057, [arXiv:1706.04018 \[hep-ph\]](#).
- [204] G. Soar, S. Moch, J. Vermaseren, and A. Vogt, “On Higgs-exchange DIS, physical evolution kernels and fourth-order splitting functions at large x ,” *Nucl. Phys. B* **832** (2010) 152–227, [arXiv:0912.0369 \[hep-ph\]](#).
- [205] D. de Florian, J. Mazzitelli, S. Moch, and A. Vogt, “Approximate N³LO Higgs-boson production cross section using physical-kernel constraints,” *JHEP* **10** (2014) 176, [arXiv:1408.6277 \[hep-ph\]](#).

- [206] M. Beneke, A. Broggio, M. Garny, S. Jaskiewicz, R. Szafron, L. Vernazza, and J. Wang, “Leading-logarithmic threshold resummation of the Drell-Yan process at next-to-leading power,” *JHEP* **03** (2019) 043, [arXiv:1809.10631 \[hep-ph\]](#).
- [207] M. Beneke, M. Garny, S. Jaskiewicz, R. Szafron, L. Vernazza, and J. Wang, “Leading-logarithmic threshold resummation of Higgs production in gluon fusion at next-to-leading power,” *JHEP* **01** (2020) 094, [arXiv:1910.12685 \[hep-ph\]](#).
- [208] M. Beneke, A. Broggio, S. Jaskiewicz, and L. Vernazza, “Threshold factorization of the Drell-Yan process at next-to-leading power,” [arXiv:1912.01585 \[hep-ph\]](#).
- [209] W. van Neerven, “Dimensional Regularization of Mass and Infrared Singularities in Two Loop On-shell Vertex Functions,” *Nucl. Phys. B* **268** (1986) 453–488.
- [210] R. V. Harlander, “Virtual corrections to $g g \rightarrow H$ to two loops in the heavy top limit,” *Phys. Lett. B* **492** (2000) 74–80, [arXiv:hep-ph/0007289](#).
- [211] T. Gehrmann, T. Huber, and D. Maitre, “Two-loop quark and gluon form-factors in dimensional regularisation,” *Phys. Lett. B* **622** (2005) 295–302, [arXiv:hep-ph/0507061](#).
- [212] P. A. Baikov, K. G. Chetyrkin, A. V. Smirnov, V. A. Smirnov, and M. Steinhauser, “Quark and gluon form factors to three loops,” *Phys. Rev. Lett.* **102** (2009) 212002, [arXiv:0902.3519 \[hep-ph\]](#).
- [213] J. M. Henn, T. Peraro, M. Stahlhofen, and P. Wasser, “Matter dependence of the four-loop cusp anomalous dimension,” *Phys. Rev. Lett.* **122** no. 20, (2019) 201602, [arXiv:1901.03693 \[hep-ph\]](#).
- [214] K. Chetyrkin, J. H. Kuhn, and C. Sturm, “QCD decoupling at four loops,” *Nucl. Phys. B* **744** (2006) 121–135, [arXiv:hep-ph/0512060](#).
- [215] J. C. Collins, *Sudakov form-factors*, vol. 5, pp. 573–614. 1989. [arXiv:hep-ph/0312336](#).
- [216] L. Magnea, “Analytic resummation for the quark form-factor in QCD,” *Nucl. Phys. B* **593** (2001) 269–288, [arXiv:hep-ph/0006255](#).

- [217] S. Moch, J. Vermaseren, and A. Vogt, “The Quark form-factor at higher orders,” *JHEP* **08** (2005) 049, [arXiv:hep-ph/0507039](#).
- [218] J. Kodaira and L. Trentadue, “Summing Soft Emission in QCD,” *Phys. Lett. B* **112** (1982) 66.
- [219] J. Kodaira and L. Trentadue, “Single Logarithm Effects in electron-Positron Annihilation,” *Phys. Lett. B* **123** (1983) 335–338.
- [220] A. Gonzalez-Arroyo, C. Lopez, and F. Yndurain, “Second Order Contributions to the Structure Functions in Deep Inelastic Scattering. 1. Theoretical Calculations,” *Nucl. Phys. B* **153** (1979) 161–186.
- [221] G. Curci, W. Furmanski, and R. Petronzio, “Evolution of Parton Densities Beyond Leading Order: The Nonsinglet Case,” *Nucl. Phys. B* **175** (1980) 27–92.
- [222] W. Furmanski and R. Petronzio, “Singlet Parton Densities Beyond Leading Order,” *Phys. Lett. B* **97** (1980) 437–442.
- [223] R. Hamberg and W. van Neerven, “The Correct renormalization of the gluon operator in a covariant gauge,” *Nucl. Phys. B* **379** (1992) 143–171.
- [224] R. Ellis and W. Vogelsang, “The Evolution of parton distributions beyond leading order: The Singlet case,” [arXiv:hep-ph/9602356](#).
- [225] J. Ablinger, A. Behring, J. Blümlein, A. De Freitas, A. von Manteuffel, and C. Schneider, “The three-loop splitting functions $P_{qg}^{(2)}$ and $P_{gg}^{(2,N_F)}$,” *Nucl. Phys. B* **922** (2017) 1–40, [arXiv:1705.01508 \[hep-ph\]](#).
- [226] S. Moch, B. Ruijl, T. Ueda, J. A. M. Vermaseren, and A. Vogt, “Four-Loop Non-Singlet Splitting Functions in the Planar Limit and Beyond,” *JHEP* **10** (2017) 041, [arXiv:1707.08315 \[hep-ph\]](#).
- [227] C. Anastasiou, C. Duhr, F. Dulat, F. Herzog, and B. Mistlberger, “Higgs Boson Gluon-Fusion Production in QCD at Three Loops,” *Phys. Rev. Lett.* **114** (2015) 212001, [arXiv:1503.06056 \[hep-ph\]](#).

- [228] B. Mistlberger, “Higgs boson production at hadron colliders at N^3 LO in QCD,” *JHEP* **05** (2018) 028, [arXiv:1802.00833 \[hep-ph\]](#).
- [229] D. de Florian, M. Mahakhud, P. Mathews, J. Mazzitelli, and V. Ravindran, “Quark and gluon spin-2 form factors to two-loops in QCD,” *JHEP* **02** (2014) 035, [arXiv:1312.6528 \[hep-ph\]](#).
- [230] D. de Florian, M. Mahakhud, P. Mathews, J. Mazzitelli, and V. Ravindran, “Next-to-Next-to-Leading Order QCD Corrections in Models of TeV-Scale Gravity,” *JHEP* **04** (2014) 028, [arXiv:1312.7173 \[hep-ph\]](#).
- [231] T. Ahmed, G. Das, P. Mathews, N. Rana, and V. Ravindran, “Spin-2 Form Factors at Three Loop in QCD,” *JHEP* **12** (2015) 084, [arXiv:1508.05043 \[hep-ph\]](#).
- [232] T. Ahmed, P. Banerjee, P. K. Dhani, P. Mathews, N. Rana, and V. Ravindran, “Three loop form factors of a massive spin-2 particle with nonuniversal coupling,” *Phys. Rev. D* **95** no. 3, (2017) 034035, [arXiv:1612.00024 \[hep-ph\]](#).
- [233] T. Ahmed, P. Banerjee, P. K. Dhani, M. C. Kumar, P. Mathews, N. Rana, and V. Ravindran, “NNLO QCD corrections to the Drell–Yan cross section in models of TeV-scale gravity,” *Eur. Phys. J. C* **77** no. 1, (2017) 22, [arXiv:1606.08454 \[hep-ph\]](#).
- [234] P. Banerjee, P. K. Dhani, M. C. Kumar, P. Mathews, and V. Ravindran, “NNLO QCD corrections to production of a spin-2 particle with nonuniversal couplings in the Drell-Yan process,” *Phys. Rev. D* **97** no. 9, (2018) 094028, [arXiv:1710.04184 \[hep-ph\]](#).
- [235] C. Anastasiou and K. Melnikov, “Pseudoscalar Higgs boson production at hadron colliders in NNLO QCD,” *Phys. Rev. D* **67** (2003) 037501, [arXiv:hep-ph/0208115 \[hep-ph\]](#).
- [236] R. V. Harlander and W. B. Kilgore, “Production of a pseudoscalar Higgs boson at hadron colliders at next-to-next-to leading order,” *JHEP* **10** (2002) 017, [arXiv:hep-ph/0208096 \[hep-ph\]](#).
- [237] V. Ravindran, J. Smith, and W. L. van Neerven, “NNLO corrections to the total cross-section for Higgs boson production in hadron hadron collisions,” *Nucl. Phys. B* **665** (2003) 325–366, [arXiv:hep-ph/0302135](#).

- [238] T. Ahmed, T. Gehrmann, P. Mathews, N. Rana, and V. Ravindran, “Pseudo-scalar Form Factors at Three Loops in QCD,” *JHEP* **11** (2015) 169, [arXiv:1510.01715 \[hep-ph\]](#).
- [239] T. Ahmed, M. C. Kumar, P. Mathews, N. Rana, and V. Ravindran, “Pseudo-scalar Higgs boson production at threshold N^3 LO and N^3 LL QCD,” *Eur. Phys. J.* **C76** no. 6, (2016) 355, [arXiv:1510.02235 \[hep-ph\]](#).
- [240] T. Ahmed, M. Bonvini, M. C. Kumar, P. Mathews, N. Rana, V. Ravindran, and L. Rottoli, “Pseudo-scalar Higgs boson production at N^3 LO_A + N^3 LL’,” *Eur. Phys. J.* **C76** no. 12, (2016) 663, [arXiv:1606.00837 \[hep-ph\]](#).
- [241] C. Anastasiou, C. Duhr, F. Dulat, E. Furlan, T. Gehrmann, F. Herzog, and B. Mistlberger, “Higgs Boson Gluon Fusion Production Beyond Threshold in N^3 LO QCD,” *JHEP* **03** (2015) 091, [arXiv:1411.3584 \[hep-ph\]](#).
- [242] J. Blumlein and V. Ravindran, “QCD threshold corrections to Higgs decay and to hadroproduction in $l+l-$ annihilation,” *Phys. Lett. B* **640** (2006) 40–47, [arXiv:hep-ph/0605011](#).
- [243] E. Laenen, L. Magnea, G. Stavenga, and C. D. White, “On Next-to-Eikonal Exponentiation,” *Nucl. Phys. B Proc. Suppl.* **205-206** (2010) 260–265, [arXiv:1007.0624 \[hep-ph\]](#).
- [244] S. Moch, J. A. M. Vermaseren, and A. Vogt, “Higher-order corrections in threshold resummation,” *Nucl. Phys.* **B726** (2005) 317–335, [arXiv:hep-ph/0506288 \[hep-ph\]](#).
- [245] A. A. H., G. Das, M. C. Kumar, P. Mukherjee, V. Ravindran, and K. Samanta, “Resummed Drell-Yan cross-section at N^3 LL,” [arXiv:2001.11377 \[hep-ph\]](#).
- [246] G. Grunberg and V. Ravindran, “On threshold resummation beyond leading $1-x$ order,” *JHEP* **10** (2009) 055, [arXiv:0902.2702 \[hep-ph\]](#).
- [247] K. Chetyrkin, G. Falcioni, F. Herzog, and J. Vermaseren, “Five-loop renormalisation of QCD in covariant gauges,” *JHEP* **10** (2017) 179, [arXiv:1709.08541 \[hep-ph\]](#).
[Addendum: *JHEP* 12, 006 (2017)].

- [248] T. Luthe, A. Maier, P. Marquard, and Y. Schroder, “The five-loop Beta function for a general gauge group and anomalous dimensions beyond Feynman gauge,” *JHEP* **10** (2017) 166, [arXiv:1709.07718 \[hep-ph\]](#).
- [249] F. Herzog, B. Ruijl, T. Ueda, J. Vermaseren, and A. Vogt, “The five-loop beta function of Yang-Mills theory with fermions,” *JHEP* **02** (2017) 090, [arXiv:1701.01404 \[hep-ph\]](#).